

# Helicates as Versatile Supramolecular Complexes

Claude Piguet,<sup>\*,†</sup> Gérald Bernardinelli,<sup>‡</sup> and Gérard Hopfgartner<sup>§</sup>

Department of Inorganic, Analytical and Applied Chemistry and the Laboratory of X-ray Crystallography, University of Geneva, 30 quai Ernest Ansermet, 1211 Geneva 4, Switzerland, and Pharma Division, F. Hoffmann-La Roche Ltd CH-4070 Basle, Switzerland

Received December 10, 1996 (Revised Manuscript Received April 29, 1997)

## Contents

I. Introduction	2005
II. Principles and Classification of Self-Assembled Helicates	2007
A. The Intrinsic Information	2007
1. Saturated Homotopic Helicates	2008
2. Saturated Heterotopic Helicates	2009
3. Unsaturated Homo- and Heterotopic Helicates	2010
B. Self-Assembly of Helicates	2011
III. Helicates and Molecular Helicity	2012
IV. Synthetic Single-, Double-, and Triple-Stranded Helicates	2015
A. Single-Stranded Helicates	2015
1. Mononuclear Helical Complexes as Precursors for Double-Stranded Helicates	2015
2. Dinuclear Single-Stranded Helicates	2017
B. Double-Stranded Helicates	2019
1. Saturated Homotopic Double-Stranded Helicates	2019
2. Saturated Heterotopic Double-Stranded Helicates	2030
3. Unsaturated Double-Stranded Helicates	2034
C. Triple-Stranded Helicates	2035
1. Saturated Homotopic Triple-Stranded Helicates	2035
2. Saturated Heterotopic Triple-Stranded Helicates	2041
3. Unsaturated Triple-Stranded Helicates	2043
V. Applications of Helicates	2043
VI. Characterization of Self-Assembled Helicates	2046
A. Thermodynamic Self-Assembly and Solution Structures	2047
1. Qualitative Speciation	2047
2. Quantitative Speciation	2050
3. Structural Characterization	2051
B. Crystal Structures of Helicates	2053
1. Crystal Growth and Handling	2053
2. Choice of the Counter-ion	2053
3. Data Collection and Refinement	2053
4. Molecular Symmetry and Crystal Packing	2055
VII. Summary and Outlook	2057
VIII. Addendum	2058
IX. Acknowledgments	2059
X. References	2059

## I. Introduction

The term *helicate* was introduced by Lehn and co-workers in 1987 for the description of a polymetallic

helical double-stranded complex, in effect a metal-containing helix.<sup>1</sup> It is formed by the contraction of the word *helix* (Greek:  $\epsilon\lambda\iota\xi$  = winding, convolution, spiral) with the suffix *-ate*, characterizing host–guest complexes between (pre)organized receptors and metal ions in the same way as *coronates* (macrocyclic complexes of alkali or alkaline earth)<sup>2</sup> or *cryptates* (macropolycyclic complexes with one or more encapsulated metal ions).<sup>3</sup> One may draw a rough analogy between the structure of nucleic acids and that of helicates with, on one hand, the two right-handed polynucleotide chains wound around a central axis defined by the hydrogen-bonded complementary nucleic bases in DNA (**1**),<sup>4</sup> and on the other, the two polyatomic ligand strands wrapped about a series of coordinated metal ions in helicates (**2**) (Figure 1). However, the similarities between these helical structures are very limited and the helicates present only a limited interest as biomimetic models.<sup>5</sup> The importance of the helicates is related to the development and the understanding of self-processes in supramolecular chemistry.<sup>6</sup> The spontaneous generation of the helix **2** was perceived at that time as a self-assembly process similar to those studied in biology<sup>7</sup> and in physics.<sup>8</sup> Intense research activities have been focused on this new field in order to explore and apply its power of design and control for the selective preparation of complicated organized chemical architectures. Among the numerous concepts which have emerged from the work dedicated to helicates, four are crucial in supramolecular chemistry:<sup>6</sup> *molecular recognition* which represents the selective interaction between two or more components in a self-process, *self-organization* which is related to systems capable of spontaneously generating a well-defined (functional) supramolecular architecture from its complementary components under a given set of conditions, *self-assembly* which corresponds to an elemental step within a self-organization process, and (*supra*)*molecular programming* which involves the incorporation of instructions into the components of a self-assembly.<sup>6</sup> The fundamental research on helicates has led recently to new fascinating extended programmed metallosupramolecular architectures based on multicomponents self-assemblies such as directional light-converting devices,<sup>9</sup> inorganic two-dimensional racks, ladders<sup>10</sup> and grids,<sup>11</sup> intertwined catenanes and knots,<sup>12</sup> and allosteric ionophores.<sup>13</sup>

The self-assembly of supramolecular complexes resulting from noncovalent interactions has been reviewed recently by Lawrence, Jiang, and Levett<sup>14</sup> and detailed discussions of interlocked and intertwined structures have been reported by Stoddart and co-workers.<sup>15</sup> In these reviews, some aspects of

<sup>†</sup> Department of Inorganic, Analytical and Applied Chemistry, Geneva.

<sup>‡</sup> Laboratory of X-ray Crystallography, Geneva.

<sup>§</sup> Pharma Division, Hoffmann-La Roche, Basle.

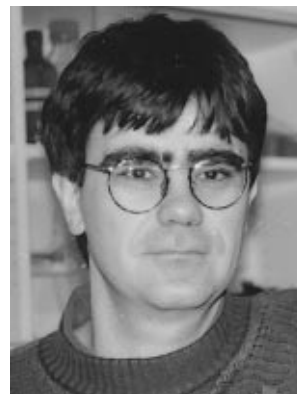


Claude Piguet was born in Geneva, Switzerland, in 1961. He studied chemistry at the University of Geneva and received his M.S. degree in Chemistry in 1986. From 1986 to 1989 he was a graduate student at the Department of Inorganic Chemistry of the University of Geneva where he obtained his Ph.D. thesis with felicitations in 1989 in the domain of coordination chemistry and dioxygen complexes. He pursued his formation as a postdoctoral fellow in the group of Professor J.-M. Lehn at the University of Strasbourg, France (1989–1990), then he returned to Geneva in the group of Professor A. F. Williams (1990–1994), and finally he moved to Lausanne, Switzerland, in the group of Professor J.-C. G. Bünzli (1995). In 1995 he received the *Werner Medal* of the New Swiss Chemical Society for his research in the field of supramolecular chemistry of lanthanide metal ions and luminescent sensors. Since 1995, he has been an Assistant-Professor in the Department of Inorganic Chemistry at the University of Geneva and recipient of the Werner grant for the project "Toward Organized Luminescent Materials". His research topics and interests are the methodical studies of self-assembled supramolecular complexes with d-block and f-block metal ions, the development of lanthanide probes and sensors with predetermined structural, photophysical and magnetic properties, and the preparation of luminescent metallo-mesogens containing lanthanide metal ions.



Gérald Bernardinelli was born in Nice, France, in 1945. He studied chemical engineering from 1963 to 1968 at the Engineer School of Geneva and the chemistry from 1968 to 1973 at the University of Geneva. He received his M.S. degree in chemistry in 1973 and his Ph.D. in 1978 in the domain of structural chemistry of macrocyclic musks. From 1978 to 1983, he was a Research Chemist in the field of X-ray crystallography. Since 1983 he has worked as an Associated Professor in the Laboratory of Crystallography of the University of Geneva where he is responsible for the structural determination of organic and organometallic compounds by X-ray diffraction for the Chemistry and Pharmacy Departments. His scientific interests are X-ray diffraction analysis in relation to structural chemistry of small and medium-size molecules.

helical arrays obtained by hydrogen bonding and coordination interactions have been presented, but the field of supramolecular chemistry has expanded rapidly and the study of helical complexes resulting from metal ions and coordinated organic receptors has become a domain on its own.<sup>16</sup> This review aims to report a classification and a presentation of the helicates according to the intrinsic informations



Gérard Hopfgartner was born in Zürich, Switzerland, in 1960. He studied chemistry at the University of Geneva and received his M.S. degree in Chemistry in 1985 and his Ph.D. in 1991 in the field of organic geochemistry and mass spectrometry. He pursued his formation as a postdoctoral fellow at Cornell University in the group of Professor J. Henion in the domain of liquid chromatography combined with tandem mass spectrometry (LC–MS) (1991–1992). He then joined Hoffmann-La Roche in Basel. He is currently in charge as a senior scientist of the LC–MS group in the department of drug metabolism and kinetics. His scientific interests are LC–MS, CE–MS, quantitative analysis, structure elucidation of metabolites, and fragmentation mechanism in collision-induced dissociation.

required for their spontaneous generation. Particular attention will be focused on (i) the molecular helicity in helicates, (ii) the physical and chemical factors controlling the thermodynamic self-assembly leading to the helicates, and (iii) the structural characterization of these metallosupramolecular edifices.

There is a large variety of coordination compounds whose molecular structure may be loosely described as helical. Pseudotetrahedral complexes possessing two unsymmetrical bidentate AB-type ligands coordinated to a central metal ion  $[M(AB)_2]$  (Figure 2a) or pseudooctahedral complexes  $[M(AB)_3]$  or  $[M(AA)_3]$  (Figure 2b) correspond to helical complexes since the absolute configuration of the metal ion produces right-handed ( $\Delta = P$ ) or left-handed ( $\Lambda = M$ ) helicity along their principal  $C_2^{17}$  or  $C_3^{18}$  axes.

The concept of a helicate indeed implies an extension of these classical coordination complexes toward more complicated helical supermolecules in which *two or more* ions (in general cations) lie on the helical axis.<sup>1,6</sup> A helicate is thus a *discrete* helical supramolecular complex constituted by one or more covalent organic *strands* wrapped about and *coordinated* to a series of ions defining the *helical axis*. This review covers the field of metallosupramolecular helicates which match the two following requirements:

(1) One or more organic acyclic ligand strands are helically wrapped and coordinated to cations (or anions) by coordinate bonds (dative bonds).<sup>14</sup> This condition excludes helical arrays produced by hydrogen bonds as found in DNA<sup>4</sup> and in other supramolecular assemblies.<sup>14,19</sup> Helically distorted macrocyclic, macrobicyclic and knotted structures are also excluded, but the acyclic double-stranded helical precursors of knots and interlocked [2]-catenates will be considered together with helicates derived from podand ligands.<sup>2</sup>

(2) A helicate contains a minimum of two ions ( $n \geq 2$ ,  $n$  is the nuclearity) and forms a discrete

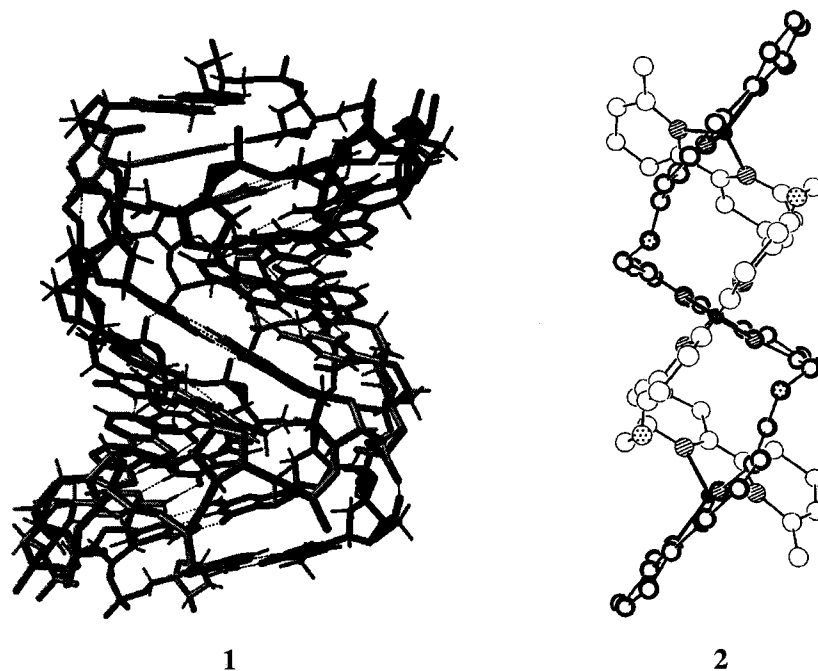


**Figure 1.** X-ray structures of a double-stranded A-DNA (**1**)<sup>4</sup> and a trinuclear double-stranded helicate **2**.<sup>1</sup> (Reproduced with permission from ref 1. Copyright 1987 National Academy of Sciences USA.)

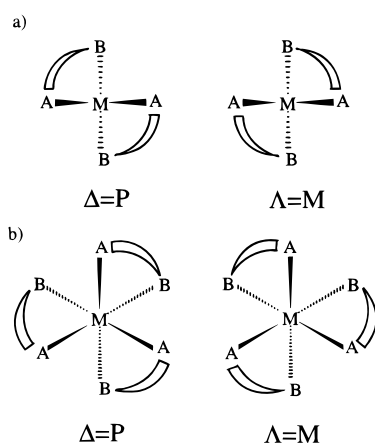


**Figure 2.** Absolute configurations of (a) bis-chelate complexes viewed down the C<sub>2</sub> axis and (b) tris-chelate complexes viewed down the C<sub>3</sub> axis. Δ corresponds to a right-handed helix (symbol P according to Cahn–Ingold–Prelog notation),<sup>24</sup> and Λ to a left-handed helix (M) along the principal axis.

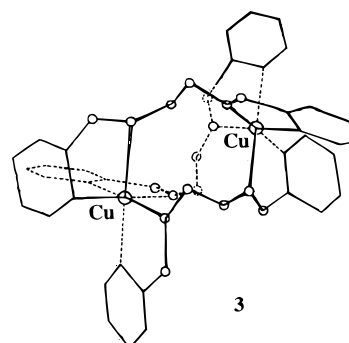
polynuclear oligomer. Classical mononuclear propellers<sup>20</sup> derived from tetrahedral,<sup>17</sup> octahedral,<sup>18</sup> and tricapped trigonal prismatic complexes<sup>21</sup> will not be considered. Polynuclear or infinite helical arrays resulting from crystallization or packing processes (other forms of self-assembly)<sup>22</sup> will not be mentioned.

Although the term *helicate* appeared only in 1987,<sup>1</sup> some early reports describing double- and triple-stranded polynuclear coordination complexes will be considered in this review which will thus cover the subject from the report of Harris and McKenzie<sup>23</sup> who proposed for the first time a helical structure for their dinuclear Cu(II) complex **3** (Chart 1), reminiscent of what is now termed a triple-stranded helicate. The literature has been covered until March 1997.

## II. Principles and Classification of Self-Assembled Helicates

One of the most fascinating aspects of supramolecular chemistry is the spontaneous formation of

**Chart 1**

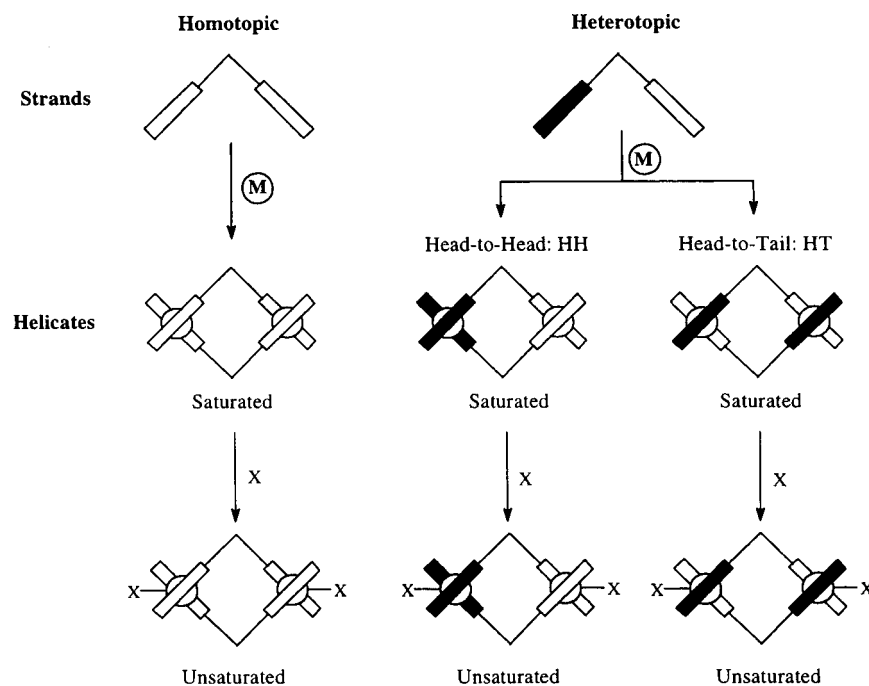


organized architectures from successive molecular recognition processes between various components. The selectivity of the self-assembly process depends on (i) the stereoelectronic molecular informations encoded in the components (i.e., the intrinsic information)<sup>25</sup> and (ii) the external conditions used for the reading, the recognition and the expression of this information in the final supramolecular edifices.

### A. The Intrinsic Information

The generation of the final metallosupramolecular helicate results from specific interactions between the covalent organic ligand strands and the central ions. With one exception,<sup>26</sup> metallic cations are systematically used in helicate self-assembly since they possess useful properties for the assembly process: (i) a set of coordination numbers and stereochemical preferences depending on their size, charge and electronic structure, (ii) a large variation in binding strength and kinetic stability (for instance, d<sup>6</sup> low-spin Ru(II) and Os(II) produce inert and strongly covalent bonds while weak and labile electrostatic bonds are found in Na(I) complexes), (iii) variable affinities for different binding units, and (iv) specific magnetic, electronic, and spectroscopic properties expressed in the final helicates.<sup>6</sup> Points i–iv correspond to the intrinsic information borne by the metal ion which

Scheme 1



should closely match the binding possibilities of the organic ligand strands if these assemblies are to give predictable and well-defined products.<sup>6,25</sup> The use of covalent synthesis for the preparation of organic strands offers almost unlimited possibilities for designing receptors with suitable and complementary intrinsic informations. These ligands should possess (i) several binding units along the strand allowing the recognition and coordination of the various metal ions, (ii) judicious spacers between the binding units which are rigid enough to prevent the coordination of several binding units of one strand to the same metal ion, but flexible enough to undergo helication and to wrap about the metal ions to produce stable polynuclear complexes. It has been shown recently that severe steric constraints in the ligand backbone prevent the self-assembly of helicates and generate symmetry-driven metal-containing clusters derived from the combination of incommensurate symmetry requirements.<sup>27</sup> As one can foresee, there are several possibilities for programming suitable molecular informations within the components (i.e., the ligand strands and the metal ions) and this is the basic point of the classification of helicates proposed in this review. First, the number of coordinated strands are associated with *single*-, *double*-, and *triple*-stranded helicates possessing respectively, one, two and three strands wrapped about the metal ions. Identical coordinated strands correspond to *homostranded* helicates while the presence of different strands leads to *heterostranded* helicates. Intuitively, it is obvious that there are two major types of strands in helicates. The first category contains coordinated ligand strands possessing a sequence of similar binding units along the strand with similar intrinsic informations leading to *homotopic* helicates. The second category results from coordinated ligand strands possessing different binding units providing a directionality within the strand. The resulting helicates are termed *heterotopic* and exist in two isomeric forms according to the orientations of the coordinated binding units (head-to-head, HH, or head-to-tail, HT). Each category is

further split into *saturated* helicate when the stereochemical requirements of the metal ions are fulfilled by the donor atoms of the strands and *unsaturated* when supplementary ligands (X in the Scheme 1) complete the coordination sphere of the metals.

### 1. Saturated Homotopic Helicates

*Dinuclear* ( $n = 2$ ) saturated homotopic helicates possess at least one coordinated strand with a  $C_2$  axis or a  $\sigma$ -symmetry plane passing through the ligand and perpendicular to the helical axis. They result from the assembly of symmetrical organic ligands possessing two identical binding units (*homotopic* = same denticity, same connectivity, same donor atoms) disposed along the strand with metal ions whose stereochemical requirements are completely fulfilled (*saturated*) by the coordinating units of the organic strands. For helicates with *higher nuclearities* ( $n \geq 3$ ), these symmetry requirements are not sufficient since they only relate two parts of the coordinated strand, but they do not ensure that the binding units are similar along the strand. Therefore, homotopic helicates with  $n \geq 3$  result when (i) at least one coordinated strand possesses a  $C_2$  axis or a  $\sigma$ -symmetry plane perpendicular to the helical axis and (ii) the binding units along the strands are similar (same denticity, same connectivity and same donor atoms) and separated by similar spacers. Ideally, homotopic helicates lead to palindromic helices (constant pitch). Let us consider spherical  $d^{10}$  Cu(I) ions which display a preference for pseudotetrahedral ( $D_{2,d}$ ) coordination with 2,2'-bipyridine or analogous  $\alpha,\alpha'$ -diimine ligands,<sup>28</sup> and the  $C_2$ -symmetrical oligobipyridine **4** which possesses three 2,2'-bipyridine units connected by two oxopropylene spacers. Reaction of **4** with Cu(I) in a chloroform/acetonitrile mixture produces quantitatively and selectively the  $D_2$ -symmetrical double-stranded trinuclear helicate  $[\text{Cu}_3(\mathbf{4})_2]^{3+}$  (**2**) where the two ligand strands are wrapped around the three metal ions, each Cu(I) being pseudotetrahedrally coordinated by two bidentate 2,2'-bipyridine

**Table 1. Classification of Saturated Homotopic Dinuclear Homo- and Heterostranded Helicates According to Their Intrinsic Information**

denticity of the binding units	stereochemical preferences of the metal ion	helicates	idealized symmetry	example	ref
monodentate–monodentate	two-coordinate (linear)	double-stranded	$D_2$	$[\text{Cu}_2(\mathbf{41})_2]^{2+}$	91
monodentate–monodentate	three-coordinate (trigonal)	triple-stranded	$D_3$	$[\text{Cu}_3(\mathbf{114})_3]^{3+}$ <sup>a</sup>	158
bidentate–bidentate	four-coordinate (tetrahedral)	double-stranded	$D_2$	$[\text{Zn}_2(\mathbf{32})_2]^{4+}$	58
bidentate–bidentate	six-coordinate (octahedral)	triple-stranded	$D_3$	$[\text{Co}_2(\mathbf{5})_2]^{4+}$	29
tridentate–tridentate	six-coordinate (octahedral)	double-stranded	$D_2$	$[\text{Cd}_2(\mathbf{33})_2]^{4+}$	80
tridentate–tridentate	nine-coordinate (ttp) <sup>b</sup>	triple-stranded	$D_3$	$[\text{Eu}_2(\mathbf{98})_3]^{6+}$	185
mono–mono + bi–bi <sup>c</sup>	three-coordinate	double-stranded	$C_2$	unknown	
mono–mono + tri–tri <sup>c</sup>	four-coordinate	double-stranded	$C_2$	unknown	
bi–bi + tri–tri <sup>c</sup>	five-coordinate	double-stranded	$C_2$	$[\text{Cu}_3(\mathbf{4})(\mathbf{6})_3]^{6+}$ <sup>a</sup>	30
mono–mono + mono–mono + bi–bi <sup>c</sup>	four-coordinate	triple-stranded	$C_2$	unknown	
mono–mono + mono–mono + tri–tri <sup>c</sup>	five-coordinate	triple-stranded	$C_2$	unknown	
mono–mono + bi–bi + bi–bi <sup>c</sup>	five-coordinate	triple-stranded	$C_2$	unknown	
mono–mono + tri–tri + tri–tri <sup>c</sup>	seven-coordinate	triple-stranded	$C_2$	unknown	
mono–mono + bi–bi + tri–tri <sup>c</sup>	six-coordinate	triple-stranded	$C_1$	unknown	
bi–bi + bi–bi + tri–tri <sup>c</sup>	seven-coordinate	triple-stranded	$C_2$	unknown	
bi–bi + tri–tri + tri–tri <sup>c</sup>	eight-coordinate	triple-stranded	$C_2$	unknown	

<sup>a</sup> Only a trinuclear example has been reported. <sup>b</sup> ttp: tricapped trigonal prismatic. <sup>c</sup> Heterostranded helicates: mono, monodentate; bi, bidentate; and tri, tridentate.

units satisfying its stereochemical requirements (Figure 3).<sup>1</sup>  $[\text{Cu}_3(\mathbf{4})_2]^{3+}$  is classified as a homotopic helicate because the coordinated ligand strands possess a  $C_2$ -axis perpendicular to the helical axis and the three binding units are *similar* (2,2'-bipyridine) although the central bidentate binding units is not *identical* (symmetrically speaking) to the terminal binding units.

According to the terminology developed by Lehn,<sup>6</sup> the assembly of **2** amounts to a "tetrahedral reading by Cu(I) of the molecular information stored in the strand **4**" and variations on this unifying theme have led to an important part of the research work dedicated to helicates. One major goal is thus to encode suitable intrinsic informations into the components to generate programmed helicates based on bidentate or tridentate binding units and various metal ions. Tetrahedral metal ions react with oligobidentate ligands to give double-stranded helicates, while octahedral metal ions require oligotridentate strands to produce analogous double-stranded helicates. Triple-stranded helicates result from octahedral metal ions with oligobidentate organic strands or tricapped trigonal prismatic ions with oligotridentate ligands (Table 1).<sup>6,29</sup> A higher level of molecular programming may result from ligands or metal ions possessing ambivalent intrinsic informations. For instance, the bis-bidentate ligand **5** possesses binding units which are compatible with tetrahedral or octahedral metal ions and reaction with Cu(I) gives quantitatively the double-stranded helicate  $[\text{Cu}_2(\mathbf{5})_2]^{2+}$  where each Cu(I) is tetrahedrally coordinated by two bidentate units, while the triple-stranded helicate  $[\text{Co}_2(\mathbf{5})_3]^{4+}$  is obtained with pseudooctahedral Co(II) (Figure 4a).<sup>29</sup> On the other hand, Cu(II) is well known to produce variable and distorted coordination geometries among which five-coordinate complexes are often observed. Its stereochemical requirements are fulfilled by the simultaneous complexation of one bidentate and one tridentate binding unit leading to the self-assembled saturated homotopic trinuclear double-stranded helicate  $[\text{Cu}_3(\mathbf{4})(\mathbf{6})]^{6+}$  which is the

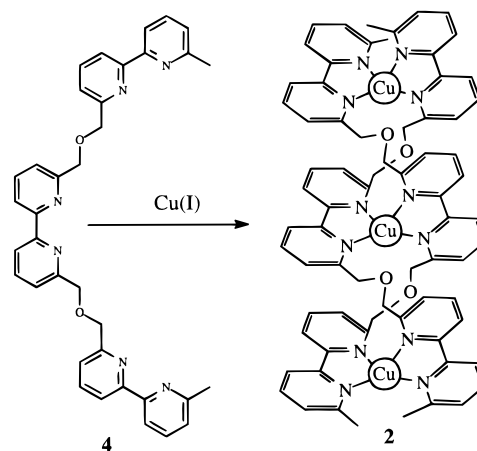


**Figure 3.** Self-assembly of the trinuclear saturated homotopic double-stranded helicate **2**.<sup>1</sup>

only fully characterized helicate possessing different strands **4** and **6**. It is thus termed a double-*hetero*-stranded helicate in contrast to *homost*-stranded helicates which contain identical strands (Figure 4b).<sup>30</sup> Table 1 summarizes the possible saturated dinuclear homotopic helicates generated from a suitable match of intrinsic informations.

## 2. Saturated Heterotopic Helicates

When the coordinated strands in a *dinuclear* helicate do not possess a  $C_2$  axis or a  $\sigma$ -symmetry passing through the ligand and perpendicular to the helical axis, the strands exhibit a directionality analogous to that defined by Mislow for cycles<sup>31</sup> and the resulting helicates are termed *heterotopic*. Stereoisomeric helicates result from the various possible arrangements of the strands: For a double-stranded helicate, two different orientations must be considered (i) a head-to-head arrangement (HH) where the identical binding units of each strand are coordinated to the same metal ion and (ii) a head-to-tail arrangement (HT) corresponding to the coordination of the different binding units of each strand to the same metal. For *higher nuclearities* ( $n \geq 3$ ), the existence

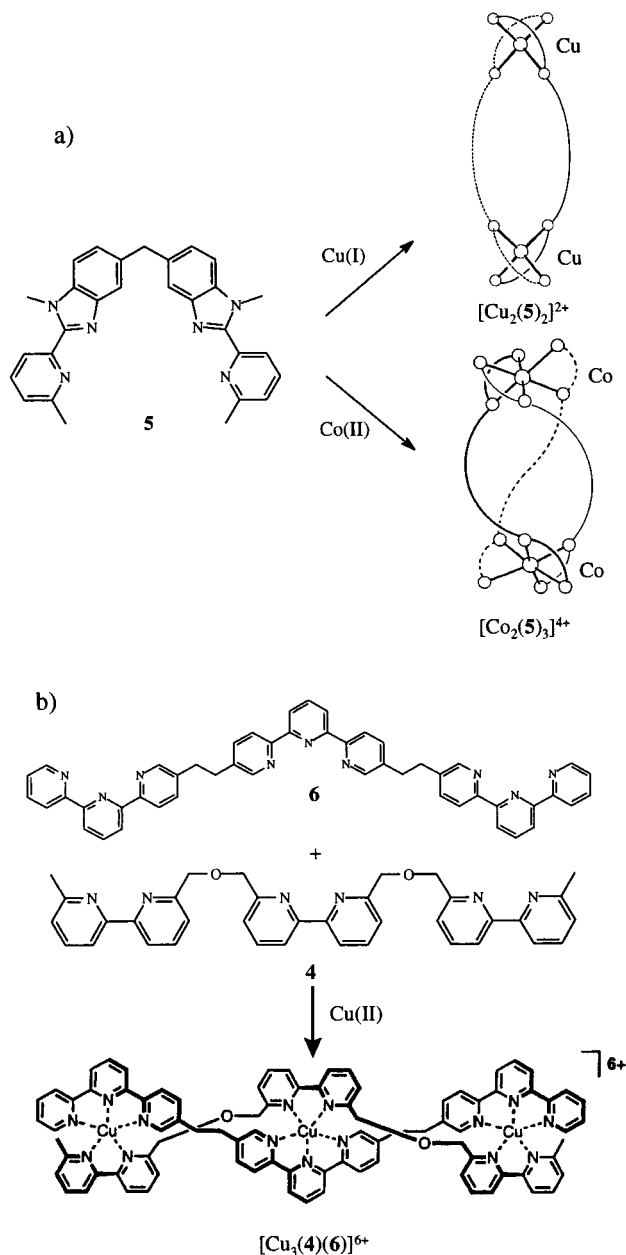


**Figure 4.** Self-assembly of (a) saturated homotopic double-stranded  $[\text{Cu}_2(\mathbf{5})_2]^{2+}$  and triple-stranded  $[\text{Co}_2(\mathbf{5})_3]^{4+}$  helicates according to tetrahedral (Cu(I)) or octahedral (Co(II)) reading of the molecular information stored in **5**,<sup>29</sup> and (b) a saturated homotopic double-heterostranded helicate  $[\text{Cu}_3(\mathbf{4})(\mathbf{6})]^{6+}$  obtained from two different strands.<sup>30</sup> (Reproduced with permission from ref 30, Copyright 1996 National Academy of Sciences USA.)

of different coordinated binding units along the strand is a sufficient condition to produce a heterotopic helicate. The quinquepyridine strand **7** provides a simple example because it may be separated into one bidentate “bipyridine” segment and one tridentate “terpyridine” segment upon complexation to metal ions (Figure 5).<sup>32–34</sup> With Pd(II), the two strands adopt a head-to-tail arrangement leading to the  $C_2$ -symmetrical saturated heterotopic double-stranded helicate  $(\text{HT})\text{-}[\text{Pd}_2(\mathbf{7})_2]^{4+}$  (the  $C_2$  axis is perpendicular to the helical axis, but does not pass through the coordinated strand). Each Pd(II) lies in a distorted five-coordinate environment produced by the coordination of one bipyridine and one terpyridine subunit of each strand.<sup>33</sup> The reaction of the same ligand with one tetrahedral metal ion Ag(I) and one

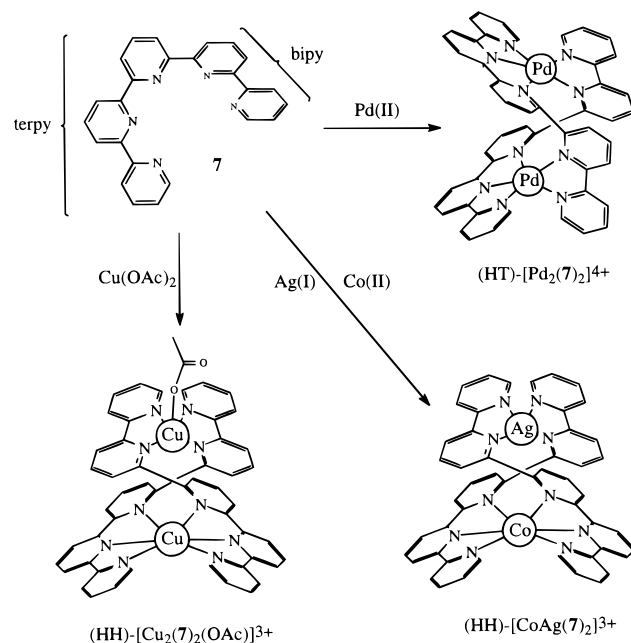


**Figure 5.** Self-assembly of heterotopic double-stranded helicates with 2,2':6',2'':6'',2''':6''',2'''' quinquepyridine **7**:  $(\text{HT})\text{-}[\text{Pd}_2(\mathbf{7})_2]^{4+}$  (saturated, head-to-tail),<sup>33</sup>  $(\text{HH})\text{-}[\text{CoAg}(\mathbf{7})_2]^{3+}$  (saturated, head-to-head),<sup>34</sup> and  $(\text{HH})\text{-}[\text{Cu}_2(\mathbf{7})_2(\text{OAc})]^{3+}$  (unsaturated, head-to-head).<sup>39</sup>

octahedral ion Co(II) leads to the isomeric  $C_2$ -symmetrical ( $C_2$  axis along the helical axis) head-to-head saturated heterotopic helicate  $(\text{HH})\text{-}[\text{CoAg}(\mathbf{7})_2]^{3+}$  where each metal ion occupies a coordination site satisfying its stereochemical requirements (Figure 5).<sup>34</sup>

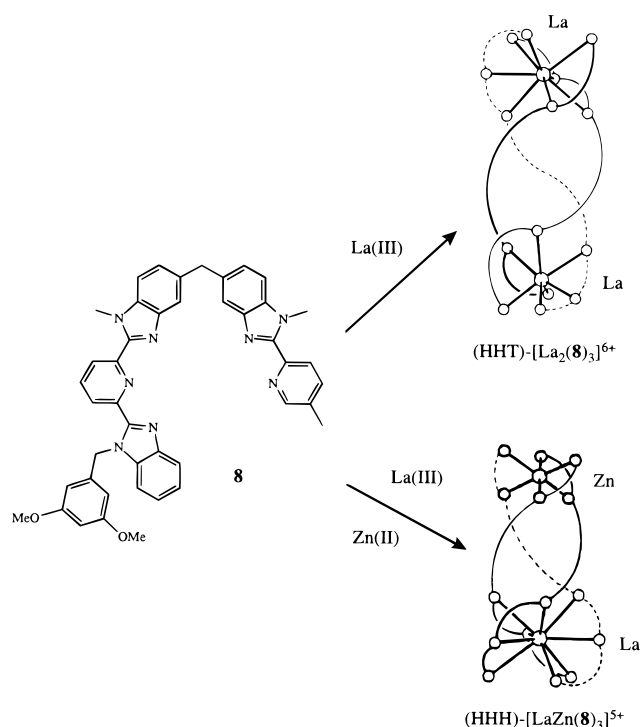
An analogous behavior, reminiscent of the facial–meridional isomerism found in mononuclear octahedral complexes,<sup>35</sup> is expected for triple-stranded helicates. The segmental ligand **8** reacts with La(III) in acetonitrile to give selectively the  $C_1$ -symmetrical triple-stranded helicate  $(\text{HHT})\text{-}[\text{La}_2(\mathbf{8})_3]^{6+}$  where two strands adopt a head-to-head arrangement while the third ligand is oriented head-to-tail leading to different metal environments with respectively seven and eight-coordinated N-donor atoms.<sup>36,37</sup> The isomeric  $C_3$ -symmetrical saturated heterotopic head-to-head triple-stranded helicate  $(\text{HHH})\text{-}[\text{LaZn}(\mathbf{8})_3]^{5+}$  is obtained when La(III) and Zn(II) react with **8** in acetonitrile (Figure 6).<sup>37</sup>

### 3. Unsaturated Homo- and Heterotopic Helicates

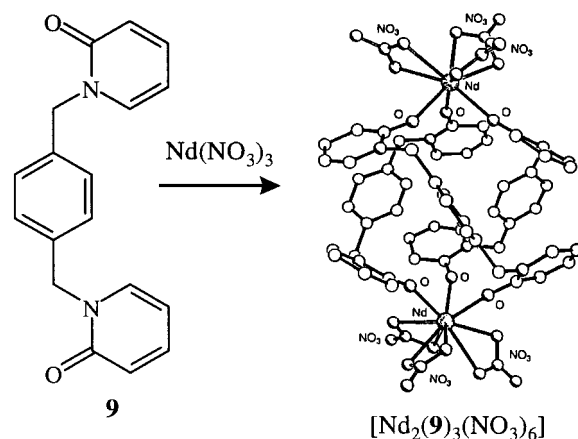
A mismatch between the intrinsic informations encoded in the components does not lead systematically to intricate mixtures of complexes, and the selective generation of a well-defined self-assembled helicate may result from (i) a partial use of the binding possibilities of the strands and (ii) an incomplete filling of the coordination sphere of the metal ion by the ligand strands (*unsaturated*) combined with the binding of supplementary ligands (anions, solvent molecules) to fulfill the stereochemical requirements of the metal. Among the numerous possibilities, only few single-, double-, and triple-stranded unsaturated helicates have been investigated and characterized, probably as a result of the lower selectivity of these type of multicomponent assemblies.<sup>29,32</sup> As described for saturated helicates,  $C_2$ - or  $\sigma$ -symmetrical ligand strands generally produce unsaturated homotopic helicates as exemplified

**Table 2. Classification of Homostranded Saturated Heterotopic Dinuclear Helicates According to Their Intrinsic Information**

denticity of the binding units	stereochemical preferences of the metal ions	arrangement	helicates	idealized symmetry	example	ref
monodentate–bidentate	three-coordinate	head-to-tail	double-stranded	$C_2$	unknown	
monodentate–bidentate	four-coordinate + five-coordinate	head-to-tail	triple-stranded	$C_1$	unknown	
monodentate–bidentate	two-coordinate + four-coordinate	head-to-head	double-stranded	$C_2$	$[\text{Cu}_2(\mathbf{47})_2]^{2+}$	97
monodentate–bidentate	six-coordinate + three-coordinate	head-to-head	triple-stranded	$C_3$	unknown	
monodentate–tridentate	four-coordinate	head-to-tail	double-stranded	$C_2$	unknown	
monodentate–tridentate	five-coordinate + seven-coordinate	head-to-tail	triple-stranded	$C_1$	unknown	
monodentate–tridentate	two-coordinate + six-coordinate	head-to-head	double-stranded	$C_2$	unknown	
monodentate–tridentate	three-coordinate + nine-coordinate	head-to-head	triple-stranded	$C_3$	unknown	
bidentate–tridentate	five-coordinate	head-to-tail	double-stranded	$C_2$	$[\text{Pd}_2(\mathbf{7})_2]^{4+}$	33
bidentate–tridentate	seven-coordinate + eight-coordinate	head-to-tail	triple-stranded	$C_1$	$[\text{La}_2(\mathbf{8})_3]^{6+}$	37
bidentate–tridentate	four-coordinate + six-coordinate	head-to-head	double-stranded	$C_2$	$[\text{CoAg}(\mathbf{7})_2]^{3+}$	34
bidentate–tridentate	six-coordinate + nine-coordinate	head-to-head	triple-stranded	$C_3$	$[\text{EuZn}(\mathbf{109})_5]^{5+}$	190

**Figure 6.** Self-assembly of saturated heterotopic triple-stranded helicates with the segmental ligand **8**. (HHT)- $[\text{La}_2(\mathbf{8})_3]^{6+}$  is head-to-tail while (HHH)- $[\text{LaZn}(\mathbf{8})_3]^{5+}$  is head-to-head.<sup>36,37</sup>

by the bis-monodentate ligand **9** which reacts with Nd(III) to give the unsaturated homotopic triple-stranded helicate  $[\text{Nd}_2(\mathbf{9})_3(\text{NO}_3)_6]$  where the coordination sphere of each Nd(III) is completed by three bidentate  $\text{NO}_3^-$  (Figure 7).<sup>38</sup> Unsaturated heterotopic helicates result from the assembly of unsymmetrical organic strands with metal ions whose stereochemical requirements are not fulfilled by head-to-head or head-to-tail arrangements of the ligands. For instance, the reaction of the quinquepyridine **7** with the versatile Cu(II) readily gives the head-to-head unsaturated heterotopic double-stranded helicate (HH)- $[\text{Cu}_2(\mathbf{7})_2(\text{OAc})]^{3+}$ . One Cu(II) is six-coordinated by the two terpyridine subunits and the

**Figure 7.** Self-assembly of an unsaturated homotopic triple-stranded helicate  $[\text{Nd}_2(\mathbf{9})_3(\text{NO}_3)_6]$ .<sup>38</sup> (Reproduced with permission from ref 38, Copyright 1993 Royal Society of Chemistry.)

second Cu(II) lies in a strongly distorted five-coordinate site produced by the two remaining bipyridine units and one monodentate acetate anion (Figure 5).<sup>39</sup>

## B. Self-Assembly of Helicates

In order to generate programmed helicates, the intrinsic informations of the components must be recognized and expressed efficiently and completely by the assembly process. In general, the reaction between the ligand strands and the metal ions belongs to the category described by Lindsey as strict self-assembly,<sup>7</sup> in which the final helicate corresponds to the most thermodynamically stable product.<sup>6,25</sup> Since the final product requires the formation of several bonds, the kinetic of bond formation and dissociation must be rapid in order (i) to explore completely the potential energy hypersurface of the assembly process leading to the minimum of free energy and (ii) to allow the rejection of "errors" corresponding to only local energy minima. Coordinate bonds appear to be particularly suitable because their considerable strength<sup>35</sup> (compared to other

**Table 3. Classification of Reported Homostranded Unsaturated Dinuclear Helicates According to Their Intrinsic Information**

denticity of the binding units	stereochemical preferences of the metal ions	arrangement	other ligands	helicates	example	ref
monodentate–monodentate	nine-coordinate	/	NO <sub>3</sub> <sup>−</sup>	triple-stranded	[Nd <sub>2</sub> ( <b>9</b> ) <sub>3</sub> (NO <sub>3</sub> ) <sub>6</sub> ]	38
bidentate–bidentate	six-coordinate	/	bipy <sup>a</sup>	single-stranded	[Ru <sub>2</sub> ( <b>37</b> )(bipy) <sub>4</sub> ] <sup>4+</sup>	87
bidentate–bidentate	six-coordinate	/	OAc <sup>−</sup>	double-stranded	[Ni <sub>2</sub> ( <b>73</b> ) <sub>2</sub> (OAc) <sub>2</sub> ] <sup>2+</sup>	119
bidentate–tridentate	six-coordinate	/	terpy <sup>b</sup> , Cl <sup>−</sup>	single-stranded	[Ru <sub>2</sub> ( <b>7</b> )(terpy) <sub>2</sub> (Cl)] <sup>3+</sup>	86
bidentate–tridentate	five-coordinate + six-coordinate	head-to-head	OAc <sup>−</sup>	double-stranded	[Cu <sub>2</sub> ( <b>7</b> ) <sub>2</sub> OAc] <sup>3+</sup>	39

<sup>a</sup> bipy = 2,2′-bipyridine. <sup>b</sup> terpy = 2,2′:6′,2′′-terpyridine.

labile noncovalent hydrogen bonds<sup>40</sup> or dispersion forces<sup>41</sup>) leads to large free energy changes upon the formation of the final metallosupramolecular complexes, and their lability<sup>42</sup> allows strict self-assembly. Obviously, the kinetic and thermodynamic behavior is controlled by the usual external factors (temperature, pressure, activities) which are as important as the intrinsic stereochemical informations for the selective production of stable helicates. The thermodynamic parameters of multicomponent self-assemblies<sup>6</sup> are particularly sensitive to external conditions<sup>37,43</sup> as exemplified by the self-assembly of the saturated heterotopic triple-stranded helicate (HHH)-[LaZn(**8**)<sub>3</sub>]<sup>5+</sup> which dissociates into its mononuclear precursors [Zn(**8**)<sub>2</sub>]<sup>2+</sup> and (HHT)-[La<sub>2</sub>(**8**)<sub>3</sub>]<sup>6+</sup> upon dilution and whose quantitative formation is limited to a stoichiometric ratio La:Zn:**8** = 1:1:3 and concentrations larger than 0.005 M (Figure 46).<sup>37,44</sup> Similarly, the analogous double-stranded helicate (HH)-[CoAg(**7**)<sub>2</sub>]<sup>3+</sup> exists in thermodynamic equilibrium with its mononuclear precursors [Co(**7**)(CH<sub>3</sub>CN)<sub>2</sub>]<sup>2+</sup> and [Ag(**7**)]<sup>+</sup> and it is quantitatively formed under suitable external conditions.<sup>34</sup> Three interrelated secondary thermodynamic factors are associated with self-assembly: allostery, regulation and cooperativity<sup>6</sup> which are often crucial for the spontaneous generation of helicates. These features are observed when the occupation of a given site leads to a change in the binding properties of the other site(s) making binding easier or more difficult associated respectively with positive or negative cooperativity.<sup>45</sup> Polynuclear helicates offer fascinating possibilities for the study of these phenomena and positive cooperativity has been reported for the selective formation of trinuclear double-stranded helicates similar to **2**.<sup>46,47</sup>

### III. Helicates and Molecular Helicity

A helix is characterized by a *helical axis*, a *screw sense* (i.e., its chirality), and a *pitch* (rate of axially linear to angular properties). Thus helicity is a special case of chirality, because it implies two additional properties: When a chiral object has not all the helical properties, nor by a simple adaptation can be given them, the specialized helical model is inapplicable, and the object belongs to the general case of chirality as noted by Cahn, Ingold, and Prelog.<sup>24</sup> Geometrically speaking, a helix is the figure generated by the motion of a point *around* and *along* a line: the helical axis. Ideally, the axis is a straight line and the two kinds of motion are *circular* and *linear* at a constant *distance* *r* from the axis producing a cylindrical (constant radius) palindromic (constant pitch) helix (Figure 8).<sup>48</sup> It may be right-

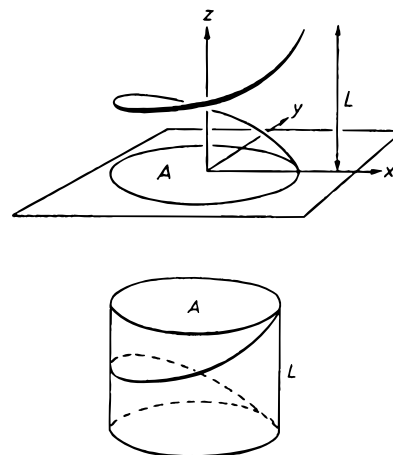


**Figure 8.** A single turn of a right-handed helix (*P*). *L* is the pitch, *z* is the helical axis, and *A* is the area of the subtended circle in the plane *xy*.

handed (plus, *P*) or left-handed (minus, *M*) according to whether the rotation is clockwise or anticlockwise when the helix is considered to wind from the viewer's eye toward a point distant from the viewer.<sup>49</sup> One turn of the helix along the helical axis (*z*) subtends a circle of area *A* in the plane *xy* measuring the motion in the *x* and *y* directions, while the projection of both extremities of the helix onto the *z* axis measures the pitch *L* (i.e., the motion in the *z* direction, Figure 8). The product *A* × *L* gives the volume *V* of the helix domain defined by the thread. When the line changes its helicity, domains of opposite helicity arise, leading to an *amphiverse* helix.

The *net helicity* is measured by the difference in volume of the right- and the left-handed helix domains while the *absolute helicity* is given by the total volume of the helix domain.<sup>48</sup> These strict definitions require some modifications to be applied to chemical edifices. For a molecular helix, the arrangement of atoms can be described by a combination of rotation and translation processes characterized by a pitch, a helical axis, a screw direction, and a radius, but with nonideal subtended geometrical figures.<sup>49</sup> Brewster<sup>48</sup> has studied in detail the helical arrays produced by short chains of tetrahedral atoms (*n* = 4–6) and has extended his “helical conductor model” for the description of many-turn [2]-helices. Depending on the orientation and the sign of the successive dihedral angles within the chain of atoms, complex geometrical figures are obtained and ring, star, rectangular, amphiverse, radial, and step helices have been differentiated.<sup>48</sup>

For ideal helicates, the helical axis is defined by the root-mean-square line passing through the metal

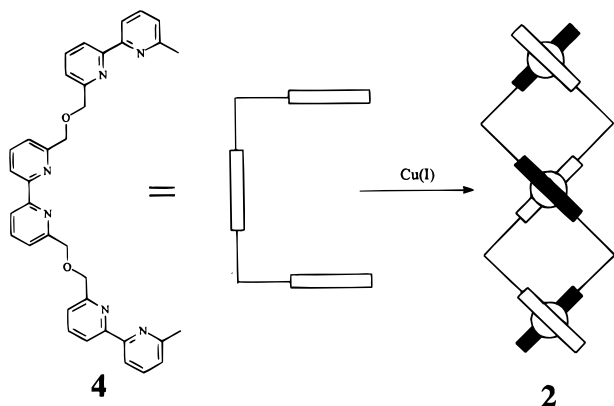


**Figure 9.** Simplified representation of ligand strands by crooked lines made of binding units separated by spacers in helicates.<sup>1,50</sup>

ions while the organic strands provide the helical arrays of atoms. However, this helical system is significantly more complicated than the two atom and two bond motif of [2]-helices treated by Brewster<sup>48</sup> because (i) different motif of atoms arise along the strand and (ii) cyclic subunits (pyridine, benzimidazole, cyclohexane, etc.) are often incorporated into the organic ligand leading to a spatial expansion of the strand roughly perpendicular to the helical axis: the screw thread. A complete mathematical treatment of helicity in helicates has yet to be given, but a simplified approach considering the ligand strands as a crooked line constituted of binding units separated by spacers and wrapped around the metal ions, is usually used for the qualitative description of idealized helicate structures (Figure 9).<sup>29,32,50</sup>

If we neglect the helical domain produced by the spacers between the binding units (i.e., we assign a negligible contribution of the spacer to the total helical pitch), the helicity of the helicate may be deduced from the absolute configurations of the metal ions (Figure 2). For a simple dinuclear saturated homotopic helicate (i.e., a palindromic helix), two extreme situations must be considered: (i) the two metals display opposite absolute configurations (*P* and *M*) leading to a subtended line with no generated area and corresponding to a side-by-side<sup>44,50</sup> arrangement of the ligand strands around the metal ions and (ii) the two metal ions possess identical absolute configurations (*P,P* or *M,M*) leading to a fraction of a subtended circle compatible with a helical arrangement of the strands.<sup>44,48,50</sup> This simple analysis may be applied to the various type of helicates described in section IV and Figures 10–12 summarize the geometrical characteristics of idealized di- and trinuclear single-, double-, or triple-stranded helicates produced by the various combinations of side-by-side and helical arrangement of the strand(s) with metal ions of *P* or *M* absolute configurations.

A careful examination of Figures 10–12 shows that the chiral and helical properties of the helicates depend on the parity of the number of metal ions *n* (i.e., the nuclearity). When *n* = 2, the side-by-side helicates are achiral (i.e., they possess a symmetry plane  $\sigma$ ) and correspond to amphiverse helices with a zero net helicity. Chiral helices result when the two metal ions display the same absolute configuration. More complicated chiral or achiral irregular helicates are expected when *n* is even and *n* ≥ 4 and

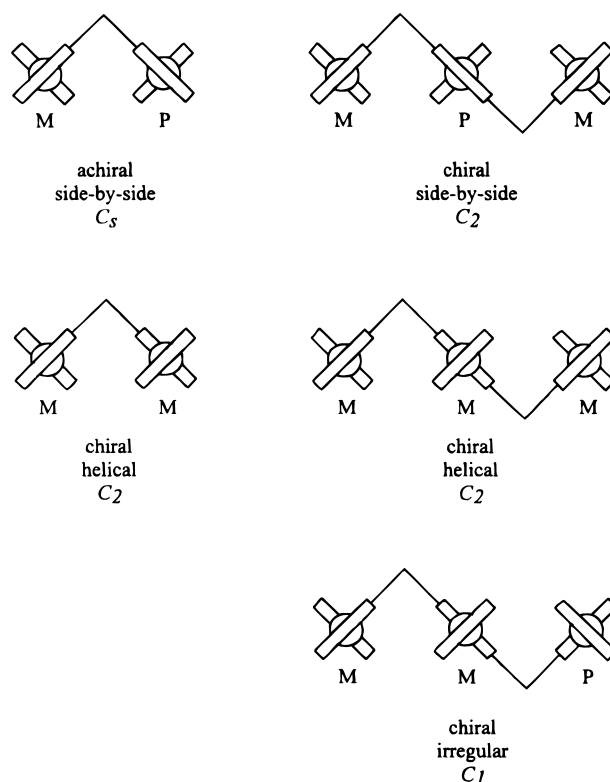


**Figure 10.** Helical and chiral properties of single-stranded dinuclear and trinuclear helicates with  $C_2$ -symmetrical ligand strands. Regular helicates are homotopic while irregular helicates are heterotopic.

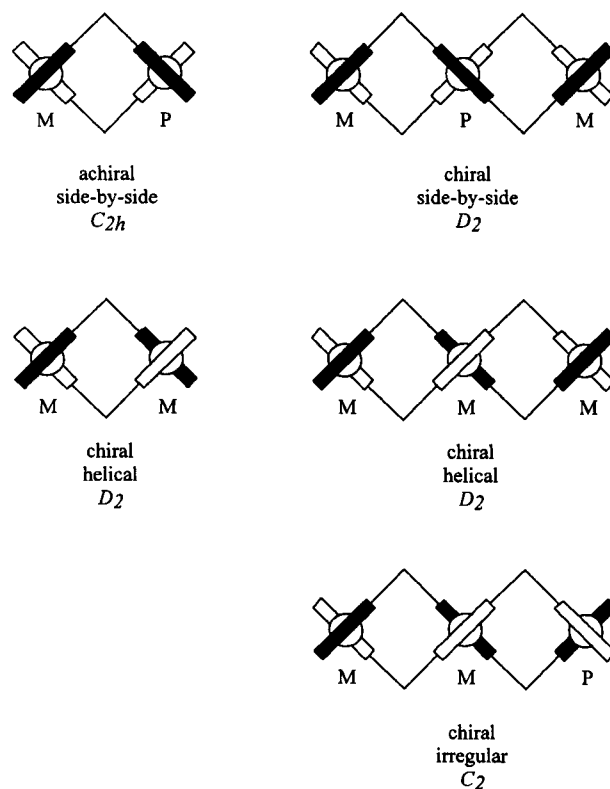


**Figure 11.** Helical and chiral properties of double-stranded dinuclear and trinuclear helicates with  $C_2$ -symmetrical ligand strands. Regular helicates are homotopic while irregular helicates are heterotopic.

for different combinations of *P* and *M* metal ions along the helical axis. These cases are not considered further in this review since only one tetranuclear homotopic  $D_2$ -symmetrical helicate have been char-

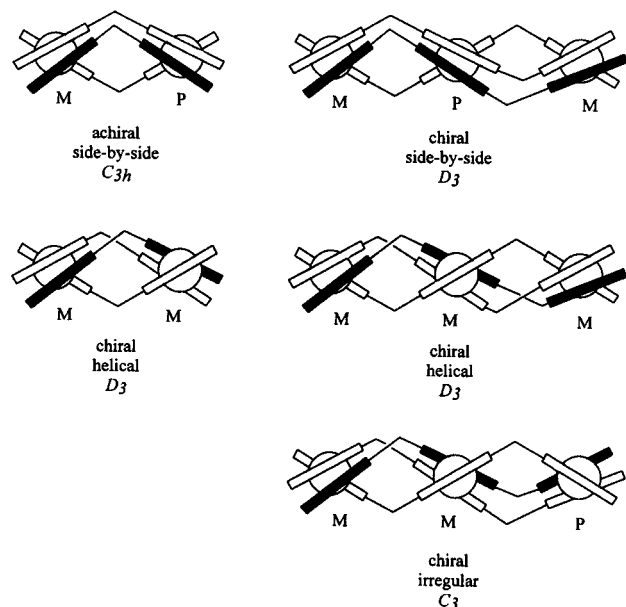
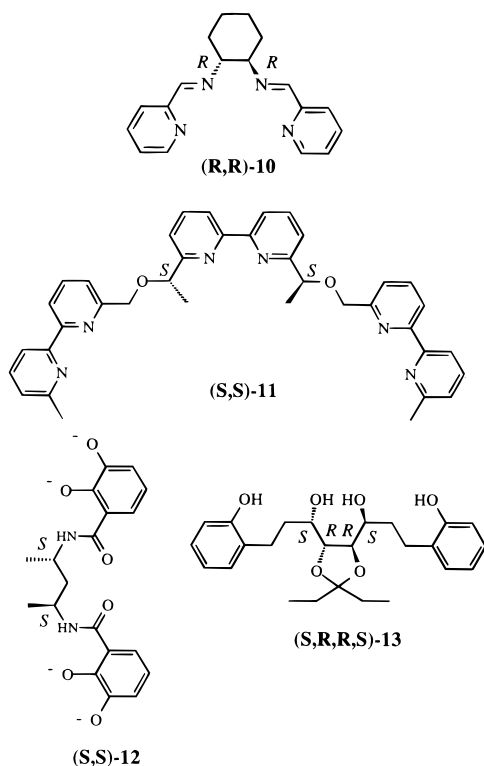


**Figure 12.** Helical and chiral properties of triple-stranded dinuclear and trinuclear helicates with  $C_2$ -symmetrical ligand strands. Regular helicates are homotopic while irregular helicates are heterotopic.

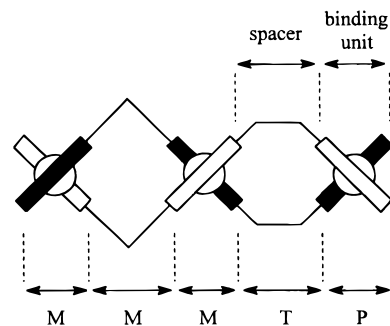
### Chart 2



acterized.<sup>51</sup> When  $n$  is odd, both side-by-side and helical arrangement of the strands lead to chiral helicates belonging to the same point group (single-stranded,  $C_2$ ; double-stranded,  $D_2$ ; and triple-stranded,  $D_3$ ). An irregular succession of  $P$  and  $M$  metal ions (shown for  $n = 3$  in Figures 10–12) leads to chiral irregular helicates.

The use of enantiomerically pure chiral strands introduces a second source of chirality in the helicate leading to the formation of diastereomers according to the screw turn and the ligand arrangement. The ligands **10**,<sup>52</sup> **11**,<sup>50</sup> **12**,<sup>53</sup> and **13**<sup>54</sup> (Chart 2) possess two stereogenic centres in order to induce specific

### Chart 3



helicity in the final helicates and may lead to complicated mixtures of stereoisomers. For instance, the ligand strand  $(R,R)$ -**12** reacts with Ga(III) to give the saturated triple-stranded helicate  $[Ga_2((R,R)$ -**12**)<sub>3</sub>]<sup>6-</sup>. Depending on the absolute configuration of Ga(III), we expect the generation of two chiral  $D_3$ -helical homotopic diastereomeric helicates  $[(P,P)$ - $Ga_2((R,R)$ -**12**)<sub>3</sub>]<sup>6-</sup> and  $[(M,M)$ - $Ga_2((R,R)$ -**12**)<sub>3</sub>]<sup>6-</sup> and one chiral heterotopic  $C_3$  side-by-side helicate  $[(P,M)$ - $Ga_2((R,R)$ -**12**)<sub>3</sub>]<sup>6-</sup>. <sup>1</sup>H NMR data show that the  $(M,M)$ -helicate is the only complex formed in solution and that the  $(P,P)$ - or  $(P,M)$ -helicates are destabilized by at least 8.4 kJ mol<sup>-1</sup> at 297 K.<sup>53</sup> The meso form  $(R,S)$ -**12** leads to new isomers resulting from head-to-head and head-to-tail arrangement of the ligands in the final helicates. For the dinuclear Ga(III) helicate, we expect the formation of eight diastereomers: (i) two chiral heterotopic head-to-head  $C_3$ -helical helicates (HHH)- $[(P,P)$ - $Ga_2((R,S)$ -**12**)<sub>3</sub>]<sup>6-</sup> and (HHH)- $[(M,M)$ - $Ga_2((R,S)$ -**12**)<sub>3</sub>]<sup>6-</sup>, (ii) two chiral heterotopic head-to-tail  $C_1$ -helical helicates (HHT)- $[(P,P)$ - $Ga_2((R,S)$ -**12**)<sub>2</sub>((S,R)-**12**)]<sup>6-</sup> and (HHT)- $[(M,M)$ - $Ga_2((R,S)$ -**12**)<sub>2</sub>((S,R)-**12**)]<sup>6-</sup>, (iii) two achiral homotopic head-to-head  $C_{3h}$ -side-by-side helicates (HHH)- $[(P,M)$ - $Ga_2((R,S)$ -**12**)<sub>3</sub>]<sup>6-</sup> and (HHH)- $[(M,P)$ - $Ga_2((R,S)$ -**12**)<sub>3</sub>]<sup>6-</sup>, and (iv) two achiral homotopic head-to-tail  $C_s$ -side-by-side helicates (HHT)- $[(P,M)$ - $Ga_2((R,S)$ -**12**)<sub>2</sub>((S,R)-**12**)]<sup>6-</sup> and (HHT)- $[(M,P)$ - $Ga_2((R,S)$ -**12**)<sub>2</sub>((S,R)-**12**)]<sup>6-</sup>.

Finally, further complications arise from two deviations not considered in the ideal case described in Figures 10–12. First, the metal ions do not invariably display  $P$  or  $M$  absolute configurations. A tetragonal four-coordinate (or a trigonal prismatic six-coordinate) metal ion bound to two (three) bidentate binding units displays a  $T$  conformation ( $T = trans$  as proposed by Brewster)<sup>48</sup> leading to nonhelical domains within the final helicate. Secondly, the length of the spacer is often not negligible, which produces supplementary helical domains corresponding to either  $P$ ,  $M$  absolute configurations or  $T$  conformations. The complete description of the helicity of a particular helicate should thus consider the following points: (i) the helicate is divided into different helical domains corresponding to the binding units coordinated to the metal ions and the spacers between them (Chart 3), (ii) each domain gives a helical contribution to the net helicity according to its absolute configuration  $P$ ,  $M$  or conformation  $T$  and (iii) other sources of chirality associated with asymmetric centers in the strand may lead to diastereomers.

## IV. Synthetic Single-, Double-, and Triple-Stranded Helicates

### A. Single-Stranded Helicates

An abundant literature reports the formation of single-stranded mononuclear helical complexes resulting from the reactions of acyclic receptors with alkali, alkaline earth, and transition metal ions.<sup>2,55</sup> Although mononuclear complexes are not considered in our definition of helicates (see section I), some single-stranded mononuclear helical complexes are important precursors of double-stranded helicates<sup>56–67</sup> and merit further comments.

#### 1. Mononuclear Helical Complexes as Precursors for Double-Stranded Helicates

The general strategy uses a central metal ion which is too small to fit the cavity of the bound multidentate ligand. Steric interactions between the extremities of the strand induce a slight twisting of the ligand reminiscent of that found in organic helicenes.<sup>49</sup> Several acyclic polyglycols and linear podands wrap around group I and II metals<sup>55</sup> as exemplified by the carbocyclic antibiotic monensin (**14**, Chart 4) which gives the mononuclear single-stranded helical complex  $[\text{Ag}(\mathbf{14})]^+$ .<sup>68</sup> The helical twist may be favored by the attachment of rigid and bulky terminal aromatic groups to oligo(ethylene glycol) units.<sup>69</sup>

#### Chart 4

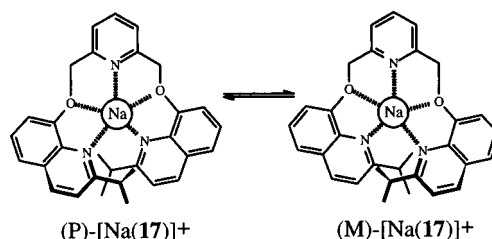
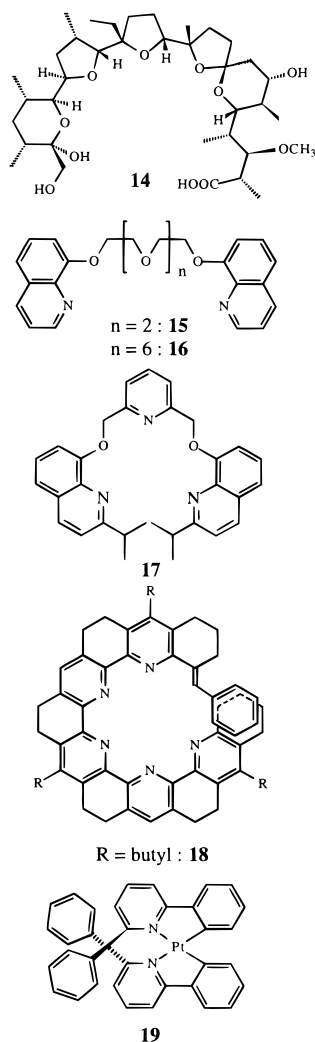


**Figure 13.** Configurational interconversion between P and M helical enantiomers of  $[\text{Na}(\mathbf{17})]^+$ .<sup>72</sup>

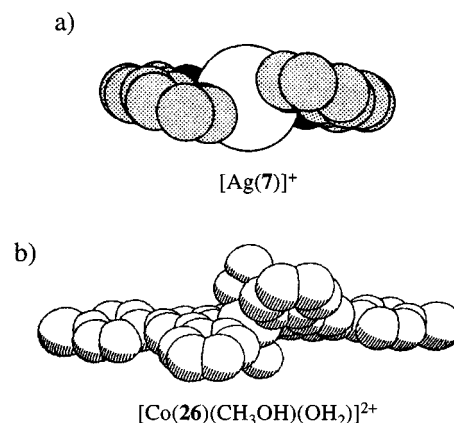
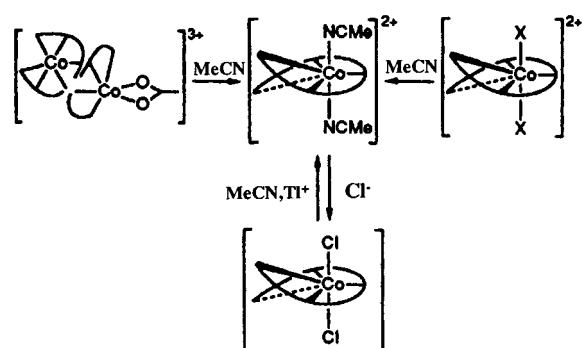


**Figure 14.** Space-filling representation of the mononuclear single-stranded helical cations a)  $[\text{Ag}(\mathbf{7})]^+$ ,<sup>59</sup> and b)  $[\text{Co}(\mathbf{26})(\text{CH}_3\text{OH})(\text{OH}_2)]^{2+}$ .<sup>61</sup> (Reproduced with permission from refs 59 and 61. Copyright 1988 and 1992 Royal Society of Chemistry.)

Compounds **15** and **16** react with  $\text{Rb}^+$  to give helically twisted mononuclear complexes  $[\text{Rb}(\mathbf{15})]^+$ <sup>70</sup> and  $[\text{Rb}(\mathbf{16})]^+$ <sup>71</sup> in the solid state while  $^1\text{H}$  and  $^{13}\text{C}$  NMR spectra of the analogous complex  $[\text{Na}(\mathbf{17})]^+$  indicate that *P*- and *M*-helices interconvert rapidly on the NMR time scale at room temperature ( $\Delta G^\ddagger \approx 41 \text{ kJ mol}^{-1}$ , Figure 13).<sup>72</sup> The  $P \leftrightarrow M$  interconversion process may be slowed down by using (i) a more rigid organic backbone as in the carbocyclic helicene **18**<sup>73</sup> whose single-stranded helical complex  $[\text{Na}(\mathbf{18})]^+$  racemizes slowly at room temperature, and (ii) a strongly bound and inert metal ion which prevents dissociative pathways for helical interconversion as found in the inert cyclometallated Pt(II) complex **19**.<sup>74</sup>

Constable and co-workers<sup>61–64</sup> and Potts and co-workers<sup>60</sup> have shown that the quinquepyridine **7** and its substituted analogues **20–22** and **24–28** may act as pentadentate ligands with transition metal ions to give mononuclear single-stranded helical complexes. The large silver(I) cation ( $1.09 \text{ \AA}$ )<sup>75</sup> almost fits the cavity produced by the *cisoid* arrangement of the five pyridine rings leading to a slight helical twisting of the strand in the crystal structure of  $[\text{Ag}(\mathbf{7})]^+$ .<sup>62</sup> The X-ray crystal structures of  $[\text{Co}(\mathbf{21})\text{-Cl}_2]$ ,<sup>60</sup>  $[\text{Co}(\mathbf{26})(\text{CH}_3\text{OH})(\text{OH}_2)](\text{PF}_6)_2$ ,<sup>61,62</sup> and  $[\text{Re}(\mathbf{7})\text{-Cl}_2]\text{ClO}_4$ <sup>76</sup> show the quinquepyridine strand acting as a pentadentate ligand and forming a more pronounced shallow helical twist about the equatorial plane of a pentagonal bipyramidal seven-coordinate metallic center as a result of the smaller size of Co(II) and Re(III) metal ions (Figure 14). The two axial coordination sites are occupied by solvent molecules<sup>61,62</sup> or chloride anions.<sup>60</sup> In solution,  $[\text{Ag}(\mathbf{7})]^+$  and  $[\text{Co}(\mathbf{L})\text{S}_2]^{2+}$  ( $\mathbf{L} = \mathbf{24–28}$ ; S = solvent) display an average planar arrangement of the quinquepyridine ligands resulting from rapid inter-

a)



b)

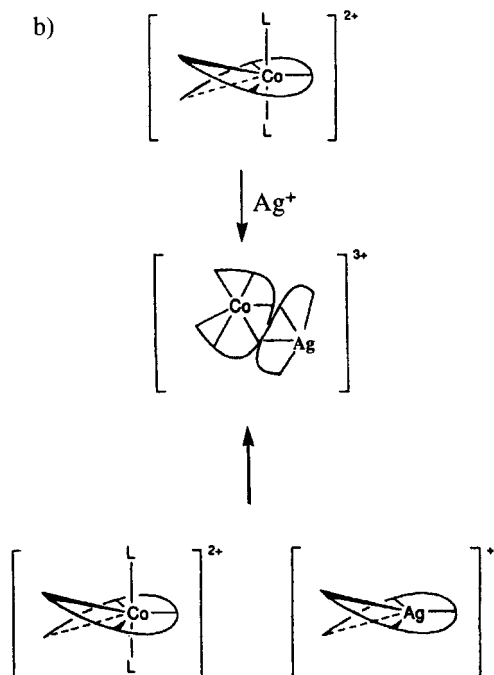
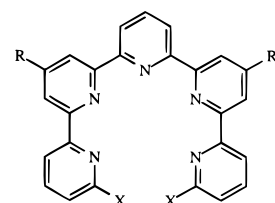


**Figure 15.** Interconversion between mononuclear single-stranded helical complexes and dinuclear double-stranded helicates with quinquepyridine **7**: (a) homonuclear<sup>61</sup> and (b) heteronuclear complexes.<sup>34</sup> (Reproduced with permission from refs 34 and 61. Copyright 1992 Royal Society of Chemistry.)

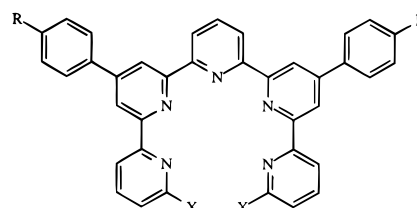
conversion between the right- and left-handed helical enantiomers.

Surprisingly, the assembly of **7** with cobalt(II) acetate in methanol provides a yellow solid whose elemental analysis corresponds to the dinuclear complex  $[\text{Co}_2(\text{7})_2(\text{OAc})](\text{PF}_6)_3$ .<sup>64</sup> The crystal structure of this unsaturated heterotopic double-stranded helicate  $(\text{HH})\text{-}[\text{Co}_2(\text{7})_2(\text{OAc})]^{3+}$  reveals a head-to-head arrangement of the quinquepyridine ligands which are essentially separated into bidentate and tridentate binding units. Two terpyridine subunits are bound to a pseudooctahedral  $\text{Co}(\text{II})$  and the two remaining bidentate bipyridine units and the bidentate acetate anion are bound to the second six-coordinate  $\text{Co}(\text{II})$  (Figure 15a). Interconversion between the double-stranded helicate  $[\text{Co}_2(\text{7})_2(\text{OAc})]^{3+}$  and the mononuclear precursor  $[\text{Co}(\text{7})\text{S}_2]^{2+}$  occurs in solution and corresponds to a change from six-coordinate to seven-coordinate  $\text{Co}(\text{II})$  associated with the only modest ligand-field preference of  $\text{Co}(\text{II})$  for octahedral geometry (Figure 15).<sup>32</sup> This process may be reversed by the addition of a metal ion with a

## Chart 5



- X = H, R = S-Me : **20**  
 X = H, R = S-Prop : **21**  
 X = H, R =  : **22**  
 X = Me, R = H : **23**

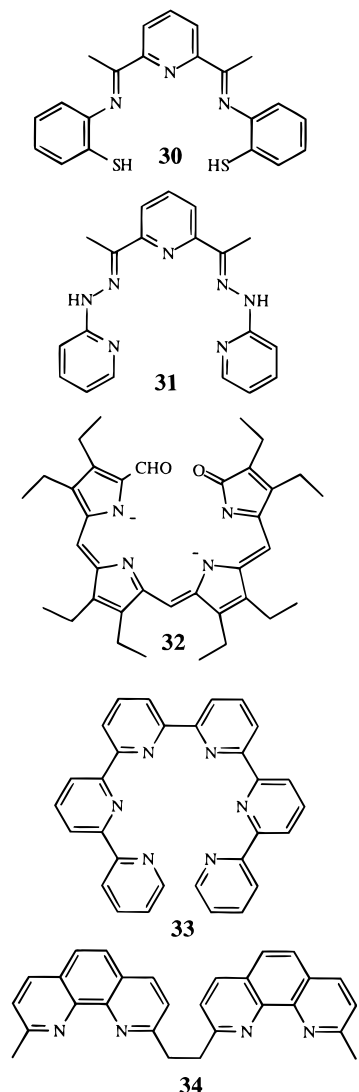


- X = H, R = H : **24**  
 X = H, R = Me : **25**  
 X = H, R = Cl : **26**  
 X = H, R = OH : **27**  
 X = H, R = NMe<sub>2</sub> : **28**  
 X = Me, R = H : **29**

strong preference for tetrahedral coordination which should occupy the site created by the two bipyridine subunits and forces  $\text{Co}(\text{II})$  to lie in the remaining pseudooctahedral site defined by the terpyridine moieties. This is indeed observed and reaction between the mononuclear helical complexes  $[\text{Ag}(\text{7})]^+$  and  $[\text{Co}(\text{7})(\text{CH}_3\text{CN})_2]^{2+}$  spontaneously generates the heterodinuclear heterotopic double-stranded helicate  $(\text{HH})\text{-}[\text{CoAg}(\text{7})_2]^{3+}$  which was characterized by  $^1\text{H}$  NMR in solution and by X-ray diffraction studies in the solid state (Figure 15b).<sup>34</sup> The introduction of methyl groups at the 6 and 6''' positions of the quinquepyridines **23** and **29** increases the steric constraints between the extremities of the strand resulting in a higher degree of twisting within the pentacoordinated quinquepyridine strand in the bridged single-stranded helicate  $[\text{Mn}(\text{23})(\text{OH}_2)]_2\text{Cl}$ .<sup>77</sup> Surprisingly, the expected single-stranded helical complexes  $[\text{Ag}(\text{L})]^+$  ( $\text{L} = \text{23}, \text{29}$ ) are not formed in the solid state, but saturated homo- and heterotopic double-stranded helicates  $[\text{Ag}_2(\text{L})_2]^{2+}$  ( $\text{L} = \text{23}, \text{29}$ ) are observed in the X-ray crystal structures of  $[\text{Ag}_2(\text{L})_2](\text{ClO}_4)_2$  ( $\text{L} = \text{23}, \text{29}$ ).<sup>78</sup>  $^1\text{H}$  NMR spectra in acetonitrile display a higher symmetry in solution compatible with the homotopic  $D_2$ -symmetrical double-stranded helicate  $[\text{Ag}_2(\text{L})_2]^+$  or the possible formation of an average  $C_{2v}$ -symmetrical single-stranded complex  $[\text{Ag}(\text{L})]^+$  in solution.<sup>78</sup> The situation is somewhat clearer with  $\text{Cu}(\text{II})$  and  $\text{Ni}(\text{II})$  where only unsaturated heterotopic double-stranded helicates are obtained with ligands **20–28** (Chart 5) which act as bidentate-tridentate coordinating units.

Although less investigated, similar subtle interconversions between mononuclear helical precursors and dinuclear double-stranded helicates have been reported for several pentadentate ligand strands. The

## Chart 6



2,6-bis[1-[(2-mercaptophenyl)imino]ethyl]diacetylpyridine **30** (Chart 6) is known to form only the mononuclear five-coordinate  $C_2$ -symmetrical helical complex  $[Zn(\mathbf{30}\cdot 2H)]$ ,<sup>56</sup> but the analogous pyridyl-hydrazone derivatives **31** leads to two different complexes: a seven-coordinate pentagonal bipyramidal single-stranded complex  $[Co(\mathbf{31}\cdot 2H)(H_2O)_2]$  and a dinuclear double-stranded helicate  $[Zn_2(\mathbf{31}\cdot 2H)_2]$  depending on the metal ion.<sup>57</sup> These complexes were characterized by X-ray diffraction studies after crystallization and no attempt to investigate possible chemical equilibria in solution has been reported. In an effort to explain versatile metal-templated cyclization reactions, Furhop and co-workers<sup>58</sup> have investigated the octaethylformylbiliverdin (**32**) which provides a brown complex with Zn(II) in neutral solution ( $\lambda_{max} = 830$  nm) which turns green upon addition of a strong acid ( $\lambda_{max} = 750$  nm). Both green and brown crystals may be separated from a methylene chloride/methanol solution of the complex and X-ray diffraction studies show that the neutral form (brown crystals) corresponds to a mononuclear single-stranded helical complex  $[Zn(\mathbf{32})(OH_2)]$  where Zn(II) is coordinated by the four nitrogen atoms of the helically wrapped ligand, the fifth axial position being occupied by a water molecule. The substitution of the axial water molecule by chiral amines or amino acids esters has recently allowed the induction of

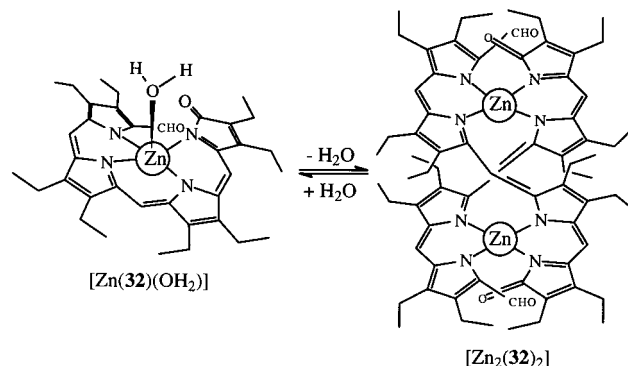


**Figure 16.** Schematic drawing of the double-stranded helicate  $[Zn_2(\mathbf{32})_2]$  and its mononuclear helical precursor  $[Zn(\mathbf{32})(OH_2)]$ .<sup>58</sup>

helical chirality with diastereomeric excesses of 10–73%.<sup>79</sup> The acid form (green crystals) corresponds to a dinuclear double-stranded helicate  $[Zn_2(\mathbf{32})_2]$  which results from the removal of the coordinated water molecule bound to Zn(II) in the mononuclear precursor (Figure 16).<sup>58</sup> The sexipyridine **33** is the next higher oligobipyridine after quinquepyridine **7** and it forms a mononuclear single-stranded helical complex  $[Eu(\mathbf{33})(NO_3)_2]^+$  with the large Eu(III) metal ion. Its crystal structure shows the sexipyridine ligand helically twisted about the equatorial plane, two bidentate nitrate group occupying axial positions eventually leading to a ten-coordinate metal center.<sup>65</sup> <sup>1</sup>H NMR data suggests that a  $C_2$ -symmetrical complex exists in solution which is compatible with the mononuclear complex (whose helical enantiomers interconvert rapidly) or a dinuclear double-stranded homotopic helicate similar to those found for  $[Cd_2(\mathbf{33})_2]^{4+}$ <sup>80</sup> or  $[Ni_2(\mathbf{33})_2]^{4+}$  (see section IV.B).<sup>81,82</sup>

Finally, the interconversion between mononuclear single-stranded and dinuclear double-stranded helicates is not limited to constrained oligopyridines or pentadentate ligands displaying some ambiguities concerning their binding mode. The segmental ligand **34** which possesses two well-defined binding units separated by an ethylene spacer and designed for the assembly of polynuclear helicates,<sup>66,67</sup> also gives mononuclear single-stranded helical complexes  $[Co(\mathbf{34})(CF_3SO_3)_2]$ <sup>66</sup> and  $[Cu(\mathbf{34})(OH_2)]^{2+}$ .<sup>67</sup> In these complexes, the bis-bidentate ligand is wrapped about the metal ion and acts as a tetradentate binding unit occupying the four equatorial positions around the metal ion in the solid state, triflate anions, or water molecules occupying axial position in the crystal structures (Figure 17). The reduction of  $[Cu(\mathbf{34})(OH_2)]^{2+}$  in acetonitrile produces the homotopic double-stranded helicate  $[Cu_2(\mathbf{34})_2]^{2+}$  as a result of the preference of spherical  $d^{10}$  Cu(I) for tetrahedral coordination with constrained 1,10-phenanthroline or 2,2'-bipyridine binding units.<sup>28,83</sup>

## 2. Dinuclear Single-Stranded Helicates

According to our definition of helicates, a single-stranded helicate results when a ligand strand is helically wrapped around and coordinated to two or more metal ions. This definition is close to the many-turn helix model proposed by Brewster<sup>48</sup> for crooked lines, the main difference lying in the presence of coordinated metal ions on the helical axis. For instance, the glyme ligand strand **35** (Chart 7) reacts

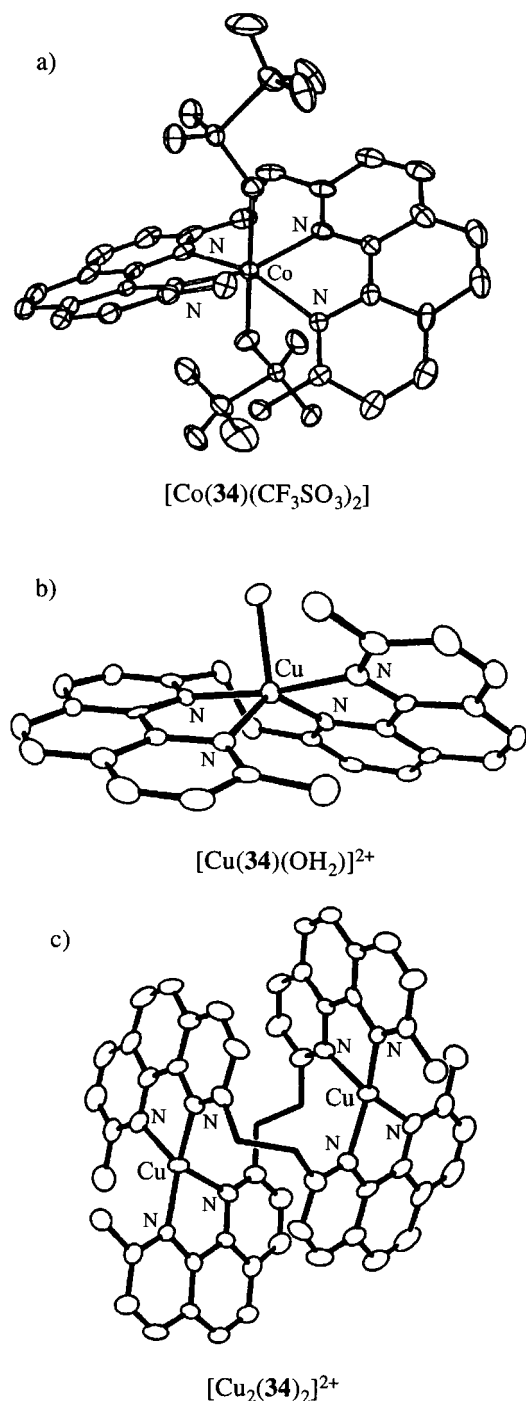
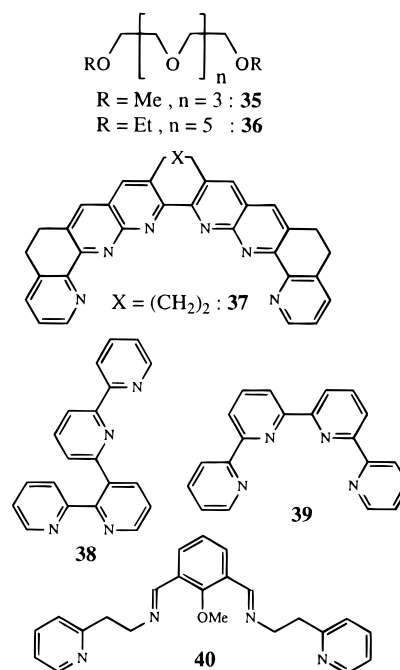


**Figure 17.** ORTEP representations of the crystal structures of (a) [Co(**34**)(CF<sub>3</sub>SO<sub>3</sub>)<sub>2</sub>],<sup>66</sup> (b) [Cu(**34**)(OH<sub>2</sub>)<sub>2</sub>]<sup>2+</sup>, and (c) [Cu<sub>2</sub>(**34**)<sub>2</sub>]<sup>2+</sup>.<sup>67</sup> (Reproduced from refs 66 and 67. Copyright 1991 and 1992 American Chemical Society.)

with HgCl<sub>2</sub> to give only a mononuclear complex. The five oxygen atoms of **35** are almost coplanar, directed inward, and closely embrace the central Hg(II) cation, but the extended hexamethylene glycol–diethyl ether **36** utilizes its seven oxygen donor atoms to complex two Hg(II).<sup>84</sup> The detailed conformation of the strand in the single-stranded helicate [Hg<sub>2</sub>(**36**)Cl<sub>4</sub>] was analyzed according to the successive dihedral angles of the molecular thread (antiperiplanar or synclinal) as described for [2]-helices.<sup>48</sup> The adjacency of two synclinal sequences at the central oxygen atom is responsible for the separation of the strand into two binding domains occupied by two Hg(II) ions.<sup>85</sup>

As discussed in the previous section for mononuclear helical complexes, dinuclear single-stranded

**Chart 7**



helicates are also interesting as precursors of double-stranded helicates and the quinquepyridine **7** is particularly suitable to investigate these interconversion processes because of its various binding modes. Compound **7** is pentadentate in mononuclear helical complexes,<sup>60–63</sup> but it acts as a segmental bidentate–tridentate ligand strand in dinuclear heterotopic double-stranded helicates (Figure 5)<sup>33,34,39,64</sup> and in the unsaturated heterotopic dinuclear single-stranded helicate [Ru<sub>2</sub>(**7**)(terpy)<sub>2</sub>Cl]<sup>3+</sup>,<sup>86</sup> whose crystal structure shows two different six-coordinate metallic sites, with one Ru(II) coordinated to the terpyridine subunit of the ligand **7** and the second Ru(II) bound to the remaining bipyridine subunit (Figure 18a). The helical twist of the strand results from a torsion between the two connected pyridine rings of each subunit and amounts to 74.9°, one of the largest values found for helicates of this ligand (Table 5).<sup>86</sup> The remaining vacant coordination sites around Ru(II) are occupied by two tridentate terpyridine (terpy) ligands and one chloride anion (Figure 18a). In the homotopic single-stranded helicate [Re<sub>2</sub>(**7**)(py)<sub>2</sub>(CO)<sub>6</sub>]<sup>2+</sup>, **7** adopts an unusual bis-bidentate binding mode where each Re(I) is coordinated to a terminal bipyridine binding unit of the strand, the central uncoordinated pyridine ring acting as a spacer (Figure 18b).<sup>76</sup> As expected, the intermetallic distance significantly increases in the latter binding mode (5.38 Å for [Ru<sub>2</sub>(**7**)(terpy)<sub>2</sub>Cl]<sup>3+</sup> and 7.723 Å for [Re<sub>2</sub>(**7**)(py)<sub>2</sub>(CO)<sub>6</sub>]<sup>2+</sup>) and it reaches 8.12 Å in the related homotopic single-stranded helicate [Ru<sub>2</sub>(**37**)-(bipy)<sub>4</sub>]<sup>4+</sup> where an elongated spacer separates the two bipyridine binding units.<sup>87</sup> An analogous single-stranded helical structure has been proposed for [Pd<sub>2</sub>(**33**)(OAc)<sub>2</sub>](PF<sub>6</sub>)<sub>2</sub> in the solid state<sup>82</sup> but no crystal structure has been reported.

A problem arises for the nonsymmetrical 2,2':3',2'':6'',2''' quaterpyridine ligand **38** (Chart 7) synthesized by Barigelletti, Ward, and co-workers since the resulting heterodinuclear cation [Cl(CO)<sub>3</sub>Re(**38**)Ru-(bipy)<sub>2</sub>]<sup>2+</sup> still corresponds to our definition of a heterotopic single-stranded helicate despite the un-

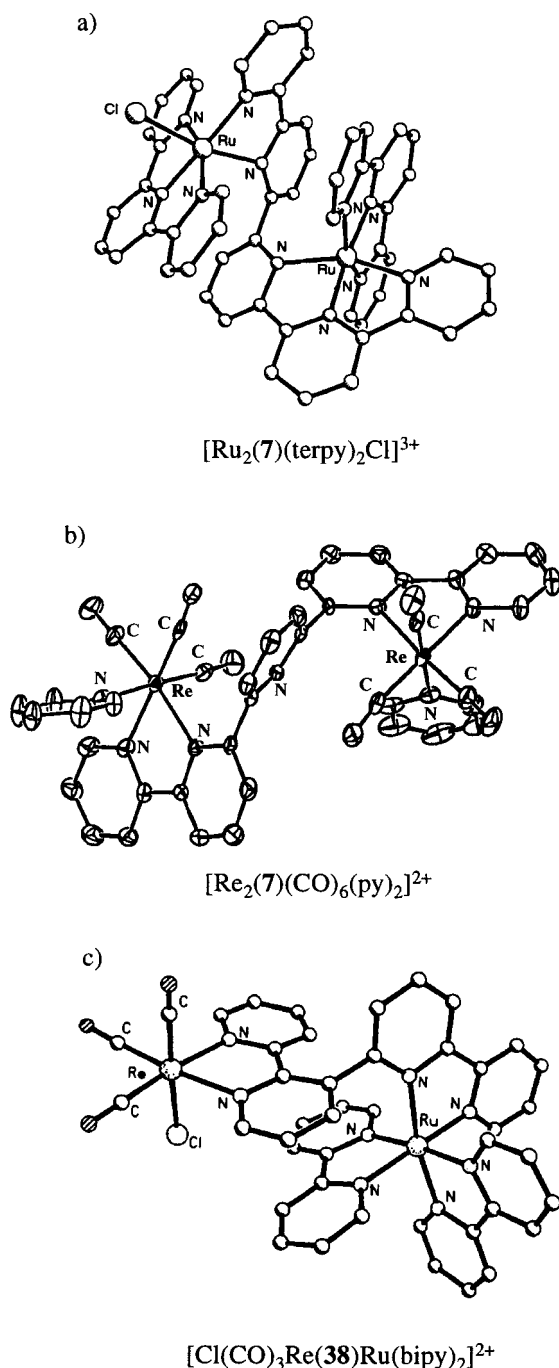


**Figure 18.** Crystal structures of the single-stranded dinuclear helicates (a)  $[\text{Ru}_2(7)(\text{terpy})_2\text{Cl}]^{3+}$ ,<sup>86</sup> (b)  $[\text{Re}_2(7)(\text{CO})_6(\text{py})_2]^{2+}$ ,<sup>76</sup> and (c)  $[\text{Cl}(\text{CO})_3\text{Re}(\mathbf{38})\text{Ru}(\text{bipy})_2]^{2+}$ .<sup>88</sup> (Reproduced with permission from ref. 76, 86, and 88. Copyright 1990 and 1996 Royal Society of Chemistry, and 1995 American Chemical Society.)

usual conformation of the ligand strand which is obviously not compatible with our intuitive representation of a helix (Figure 18c).<sup>88</sup> A general approach considers the segmental ligand **38** (or its symmetrical analogue **39**) as a strand adopting *P* or

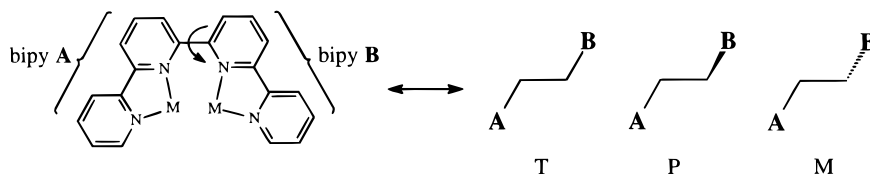


**Figure 19.** Possible conformation of the quaterpyridine **39** acting as a bis-bidentate chelate bridging ligand.

*M* helicity (or *T* conformation).<sup>48</sup> According to this statement, almost any dinuclear complex possessing a linear nonplanar (*P* or *M* configuration) chelating strand may be loosely described as a single-stranded helicate (Figure 19).<sup>89</sup> In this review, we have thus limited our discussions to single-stranded helicates possessing a ligand strand closely related to those used in the self-assembly of double- and triple-stranded helicates.

The ligand strand **40** merits particular attention because it reacts with Cu(I) in dichloromethane to give the orange dinuclear complex  $[\text{Cu}_2(\mathbf{40})(\text{CH}_3\text{CN})_4]^{2+}$  where each Cu(I) is probably four-coordinated by one bidentate  $\alpha, \alpha'$ -diimine binding unit and two acetonitrile molecules (Figure 20a).<sup>90</sup> The addition of a large excess of acetonitrile leads to a mixture of  $[\text{Cu}(\text{CH}_3\text{CN})_4]^+$  and a pale yellow and poorly soluble polymer  $[\text{Cu}(\mathbf{40})\text{BF}_4]_n$  whose crystal structure reveals the formation of an infinite linear helical string based on single-stranded helical motives connected by metal ions (Figure 20b).<sup>90</sup> Such a polymeric arrangement of two helical threads represents a structural alternative to classical discrete double-stranded helicates. According to Feringa and co-workers,<sup>90</sup> the infinite helical polymer is in equilibrium with its single-stranded helical precursor in solution.

## B. Double-Stranded Helicates

### 1. Saturated Homotopic Double-Stranded Helicates

a. *Two-Coordinate Metal Ions.* If we limit the metal ion to be strictly two-coordinate (Table 1, entry 1), the white dinuclear complexes  $[\text{Cu}_2(\mathbf{L})_2]^{2+}$  ( $\mathbf{L} = \mathbf{41}, \mathbf{42}$ ; Chart 8) characterized by Williams and co-workers are the only example of this category.<sup>91</sup> The crystal structure of  $[\text{Cu}_2(\mathbf{41})_2](\text{ClO}_4)_2$  shows the dinuclear cation  $[\text{Cu}_2(\mathbf{41})_2]^{2+}$  to exhibit a centrosymmetrical structure in which each Cu(I) is essentially linearly coordinated by one benzimidazole group of each ligand (Figure 21a).<sup>91</sup> Despite the lack of crystallographic  $C_2$  axis in the solid state, the idealized structure of  $[\text{Cu}_2(\mathbf{41})_2]^{2+}$  corresponds to a dinuclear homotopic double-stranded  $C_{2h}$ -side-by-side helicate with a zero net helicity associated with *T* conformations for the metal ions and for the benzene-1,3-diyl spacer.<sup>91</sup> In nitromethane solution, conductivity measurements show that the dinuclear structure of the cation is maintained, but <sup>1</sup>H NMR studies of the analogous helicate  $[\text{Cu}_2(\mathbf{42})_2]^{2+}$  indicate that the geminal methylene protons bound to the benzimidazole side arms are enantiotopic pointing to  $D_{2h}$  symmetry in solution resulting from a fast in-out interconversion of the central benzene-1,3-diyl spacer on the NMR time scale.<sup>91,92</sup> When the rigid benzene spacer is replaced by a more flexible propylene unit in **43**, the dimeric structure is lost and only a mononuclear complex  $[\text{Cu}(\mathbf{43})(\text{CH}_3\text{CN})]^+$  is formed because **43** acts as a bidentate chelate to one metal

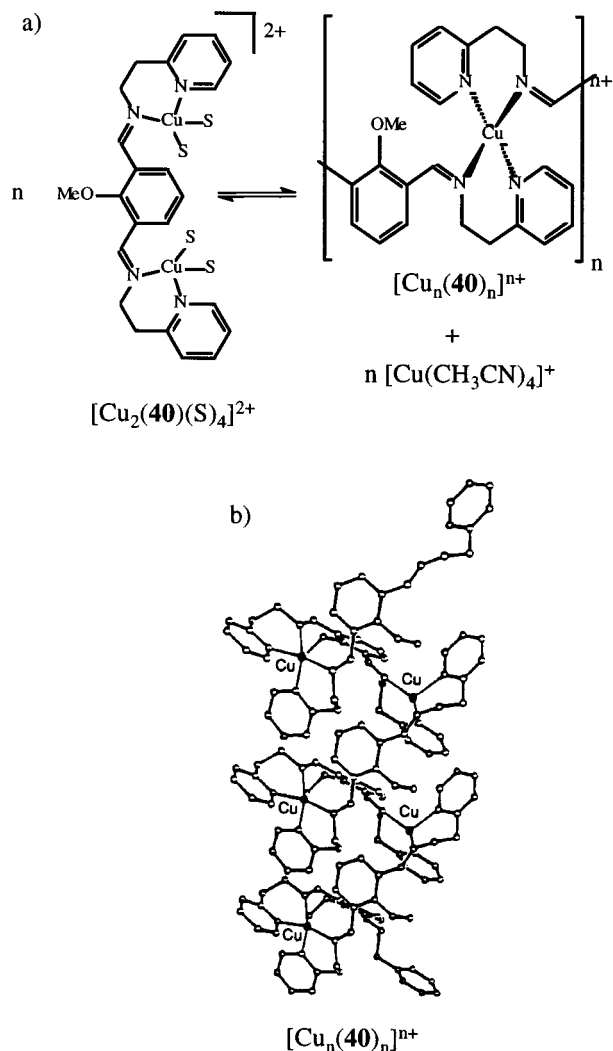
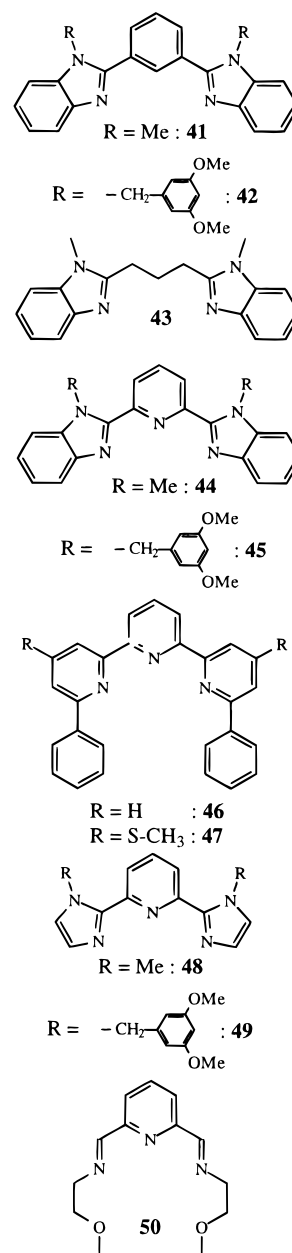


**Figure 20.** Self-assembly of an infinite linear helical polymer based on single-stranded helical motives: (a) equilibrium in solution and (b) part of the X-ray crystal structure of the infinite helicate  $[Cu_n(40)_n]^{n+}$ .<sup>90</sup> (Reproduced with permission from ref 90. Copyright 1991 Royal Society of Chemistry.)

ion.<sup>93</sup> The introduction of a rigid pyridine spacer between the benzimidazole side arms restores the dinuclear structure and the orange double-stranded helicates  $[Cu_2(L)_2]^{2+}$  ( $L = 44, 45$ ) are readily formed in solution.<sup>91</sup> The crystal structure of the cation  $[Cu_2(44)_2]^{2+}$  reveals a pseudo- $D_2$  helical arrangement of the two organic strands wrapped about a helical axis defined by the metal ions (Figure 21b).<sup>94</sup> Each copper is still essentially linearly two-coordinated by the benzimidazole side arms of each strand ( $Cu-N(\text{bzim}) = 1.901-1.933 \text{ \AA}$ ), but the central pyridine units act as weakly bridging ligands producing a minor tetrahedral distortion of the Cu(I) coordination sites ( $Cu-N(\text{py}) = 2.415-2.622 \text{ \AA}$ ).<sup>94</sup> As a result of the helication in  $[Cu_2(44)_2]^{2+}$ , the intermetallic distance is shortened ( $7.14 \text{ \AA}$  in  $[Cu_2(41)_2]^{2+}$  and  $2.854 \text{ \AA}$  in  $[Cu_2(44)_2]^{2+}$ ), and two strong intramolecular  $\pi$ -stacking interactions occur between the benzimidazole rings of each strand (Figure 21b). A related behavior is observed when the distal benzimidazole rings are replaced by substituted pyridine (**46** and **47**) or imidazole side arms (**48** and **49**). The core of the X-ray crystal structure of the double-stranded helicate  $[Cu_2(48)_2]^{2+}$  is almost superimposable with that of  $[Cu_2(44)_2]^{2+}$  despite the removal of intramolecular

**Chart 8**



interstrand stacking interactions which strongly suggests that the weakly bridging pyridine units are crucial for the helication process.<sup>95</sup> Intermolecular  $\pi$ -stacking interactions between imidazole rings of successive helicates produce columns of packed cations  $[Cu_2(48)_2]^{2+}$  with the same helicity in the solid state.<sup>95</sup> Constable and co-workers<sup>96</sup> and Potts and co-workers<sup>97</sup> have shown that analogous substituted 6,6''-diphenylterpyridine ligands **46** and **47** also react with Cu(I) to give orange dinuclear double-stranded helicates  $[Cu_2(L)_2]^{2+}$  ( $L = 46, 47$ ), but their crystal structures exhibit different coordination sites for the two metal ions leading to (strictly speaking) heterotopic helicates in the solid state. The ligand strands have essentially distributed themselves to present bidentate domains coordinated to a distorted tetrahedral Cu(I) and monodentate pyridines coordinated to a quasi-linear Cu(I) ion (Figure 21c).<sup>96,97</sup> The central pyridine rings are still bridging, but in a very unsymmetrical fashion ( $Cu-N(\text{central pyridine}) = 2.180-2.480 \text{ \AA}$ ). Several stacking interactions occur between the aromatic rings of the two strands and

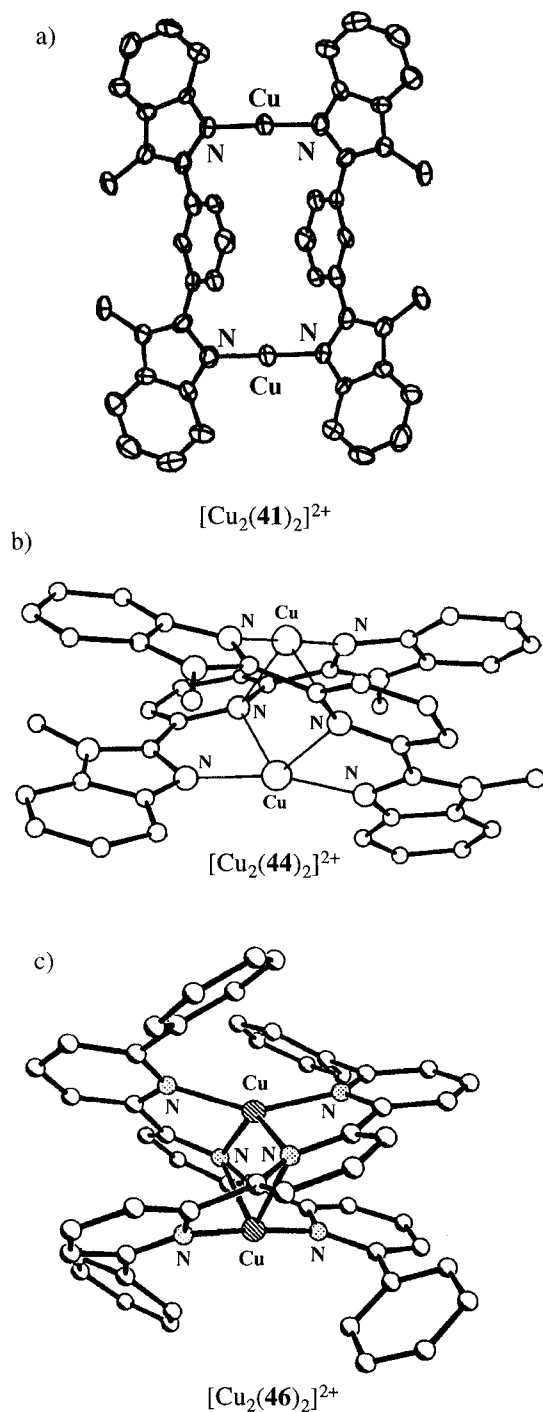


**Figure 21.** X-ray crystal structures of the double-stranded helicates  $[\text{Cu}_2(\mathbf{41})_2]^{2+}$ ,<sup>91</sup>  $[\text{Cu}_2(\mathbf{44})_2]^{2+}$ ,<sup>94</sup> and  $[\text{Cu}_2(\mathbf{46})_2]^{2+}$ .<sup>96</sup> (Reproduced with permission from refs 91, 94, and 96. Copyright 1994 Royal Society of Chemistry, and 1989 and 1992 American Chemical Society.)

subtle substituent effects finely control the helical pitch which is larger for thio-substituted terpyridine **47** (Table 4).<sup>96</sup>

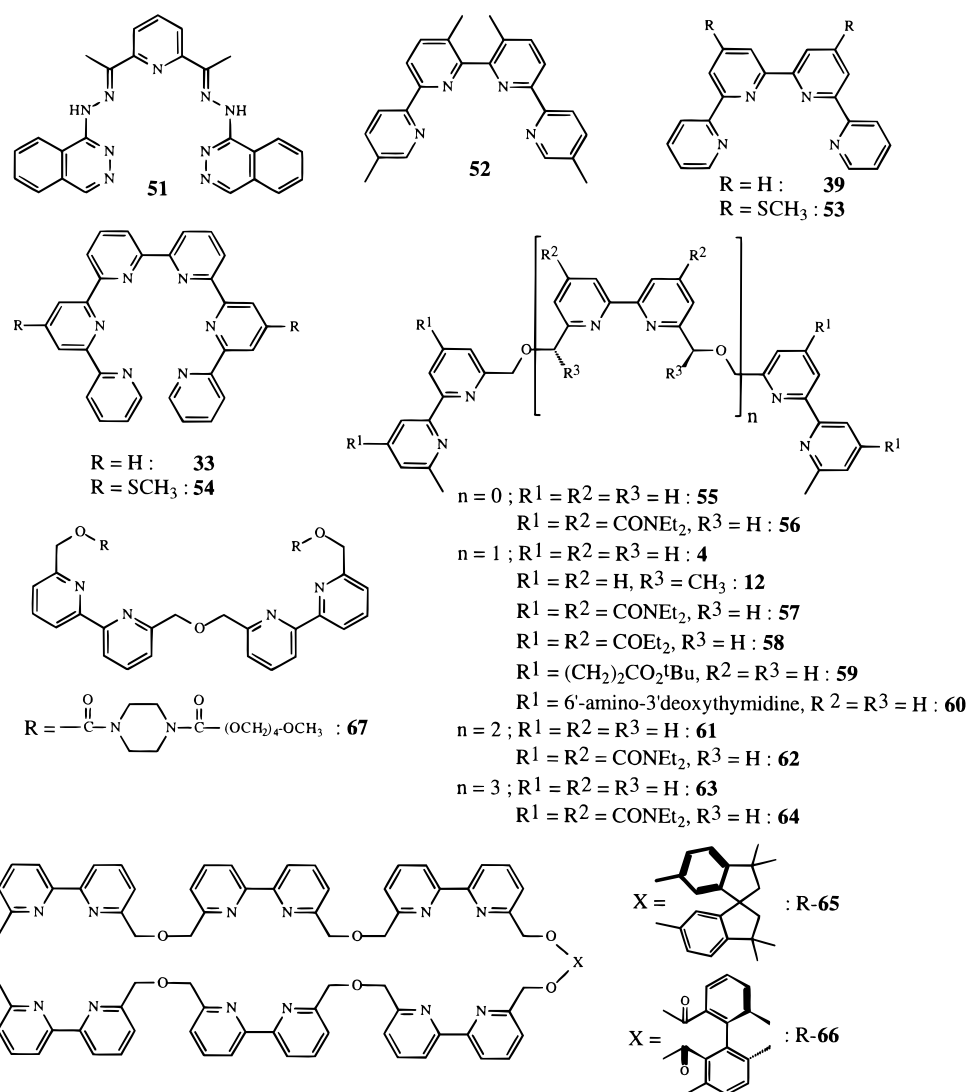
The idealized dinuclear double-stranded helical structures found in the solid state for the helicate series  $[\text{Cu}_2(\mathbf{L})_2]^{2+}$  ( $\mathbf{L} = \mathbf{44}–\mathbf{49}$ ) are maintained in solution as established by various spectroscopic techniques (<sup>1</sup>H NMR, UV–vis,<sup>91,97</sup> and ES–MS<sup>98</sup>) and conductivity measurements.<sup>91</sup> The orange color is characteristic of the Cu(I)  $\rightarrow \pi^*$  MLCT transition associated with tetrahedrally distorted Cu<sup>I</sup>–polypyridine chromophores<sup>99</sup> which implies that the central bridging pyridine ring still interacts with

Cu(I) in solution for the helical dinuclear complexes.<sup>91</sup> A detailed analysis of the variable-temperature <sup>1</sup>H NMR signals of the diastereotopic methylene protons in  $[\text{Cu}_2(\mathbf{L})_2]^{2+}$  ( $\mathbf{L} = \mathbf{45}, \mathbf{49}$ ) indicates that the chiral  $D_2$ -symmetrical double-stranded helical structure is kinetically stable at room temperature<sup>91,95,97</sup> which strongly contrasts with the fast exchange rate found for the side-by-side analogue  $[\text{Cu}_2(\mathbf{42})_2]^{2+}$ . Fast racemization between (*P,P*), (*P,M*) and (*M,M*) isomers occurs at higher temperature on the <sup>1</sup>H NMR time scale and free energies of  $\Delta G^\ddagger = 65.1(4)$  kJ mol<sup>-1</sup> and 50.8(4) kJ mol<sup>-1</sup> have been calculated for  $[\text{Cu}_2(\mathbf{45})_2]^{2+}$  and  $[\text{Cu}_2(\mathbf{49})_2]^{2+}$  in DMF-*d*<sub>7</sub>, respectively.<sup>92</sup> Attempts to oxidize the dinuclear double-stranded helicates  $[\text{Cu}_2(\mathbf{47})_2]^{2+}$  show two mono-electronic and quasi-reversible waves (0.12 and 0.98 V vs SCE) attributed to successive oxidation of the metals which strongly interact in the dinuclear helicate.<sup>97</sup> However, it is not clear whether the oxidized helicate can survive in solution and an alternative explanation involves the decomposition of the dinuclear complex after the first oxidation step to give  $[\text{Cu}(\mathbf{47})]^{2+}$  and  $[\text{Cu}(\text{CH}_3\text{CN})_4]^+$ , the latter complex being then oxidized at 0.98 V to give  $[\text{Cu}(\text{CH}_3\text{CN})_4]^{2+}$ . The attachment of pendant ether groups in **50** offers new binding possibilities and reaction with Cu(I) in ethanol gives brown crystals of  $[\text{Cu}_2(\mathbf{50})_2](\text{ClO}_4)_2$ .<sup>100</sup> The crystal structure of the cation  $[\text{Cu}_2(\mathbf{50})_2]^{2+}$  is similar to those described for  $[\text{Cu}_2(\mathbf{L})_2]^{2+}$  ( $\mathbf{L} = \mathbf{46}, \mathbf{47}$ ) and shows the ligand strands separated into bidentate and monodentate nitrogen donor domains. One Cu(I) is thus pseudo-tetrahedrally coordinated by two iminopyridine units while the other is essentially linearly coordinated by the remaining imine groups of each ligand. Weak interactions with the pendant ether groups and the central bridging pyridine rings complete the coordination spheres of the metals.

We conclude that double-stranded helicates with essentially two-coordinate metal ions require a rigid spacer between the binding units. However, the use of a pyridine is not innocent and its weak bridging properties favor the helical twist required for the generation of  $D_2$ -symmetrical double-stranded helicates in solution. In the solid state, slightly different arrangements of the central pyridine rings are observed in the crystal structures which are probably associated with a rather flat structural energy minimum controlled by packing forces and leading to symmetrical or unsymmetrical bridges between the metal ions. Very subtle forces control the assembly of these helicates, and in this context, it is worth noting that  $[\text{Ag}_2(\mathbf{44})_2]^{2+}$  displays a helical double-stranded structure in solution similar to that found for its Cu(I) analogue,<sup>101</sup> but  $[\text{Ag}(\mathbf{46})]^+$  is mononuclear,<sup>96</sup> while the unsubstituted precursor ligand strand 2,2':6',2''-terpyridine leads to complicated polynuclear complexes with Ag(I).<sup>102</sup>

*b. Four-Coordinate Metal Ions.* The spontaneous generation of homotopic double-stranded helicates from  $C_2$ - or  $\sigma$ -symmetrical ligand strands with tetrahedral metal ions (Table 1, entry 3) is probably the best studied helicate self-assembly. The first fully characterized helicates belonged to this category and were often the fortuitous result of efforts to design coordination complexes with constrained environments. In section IV.A, we have shown how penta-

## Chart 9



dentate ligands are strongly sensitive to minor structural changes leading to mononuclear single-stranded helical complexes or dinuclear double-stranded helicates, and in 1975, Palenik and Wester reported the crystal structure of one of the first homotopic dinuclear double-stranded helicate [Zn<sub>2</sub>(**31-2H**)<sub>2</sub>] based on the deprotonated pentadentate ligand [**31-2H**]<sup>2-</sup>.<sup>57</sup> The crystal structure reveals that two ligand strands are wrapped around two Zn(II) cations and the central pyridine rings of **31** weakly bridge the two metals (Zn–N(central pyridine) = 2.39–2.62 Å) leading to distorted coordination sites around Zn(II) as previously discussed for ligands **44**–**50** with Cu(I). A similar double-stranded helicate [Ni<sub>2</sub>(**51-2H**)<sub>2</sub>] possessing two bridging pyridine units may be isolated when the terminal pyridine side arms are replaced with phthalazine groups.<sup>103</sup> The first planned strategy for the generation of a dinuclear double-stranded helicate may be attributed to Lehn, Sauvage, Ziessel, and co-workers who prepared the conformationally restricted and preorganized quaterpyridine **52**<sup>104</sup> (Chart 9). The methyl groups bound to the 5' and 3'' positions maintain the two bipyridine subunits in a twisted conformation which favors the formation of dinuclear helical complexes. Reaction of **52** with Cu(I) selectively produces a dinuclear complex [Cu<sub>2</sub>(**52**)<sub>2</sub>]<sup>2+</sup> whose

**Table 4. Intermetallic Distances (*d*) and Interplanar Angles ( $\omega_1$  and  $\omega_2$ ) between the Central Pyridine Ring and the Two Connected Planar Aromatic Side Arms in the Crystal Structures of Dinuclear Double-Stranded Helicates with Ligand Strands 41–50**

metal	ligand	helicate	<i>d</i> , Å	$\omega_1$ , deg	$\omega_2$ , deg	ref
Cu(I)	<b>41</b>	[Cu <sub>2</sub> ( <b>41</b> ) <sub>2</sub> ] <sup>2+</sup>	7.140	36.7	43.7	91
Cu(I)	<b>44</b>	[Cu <sub>2</sub> ( <b>44</b> ) <sub>2</sub> ] <sup>2+</sup>	2.854	18.4–22.6	41.8–44.6	94
Cu(I)	<b>46</b>	[Cu <sub>2</sub> ( <b>46</b> ) <sub>2</sub> ] <sup>2+</sup>	2.570	/	/	96
Cu(I)	<b>47</b>	[Cu <sub>2</sub> ( <b>47</b> ) <sub>2</sub> ] <sup>2+</sup>	2.631	27.5	37.0	97
Cu(I)	<b>48</b>	[Cu <sub>2</sub> ( <b>48</b> ) <sub>2</sub> ] <sup>2+</sup>	2.821	27.7	25.1	95
Cu(I)	<b>50</b>	[Cu <sub>2</sub> ( <b>50</b> ) <sub>2</sub> ] <sup>2+</sup>	2.626	7.1–9.0	28.9–30.6	100

crystal structure confirms the helical arrangement of the two strands around the metal ions. As expected, each ligand is separated into two bipyridine subunits with interplanar angles of 75.4–75.6° between them (Figure 22).<sup>104</sup> Electrochemical studies have established that the dinuclear helicate [Cu<sub>2</sub>(**52**)<sub>2</sub>]<sup>2+</sup> is oxidized in two successive steps (0.53 and 0.72 V vs SCE) to give an unstable dinuclear complex [Cu<sub>2</sub>(**52**)<sub>2</sub>]<sup>4+</sup> which rapidly dissociates in solution providing the final mononuclear product [Cu(**52**)-(OH<sub>2</sub>)]<sup>2+</sup>.<sup>105</sup> The separation of the two oxidation waves  $\Delta E_{1/2} = 0.19$  V implies a significant electronic interaction between the Cu(I) (Cu–Cu = 3.90 Å)<sup>104</sup> which can be compared to that found in [Cu<sub>2</sub>(**47**)<sub>2</sub>]<sup>2+</sup>

**Table 5. Intermetallic Distances ( $d$ ) and Interplanar Angles ( $\omega$ ) between the Central Pyridine Rings of the Coordinated Binding Units in the Crystal Structures of Dinuclear Single- and Double-Stranded Helicates with Oligopyridine Ligands**

metal	ligand	helicate	$d$ Å	$\omega$ deg	binding mode	ref
Quaterpyridines						
Cu(I)	<b>39</b>	[Cu <sub>2</sub> ( <b>39</b> ) <sub>2</sub> ] <sup>2+</sup>	3.17	35.2–40.2	bidentate + bidentate	106
Ag(I)	<b>39</b>	[Ag <sub>2</sub> ( <b>39</b> ) <sub>2</sub> ] <sup>2+</sup>	3.107	45.1–46.9	bidentate + bidentate	106
Cu(I)	<b>53</b>	[Cu <sub>2</sub> ( <b>53</b> ) <sub>2</sub> ] <sup>2+</sup>	3.32	55.4–59.7	bidentate + bidentate	107
Cu(I)	<b>52</b>	[Cu <sub>2</sub> ( <b>52</b> ) <sub>2</sub> ] <sup>2+</sup>	3.90	75.4–75.6	bidentate + bidentate	104
Quinquepyridines						
Re(I)	<b>7</b>	[Re <sub>2</sub> ( <b>7</b> )(CO) <sub>6</sub> (py) <sub>2</sub> ] <sup>2+</sup>	7.723	68–69.6	bidentate + bidentate	76
Ag(I)	<b>29</b>	[Ag <sub>2</sub> ( <b>29</b> ) <sub>2</sub> ] <sup>2+</sup>	3.22	36.1–36.8	bidentate + bidentate	77
Ru(II)	<b>7</b>	[Ru <sub>2</sub> ( <b>7</b> )(terpy) <sub>2</sub> Cl] <sup>3+</sup>	5.38	74.9	bidentate + tridentate	86
Pd(II)	<b>7</b>	[Pd <sub>2</sub> ( <b>7</b> ) <sub>2</sub> ] <sup>4+</sup>	4.96	70	bidentate + tridentate	33
Ag(I)	<b>23</b>	[Ag <sub>2</sub> ( <b>23</b> ) <sub>2</sub> ] <sup>2+</sup>	3.48	47.2	bidentate + tridentate	77
Cu(II) + Cu(I)	<b>7</b>	[Cu <sub>2</sub> ( <b>7</b> ) <sub>2</sub> ] <sup>3+</sup>	3.957	47.7–48.3	bidentate + tridentate	39
Cu(II) + Cu(I)	<b>20</b>	[Cu <sub>2</sub> ( <b>20</b> ) <sub>2</sub> ] <sup>3+</sup>	4.25	63.5–70.1	bidentate + tridentate	107
Co(II) + Ag(I)	<b>7</b>	[CoAg( <b>7</b> ) <sub>2</sub> ] <sup>3+</sup>	4.224	60	bidentate + tridentate	34
Co(II)	<b>7</b>	[Co <sub>2</sub> ( <b>7</b> ) <sub>2</sub> (OAc)] <sup>3+</sup>	4.46	58.1–59.9	bidentate + tridentate	64
Ni(II)	<b>7</b>	[Ni <sub>2</sub> ( <b>7</b> ) <sub>2</sub> (OAc)] <sup>3+</sup>	4.45	58–60	bidentate + tridentate	154
Ni(II)	<b>20</b>	[Ni <sub>2</sub> ( <b>20</b> ) <sub>2</sub> (OAc)] <sup>3+</sup>	4.42	44.0	bidentate + tridentate	108
Ni(II)	<b>20</b>	[Ni <sub>2</sub> ( <b>20</b> ) <sub>2</sub> (OAc)] <sup>3+</sup>	4.44	45.5	bidentate + tridentate	62
Cu(II)	<b>7</b>	[Cu <sub>2</sub> ( <b>7</b> ) <sub>2</sub> (OAc)] <sup>3+</sup>	4.503	51–55	bidentate + tridentate	39
Cu(II)	<b>20</b>	[Cu <sub>2</sub> ( <b>20</b> ) <sub>2</sub> (OAc)] <sup>3+</sup>	4.44	40.4	bidentate + tridentate	107
Ru(II)	<b>7</b>	[Ru <sub>2</sub> ( <b>7</b> ) <sub>2</sub> (C <sub>2</sub> O <sub>4</sub> )] <sup>2+</sup>	4.611	65.8–66.4	bidentate + tridentate	155
Sexipyridines						
Cu(II)	<b>90</b>	[Cu <sub>2</sub> ( <b>90</b> ) <sub>2</sub> ] <sup>4+</sup>	4.89	62.8–66.9	tridentate + tridentate	108
Cd(II)	<b>33</b>	[Cd <sub>2</sub> ( <b>33</b> ) <sub>2</sub> ] <sup>4+</sup>	4.173	57.3	tridentate + tridentate	80
Septipyridine						
Co(II)	<b>111</b>	[Co <sub>2</sub> ( <b>111</b> ) <sub>2</sub> ] <sup>4+</sup>	4.606	40.2	tridentate + tridentate	152
Zn(II)	<b>112</b>	[Zn <sub>2</sub> ( <b>112</b> ) <sub>2</sub> ] <sup>4+</sup>	4.333	47.4	tridentate + tridentate	153

( $\Delta E_{1/2} = 0.86$  V) where the intermetallic distance is shorter (Cu...Cu = 2.631 Å).<sup>97</sup> Upon reduction of [Cu(**52**)(OH<sub>2</sub>)]<sup>2+</sup>, the dinuclear double-stranded helicate [Cu<sub>2</sub>(**52**)<sub>2</sub>]<sup>2+</sup> is rapidly restored.<sup>105</sup> However, the intrinsic information coded in the quaterpyridines **39** and **53** is sufficient to produce similar self-assembled dinuclear double-stranded helicates [Cu<sub>2</sub>(**39**)<sub>2</sub>]<sup>2+</sup><sup>106</sup> and [Cu<sub>2</sub>(**53**)<sub>2</sub>]<sup>2+</sup><sup>107</sup> pointing to the fact that sterically demanding substituents are not essential to induce helication. The crystal structures show that the Cu...Cu contact distances are shorter (3.17–3.32 Å, Table 5) and the interplanar angles between the bipyridine subunits are reduced (35.2–40.2° for [Cu<sub>2</sub>(**39**)<sub>2</sub>]<sup>2+</sup>, 55.4–62.7° for [Cu<sub>2</sub>(**53**)<sub>2</sub>]<sup>2+</sup>).<sup>106,107</sup> The role of the methyl substituents in **52** is now clear: their primary function is not to preorganize the ligand, but to control (i) the helical wrapping via steric interactions providing a longer pitch in [Cu<sub>2</sub>(**52**)<sub>2</sub>]<sup>2+</sup> and (ii) the redox behavior since the analogous complexes [Cu<sub>2</sub>(**39**)<sub>2</sub>]<sup>2+</sup> and [Cu<sub>2</sub>(**53**)<sub>2</sub>]<sup>2+</sup> display only irreversible oxidation processes and show no evidence for the formation of stable mixed-valence Cu<sup>II</sup>Cu<sup>I</sup> compounds in solution.<sup>106,107</sup> The larger cation Ag(I) gives the analogous helicate [Ag<sub>2</sub>(**39**)<sub>2</sub>]<sup>2+</sup> with an Ag...Ag distance of 3.107 Å, actually shorter than the Cu...Cu distance which suggests that the intermetallic separation depends on a set of subtle structural features such as metal–nitrogen bond lengths, successive interplanar angles and intra- and interstrand interactions. As a consequence of the helical wrapping of the quaterpyridine ligands in the helicates,  $\pi$ -stacking interactions between the pyridine rings of the different strands are systematically observed in the solid state. The charge and the charge-to-radius ratio seem to be as important as ligand-field effects in quaterpyridine helical complexes since stereochemically demanding d<sup>8</sup> (Ni(II), Pd(II), Pt(II)) and spherical d<sup>10</sup> (Zn(II), Cd(II), and Pb(II) ions) produce only mononuclear complexes

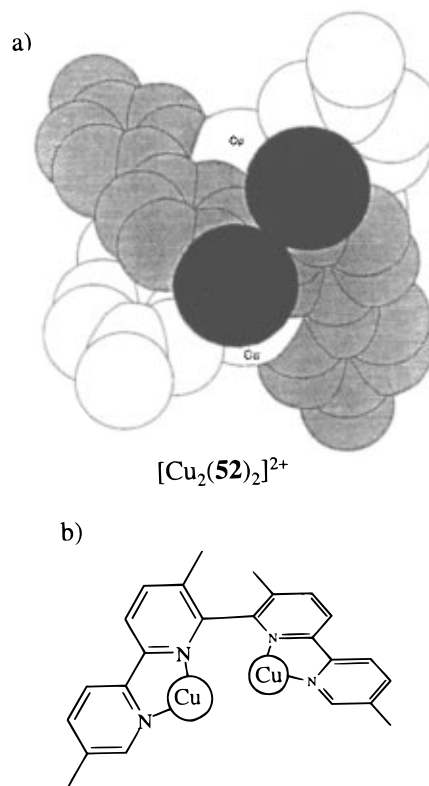


**Figure 22.** (a) Representation of the crystal structure of the double-stranded helicate [Cu<sub>2</sub>(**52**)<sub>2</sub>]<sup>2+</sup>,<sup>104</sup> with the methyl groups (3', 5') showing steric interactions in black<sup>29</sup> and (b) structural formula for a single quaterpyridine unit. (Part a: reproduced with permission from ref 32. Copyright 1994 John Wiley & Sons Inc.)

[M(**39**)]<sup>2+</sup> where the strand **39** acts as a tetradentate donor occupying the four equatorial positions around the metal ion, while Cu(I) and Ag(I) lead to dinuclear double-stranded helicates.<sup>106</sup>

The next even oligopyridines (sexipyridines) **33**<sup>80</sup> and **54**<sup>108</sup> are expected to act as tris-bidentate seg-

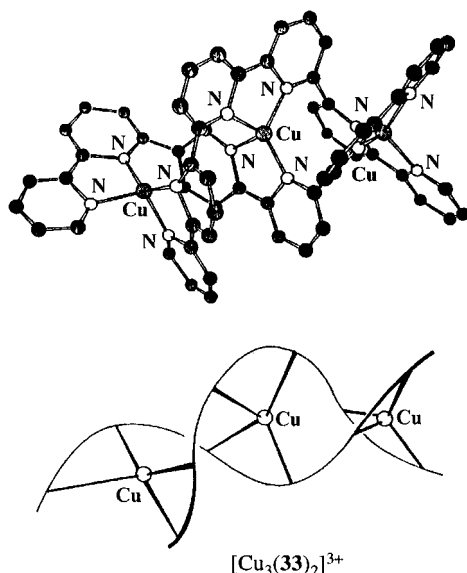


**Figure 23.** Proposed  $D_2$ -symmetrical helical structures for the trinuclear double-stranded helicate  $[\text{Cu}_3(\mathbf{33})_2]^{3+}$  in solution.<sup>82</sup> (Reproduced with permission from ref 82. Copyright 1991 Royal Society of Chemistry.)

mental ligands with four-coordinate metal ions. The isolations of the trinuclear complexes  $[\text{Cu}_3(\mathbf{33})_2]^{3+}$  by Constable and co-workers<sup>80</sup> and of  $[\text{Cu}_3(\mathbf{54})_2]^{3+}$  by Potts and co-workers<sup>108</sup> confirm this statement even though no crystal structure has been reported and the characterization of the double-stranded helicates results from FAB-MS spectra and  $^1\text{H}$  NMR data ( $D_2$ -symmetrical in solution, Figure 23).<sup>80,108</sup> Oxidation of the trinuclear helicate  $[\text{Cu}_3(\mathbf{L})_2]^{3+}$  ( $\mathbf{L} = \mathbf{33}, \mathbf{54}$ ) shows complicated electrochemical processes eventually leading to the formation of the double-stranded Cu(II) helicate  $[\text{Cu}_2(\mathbf{L})_2]^{4+}$  and the expulsion of one solvated Cu(I) ion.

In order to remove any ambiguities concerning the binding mode of the ligands, suitable spacers have been introduced between the coordinating units which allow (i) the helical wrapping of the strands, (ii) the efficient coordination of the metal ions, and (iii) the selective formation of polynuclear complexes.<sup>1,29,32</sup> A famous spacer is the oxopropylene unit  $\text{CH}_2\text{-O-CH}_2$  which has been used by Lehn and co-workers to connect the 6 positions of substituted 2,2'-bipyridine units leading to the segmental  $C_2$ -symmetrical oligobipyridine ligands **4**, **11**, and **55–64**.<sup>1,50,109,110</sup> The complete series of the unsubstituted oligobipyridine strands **4**, **55**, **61**, and **63** self-assembles with Cu(I) in acetonitrile–chloroform (1:1) to generate the di- to pentanuclear double-stranded helicates  $[\text{Cu}_2(\mathbf{55})_2]^{2+}$ ,  $[\text{Cu}_3(\mathbf{4})_2]^{3+}$ ,  $[\text{Cu}_4(\mathbf{61})_2]^{4+}$ , and  $[\text{Cu}_5(\mathbf{63})_2]^{5+}$  (Figure 24). Figure 1 shows the crystal structure of the trinuclear double-stranded helicate  $[\text{Cu}_3(\mathbf{4})_2]^{3+}$  which displays a helical structure with a pitch of  $\sim 12$  Å and a radius of  $\sim 6$  Å for the circumscribed cylinder; each Cu(I) being pseudo-tetrahedrally coordinated by two bipyridine binding units.<sup>1</sup> As found for oligopyridines **39**, **52**, and **53**, the helical wrapping of the strand produces intramolecular interstrand stacking interactions between the aromatic pyridine units of the segmental ligands. Thermodynamic studies of the formation of the analogous soluble helicate  $[\text{Cu}_3(\mathbf{58})_2]^{3+}$  in dichloromethane–acetonitrile (1:1) using spectrophotomet-

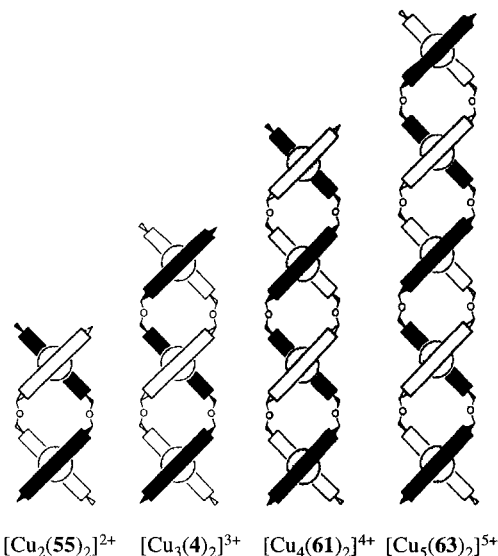
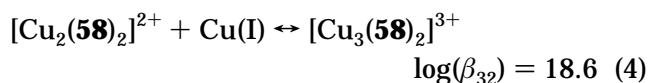
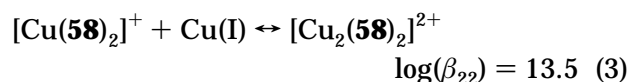
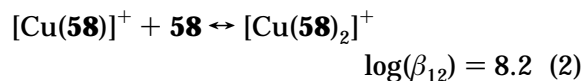
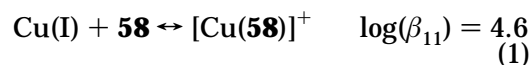


**Figure 24.** Schematic representation of di- to pentanuclear double-stranded helicates with unsubstituted oligobipyridines.<sup>1,50</sup>

ric titrations involve the following four equilibria eqs 1–4:



Scatchard and Hill plots clearly indicate positive cooperativity for the overall process which means that the formation of the precursor complex favors the fixation of the following metal ions leading to completion of the helicate formation (Figure 58).<sup>47</sup> Similar results have been obtained with the analogous silver(I) helicate  $[\text{Ag}_3(\mathbf{4})_2]^{3+}$  whose crystal structure confirms the double-stranded arrangement of the strands.<sup>111</sup> Potentiometric and spectrophotometric studies<sup>46</sup> also imply a homotropic cooperative process for the formation of the trinuclear helicate, but a careful examination of the data suggest that the cooperativity is more pronounced for helicates derived from the less hindered strand **4** compared to **58**. Intramolecular interstrand  $\pi$ -stacking of the pyridine bases is thought to induce a favorable conformation for progressive metal coordination which might explain the observed cooperativity.<sup>46</sup>

These helicates are systematically formed in solution as racemic mixtures of helical *P* and *M* enantiomers, but the synthesis of the enantiomerically pure oligobipyridine (*S,S*)-**11** offers new perspectives for the separation of helical conformers since self-assembly with Cu(I) should generate two  $D_2$ -symmetrical homotopic helical diastereomers with opposite helicity [*(P,P,P)*- $\text{Cu}_3(\text{S,S})\text{-11}$ ]<sub>2</sub><sup>3+</sup> and [*(M,M,M)*- $\text{Cu}_3(\text{S,S})\text{-11}$ ]<sub>2</sub><sup>3+</sup>. The  $^1\text{H}$  NMR data and a large Cotton effect in the CD spectrum point to the

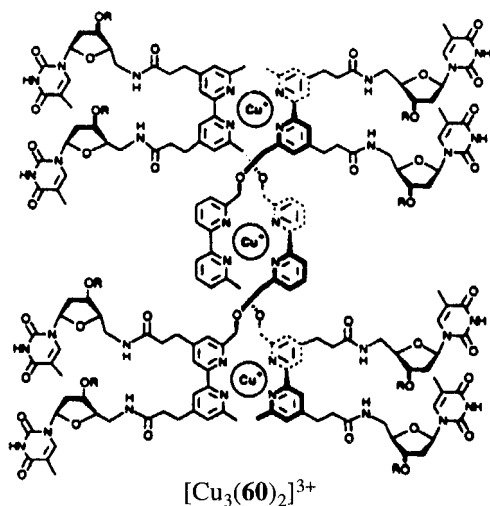


**Figure 25.** Schematic representation of the trinuclear deoxyribonucleohelicate  $[\text{Cu}_3(\mathbf{60})_2]^{3+}$ .<sup>110</sup> (Reproduced with permission from ref 110. Copyright 1990 Macmillan Magazines Limited.)

preferential formation of a single diastereomer resulting from a high degree of helical induction (>95%) from the chiral carbon atoms.<sup>50</sup> Molecular mechanics calculations suggest that the steric crowding induced by the methyl groups ( $\text{R}^3 = \text{Me}$ ) favors a right-handed screw sense at the Cu(I) center leading to the quantitative formation of the right-handed helicate  $[(P,P,P)\text{-Cu}_3((S,S)\text{-}\mathbf{11})_2]^{3+}$ . Alternatively, Siegel and co-workers have connected two oligobipyridine strands to enantiomerically pure dipoles leading to the chiral elongated strands (*R*)-**65** and (*R*)-**66**.<sup>112</sup> Upon reaction with Cu(I), the expected trinuclear double-stranded helicates  $[\text{Cu}_3(\mathbf{L})]^{3+}$  ( $\mathbf{L} = (\text{R})\text{-}\mathbf{65}, (\text{R})\text{-}\mathbf{66}$ ) are quantitatively formed. <sup>1</sup>H-NMR spectra indicate that the helicate formation is diastereoselective and CD spectra suggest that the right-handed helices  $[(P,P,P)\text{-Cu}_3(\mathbf{L})]^{3+}$  ( $\mathbf{L} = (\text{R})\text{-}\mathbf{65}, (\text{R})\text{-}\mathbf{66}$ ) are the only products of the self-assembly. Although these two helicates are strictly speaking heterotopic (no  $C_2$  or  $\sigma$  symmetry of the ligand perpendicular to the helical axis) and correspond to head-to-head isomers, we have

discussed them in this part of the review because (i) no head-to-tail isomers are possible with podand-type ligand and (ii) the induction of chirality in these complexes is closely related to that described by Lehn for the homotopic helicates  $[(P,P,P)\text{-Cu}_3((S,S)\text{-}\mathbf{11})_2]^{3+}$ .

Another interesting feature of Lehn's helicates is their organization framework which allows the arrangement in space in a double-helical fashion of substituents attached to the bipyridine units. The connection of nucleosides is particularly attractive and the alternated thymidine-substituted strands **60** react with Cu(I) to give the expected double-stranded helicate  $[\text{Cu}_3(\mathbf{60})_2]^{3+}$ ; an inside-out analogue of double-stranded nucleic acids which is termed deoxyribonucleohelicate.<sup>110</sup> Because these species are positively charged and present the hydrogen-binding bases on the periphery, they bind to nucleic acids with formation of mixed natural-artificial adducts (Figure 25).<sup>113</sup> Recently, long lipophilic organic chains have been connected to the 6 positions of the bipyridine units in **67** leading to block copolymers containing helically wrapped oligobipyridine units in  $[\text{Cu}_2(\mathbf{67})_2]^{2+}$ .<sup>114</sup>

In addition to high efficiency, selectivity, and cooperativity, helicate formation has been reported to exhibit self-recognition.<sup>115</sup> A mixture of di- to pentabipyridine strands **56**, **57**, **62**, and **64** reacts with Cu(I) to produce exclusively and selectively the double-stranded helicates  $[\text{Cu}_2(\mathbf{56})_2]^{2+}$ ,  $[\text{Cu}_3(\mathbf{57})_2]^{3+}$ ,  $[\text{Cu}_4(\mathbf{62})_2]^{4+}$ , and  $[\text{Cu}_5(\mathbf{64})_2]^{5+}$  with no trace of mixed species according to <sup>1</sup>H NMR data (Figure 26).<sup>115</sup> Such self-recognition processes involve a judicious structural information combined with suitable thermodynamic factors (see section II). The oligobipyridine ligands **56**, **57**, **62**, and **64** are structurally adapted to generate double-stranded helicates with tetrahedral Cu(I) (the intrinsic informations) and the energy-related principle of "maximal site occupancy" and the entropy factors prevent the formation of intricate mixtures of polymers or mixed helicates (the thermodynamic factors).<sup>6</sup>

However, the self-assembly of double-stranded helicates with oligobipyridine strands is not limited

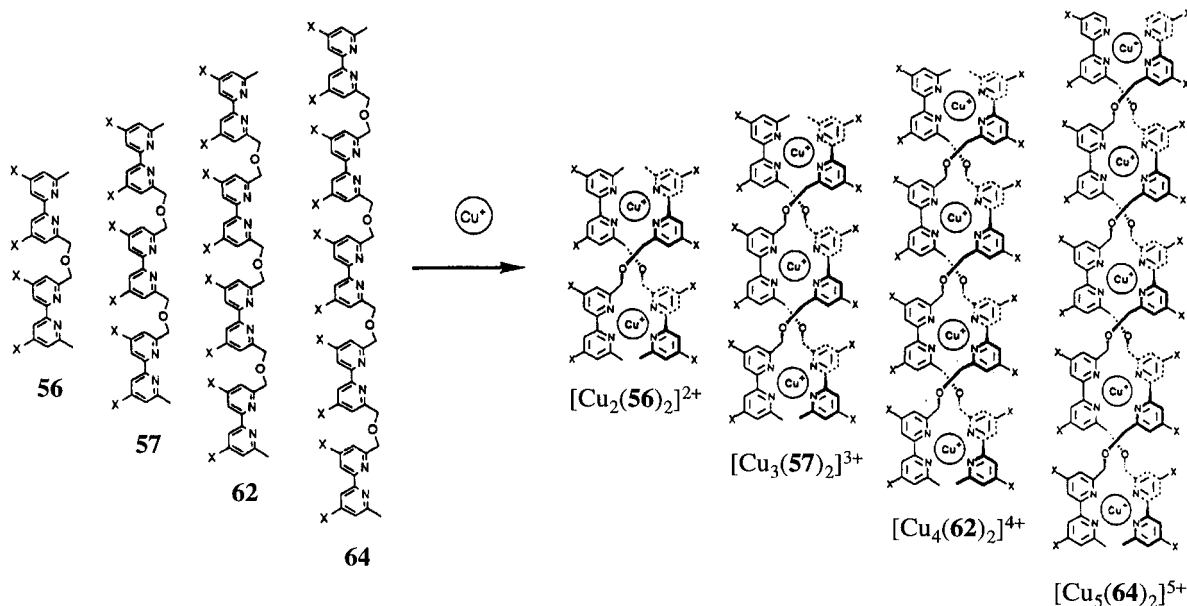
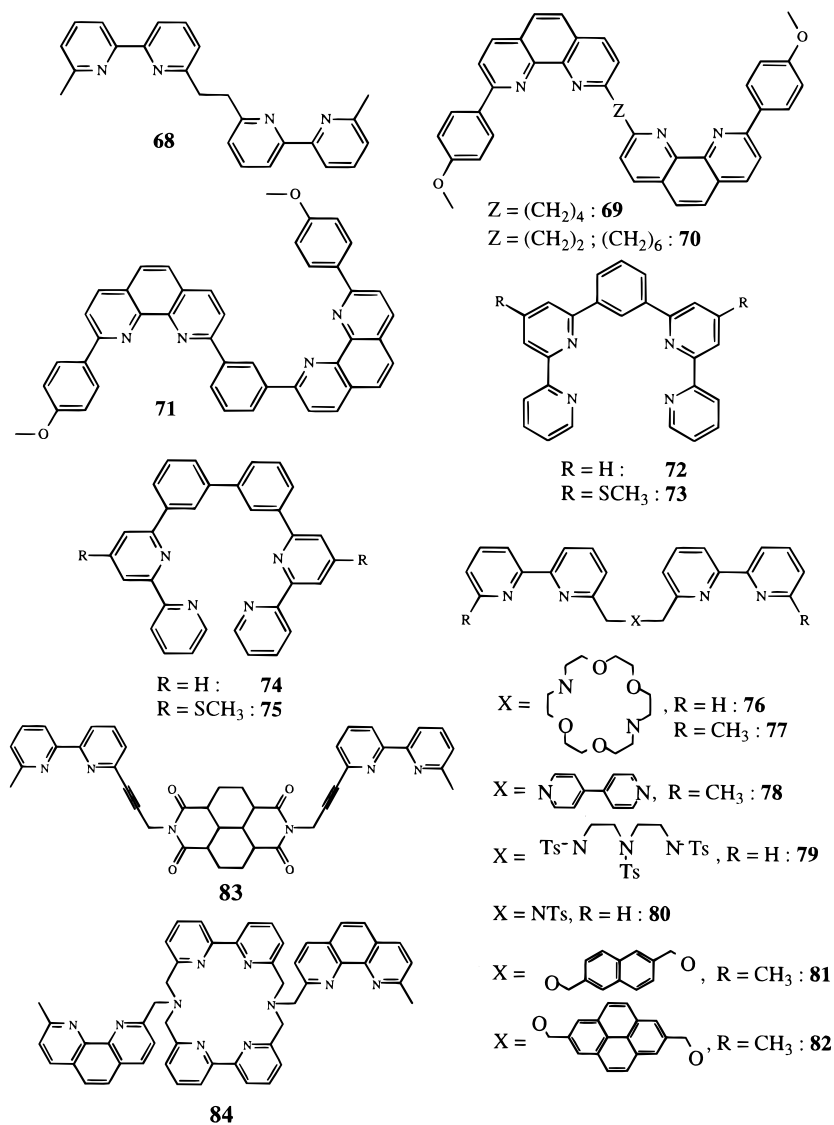


**Figure 26.** Self-recognition in the self-assembly of double-stranded helicates from a mixture of oligobipyridine strands.<sup>115</sup> (Reproduced with permission from ref 115. Copyright 1993 National Academy of Sciences USA.)

## Chart 10



to oxopropylene bridges and several other suitable spacers have been used to connect 2,2'-bipyridine or 1,10-phenanthroline units. The ethane-bridged bis-bidentate ligands **34**<sup>66,67</sup> and **68**<sup>66</sup> (Chart 10) are analogous to **55** and similarly spontaneously generate self-assembled dinuclear double-stranded  $D_2$ -symmetrical helicates  $[\text{Cu}_2(\text{L})_2]^{2+}$  ( $\text{L} = \mathbf{34}, \mathbf{68}$ ) whose crystal structures are almost superimposable except for a small increase in the intermetallic distance for  $[\text{Cu}_2(\mathbf{68})_2]^{2+}$  (Table 6). Surprisingly, the analogous ligand **70** ( $Z = (\text{CH}_2)_2$ ) and its elongated analogues ( $Z = (\text{CH}_2)_4$  and  $(\text{CH}_2)_6$ ) synthesized by Dietrich-Buchecker, Sauvage, and co-workers reacts with Cu(I) in acetonitrile to give equilibrated mixtures of  $D_2$ -helical and  $C_{2h}$ -side-by-side dinuclear double-stranded helicates (Figure 27).<sup>116</sup> For **69**, the respective proportion of helical vs side-by-side helicates is about 1:8 as estimated from <sup>1</sup>H NMR data which strongly limits the synthetic yield of the trefoil knot derived from the helical precursor.<sup>12,116</sup> The more rigid benzene-1,3-diyl spacer in **71** appears to be more suitable since quantitative formation of the  $D_2$ -helical complex  $[\text{Cu}_2(\mathbf{71})_2]^{2+}$  is observed in solution.<sup>117</sup> Compared to the ethane bridged ligand **34**, the benzene-1,3-diyl spacer in **71** produces a more compact double-helical edifice with a  $\text{Cu}\cdots\text{Cu}$  distance of only 4.76 Å

**Table 6. Intermetallic Distances ( $d$ ) in the Crystal Structures of Dinuclear Double-Stranded Helicates with Segmental Ligands**

metal	ligand	helicate	$d$ , Å	ref
Ni(II)	<b>81</b>	$[\text{Ni}_2(\mathbf{81})_2]^{4+}$	12.02	139
Cu(I)	<b>68</b>	$[\text{Cu}_2(\mathbf{68})_2]^{2+}$	5.926	66
Cu(I)	<b>34</b>	$[\text{Cu}_2(\mathbf{34})_2]^{2+}$	5.729	67
Cu(I)	<b>71</b>	$[\text{Cu}_2(\mathbf{71})_2]^{2+}$	4.76	117
Cu(I)	<b>75</b>	$[\text{Cu}_2(\mathbf{75})_2]^{2+}$	6.26	120
Cu(I)	<b>84</b>	$[\text{Cu}_4(\mathbf{84})_2]^{4+}$	13.372	125
Zn(II)	<b>32</b>	$[\text{Zn}_2(\mathbf{32})_2]$	3.37	58
Zn(II)	<b>82</b>	$[\text{Zn}_2(\mathbf{82})_2]^{4+}$	14.42	139
Ag(I)	$(S,S)$ - <b>86</b>	$[\text{Ag}_2((R,R)\text{-}\mathbf{86})_2]^{2+}$	6.072	131
Ag(I)	$(R,S)$ - <b>10</b>	$[\text{Ag}_2((R,S)\text{-}\mathbf{10})_2]^{2+}$	3.254	52
Ag(I)	<b>110</b>	$[\text{Ag}_2(\mathbf{110})_2]^{2+}$	3.14	151
Ni(II)	<b>73</b>	$[\text{Ni}_2(\mathbf{73})_2(\text{OAc})_2]^{2+}$	5.875	119
Ni(II)	<b>75</b>	$[\text{Ni}_2(\mathbf{75})_2(\text{OAc})_2]^{2+}$	7.7	120
Cu(II)	<b>4 + 6</b>	$[\text{Cu}_3(\mathbf{4})(\mathbf{6})]^{6+}$	7.3	30

(Table 6). Photophysical and <sup>1</sup>H NMR data suggest that protonation of the free ligand **71** give the dimeric species  $[\text{H}_2(\mathbf{71})_2]^{2+}$  which possesses a similar double-stranded structure where two protons replace the Cu(I).<sup>118</sup>

A related structural motif has been introduced by Constable and co-workers between two bipyridine units in ligands **72** and **73** which give the expected self-assembled double-stranded helicates  $[\text{Cu}_2(\text{L})_2]^{2+}$

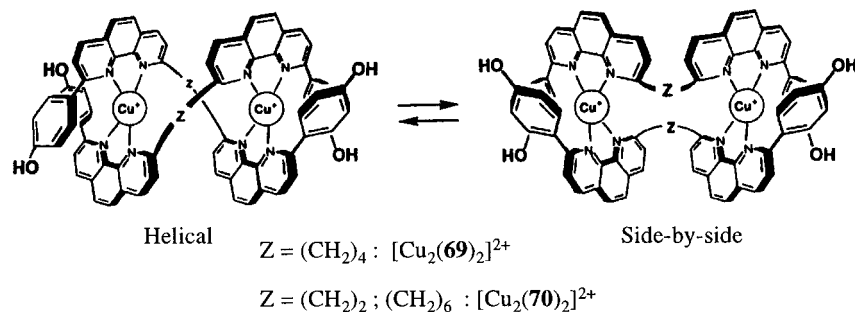


**Figure 27.** The acyclic double-stranded precursor helicates of trefoil knots: left, the  $D_2$ -helical conformer; right, the  $C_{2h}$ -side-by-side conformer.<sup>116</sup> (Reproduced with permission from ref 116. Copyright 1992 Gauthier-Villars Publishers.)

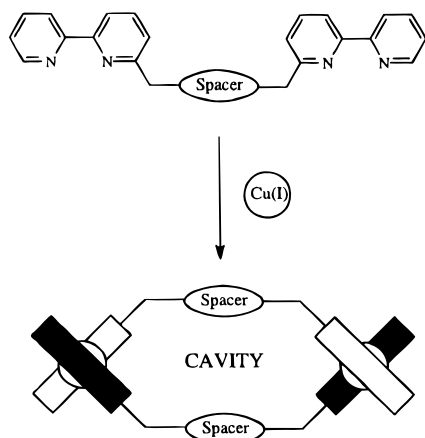


**Figure 28.** Principle of self-assembled double-stranded helicites possessing an internal macrocyclic host cavity.

and  $[\text{Ag}_2(\mathbf{L})_2]^{2+}$  ( $\mathbf{L} = \mathbf{72}, \mathbf{73}$ ).<sup>119</sup> The addition of a supplementary aromatic benzene ring between the bipyridine binding units in  $\mathbf{74}$  and  $\mathbf{75}$  is still compatible with the formation of the double-stranded helicites  $[\text{Cu}_2(\mathbf{L})_2]^{2+}$  ( $\mathbf{L} = \mathbf{74}, \mathbf{75}$ ) and the crystal structure of  $[\text{Cu}_2(\mathbf{75})_2]^{2+}$  reveals a rather large intermetallic distance (6.26 Å) associated with the biphenyl-3,3'-diyl spacer.<sup>120</sup> It is worth noting that the substitution of the biphenyl spacer is crucial for the generation of dinuclear double-stranded helicites since the biphenyl-2,2'-diyl spacer produces only a mononuclear complex with Cu(I).<sup>121</sup> A related spacer is found in the quinquepyridine  $\mathbf{29}$  where the central pyridine ring is essentially noncoordinated to the metal ions in the homotopic double-stranded helicate  $[\text{Ag}_2(\mathbf{29})_2]^{2+}$  (Ag–N distances: 2.726, 2.755 Å). Each Ag(I) is pseudotetrahedrally coordinated by two terminal bipyridine subunits.<sup>77</sup> This symmetrical bis-bidentate binding mode is unusual for quinquepyridine ligands, but it has been also observed in the single-stranded helicate  $[\text{Re}_2(\mathbf{7})_2(\text{CO})_6(\text{py})_2]^{2+}$  (Table 5).<sup>76</sup>

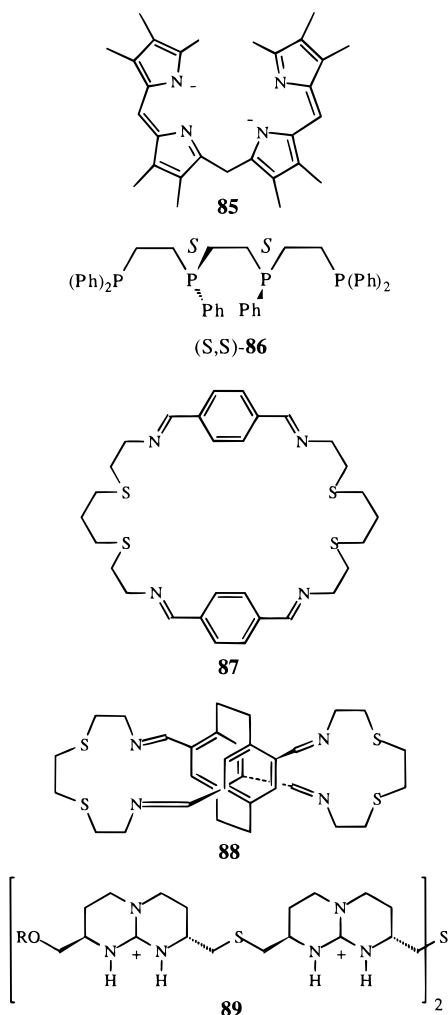
Large spacers may be used to generate internal macrocyclic metal-containing cavities between the coordinated byridine units suitable for host–guest interactions (Figure 28). Ligand strands  $\mathbf{76}$ – $\mathbf{80}$  have been designed for this purpose and dinuclear complexes of the general formula  $[\text{Cu}_2(\mathbf{L})_2](\text{PF}_6)_2$  ( $\mathbf{L} = \mathbf{76}$ – $\mathbf{80}$ ) have been isolated in the solid state.<sup>122</sup> However,  $^1\text{H}$  NMR spectra systematically show the existence of intricate mixtures of  $[\text{Cu}(\mathbf{L})]^+$ ,  $C_{2h}$ -side-by-side and  $D_2$ -helical dinuclear  $[\text{Cu}_2(\mathbf{L})_2]^{2+}$  complexes in solution. A related behavior is found for  $\mathbf{81}$  and  $\mathbf{82}$  which form only dinuclear complexes  $[\text{Cu}_2(\mathbf{L})_2]^{2+}$  in solution, but as 1:1 mixtures of side-by-side and helical conformers.<sup>123</sup> The selective self-as-

sembly of the  $D_2$ -helical double-stranded helicate  $[\text{Zn}_2(\mathbf{83})_2]^{2+}$  as a single conformer may be induced by the simultaneous complexation of a suitable guest in the internal cavity.<sup>124</sup>  $^1\text{H}$  NMR data clearly demonstrate that *o*- and *m*-dimethoxybenzene are bound in the cavity of  $[\text{Zn}_2(\mathbf{83})_2]^{2+}$  while *p*-dimethoxybenzene displays a weaker affinity. The ligand  $\mathbf{84}$  possesses a macrocyclic spacer which is able to coordinate metal ions, and reaction with Cu(I) gives a tetranuclear complex  $[\text{Cu}_4(\mathbf{84})_4]^{4+}$  where the two strands adopt the expected double-stranded arrangement with one terminal phenanthroline unit of each ligand coordinated to a pseudotetrahedral Cu(I) and leading to the double-helical feature. Two supplementary Cu(I) are coordinated within the macrocyclic spacers.<sup>125</sup> As a result of the considerable length of the spacer, the intramolecular distance between the Cu(I) ions located on the helical axis amounts to 13.772 Å and severe distortions of the coordination sites lead to a complete quenching of the MLCT luminescence usually observed for less constrained helicites  $[\text{Cu}_2(\mathbf{34})_2]^{2+}$  and  $[\text{Cu}_2(\mathbf{68})_2]^{2+}$ .<sup>126</sup>

Although less common than 2,2'-bipyridine or 1,10-phenanthroline binding units, a few other bidentate aromatic nitrogen donor units have been introduced into segmental ligands for the self-assembly of double-stranded helicites with four coordinate metal ions. Early evidence for the formation of double-helical features arose from the detailed studies of metal-templated cyclization of corrinoid and porphyrinoid macrocycles.<sup>127</sup> The lack of ring closure for the Zn(II) complexes of biliverdinate  $\mathbf{32}$  and decamethylbiladiene  $\mathbf{85}$  (Chart 11) led Furhop and co-workers<sup>58</sup> and Sheldrick and co-workers<sup>128</sup> to investigate these complexes. Unexpectedly at that time, the crystal structures revealed the formation of dinuclear double-stranded helicites  $[\text{Zn}_2(\mathbf{32})_2]$  and  $[\text{Zn}_2(\mathbf{85})_2]$  where the tetradentate ligands adopt a bis-bidentate binding mode with two aromatic units separated by a methylene spacer (Figure 16). As discussed for quaterpyridine  $\mathbf{39}$ ,  $\mathbf{52}$ , and  $\mathbf{53}$ , the wrapping of the strands results from a helical twist between the two coordinated bidentate binding units. The methylene spacer used in ligand  $\mathbf{5}$  to connect the two bidentate pyridine–benzimidazole units is reminiscent of this pioneer work and the planned self-assembly of the double-stranded helicate  $[\text{Cu}_2(\mathbf{5})_2]^{2+}$  demonstrates the wide scope of helicate self-assembly (Figure 4a).<sup>29</sup>

Alkali metal ions also interact with aromatic nitrogen donor atoms incorporated into sterically constrained and preorganized ligands. The large cation  $\text{K}^+$  matches the cavity of the ligand  $\mathbf{18}$  and

## Chart 11



forms a mononuclear complex,<sup>129</sup> but the smaller cation Na<sup>+</sup> induces a significant contraction of the structure to improve metal–ligand interactions and leads to the formation of the complex [Na<sub>2</sub>(**18**)<sub>2</sub>]<sup>2+</sup> in solution, the first example of a dinuclear double-stranded helicate with alkali ions.<sup>130</sup>

Other donor groups are compatible with the formation of double-stranded helicates and the enantiomerically pure phosphorus containing ligand (*S,S*)-**86** reacts with Ag(ClO<sub>4</sub>) in methanol to give 92% of [Ag<sub>2</sub>((*R,R*)-**86**)<sub>2</sub>](PF<sub>6</sub>)<sub>2</sub> after crystallization.<sup>131</sup> The X-ray crystal analysis reveals that only two diastereomers are formed and they coexist in the unit cell: the left-handed *D*<sub>2</sub>-symmetrical helicate [(*M,M*)-Ag<sub>2</sub>((*R,R*)-**86**)<sub>2</sub>]<sup>2+</sup> and the *C*<sub>2</sub>-symmetrical side-by-side cation [(*M,P*)-Ag<sub>2</sub>((*R,R*)-**86**)<sub>2</sub>]<sup>2+</sup> (Figure 29).<sup>131</sup> N<sub>2</sub>S<sub>2</sub> donor sets, suitable for the coordination of pseudotetrahedral Cu(I), have been incorporated into the macrocycles **87** and **88**, and the dinuclear macrocyclic complexes [Cu<sub>2</sub>(**L**)]<sup>2+</sup> (**L** = **87**, **88**) display a helical twist reminiscent of that found in the double-stranded helicates together with intramolecular stacking interactions between the aromatic rings.<sup>132</sup> Finally, a chiral and enantiomerically pure tetra-guanidium receptor **89** has been synthesized for the complexation and transport of oligonucleotides across biological membranes.<sup>26</sup> Detailed ROESY NMR data suggest that the sulfate salt [(**89**)<sub>2</sub>(SO<sub>4</sub>)<sub>4</sub>] is in fact a double-stranded helicate with two polyguanidium strands wrapped about the sulfate anions lying on

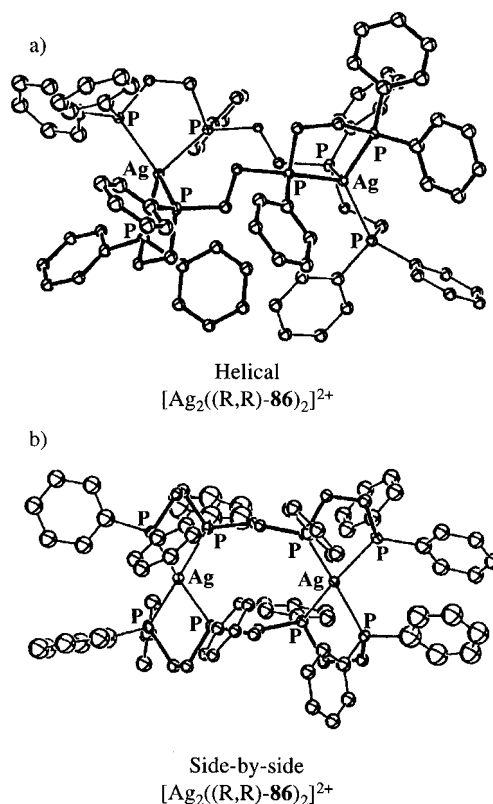


**Figure 29.** ORTEP plots of the double-stranded (a) helical and (b) side-by-side conformers of [Ag<sub>2</sub>((*R,R*)-**86**)<sub>2</sub>]<sup>2+</sup>.<sup>131</sup> (Reproduced with permission from ref 131. Copyright 1995 Royal Society of Chemistry.)

the helical axis in agreement with molecular mechanics calculations.

*c. Five-Coordinate Metal Ions.* Cu(II) is well known to accommodate five-coordination in the complex [Cu(bipy)(terpy)]<sup>2+</sup> and Hasenknopf, Lehn, and co-workers have taken advantage of this particular intrinsic information for the self-assembly of the first homotopic *C*<sub>2</sub>-symmetrical double-heterostranded helicate [Cu<sub>3</sub>(**4**)(**6**)]<sup>6+</sup> where an oligo-bidentate (**4**) and an oligo-tridentate ligand (**6**) are wrapped around the helical axis (Figure 4b).<sup>30</sup> The X-ray crystal structure reveals that each Cu(II) is five-coordinated by one bipyridine and one terpyridine subunits and has a distorted coordination geometry: the central Cu(II) being close to a trigonal bipyramid and the terminal Cu(II) may be best described as distorted square pyramids. The structural characteristics of this heterostranded helicate (pitch ≈ 12 Å, radius ≈ 9 Å, length ≈ 20 Å) are similar to those previously reported for the analogous double-homostranded helicate [Cu<sub>3</sub>(**4**)<sub>2</sub>]<sup>3+</sup>.

*d. Six-Coordinate Metal Ions.* There is a strict structural analogy between entries 3 and 5 of Table 1 and we can replace tetrahedral metal ions by octahedral ions when bidentate binding units are replaced by tridentate units in the ligand strand.<sup>6,29,32</sup> It is thus not surprising that sexipyridine **33**, the next even oligopyridine after **39**, forms a double-stranded dinuclear helicate [Cd<sub>2</sub>(**33**)<sub>2</sub>]<sup>4+</sup> with the large and spherical six-coordinate d<sup>10</sup> Cd(II). As expected, the two ligand strands are essentially separated into two tridentate binding domains and coordinated to two pseudooctahedral six-coordinate Cd(II) lying on the helical axis (Figure 30).<sup>80</sup> As previously discussed for the related helicates with quaterpyridine [Cu<sub>2</sub>(**39**)<sub>2</sub>]<sup>2+</sup>

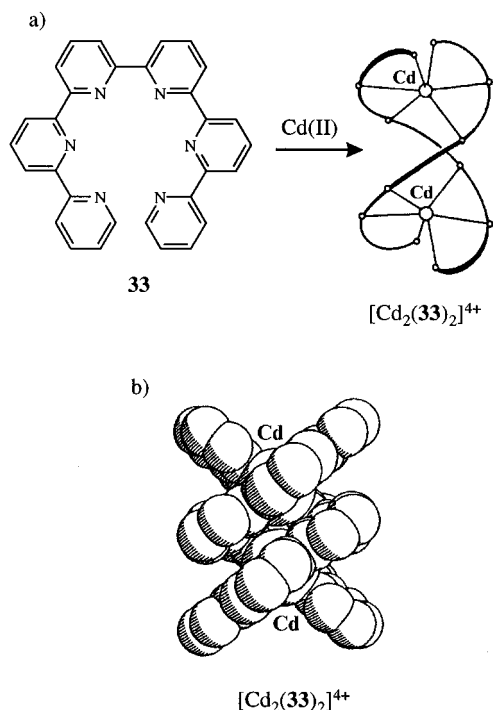


**Figure 30.** (a) Self-assembly of a dinuclear double-stranded helicate obtained from two bis-tridentate ligand strands and (b) space-filling representation of the double-stranded helicate  $[\text{Cd}_2(\mathbf{33})_2]^{4+}$ .<sup>80</sup> (Reproduced with permission from ref 80. Copyright 1990 American Chemical Society.)

and  $[\text{Cu}_2(\mathbf{53})_2]^{2+}$ , the helical twist of the strand in  $[\text{Cd}_2(\mathbf{33})_2]^{4+}$  and in the analogous double-stranded helicate  $[\text{Cu}_2(\mathbf{90})_2]^{4+}$ <sup>108</sup> results from a rotation about the interanular C–C bond connecting the two tridentate coordinated terpyridine subunits which is slightly more pronounced for sexipyridine (57.3–66.9°) than for quaterpyridine (35.2–59.7°, Table 5). The intermetallic distance is also affected and significantly increases when going from  $[\text{Cu}_2(\mathbf{39})_2]^{2+}$  to  $[\text{Cd}_2(\mathbf{33})_2]^{4+}$ , but great similarities are found if we consider (i) the intramolecular interstrand  $\pi$ -stacking interactions between the packed aromatic pyridine rings and (ii) the effect of alkylthio substituents in **90** which slightly increase the helical pitch as found for **53**. Related dinuclear double-stranded helicates have been characterized with other six-coordinate metal ions  $[\text{M}_2(\mathbf{33})_2]^{4+}$  (M = Mn(II), Fe(II), Ni(II), Cu(II))<sup>80–82</sup> and  $[\text{M}_2(\mathbf{90})_2]^{4+}$  (M = Fe(II), Co(II), Ni(II)),<sup>108</sup> and it has been reported that the symmetrical aromatic coupling<sup>133</sup> of 6-bromo-2,2':6',2''-terpyridine with Ni(0)–phosphine complexes readily gives the double-stranded helicate  $[\text{Ni}_2(\mathbf{33})_2]^{4+}$ .<sup>81</sup> The introduction of ferrocenyl groups in the 4, 4''' positions does not affect the complexation properties of the sexipyridine strand leading to similar helicates  $[\text{M}_2(\mathbf{91})_2]^{4+}$  (M = Fe(II), Co(II), Ni(II), Zn(II)).<sup>134</sup> However, the reversibility of the redox process centered on the metal ions coordinated to the terpyridine subunits is affected by the ferrocenyl substituents which are first oxidized into ferricenium by cyclic voltammetry. As mentioned in the previous section, reduction of the double-stranded helicate  $[\text{Cu}_2(\mathbf{90})_2]^{4+}$  is complicated, but eventually gives the trinuclear double-stranded Cu(I) helicate  $[\text{Cu}_3(\mathbf{90})_2]^{3+}$ .<sup>108</sup> This corresponds to an interconversion between two different binding modes of sexipyridine: bis-tridentate

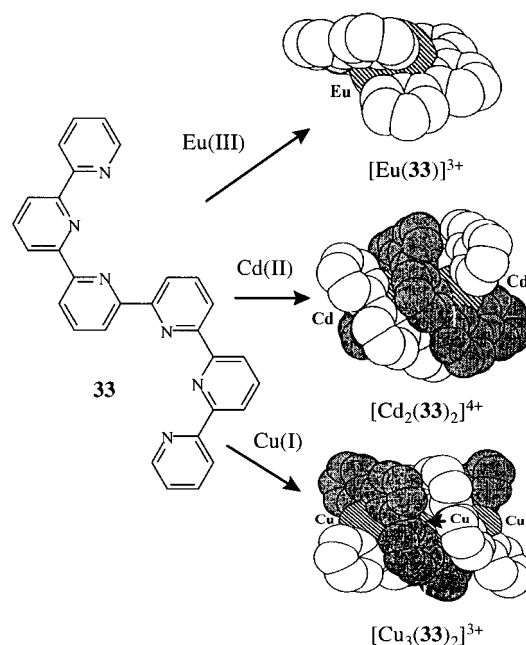
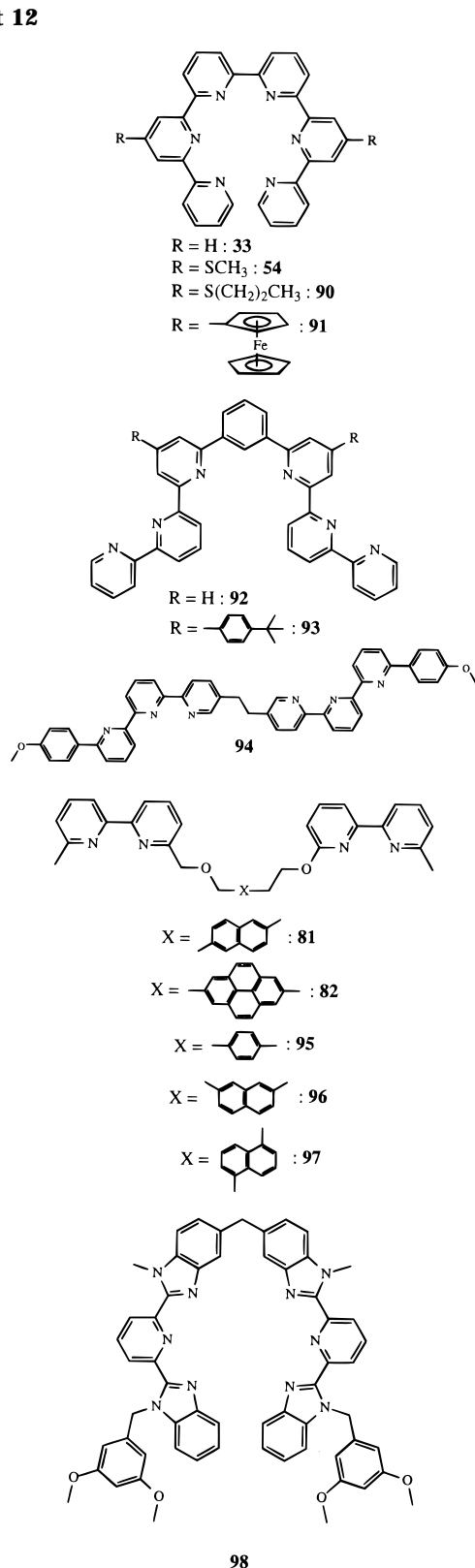


**Figure 31.** The different binding modes of sexipyridine.<sup>134</sup> (Reproduced with permission from ref 134. Copyright 1995 Royal Society of Chemistry.)

versus tris-bidentate which exemplifies the rich and varied chemistry of the oligopyridine ligand strands (Figure 31).

Various spacers have been introduced between the tridentate units. A benzene-1,3-diyl spacer is again suitable and Che and co-workers<sup>135</sup> have synthesized the segmental ligands **92** and **93** (Chart 12). Solution studies based on ES–MS and <sup>1</sup>H NMR data show the selective formation of the dinuclear cations  $[\text{Ag}_2(\mathbf{L})_2]^{2+}$  (L = **92**, **93**) and  $[\text{Cu}_2(\mathbf{L})_2]^{4+}$  (L = **92**, **93**) upon reaction with Ag(I) and Cu(II), respectively. The crystal structures of  $[\text{Cu}_2(\mathbf{L})_2]^{4+}$  (L = **92**, **93**) confirm the formation of double-stranded helicates. Each Cu(II) occupies a distorted octahedral site produced by the terpyridine subunits of each strand. As expected, the reduction of  $[\text{Cu}_2(\mathbf{L})_2]^{4+}$  (L = **92**, **93**) does not give the trinuclear double-stranded helicate as observed for sexipyridine **90** because of the presence of the rigid spacer in **92** and **93** which prevents the strands to act as tris-bidentate ligands. However, it is surprising that each Cu(II) in  $[\text{Cu}_2(\mathbf{L})_2]^{4+}$  (L = **92**, **93**) is successively and reversibly reduced to give the dinuclear complexes  $[\text{Cu}_2(\mathbf{L})_2]^{2+}$  (L = **92**, **93**) when we consider the different stereochemical requirements of Cu(II) and Cu(I). A significant interaction occurs between the metallic centers ( $\Delta E_{1/2} = 190$  mV), but no attempt has been made to unravel the coupling mechanism.<sup>135</sup> Compared to 2,2'-bipyridine units which are generally bound to the spacer by the 6,6' positions, tridentate 2,2':6',2''-terpyridine units require aliphatic spacers attached to the synthetically less accessible<sup>136</sup> 5,5'' positions to allow helication.<sup>137</sup> According to this strategy, Sauvage and Crane have synthesized the segmental ligand **94** which reacts with Fe(II) or Ru(II) to give the double-stranded helicates  $[\text{M}_2(\mathbf{94})_2]^{4+}$ .<sup>137</sup> The similar, but elongated strand **6** prepared by Lehn and co-workers leads to the trinuclear *D*<sub>2</sub>-symmetrical double-stranded helicates  $[\text{Fe}_3(\mathbf{6})_2]^{6+}$  and  $[\text{Ni}_3(\mathbf{6})_2]^{6+}$  based on octahedral metal ions.<sup>138</sup> The kinetic inertness of  $[\text{Fe}_3(\mathbf{6})_2]^{6+}$  allows its chromatographic separation into

## Chart 12



its two helical enantiomers  $[(P,P,P)\text{-Fe}_3(\mathbf{6})_2]^{6+}$  and  $[(M,M,M)\text{-Fe}_3(\mathbf{6})_2]^{6+}$  which are characterized by their inverted CD spectra. The optical activity of the solution is constant over seven weeks at 52 °C pointing to a greater stability of the trinuclear architecture, compared to analogous mononuclear species.<sup>138</sup>

Harding and co-workers have reacted the segmental "bis-bidentate" ligands **81**, **82**, and **95-97** with Zn(II) and Ni(II) and they have realized that each metal ion does not adopt the expected pseudotetra-

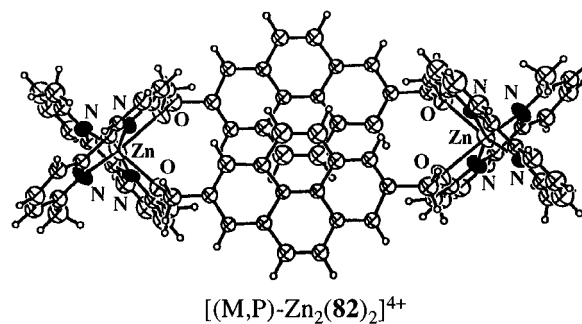


**Figure 32.** ORTEP representation of the side-by-side helicate  $[(M,P)\text{-Zn}_2(\mathbf{82})_2]^{4+}$ .<sup>139</sup> (Reproduced with permission from ref 139. Copyright 1994 Royal Society of Chemistry.)

**Table 7. Relative Amounts of Helical and Side-by-side Dinuclear Double-Stranded Helicates Formed in Solution for Ligand Strands **81**, **82**, and **95** with Cu(I), Zn(II), and Cd(II)**<sup>123,124,139</sup>

ligand	metal	% helical	% side-by-side
<b>81</b>	Cu(I)	50	50
<b>82</b>	Cu(I)	50	50
<b>82</b>	Zn(II)	not detected	> 98
<b>81</b>	Zn(II)	70	30
<b>81</b>	Cd(II)	45	55
<b>95</b>	Zn(II)	57	43

hedral coordination, but the two oxygen atoms of the ether links in  $[\text{Ni}_2(\mathbf{81})_2]^{4+}$  and  $[\text{Zn}_2(\mathbf{82})_2]^{4+}$  interact with the metals leading to distorted pseudo-octahedral coordination sites (Figure 32).<sup>139</sup> The two strands adopt a face-to-face arrangement in the crystal structures leading to opposite absolute configurations for the metal ions corresponding to side-by-side helicates with zero net helicity. Only weak stacking interactions are observed between the parallel aromatic planes of the spacers which are probably not responsible for the exclusive formation of the non-helical conformer. Detailed <sup>1</sup>H NMR studies show that dynamic equilibria occur between *D*<sub>2</sub>-helical and *C*<sub>2*h*</sub>-side-by-side conformers in solution (Table 7), the latter being favored by rigid and constrained spacers incompatible with a helical twisting of the strands in  $[\text{Zn}_2(\mathbf{82})_2]^{4+}$ .

However, an oligo-tridentate ligand strand combined with octahedral metal ions does not systematically give polynuclear double-stranded helicates. For instance, Hopfgartner, Piguet, and co-workers<sup>140</sup> have reported that the bis-tridentate ligand **98**, which possesses two tridentate binding units analogous to terpyridine<sup>141</sup> separated by a 5,5'-diphenylmethane spacer, reacts with octahedral ions M(II) = Fe(II), Co(II), Ni(II) to give the *D*<sub>3</sub>-symmetrical trinuclear toroidal complex  $[\text{M}_3(\mathbf{98})_3]^{6+}$  instead of the expected dinuclear double-stranded helicate  $[\text{M}_2(\mathbf{98})_2]^{6+}$  (Figure 33). CPK space-filling molecular models suggest that the ligand strands are helically wrapped in the torus as found in double-stranded helicates, but steric constraints induced by the 5,5'-diphenylmethane spacer exclude the large interplanar angles between the tridentate units required for the formation of the dinuclear helicate.<sup>140</sup>  $[\text{M}_3(\mathbf{98})_3]^{6+}$  may be viewed as a circular single-stranded helicate by analogy with DNA and circular DNA.

## 2. Saturated Heterotopic Double-Stranded Helicates

As described in section II, a heterotopic double-stranded helicate results when different binding

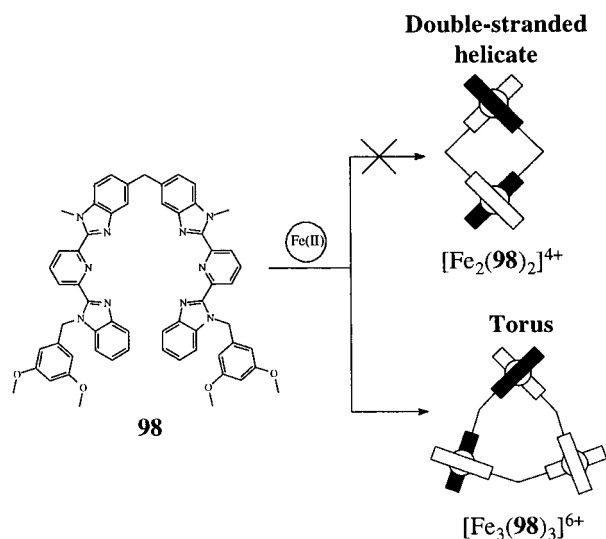


**Figure 33.** Self-assembly of a toroidal complex (= circular helicate) from the bis-tridentate ligand strands **98** and six-coordinate metal ions<sup>140</sup> vs a double-stranded helicate.

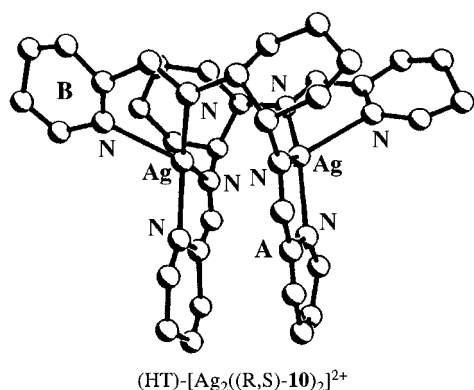


**Figure 34.** PLUTO drawing of the crystal structure of (HT)-[Ag<sub>2</sub>((R,S)-**10**)<sub>2</sub>]<sup>2+</sup>.<sup>52</sup> (Reproduced from ref 52. Copyright 1984 American Chemical Society.)

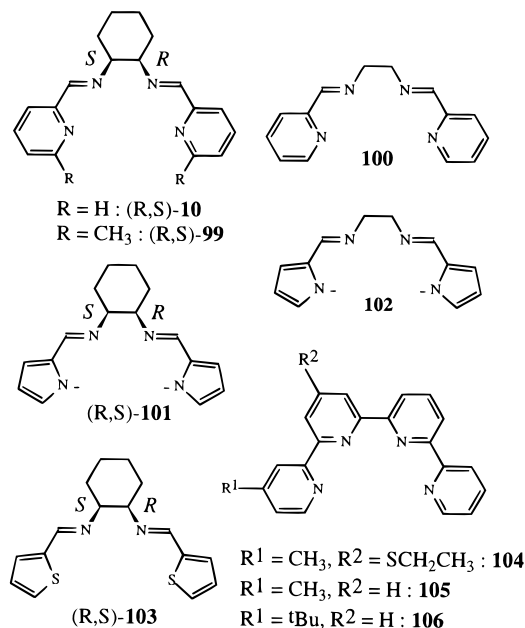
units are coordinated to the metal ions which destroy the  $C_2$  symmetry passing through the ligand and perpendicular to the helical axis expected for homotopic helicates or the  $\sigma$  symmetry for their side-by-side conformers. The enantiomerically pure “meso” bis-bidentate ligand strand (*R,S*)-**10** synthesized by Van Koten and co-workers belongs to this category since the two chiral carbon atoms remove the  $C_2$  symmetry of the ligands which can adopt head-to-head or head-to-tail arrangements in the final helicate.<sup>52</sup> Upon reaction with Ag(I), the dinuclear complex [Ag<sub>2</sub>((*R,S*)-**10**)<sub>2</sub>]<sup>2+</sup> is selectively obtained in solution, but four diastereomeric helicates are expected: two chiral  $C_2$ -helical double-stranded helicates (HH)-[Ag<sub>2</sub>((*R,S*)-**10**)<sub>2</sub>]<sup>2+</sup> and (HT)-[Ag<sub>2</sub>((*R,S*)-**10**)<sub>2</sub>]<sup>2+</sup> existing as pairs of (*M,M*) ↔ (*P,P*) enantiomers and two achiral side-by-side conformers, the  $C_{2h}$ -symmetrical (HH)-[(*M,P*)-Ag<sub>2</sub>((*R,S*)-**10**)<sub>2</sub>]<sup>2+</sup> and the  $C_s$ -symmetrical (HT)-[(*M,P*)-Ag<sub>2</sub>((*R,S*)-**10**)<sub>2</sub>]<sup>2+</sup>. The X-ray crystal structure shows the exclusive formation of the heterotopic helical conformer (HT)-[Ag<sub>2</sub>((*R,S*)-**10**)<sub>2</sub>]<sup>2+</sup> with the pseudo- $C_2$  axis perpendicular to the helical axis (Figure 34).<sup>52,142</sup> Each Ag(I) lies in a distorted tetrahedral site as found for double-stranded homotopic helicates with bis-bidentate ligands, but the two binding units of the same strand in (HT)-[Ag<sub>2</sub>((*R,S*)-**10**)<sub>2</sub>]<sup>2+</sup> are not equivalent (A and B in Figure 34).<sup>52</sup> Detailed <sup>1</sup>H, <sup>13</sup>C, <sup>15</sup>N, and <sup>109</sup>Ag

NMR studies in solution have established that (i) [Ag<sub>2</sub>((*R,S*)-**10**)<sub>2</sub>]<sup>2+</sup> belongs to the point group  $C_2$ , (ii) the two ligand strands are wrapped helically around the metal ions (NOE effects), and (iii) the two Ag(I) are equivalent. These features are only compatible with the retention of the structure found in the solid state: (HT)-[Ag<sub>2</sub>((*R,S*)-**10**)<sub>2</sub>]<sup>2+</sup> is also the only diastereomer formed in solution.<sup>52,142</sup> However, intermolecular metallic exchange processes in solution induce dynamic (*P,P*) ↔ (*M,M*) interconversion between the helical enantiomers.<sup>52</sup> The rate of this exchange strongly depends on (i) the nature of the metal ion (Cu(I) or Ag(I)), (ii) the substituents bound to the 6 position of the pyridine ring (R = H, **10**; R = CH<sub>3</sub>, **99**), and (iii) the nature of the bridging groups since the ethane-1,2-diyl spacer in **100** leads to significantly faster interconversion. As a result of efforts to obtain reliable solution-state structural and dynamic informations, Van Koten and co-workers synthesized an analogous “meso” ligand with pyrrole groups (*R,S*)-**101** which reacts with Zn(II) to give the related neutral head-to-tail double-stranded helicate (HT)-[Zn<sub>2</sub>((*R,S*)-**101**)<sub>2</sub>].<sup>143</sup> The increased strength of the nitrogen–Zn<sup>II</sup> bonds in [Zn<sub>2</sub>((*R,S*)-**101**)<sub>2</sub>] compared with the Ag<sup>I</sup>–N bond in [Ag<sub>2</sub>((*R,S*)-**10**)<sub>2</sub>]<sup>2+</sup> prevents intermolecular exchange and the (*P,P*) ↔ (*M,M*) interconversion is blocked on the NMR time scale for the Zn(II) helicate.<sup>143</sup> However, fast conformational movements are observed with the less rigid ethane-1,2-diyl spacer in [Zn<sub>2</sub>(**102**)<sub>2</sub>].<sup>143</sup> As a result of the weak affinity of thiophene S atom for groups 1b metal ions, the sulfur atom only weakly interacts with Cu(I) or Ag(I), leading to the formation of only six-coordinate mononuclear complexes [M(**103**)<sub>2</sub>]<sup>+</sup> (M = Cu(I), Ag(I)).<sup>144</sup> It must be realized that subtle intra- and interstrand steric and electronic interactions are responsible for the observed high selectivity leading to the formation of a single helicate (HT)-[Ag<sub>2</sub>((*R,S*)-**10**)<sub>2</sub>]<sup>2+</sup> among four possible diastereomers, but minor structural effects are often sufficient to induce significant discrimination between diastereomers since a 95:5 mixture between two conformers requires a difference in free energies of only 7.3 kJ mol<sup>-1</sup>.

Constable and co-workers have introduced various substituents into the basic quaterpyridine motive to design the heterotopic ligands strands **104**–**106**<sup>145,146</sup> (Chart 13). The presence of alkyl groups bound to the 4,4′ positions is expected to induce a discrimination between head-to-head and head-to-tail conformers, but the first <sup>1</sup>H NMR results were disappointing because only mixtures of (HH)- and (HT)-[Cu<sub>2</sub>(**L**)<sub>2</sub>]<sup>2+</sup> (**L** = **104**, **105**) were obtained in solution.<sup>145</sup> The more sterically constrained ligand **106** appears to be more promising since the  $C_2$ -symmetrical double-stranded helicate (HH)-[Cu<sub>2</sub>(**106**)<sub>2</sub>]<sup>2+</sup> is the only complex formed in solution and in the solid state as a result of interstrand repulsion between the bulky *tert*-butyl groups in the head-to-tail conformer.

The pentadentate ligand strand quinquepyridine **7** represents the typical case of a  $C_2$ -symmetrical ligand which can generate heterotopic dinuclear helicates because it adopts an unsymmetrical bidentate-tridentate binding mode. Compound **7** reacts with Pd(II) to give exclusively the head-to-tail double-stranded helicate (HT)-[Pd<sub>2</sub>(**7**)<sub>2</sub>]<sup>4+</sup> where each Pd(II)

Chart 13

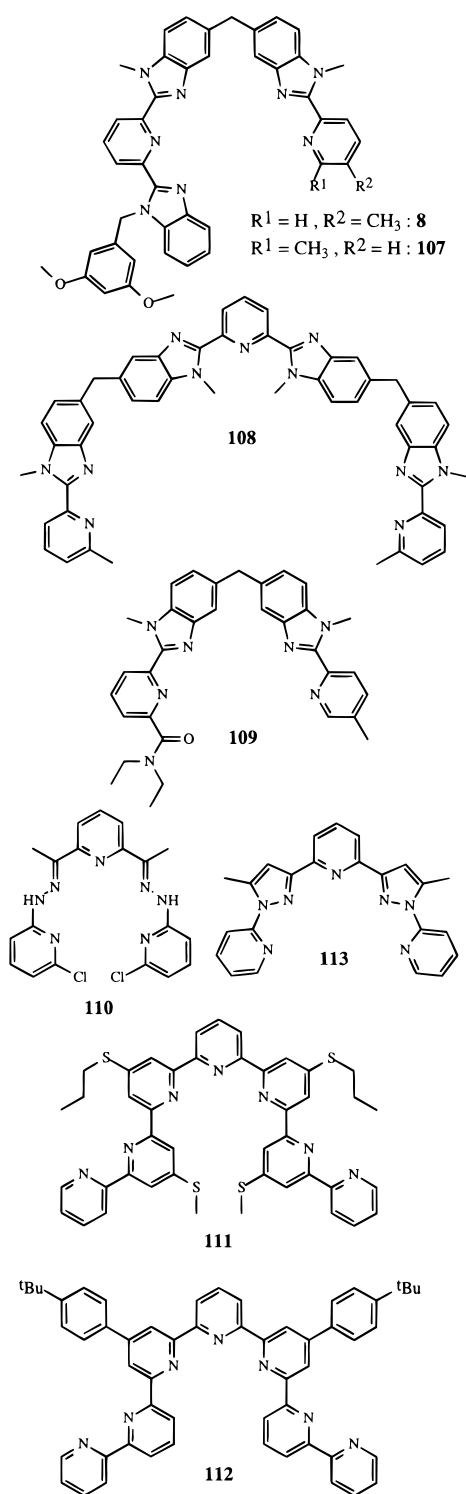


is five-coordinate in a strongly distorted coordination site provided by one terpyridine and one bipyridine subunit of each strand (Figure 5).<sup>33</sup> A very similar binding mode is observed for the analogous  $C_2$ -symmetrical helicate (HT)-[Ag<sub>2</sub>(**23**)<sub>2</sub>]<sup>2+</sup> except for a significantly shorter intermetallic distance (Ag...Ag = 3.48 Å compared to Pd...Pd = 4.96 Å, Table 5) associated with a less severe helical twist between the bound bipyridine and terpyridine subunits probably resulting from the limited stereochemical requirements of Ag(I).<sup>77</sup> <sup>1</sup>H NMR data for [Ag<sub>2</sub>(**23**)<sub>2</sub>]<sup>2+</sup> in acetonitrile indicate an average higher symmetry compatible with a relaxed homotopic dinuclear  $D_2$ -symmetrical double-stranded helicate or a  $C_{2v}$ -symmetrical mononuclear single-stranded helicate which implies that the structure in solution is different from that observed in the crystals.<sup>77</sup>

The head-to-head conformer provides one six-coordinate and one four-coordinate coordination site which may accommodate simultaneously a tetrahedral and an octahedral metal ion. This is indeed the case, and Constable and co-workers<sup>39</sup> and later Potts and co-workers<sup>107</sup> have isolated mixed-valence Cu<sup>II</sup>/Cu<sup>I</sup> double-stranded helicates (HH)-[Cu<sub>2</sub>(**7**)<sub>2</sub>]<sup>3+</sup>,<sup>39</sup> (HH)-[Cu<sub>2</sub>(**20**)<sub>2</sub>]<sup>3+</sup>,<sup>63</sup> and (HH)-[Cu<sub>2</sub>(**21**)<sub>2</sub>]<sup>3+</sup> where each copper ion occupies a coordination site satisfying its stereochemical requirements. Cu(II) lies in a distorted octahedral environment provided by the two terpyridine subunits while Cu(I) is pseudotetrahedrally coordinated by the two remaining bipyridine subunits. Extension of this concept has led to the planned and quantitative syntheses of heterodinuclear head-to-head double-stranded helicates (HH)-[CoAg(**7**)<sub>2</sub>]<sup>3+</sup><sup>34</sup> and (HH)-[NiCu(**20**)<sub>2</sub>]<sup>3+</sup><sup>147</sup> where Cu(II) is replaced with octahedral Co(II) or Ni(II) and Cu(I) with tetrahedral Ag(I) (Figure 5).

The bidentate–tridentate segmental ligand **107** (Chart 14) has been designed by Piguet and co-workers for the planned synthesis of heteronuclear double-stranded helicates.<sup>148</sup> The methyl group bound to the 6 position of the terminal pyridine ring prevents the coordination of the bidentate units to octahedral metal ions, but favors the coordination of

Chart 14



tetrahedral metal ions<sup>29</sup> leading to a segmental ligand possessing one bidentate unit coded for four-coordinate metals and one tridentate unit suitable for six-coordinate metal ions. Reaction of **107** with Fe(II) and Ag(I) generates the self-assembled  $C_2$ -symmetrical heterodinuclear double-stranded helicate (HH)-[FeAg(**107**)<sub>2</sub>]<sup>3+</sup> where Fe(II) is pseudo-octahedrally coordinated by the two tridentate units and Ag(I) lies in the pseudotetrahedral site defined by the remaining bidentate binding units as similarly found for (HH)-[CoAg(**7**)<sub>2</sub>]<sup>3+</sup>.<sup>34</sup> Molecular mechanics suggests that considerable steric constraints result from the helical twist of the ligand strands around the methylene spacers in (HH)-[FeAg(**107**)<sub>2</sub>]<sup>3+</sup>. It is

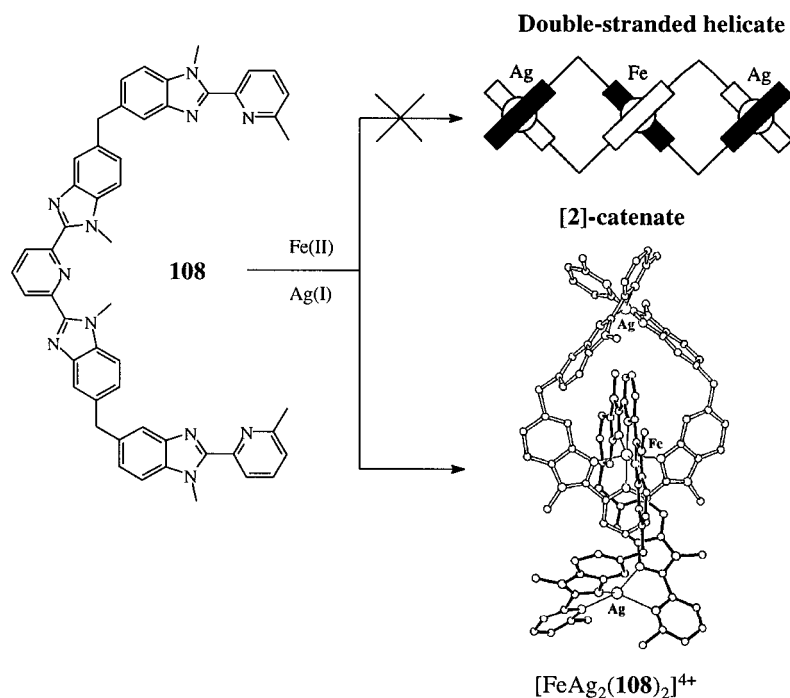


**Figure 35.** Self-assembly of the heterotrimeric metal-containing [2]-catenate  $[\text{FeAg}_2(\mathbf{108})_2]^{4+}$  vs the double-stranded helicate.<sup>149</sup>

thus not surprising that the extended bidentate–tridentate–bidentate ligand strand **108** does not produce the planned sterically demanding heterotrimeric double-stranded helicate upon reaction with Fe(II) and Ag(I), but selectively forms the isomeric helically twisted metal-containing [2]-catenate  $[\text{FeAg}_2(\mathbf{108})_2]^{4+}$  which minimizes steric constraints (Figure 35).<sup>149</sup> This observation, together with the formation of the torus  $[\text{Ni}_3(\mathbf{98})_3]^{6+}$ ,<sup>140</sup> shows that subtle variations of the intrinsic informations encoded in the ligand strands may dramatically affect the final self-assembled supramolecular architectures. This statement is exemplified by the segmental ligands **8** and **107** which react with Zn(II) to give exclusively the head-to-head double-stranded helicates (HH)- $[\text{Zn}_2(\mathbf{L})_2]^{4+}$  ( $\mathbf{L} = \mathbf{8}, \mathbf{107}$ ),<sup>37,44</sup> while the analogous ligand strand **109** possessing a terminal *N,N*-diethylcarbamoyl group selectively produces the head-to-tail double-stranded conformer (HT)- $[\text{Zn}_2(\mathbf{109})_2]^{4+}$ .<sup>150</sup>

Heterotopic double-stranded helicates may also result from ligand strands possessing too many coordinating donor atoms to match the stereochemical requirements of the metal ion in the double-stranded helicate. For instance, the pentadentate ligand **110** reacts with tetrahedral Ag(I) to give a  $D_2$ -symmetrical complex in solution according to NMR data.<sup>151</sup> Crystallization with hexafluorophosphate anions leads to the dinuclear complex  $[\text{Ag}_2(\mathbf{110})_2](\text{PF}_6)_2$  where the cation (HT)- $[\text{Ag}_2(\mathbf{110})_2]^{2+}$  corresponds to a head-to-tail double-stranded helicate with each Ag(I) coordinated by two bidentate nitrogen binding units belonging to different strands; one terminal 6-chloropyridine ring of each strand remains uncoordinated and points away from the binding cavity.<sup>151</sup> This particular binding mode leads to the heterotopic helicate (HT)- $[\text{Ag}_2(\mathbf{110})_2]^{2+}$  which is closely related to the homotopic double-stranded helicate  $[\text{Ag}_2(\mathbf{29})_2]^{2+}$  where the central pyridine rings are not coordinated to the metal ions.<sup>77</sup> A similar behavior

is exhibited by the septipyridine **111** synthesized by Potts and co-workers.<sup>152</sup> In acetonitrile, **111** reacts with Cu(I) to give a tetranuclear  $D_2$ -symmetrical double-stranded helicate  $[\text{Cu}_4(\mathbf{111})_2]^{4+}$  (Figure 36b). The four Cu(I) metal ions are symmetrically distributed among seven pyridine rings of each strand on the NMR time scale as a result of the dynamic processes previously invoked to explain the  $D_2$ -symmetry found for the related double-stranded dinuclear helicates with odd oligopyridines such as the substituted terpyridine **47** in  $[\text{Cu}_2(\mathbf{47})_2]^{3+}$ <sup>97</sup> (Figure 36a), the quinquepyridines **20** in  $[\text{Cu}_3(\mathbf{20})_2]^{3+}$  (Figure 38a),<sup>107</sup> and  $[\text{Ag}_2(\mathbf{23})_2]^{2+}$ .<sup>77</sup> Oxidation of  $[\text{Cu}_4(\mathbf{111})_2]^{4+}$  gives the mixed-valence  $\text{Cu}^{\text{II}}/\text{Cu}^{\text{I}}$  helicate  $[\text{Cu}_3(\mathbf{111})_2]^{4+}$  as found with quinquepyridine (Figures 36b and 38a).<sup>39,107</sup> Reaction of **111** with Co(II) leads to the dinuclear double-stranded helicate  $[\text{Co}_2(\mathbf{111})_2]^{4+}$  whose crystal structure reveals a low-symmetry arrangement of the ligand strands. Each Co(II) is pseudooctahedrally coordinated by two terpyridine subunits of each strand thus leaving one uncoordinated pyridine ring within each strand which occupies a terminal position in strand 1 and the central position in strand 2 (Figure 36c).<sup>152</sup> Despite the lack of a solution structure for this helicate, it is expected that dynamic processes lead to a symmetrically averaged structure in acetonitrile as found recently by Constable and co-workers<sup>153</sup> for the double-stranded helicate  $[\text{Zn}_2(\mathbf{112})_2]^{4+}$  which exists as a single head-to-head isomer (HH)- $[\text{Zn}_2(\mathbf{112})_2]^{4+}$  in the solid state (two terminal pyridine rings of each strands are uncoordinated), but gives symmetry-averaged structure on the <sup>1</sup>H NMR time scale in solutions. A similar observation has been reported for the double-stranded helicate  $[\text{Ag}_2(\mathbf{93})_2]^{2+}$  where a  $D_2$ -helical cation is observed in solution, but whose crystal structure shows a double-stranded helicate (HT)- $[\text{Ag}_2(\mathbf{93})_2]^{2+}$  where each Ag(I) is five-coordinated by one terpyridine and one bipyridine

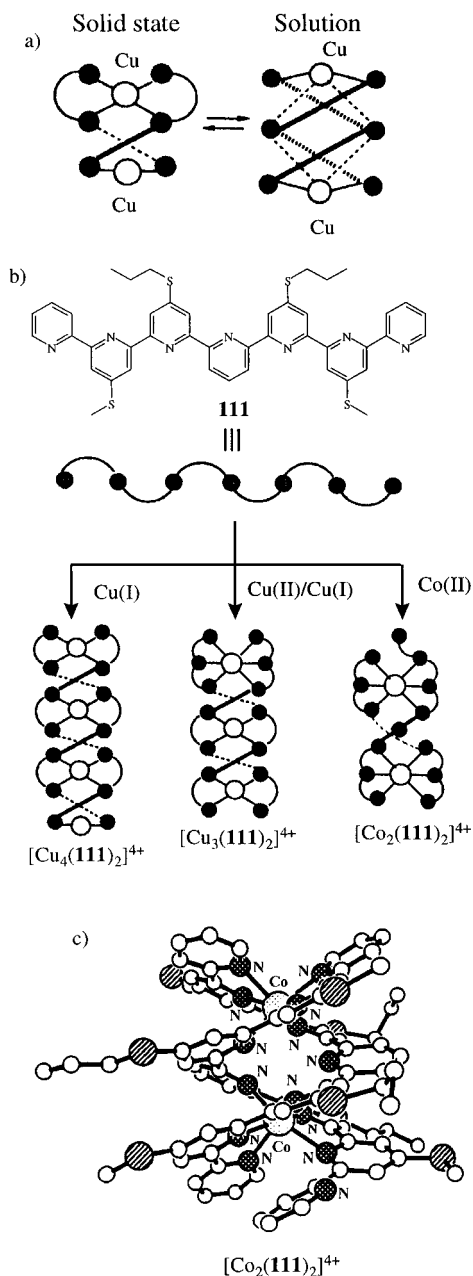


**Figure 36.** (a) Schematic representation of the solid-state and solution structures of the double-stranded helicate  $[\text{Cu}_2(\mathbf{47})_2]^{2+}$ ; (b) self-assembly of double-stranded helicites with septipyridine **111** (only one of the possible solid-state structures is schematically represented);<sup>152</sup> and (c) crystal structure of  $[\text{Co}_2(\mathbf{111})_2]^{4+}$ .<sup>152</sup> (Reproduced from ref 152. Copyright 1993 American Chemical Society.)

unit of each strand leaving one terminal pyridine ring uncoordinated on each strand.<sup>135</sup>

### 3. Unsaturated Double-Stranded Helicates

A significant mismatch between the intrinsic informations stored in the ligand strand and in the metal ion is often not compatible with the selective formation of double-stranded helicites and leads to intricate mixtures of complexes. However, the introduction of complementary mono- or bidentate coordinating ligands (anions or solvent molecules) may fulfill the stereochemical requirements of the metal ion eventually leading to stable unsaturated helicites. The best studied unsaturated helicites are those derived from the quinquepyridine ligands **7** and **20–28** combined with six-coordinate metal ions as

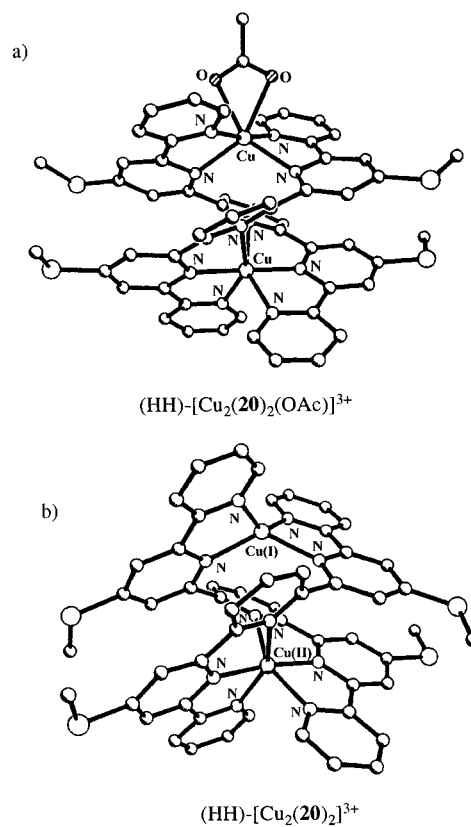


**Figure 37.** Crystal structures of heterotopic double-stranded helicites (a) unsaturated  $(\text{HH})\text{-}[\text{Cu}_2(\mathbf{20})_2(\text{OAc})]^{3+}$  and (b) saturated mixed-valence  $(\text{HH})\text{-}[\text{Cu}_2(\mathbf{20})_2]^{3+}$ .<sup>107</sup> (Reproduced from ref 107. Copyright 1993 American Chemical Society.)

in  $(\text{HH})\text{-}[\text{Cu}_2(\mathbf{7})_2(\text{OAc})]^{3+}$ .<sup>39</sup> The quinquepyridine strands display the usual separation into bipyridine and terpyridine subunits and adopt a head-to-head arrangement providing two different coordination sites: one Cu(II) is pseudooctahedrally coordinated by the two face-to-face terpyridine subunits and the second Cu(II) is five-coordinate by the two remaining bipyridine units together with a monodentate acetate anion (Figure 5).<sup>39</sup> This structure may be roughly derived from that of the mixed-valence saturated heterotopic helicate precursor  $(\text{HH})\text{-}[\text{Cu}_2(\mathbf{7})_2]^{3+}$  except for a larger intermetallic distance (4.50 Å for  $(\text{HH})\text{-}[\text{Cu}_2(\mathbf{7})_2(\text{OAc})]^{3+}$  compared to 3.957 Å for  $(\text{HH})\text{-}[\text{Cu}_2(\mathbf{7})_2]^{3+}$ , Table 5) which results from slightly different interstrand stacking interactions.<sup>39</sup> The analogous unsaturated double-stranded helicate  $(\text{HH})\text{-}[\text{Cu}_2(\mathbf{20})_2(\text{OAc})]^{3+}$  displays a very similar double-helical structure except for the presence of a bidentate acetate anion leading to two six-coordinate Cu(II) ions in the helicate (Figure 37).<sup>107</sup>

Various six-coordinate metal ions have then been introduced into unsaturated heterotopic head-to-head helicites to give related double-helical structures in the solid state for  $(\text{HH})\text{-}[\text{Co}_2(\mathbf{7})_2(\text{OAc})]^{3+}$ ,<sup>64</sup>  $(\text{HH})\text{-}[\text{Ni}_2(\mathbf{7})_2(\text{OAc})]^{3+}$ ,<sup>154</sup>  $(\text{HH})\text{-}[\text{Ni}_2(\mathbf{20})_2(\text{OAc})]^{3+}$ ,<sup>62,108</sup> and  $(\text{HH})\text{-}[\text{Ru}_2(\mathbf{7})_2(\text{C}_2\text{O}_4)]^{2+}$ .<sup>155</sup> In solution, the unsaturated Ni(II) helicites exhibit a formal Ni<sup>II</sup>/Ni<sup>I</sup> reduction process in which both Ni(II) centers are reduced at the same potential<sup>62,108</sup> while  $(\text{HH})\text{-}[\text{Ru}(\mathbf{7})_2(\text{OH}_2)]^{4+}$  may be oxidized into oxo species of Ru(IV) and Ru(VI).<sup>155</sup> The dinuclear unsaturated helicate  $(\text{HH})\text{-}[\text{Cu}_2(\mathbf{20})_2(\text{OAc})]^{3+}$  can be reduced to give the trinuclear complex  $[\text{Cu}_3(\mathbf{20})_2]^{3+}$  which is supposed to

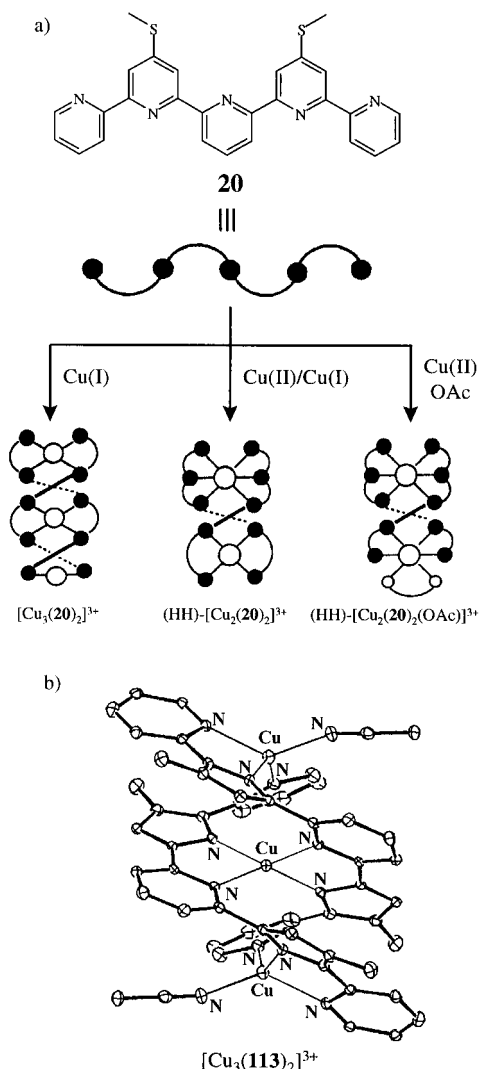


**Figure 38.** (a) Coordination behavior of quinquepyridine **20** with Cu(II) and Cu(I)<sup>107</sup> and (b) X-ray crystal structure of the unsaturated double-stranded helicate  $(\text{HT})\text{-}[\text{Cu}_3(\mathbf{113})_2]^{3+}$ .<sup>156</sup> (Reproduced from ref 156. Copyright 1996 American Chemical Society.)

adopt a double-helical structure reminiscent of that found in  $[\text{Cu}_2(\mathbf{47})_2]^{2+}$  (Figure 38a).<sup>108</sup> The crystal structure reported for the unsaturated heterotopic trinuclear double-stranded helicate  $(\text{HT})\text{-}[\text{Cu}_3(\mathbf{113})_2(\text{CH}_3\text{CN})_2]^{3+}$  strongly supports this hypothesis although the trinuclear structure is not maintained in solution according to ES-MS data (Figure 38b).<sup>156</sup> The introduction of ferrocenyl substituents into the ligand strand **22** does not sterically limit the formation of double-helical complexes and the unsaturated double-stranded helicate  $[\text{Ni}_2(\mathbf{22})_2(\text{OH}_2)]^{4+}$  has been characterized in solution.<sup>63</sup>

Segmental ligands also tolerate some degree of mismatching between the intrinsic informations and Constable and co-workers reported the formation of the unsaturated homotopic double-stranded helicate  $[\text{Ni}_2(\mathbf{73})_2(\text{OAc})_2]^{2+}$  from the bis-bidentate ligand **73** and octahedral Ni(II).<sup>119</sup> The crystal structure reveals two helically twisted strands bound to two six-coordinate Ni(II) lying in distorted  $\text{N}_4\text{O}_2$  coordination sites provided by two bipyridine units and one terminal bidentate acetate anion.<sup>119</sup> As usual, the double-helical structure is essentially achieved by twisting between the “planar” coordinated bipyridine units and the benzene-1,3-diyl spacer (interplanar

angles:  $35^\circ$  and  $38^\circ$ ).<sup>119</sup> In contrast to the usual interstrand  $\pi$ -stacking interactions observed for double-stranded helicates derived from oligopyridines, the large spacer in **73** removes any significant interactions between the strands in  $[\text{Ni}_2(\mathbf{73})_2(\text{OAc})_2]^{2+}$ . The elongated biphenyl-3,3'-diyl spacer in **75** is also suitable for the generation of unsaturated homotopic double-stranded helicates as demonstrated by the formation of  $[\text{Ni}_2(\mathbf{75})_2(\text{OAc})_2]^{2+}$  whose X-ray crystal structure is similar to that of  $[\text{Ni}_2(\mathbf{73})_2(\text{OAc})_2]^{2+}$  except for a longer intermetallic distance (7.7 Å) associated with the longer spacer.<sup>120</sup>

### C. Triple-Stranded Helicates

It was recognized very early that the tetradentate ligand triethylenetetramine (**L**) formed the unexpected dinuclear complex  $[\text{Ni}_2(\mathbf{L})_3]^{4+}$ .<sup>157</sup> Although the monobridged structure  $[(\mathbf{L})\text{Ni}(\mathbf{L})\text{Ni}(\mathbf{L})]^{4+}$  was suggested from spectroscopic and magnetic measurements, no crystal structure might be solved. Later, Harris and McKenzie found a similar 2:3 stoichiometry for their complex  $[\text{Cu}_2(\mathbf{100})_3]^{4+}$  and they suggest that the more rigid  $\alpha,\alpha'$ -diimines binding units impose structural constraints only compatible with a geometry in which all three ligands bridge the two metal ions (Chart 1).<sup>23</sup> Despite the only partial characterization of their complex, this paper reports, to the best of our knowledge, the first preparation and recognition of a synthetic dinuclear triple-stranded helicate in the literature. It is worth mentioning the more recent use of the same ligand **100** by Van Koten and co-workers for the preparation of double-stranded helicates with Ag(I).<sup>52,142–144</sup>

#### 1. Saturated Homotopic Triple-Stranded Helicates

*a. Three-Coordinate Metal Ions.* The assembly of three  $C_2$ -symmetrical oligo-monodentate ligand strands with metal ions displaying a stereochemical preference for a trigonal geometry represents the most simple case of complementary information leading to triple-stranded helicates (Table 1, entry 2). However, only one example has been reported by Potts and co-workers who have synthesized the ligand **114** (Chart 15) which produces selectively a 1:1 stoichiometric complex with Cu(I) isolated as its trinuclear hexafluorophosphate salt  $[\text{Cu}_3(\mathbf{114})_3](\text{PF}_6)_3$ .<sup>158</sup> Its crystal structure shows the cation  $[\text{Cu}_3(\mathbf{114})_3]^{3+}$  to be constituted of three ligand strands wrapped about three Cu(I) ions occupying distorted trigonal coordination sites defined by the three pyridine units of each strand. The acetylenic spacers prevent significant  $\pi$ -stacking between the pyridine rings and enforce rather long intermetallic distances ( $\sim 4.5$  Å, Table 8). Spectrophotometric and <sup>1</sup>H-NMR data suggest that the trinuclear triple-helical structure is maintained in solution and that a related dinuclear triple-stranded helicate  $[\text{Cu}_2(\mathbf{115})_3]^{2+}$  results from the reaction of **115** with Cu(I).<sup>158</sup>

*b. Six-Coordinate Metal Ions.* Parallel to the development of double-stranded helicates, oligobipyridine ligand strands have been designed for the generation of polynuclear triple-stranded helicates with six-coordinate metal ions (Table 1, entry 4). However, the usual connection of the 2,2'-bipyridines at the 6 positions fails to give self-assembled triple-

Chart 15

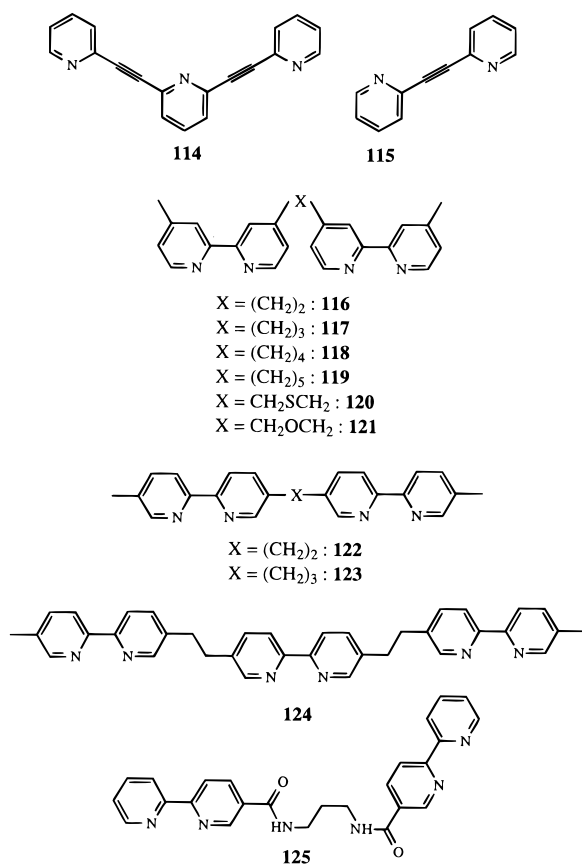


**Table 8. Intermetallic Distances (*d*) in the Crystal Structures of Dinuclear Triple-Stranded Helicates with Segmental Ligands**

metal	ligand	helicate	<i>d</i> , Å	ref
Cu(I)	<b>114</b>	[Cu <sub>3</sub> ( <b>114</b> ) <sub>3</sub> ] <sup>3+</sup>	4.494 4.519	158
Fe(II)	<b>116</b>	[Fe <sub>2</sub> ( <b>116</b> ) <sub>3</sub> ] <sup>4+</sup>	7.646	160
Fe(II)	<b>117</b>	[Fe <sub>2</sub> ( <b>117</b> ) <sub>3</sub> ] <sup>4+</sup>	7.55	161
Fe(II)	<b>118</b>	[Fe <sub>2</sub> ( <b>118</b> ) <sub>3</sub> ] <sup>4+</sup>	9.08	163
Ni(II)	<b>124</b>	[Ni <sub>3</sub> ( <b>124</b> ) <sub>3</sub> ] <sup>6+</sup>	8.6	164
Co(II)	<b>5</b>	[Co <sub>2</sub> ( <b>5</b> ) <sub>3</sub> ] <sup>4+</sup>	8.427	168
Co(II)	<b>126</b>	[Co <sub>2</sub> ( <b>126</b> ) <sub>3</sub> ] <sup>4+</sup>	8.854	169
Co(III)	<b>126</b>	[Co <sub>2</sub> ( <b>126</b> ) <sub>3</sub> ] <sup>6+</sup>	9.146	170
Fe(III)	<b>127</b>	[Fe <sub>2</sub> ( <b>127</b> ) <sub>3</sub> ] <sup>3+</sup>	7.75	174
Ga(III)	( <i>R,R</i> )- <b>12</b>	[Ga <sub>3</sub> ( <i>R,R</i> )- <b>12</b> ) <sub>3</sub> ] <sup>6-</sup>	10.78	53
Fe(III)	<b>128</b>	[Fe <sub>2</sub> ( <b>128</b> ) <sub>3</sub> ] <sup>6-</sup>	10.0	175
Eu(III)	<b>98</b>	[Eu <sub>2</sub> ( <b>98</b> ) <sub>3</sub> ] <sup>6+</sup>	8.876	185
Eu(III) + Zn(II)	<b>109</b>	[EuZn( <b>109</b> ) <sub>3</sub> ] <sup>5+</sup>	8.960	190
La(III) + Fe(II)	<b>109</b>	[LaFe( <b>109</b> ) <sub>3</sub> ] <sup>5+</sup>	9.029	225
Nd(III)	<b>9</b>	[Nd <sub>2</sub> ( <b>9</b> ) <sub>3</sub> (NO <sub>3</sub> ) <sub>6</sub> ]	9.95	38
Lu(III) + Na(I)	<b>144</b>	[ClLu( <b>144</b> ) <sub>3</sub> Na]	5.947	193

stranded helicates<sup>6</sup> as a result of steric crowding around the metal ions.<sup>159</sup> To avoid these structural restrictions, Elliott and co-workers have connected two bipyridine units via the 4 positions with various spacers: **116**–**121**.<sup>160–163</sup> Deep red 2:3 complexes are formed immediately upon reaction with Fe(II). The crystal structure of [Fe<sub>2</sub>(**116**)<sub>3</sub>]<sup>4+</sup> shows two Fe(II) pseudooctahedrally coordinated by one bipyridine units of each strand leading to a triply-bridged structure reminiscent of that proposed by Harris and McKenzie for [Cu<sub>2</sub>(**100**)<sub>3</sub>]<sup>4+</sup>.<sup>23</sup> Both metal ions in [Fe<sub>2</sub>(**116**)<sub>3</sub>]<sup>4+</sup> possess the same absolute configuration (PP or MM) leading to a global *D*<sub>3</sub>-helical triple-stranded structure if we neglect the length of the spacer (Figure 39).<sup>160</sup> A careful examination of the crystal structure of [Fe<sub>2</sub>(**116**)<sub>3</sub>]<sup>4+</sup> shows that the ethylene

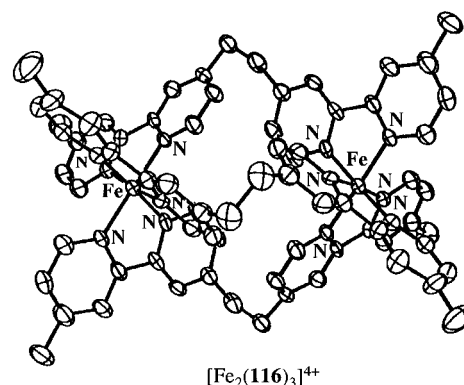


**Figure 39.** Crystal structure of the triple-stranded helicate [Fe<sub>2</sub>(**116**)<sub>3</sub>]<sup>4+</sup>.<sup>160</sup> (Reproduced from ref 160. Copyright 1988 American Chemical Society.)

bridges adopt the opposite helicity leading to a pair of enantiomeric irregular triple-stranded helices PMP and MPM (see Figure 12 and Chart 3). A similar structure is found for [Fe<sub>2</sub>(**117**)<sub>3</sub>]<sup>4+</sup> in which the intermetallic distance is not significantly affected despite the replacement of the ethylene by a propylene spacers.<sup>163</sup> Molecular mechanics suggests that ligands **116**, **117**, **120**, and **121** exhibit similar intermetallic distances in the triple-stranded helicates [Fe<sub>2</sub>(**L**)<sub>3</sub>]<sup>4+</sup> while the longer spacers in **118** and **119** significantly increase the Fe⋯Fe distance (Table 8).<sup>161,163</sup> A detailed investigation of the redox potential of the Fe<sup>III</sup>/Fe<sup>II</sup> couple indicates that a significant electrostatic interaction occurs between the two metallic centres in [Fe<sub>2</sub>(**L**)<sub>3</sub>]<sup>4+</sup> (**L** = **116**–**121**). Taking into account the intermetallic distances obtained by X-ray diffraction studies and molecular mechanics, Elliott and co-workers have estimated the relative dielectric constants ( $\epsilon_r$ ) of the medium between the two metals. For short Fe⋯Fe distances in [Fe<sub>2</sub>(**L**)<sub>3</sub>]<sup>4+</sup> (**L** = **116**, **117**),  $\epsilon_r$  amounts to 26.1–26.7, a value compatible with a pyridine/alkane-like material. The increase of  $\epsilon_r$  = 30.4 found for [Fe<sub>2</sub>(**118**)<sub>3</sub>]<sup>4+</sup> suggests that the electric field penetrates into the acetonitrile solvent only for the elongated triple helices; the short ethylene or propylene bridges preventing significant interactions with the solvent. A detailed study of the electronic coupling between the Fe(II) centers using the near-IR intervalence charge transfer transition of the mixed-valence helicates [Fe<sub>2</sub>(**L**)<sub>3</sub>]<sup>5+</sup> (**L** = **116**, **117**, **120**, **121**) demonstrates that (i) the triple-helical structure limits the access to the metal-containing macrobicyclic cavity for solvent molecules and (ii) the electronic interaction between the metals mainly involves a through space coupling mechanism mediated by the adjacent bipyridine ligands of the respective iron sites.<sup>162</sup> A significant “through-bond” contribution mediated by the bridge is limited to the short ethylene bridge in ligand **116**.<sup>162</sup> A parallel investigation of the luminescence of the analogous heterodinuclear complexes [RuFe(**L**)<sub>3</sub>]<sup>4+</sup> (**L** = **116**–**121**) confirms that energy is transferred from Ru(II) toward Fe(II) via a superexchange pathway involving through-space effects.<sup>163</sup>

Oligobipyridines connected via the 5 positions in **122** and **124** also lead to homotopic triple-stranded helicates [Fe<sub>2</sub>(**122**)<sub>3</sub>]<sup>4+</sup> and [Ni<sub>3</sub>(**124**)<sub>3</sub>]<sup>6+</sup>.<sup>164</sup> Although the triple-helical structure of [Fe<sub>2</sub>(**122**)<sub>3</sub>]<sup>4+</sup> was only suggested,<sup>66</sup> [Ni<sub>3</sub>(**124**)<sub>3</sub>]<sup>6+</sup> has been characterized by X-ray crystallography and exhibits the

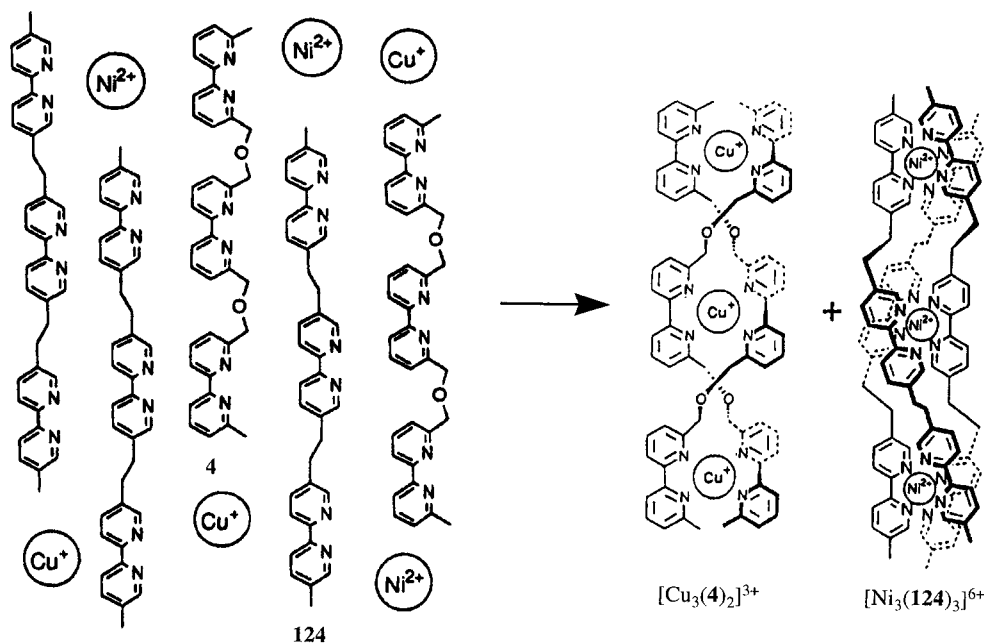
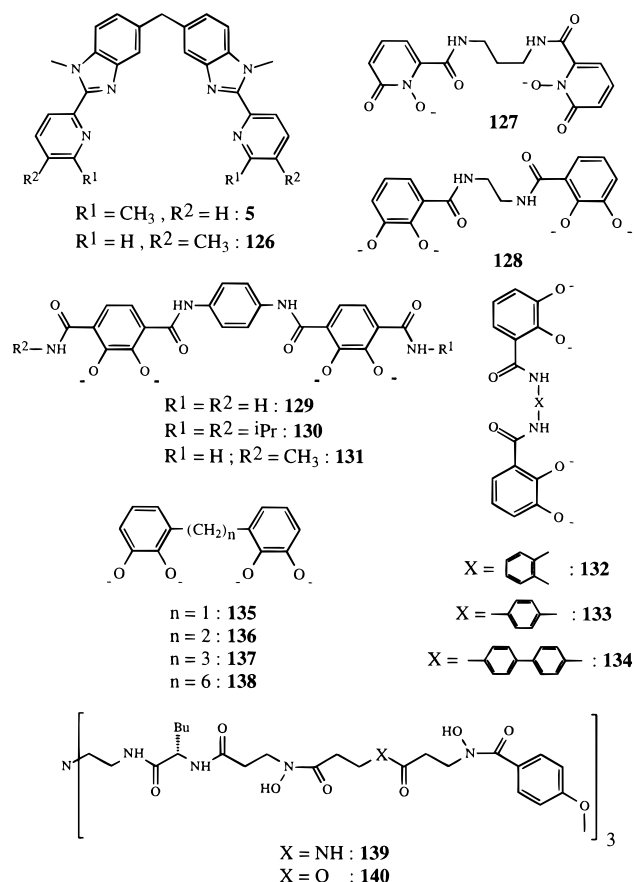


**Figure 40.** Self-recognition in the self-assembly of the double-stranded helicate  $[\text{Cu}_3(\mathbf{4})_2]^{3+}$  and the triple-stranded helicate  $[\text{Ni}_3(\mathbf{124})_3]^{6+}$ .<sup>115</sup> (Reproduced with permission from ref 115. Copyright 1993 National Academy of Sciences USA.)

expected trinuclear triple-helical structure with the three strands coordinated to three packed pseudo-octahedral Ni(II). The helical pitch is about 41 Å, a value significantly larger than the 12 Å found in the double-stranded cuprohelicate **1** and attributed to the transoid conformation of the ethylene spacers. The  $C_2$  space group of the crystals indicates that spontaneous resolution occurs during crystallization leading to only one helical enantiomer in the measured crystal.<sup>164</sup> Dissolution into acetonitrile/water maintains the absolute configuration and slow racemization occurs leading to a 23% loss of optical activity in 24 h. As a result of the different steric requirements for the assembly of double- and triple-stranded helicates with oligobipyridine strands, self-recognition occurs when ligands **4** (2 equiv) and **124** (3 equiv) are reacted with a stoichiometric mixture of Cu(I) and Ni(II) leading exclusively to the double-stranded helicate  $[\text{Cu}_3(\mathbf{4})_2]^{3+}$  and the triple-stranded helicate  $[\text{Ni}_3(\mathbf{124})_3]^{4+}$  (Figure 40).<sup>115</sup> During this self-assembly process, 11 particles of four different types generate only two supramolecular organized helicates. The more flexible spacer of **125** is still compatible with  $D_3$ -symmetrical triple-stranded helicate as demonstrated by the formation of the triple-stranded helicate  $[\text{Fe}_2(\mathbf{125})_3]^{4+}$  in solution.<sup>165</sup> Surprisingly, the ligand **123** which possesses a propylene bridge between the bipyridine units selectively generates the dinuclear homotopic  $C_{3h}$ -symmetrical side-by-side helicate  $[\text{Fe}_2(\mathbf{123})_3]^{4+}$  in solution with two metal ions of opposite chirality.<sup>166</sup> The control of the helical vs the side-by-side conformation results from the particular stereochemistry of the alkyl chain connecting the bidentate binding units as described for the analogous helicates derived from catecholate ligands **136** and **137**<sup>167</sup> (Chart 16).

As described for double-stranded helicates, triple-stranded helicates are not limited to oligobipyridine strands and Williams and co-workers reported the synthesis of a segmental ligand **5** planned for the self-assembly of triple-stranded helicates with six-coordinate metal ions.<sup>168</sup> The 5,5'-diphenylmethane spacer

**Chart 16**



in **5** is well adapted for the formation of triple-stranded helicates which requires a less pronounced helical twist between the binding units than that found for double-stranded helicates. Reaction of **5** with Co(II) produces the expected homotopic  $D_3$ -symmetrical triple-stranded helicate  $[\text{Co}_2(\mathbf{5})_3]^{4+}$  as the only complex in solution which suggests some positive cooperativity in the assembly process (Figure 4a).<sup>29</sup> The X-ray crystal structure of  $[\text{Co}_2(\mathbf{5})_3]^{4+}$  confirms the dinuclear triple-helical structure where

each Co(II) is six-coordinate in pseudooctahedral sites flattened along the  $C_3$  axis.<sup>168</sup> Detailed spectroscopic investigations ( $^1\text{H}$  NMR, UV-vis) demonstrate that the triple-helical structure is maintained in solution, but the authors were unable to oxidize electrochemically Co(II) into Co(III) in acetonitrile as normally observed for analogous mononuclear precursors.<sup>29</sup> This unexpected behavior was explained by steric constraints controlling the  $\text{Co}^{\text{III}}/\text{Co}^{\text{II}}$  redox potential.<sup>169</sup> In  $[\text{Co}_2(\mathbf{5})_3]^{4+}$ , the methyl groups bound to the 6 position of the pyridine rings prevent the contraction associated with the formation of low-spin  $d^6$  Co(III). The shift of these methyl groups from the 6 position in **5** to the 5 position in **126** minimizes the steric crowding around the metal ions and consequently (i) increases the stability of the dinuclear triple-stranded helicate  $[\text{Co}_2(\mathbf{L})_3]^{4+}$  ( $\log(\beta) = 21.9$  for  $\mathbf{L} = \mathbf{5}$  and  $\log(\beta) > 25$  for  $\mathbf{L} = \mathbf{126}$ ) and (ii) allows oxidation to Co(III).<sup>169</sup> Crystal structures of  $[\text{Co}_2(\mathbf{126})_3]^{4+}$ <sup>169</sup> and  $[\text{Co}_2(\mathbf{126})_3]^{6+}$ <sup>170</sup> have been solved and show similar triple-helical structures. The Co-N distances display the expected 0.2 Å contraction associated with the oxidation of Co(II) into Co(III) and the intermetallic distance in the oxidized form  $[\text{Co}_2(\mathbf{126})_3]^{6+}$  is slightly longer as a result of subtle variations in the helical twist of the strands.<sup>170</sup> Low-spin Co(III) complexes exhibit considerable kinetic inertness<sup>171</sup> and the triple-stranded cation  $[\text{Co}_2(\mathbf{126})_3]^{6+}$  has been separated into its two helical enantiomers  $[(P,P)\text{-Co}_2(\mathbf{126})_3]^{6+}$  and  $[(M,M)\text{-Co}_2(\mathbf{126})_3]^{6+}$  using the chiral dianion  $(+)\text{[Sb}_2(\text{C}_4\text{O}_6\text{H}_2)_2]^{2-}$ .<sup>170</sup> The reduction of  $[(P,P)\text{-Co}_2(\mathbf{126})_3]^{6+}$  with dithionite occurs with retention of configuration leading to  $[(P,P)\text{-Co}_2(\mathbf{126})_3]^{4+}$  which racemizes much slower than the mononuclear Co(II) analogues<sup>172</sup> as previously reported for  $[\text{Ni}_3(\mathbf{124})_3]^{6+}$  compared to  $[\text{Ni}(\text{bipy})_3]^{2+}$ .<sup>164</sup> This indicates that the polynuclear triple-stranded helical structure increases the kinetic inertness of the metal ion. The origin of this effect is closely related to the structural constraints arising from the second coordinated metal ion which severely limit intramolecular twist in triple-stranded helicates with short helical pitches.<sup>172</sup> For  $[(P,P)\text{-Co}_2(\mathbf{126})_3]^{4+}$ , the racemization involves an energetically costly dissociative mechanism leading to  $[\text{Co}(\mathbf{126})_3]^{2+}$  and  $\text{Co}^{2+}$  because the Baylar twist is precluded by steric constraints.<sup>172</sup> However, it is not completely clear whether ligand field effects are also important in these processes.

Segmental oxygen donors ligands based on catecholate or 1-hydroxy-2-pyridonate binding units have been designed as ferric ion sequestering agents.<sup>2</sup> Compound **127**, a biomimetic analogue of rhodotorulic acid, possesses the structural characteristics required for the formation of dinuclear complexes with Fe(III)<sup>173</sup> and a stable 2:3 complex  $[\text{Fe}_2(\mathbf{127})_3]$  ( $\log(\beta) = 52.3(3)$ ) is obtained in basic medium.<sup>174</sup>  $[\text{Fe}_2(\mathbf{127})_3]$  crystallizes to give orange-red needles whose X-ray crystal structure corresponds to a pseudo- $D_3$  triple-stranded helical structure with two pseudo-octahedrally coordinated Fe(III) as proposed for the natural siderophore  $[\text{Fe}_2(\text{rhodotorulic acid})_3]$  (Figure 41).<sup>173,174</sup> Only the left-handed helicate  $[(M,M)\text{-Fe}_2(\mathbf{127})_3]$  is observed in the measured crystal (space group  $P6_1$ ) as a result of spontaneous resolution during crystallization.<sup>174</sup>

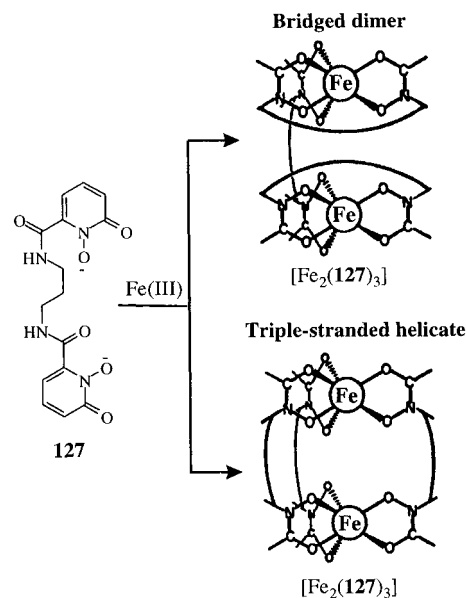


**Figure 41.** Two possible structures for the dimeric complex  $[\text{Fe}_2(\mathbf{127})_3]$ .<sup>174</sup> (Reproduced from ref 174. Copyright 1991 and 1985 American Chemical Society.)

Quantitative helical induction may be obtained with the analogous enantiomerically pure analogous ligand  $(R,R)\text{-12}$  which forms exclusively one diastereomer corresponding to the homotopic left-handed triple-stranded helicate  $[(M,M)\text{-Ga}_2((R,R)\text{-12})_3]^{6-}$  according to the X-ray crystal structure. This high selectivity implies that the helical- $(P,P)$  and the side-by-side- $(M,P)$  diastereomers are destabilized by at least  $8.4 \text{ kJ mol}^{-1}$  at 297 K in  $\text{D}_2\text{O}$ .<sup>53</sup> To probe the importance of enantiomeric purity on stereospecific helix formation, a racemic mixture of  $(R,R)\text{-12}$  and  $(S,S)\text{-12}$  was reacted with Ga(III). If we neglect the absolute configurations of the metal ions, four possible isomeric helicates are expected: two  $D_3$ -symmetrical homochiral helicates  $[\text{Ga}_2((R,R)\text{-12})_3]^{6-}$  and  $[\text{Ga}_2((S,S)\text{-12})_3]^{6-}$  and two  $C_2$ -symmetrical heterochiral helicates  $[\text{Ga}_2((R,R)\text{-12})_2((S,S)\text{-12})]^{6-}$  and  $[\text{Ga}_2((S,S)\text{-12})_2((R,R)\text{-12})]^{6-}$ . After thermodynamic equilibration, a mixture of about 6:1 heterochiral:homochiral is reached, indicating that the heterochiral isomers are energetically more stable by about  $4.2 \text{ kJ mol}^{-1}$ .<sup>53</sup> The similar achiral ligand strand **128** which possesses a shorter spacer between the catecholate binding units, also generates the self-assembled triple-stranded helicate  $[\text{Fe}_2(\mathbf{128})_3]^{6-}$  whose crystal structure is very close to that of  $[\text{Ga}_2((R,R)\text{-12})_3]^{6-}$  except for a shorter intermetallic distance (Table 8).<sup>175</sup> A detailed investigation of the assembly process allows the characterization of a bis( $\mu$ -hydroxo) dimer  $[\text{Fe}_2(\mathbf{128})_2(\text{OH})_2]^{4-}$  formed for a stoichiometric ratio  $\text{Fe(III)}:\mathbf{128}:\text{base} = 2:2:10$  and which probably corresponds to a stable intermediate within the assembly of the triple-stranded helicate. The analogous ligand strands **129–131** have been designed by Raymond and co-workers for the study of dynamic interconversion between helical enantiomers.<sup>176</sup> Upon reaction with Ga(III), the expected  $D_3$  triple-stranded helicates  $[\text{Ga}_2(\mathbf{L})_3]^{6-}$  ( $\mathbf{L} = \mathbf{129}\text{--}\mathbf{131}$ ) are formed quantitatively in solution. Variable-temperature  $^1\text{H}$  NMR investigations of the homotopic triple-stranded helicate  $[\text{Ga}_2(\mathbf{130})_3]^{6-}$  using the methyl groups of the isopropyl substituent as diastereotopic probes show that coalescence of the  $A_3B_3X$  system into a  $A_6X$  spin

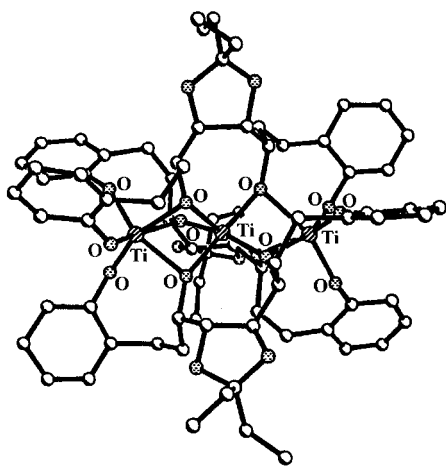
system corresponds to the fast helical interconversion  $[(P,P)\text{-Ga}_2(\mathbf{130})_3]^{6-} \leftrightarrow [(M,M)\text{-Ga}_2(\mathbf{130})_3]^{6-}$  on the NMR time scale. A line-shape analysis of the signals allows the calculation of the free energy inversion barrier which is only 1.2 times higher than that obtained for the mononuclear precursor.<sup>177</sup> The authors conclude that (i) the two metallic centres are weakly mechanically coupled in the triple-stranded helicate and (ii) the mechanism of the helical interconversion involves the heterochiral side-by-side conformer  $[(M,P)\text{-Ga}_2(\mathbf{130})_3]^{6-}$  as an intermediate which is produced by a single Bailar twist along the reaction pathway.<sup>176</sup> This result strongly contrasts with the significantly increased inertness reported for the polynuclear triple-stranded helicates  $[\text{Ni}_3(\mathbf{124})_3]^{6+}$ <sup>164</sup> and  $[\text{Co}_2(\mathbf{126})_3]^{4+}$ <sup>172</sup> and it may be tentatively attributed to the lack of ligand field effect for Ga(III) and to a larger helical pitch in  $[\text{Ga}_2(\mathbf{130})_3]^{6-}$ .<sup>172</sup> The analogous, but heterotopic helicate  $[\text{Ga}_2(\mathbf{131})_3]^{6-}$  exists in solution as a mixture of head-to-tail (HHT) and head-to-head (HHH) conformers (ratio = 1.86) which undergo helical interconversion processes similar to those found for  $[\text{Ga}_2(\mathbf{130})_3]^{6-}$ . However, no fast (HHH)- $[\text{Ga}_2(\mathbf{131})_3]^{6-} \leftrightarrow$  (HHT)- $[\text{Ga}_2(\mathbf{131})_3]^{6-}$  isomerization was observed in solution on the NMR time scale. Self-recognition of triple-stranded helicates has been demonstrated recently by Raymond and co-workers with the series of bis-catecholate ligands **132**–**134** which differ only by the length of the spacer between the binding units.<sup>27</sup> Upon reaction of a mixture of **132**–**134** with a stoichiometric amount of  $[\text{Ga}(\text{acetylacetonate})_3]$  in basic aqueous solution, the homostranded triple-stranded helicates  $[\text{Ga}_2(\mathbf{132})_3]^{6-}$ ,  $[\text{Ga}_2(\mathbf{133})_3]^{6-}$ , and  $[\text{Ga}_2(\mathbf{134})_3]^{6-}$  were exclusively formed and no trace of heterostranded helicates was detected by <sup>1</sup>H NMR or ES-MS.<sup>27</sup> This points to a remarkable cooperative process occurring between the ligands and the metal ions which is closely related to the self-recognition of double-stranded helicates with oligo-bipyridine ligands previously reported by Lehn and co-workers (Figure 26).<sup>115</sup>

The bis-catecholate ligand **136** reacts with Ti(IV) to give the  $D_3$ -symmetrical triple-stranded helicate  $[\text{Ti}_2(\mathbf{136})_3]^{4-}$  whose X-ray crystal structure reveals the incorporation of a countercation  $\text{Li}^+$  within the self-assembled metal-containing macrobicyclic cavity to give  $[\text{Li}\text{C}\text{Ti}_2(\mathbf{136})_3]^{3-}$ .<sup>178</sup> The analogous elongated ligand **137** produces selectively the  $C_{3h}$ -side-by-side triple-stranded helicate  $[(M,P)\text{-Ti}_2(\mathbf{137})_3]^{4-}$  according to the observation of diastereotopic protons for the central methylene group in the <sup>1</sup>H-NMR spectrum.<sup>167</sup> The crystal structure unambiguously confirms this statement and shows the nonhelical side-by-side structure where the two Ti(IV)s display opposite conformations in severely distorted octahedral sites. As found for  $[\text{Li}\text{C}\text{Ti}_2(\mathbf{136})_3]^{3-}$ , Albrecht and Kotila observe the inclusion of one  $\text{Na}^+$  in the larger metal-containing macrobicyclic cavity generated by the three wrapped strands in  $[\text{Na}\text{C}\text{Ti}_2(\mathbf{137})_3]^{3-}$ . In both structures, the alkali metal cation is asymmetrically bound to endohedral oxygen atoms of the catecholate binding units.<sup>167</sup> In methanol solution, the triple-helical structure is maintained, but <sup>6</sup>Li NMR spectra show no evidence for the complexation of  $\text{Li}^+$  inside the self-assembled macrobicyclic cavities. On the other hand, <sup>23</sup>Na NMR studies clearly establish that

$\text{Na}^+$  is coordinated in the macrobicyclic cavity of  $[\text{Na}\text{C}\text{Ti}_2(\mathbf{137})_3]^{3-}$  and rapidly exchanges with the bulk solution at room temperature ( $\Delta G^\ddagger = 31\text{--}36$  kJ mol<sup>-1</sup>).<sup>179</sup> Competition experiments with  $\text{K}^+$  show that  $\text{Na}^+$  is displaced by  $\text{K}^+$  which better fits the large cavity of  $[\text{Ti}_2(\mathbf{137})_3]^{4-}$ , while  $\text{Li}^+$  has only little effect because its small size. Temperature-dependent <sup>1</sup>H-NMR data show that rapid interconversion between  $P$  and  $M$  conformations of the chiral octahedral Ti(IV) centers occurs in methanol for the triple-stranded helicates with energy barriers of  $\Delta G^\ddagger = 43.1$  and  $69.4$  kJ mol<sup>-1</sup> for  $[\text{Ti}_2(\mathbf{136})_3]^{4-}$  and  $[\text{Ti}_2(\mathbf{137})_3]^{4-}$ , respectively.<sup>167,178</sup> It thus appears that the structure of the self-assembled helicate (side-by-side, vs helical) and the dynamic helical inversion of the chiral Ti(IV) centers depend on the zig zag conformation of the alkyl spacers connecting the ligand moieties. An even number of methylene units favors the helical conformation and rapid helical interconversion, while an odd number leads to the more inert side-by-side conformer.<sup>167,178</sup> This has been confirmed recently with the synthesis of the two ligands **135**<sup>180</sup> and **138**<sup>179</sup> which possess one and six methylene units between the binding units respectively. As expected, **135** produces the self-assembled  $C_{3h}$ -side-by-side triple-stranded helicate  $[(M,P)\text{-Ti}_2(\mathbf{135})_3]^{4-}$  while **138** leads to the  $D_3$ -helical triple-stranded helicate  $[\text{Ti}_2(\mathbf{138})_3]^{4-}$ . Surprisingly, no  $\text{Li}^+$  are found within the cryptand cavity in the crystal structure of  $\text{Li}_4\text{-}[(M,P)\text{-Ti}_2(\mathbf{135})_3]$ , but three  $\text{Li}^+$  are bound on the periphery of the cavity, thus blocking the access for further cations.<sup>180</sup> In  $\text{K}_4[\text{Ti}_2(\mathbf{138})_3]$ , the cavity is large enough to accommodate two  $\text{K}^+$  and the helicate is better described as  $[\text{K}_2\text{C}\text{Ti}_2(\mathbf{138})_3]^{2-}$ .<sup>179</sup>

In an effort to design effective asymmetric catalyst, Corey and co-workers have synthesized the enantiomerically pure tetraol ( $S,R,R,S$ )-**13** from D-mannitol.<sup>54</sup> Initial attempts to form the desired mononuclear Ti(IV) catalyst failed, but the careful examination of the reaction products have established the exclusive formation of a trinuclear  $D_3$ -symmetrical triple-stranded helicate  $[\text{Ti}_3((S,R,R,S)\text{-}\mathbf{13})_3]$ .<sup>54</sup> Although not considered in the original report,<sup>54</sup> it seems that only one diastereomer exists in solution which may be tentatively attributed to the left-handed helicate  $[(M,M,M)\text{-Ti}_3((S,R,R,S)\text{-}\mathbf{13})_3]$  according to the crystal structure (Figure 42).

Among the early planned preparations of triple-stranded helices, Shanzer and co-workers synthesized chiral tripodal podands **139** and **140**, possessing two hydroxamate binding units and three lateral carboxamide units which are good candidates for interstrand hydrogen bonding in order to limit the random coiling of the organic chains.<sup>181</sup> The podand **139** reacts with Fe(III) to give the mononuclear  $[\text{Fe}(\mathbf{139}\text{-3H})]$  and dinuclear  $[\text{Fe}_2(\mathbf{139}\text{-6H})]$  complexes. <sup>1</sup>H NMR and circular dichroism studies of the dinuclear complex have established (i) a restricted conformational freedom of the strands resulting from interstrand hydrogen bonds and (ii) the selective formation of the right-handed ( $P,P$ ) helical structure (Figure 43).<sup>181</sup> Minor structural variations within the chains dramatically affect the final helical edifice as exemplified by the exclusive formation of the opposite diastereomeric left-handed helicate  $[(M,M)\text{-Fe}_2(\mathbf{140}\text{-$



[(M,M,M)-Ti<sub>3</sub>((R,S,S,R)-13)<sub>3</sub>]

**Figure 42.** Crystal structure of [(M,M,M)-Ti<sub>3</sub>((R,S,S,R)-13)<sub>3</sub>].<sup>54</sup> (Reproduced with permission from ref 54. Copyright 1994 Elsevier science Ltd.)

6H)] with the analogous chiral ligand **140** where one carboxamide is replaced by an ester group.

As discussed previously for double-stranded helicates obtained from tridentate binding units and octahedral metal ions (Figure 33),<sup>140</sup> an oligo-bidentate ligand strand combined with octahedral metal ions does not systematically produce polynuclear triple-stranded helicates. Recently, Lehn and co-workers have reported that the oligo-bipyridine strand **124**, which forms the triple-stranded helicate [Ni<sub>3</sub>(**124**)<sub>3</sub>]<sup>6+</sup><sup>164</sup> produces a circular double-stranded pentanuclear helicate [Fe<sub>5</sub>(**124**)<sub>5</sub>(Cl)]<sup>9+</sup> upon reaction with FeCl<sub>2</sub> (Figure 44).<sup>182</sup> The X-ray crystal structure reveals that five Fe(II) occupy the corners of a pentagon with an edge length of 8.4 Å (Fe...Fe distance). The internal cavity has a radius of 1.75 Å, well adapted for the complexation of the central chloride anion which is strongly bound. Surprisingly, the reaction of **124** with Fe(BF<sub>4</sub>)<sub>2</sub> produces a different hexameric complex [Fe<sub>6</sub>(**124**)<sub>6</sub>]<sup>12+</sup> which strongly suggests that the resulting final architecture depends on a subtle balance between the stereochemical preferences of the metal ion and the effect of the counteranion.<sup>182</sup> This has been elegantly demon-

strated by Raymond and co-workers<sup>27</sup> who have recently used sterically constrained bis-bidentate hydroxamate ligands for the selective generation of symmetry-driven tetrahedral metal-containing clusters [Fe<sub>4</sub>L<sub>6</sub>] with pseudooctahedral Fe(III) as an alternative to the formation of the more classical triple-stranded helicate [Fe<sub>2</sub>L<sub>3</sub>] (both supramolecular complexes possess the same stoichiometric Fe:L ratio).<sup>27</sup>

*c. Nine-Coordinate Metal Ions.* An increase in the denticity of the binding units from bidentate to tridentate requires metal ions with larger coordination numbers to match the intrinsic information leading to triple-stranded helicates.<sup>29,32</sup> Table 1, entry 6, indicates that a C<sub>2</sub>-symmetrical segmental bis-tridentate ligand is suitable to generate homotopic triple-stranded helicates with nine-coordinate metal ions. Lanthanide cations Ln(III) (Ln = La–Lu) are good candidates because they tend to be nine-coordinate with simple monodentate ligands and to adopt a tricapped trigonal prismatic coordination geometry close to the idealized D<sub>3h</sub> symmetry.<sup>183</sup> The ligand strand **98** has been designed for this purpose by Piguet, Bünzli, and co-workers and the self-assembled dinuclear lanthanide complexes [Ln<sub>2</sub>(**98**)<sub>3</sub>]<sup>6+</sup> are readily obtained by the simple mixing of Ln(ClO<sub>4</sub>)<sub>3</sub> and **98** in acetonitrile (Figure 45).<sup>184</sup> Spectroscopic investigations (ES-MS, UV–vis, luminescence) have established a D<sub>3</sub>-helical triple-stranded helical structure for [Ln<sub>2</sub>(**98**)<sub>3</sub>]<sup>6+</sup> in solution<sup>184</sup> which has been confirmed by the crystal structure of [Eu<sub>2</sub>(**98**)<sub>3</sub>]<sup>6+</sup>.<sup>185</sup> Each Eu(III) is nine-coordinated by three tridentate units and efficiently protected from external interactions. The authors have taken advantage of this feature together with the particular emitting properties of Eu(III) and Tb(III) to design light-converting triple-stranded helicates.<sup>9,184</sup> The self-assembly of heterodinuclear helicates [(Ln<sup>1</sup>)(Ln<sup>2</sup>)(**98**)<sub>3</sub>]<sup>6+</sup> (Ln<sup>1</sup> ≠ Ln<sup>2</sup>) has been followed by ES-MS and <sup>1</sup>H NMR and systematic deviations from the expected statistical distribution point to an interaction between the coordination sites depending on the size of the lanthanide metal ions and mediated by the ligand backbone, a feature related to allosteric and cooperative processes in supramolecular complexes.<sup>6,186</sup>

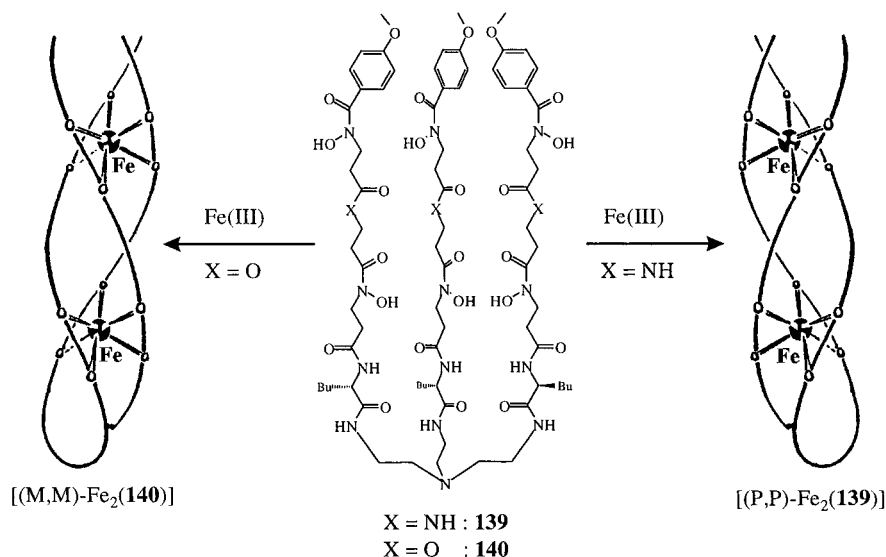


**Figure 43.** Schematic representation of the stereoselective formation of the triple-stranded helicates [(P,P)-Fe<sub>2</sub>(**139**-6H)] and [(M,M)-Fe<sub>2</sub>(**140**-6H)].<sup>181</sup>

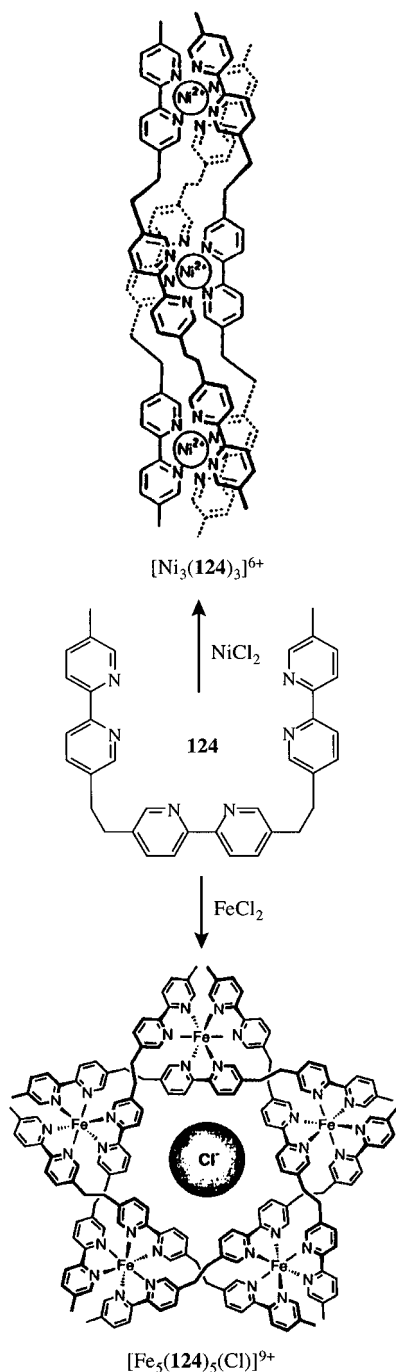


**Figure 44.** Self-assembly of a triple-stranded helicate  $[\text{Ni}_3(\mathbf{124})_3]^{6+}$  and a cyclic double-stranded pentanuclear helicate  $[\text{Fe}_5(\mathbf{124})_5(\text{Cl})]^{9+}$  from a tris-bidentate ligand strand.<sup>182</sup> (Reproduced with permission from ref 182. Copyright 1996 VCH Publishers.)

A trinuclear triple-stranded helicate  $[\text{Eu}_3(\mathbf{141})_3]^{9+}$  (Chart 17) has been evidenced in solution according to ES-MS, UV-vis, and NMR spectroscopies,<sup>187</sup> but its high positive charge makes it very sensitive to hydrolysis and requires strict anhydrous conditions to be observed.

## 2. Saturated Heterotopic Triple-Stranded Helicates

As a result of efforts to design organized luminescent and magnetically active lanthanide probes with predetermined properties, Piguet, Bünzli, and co-workers have synthesized segmental heterotopic ligands **8** and **109** possessing a bidentate and a tridentate binding unit coded for the recognition of

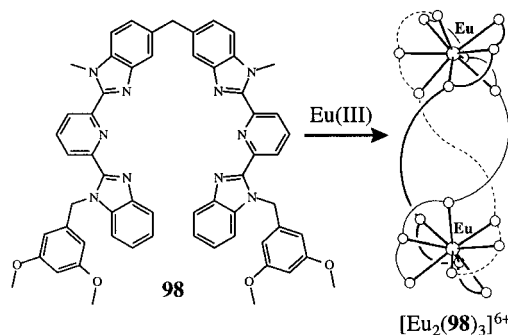
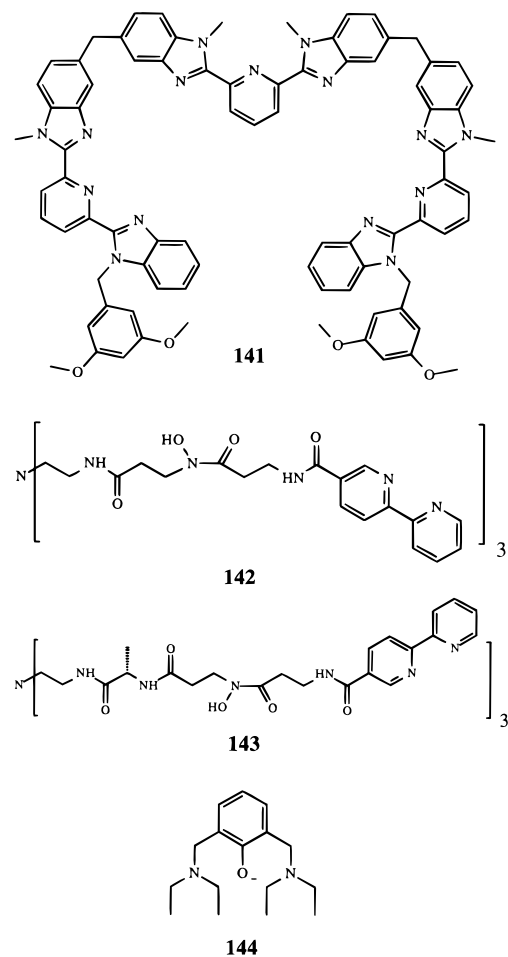


**Figure 45.** Self-assembly of  $[\text{Eu}_2(\mathbf{98})_3]^{6+}$  in acetonitrile.<sup>184</sup> (Reproduced with permission from ref 186. Copyright 1996 Chimia.)

## Chart 17



**3d** and **4f** block metal ions respectively.<sup>36,37</sup> The self-assembly of heterodinuclear d-f supramolecular complexes indeed occurs and **8** reacts with Zn(II) and Ln(III) (Ln = La–Lu) to give selectively the  $C_3$ -symmetrical heterotopic head-to-head triple-stranded helicate (HHH)- $[\text{LnZn}(\mathbf{8})_3]^{5+}$  in acetonitrile (Figure 6).<sup>36,37</sup> The detailed investigation of the multicomponent assembly process implies several equilibria between the heterodinuclear helicate and its homonuclear precursors. As a result of the limited affinity of soft aromatic nitrogen donor atoms for Ln(III), the quantitative formation of the heterotopic triple-stranded helicate is restricted to a well-defined set of suitable external conditions: (i) total ligand concentration  $\geq 10^{-2}$  M, (ii) stoichiometric ratio Ln(III): Zn(II):**8** = 1:1:3 and (iii) noncoordinating anions or solvent (Figure 46). In absence of X-ray data, the

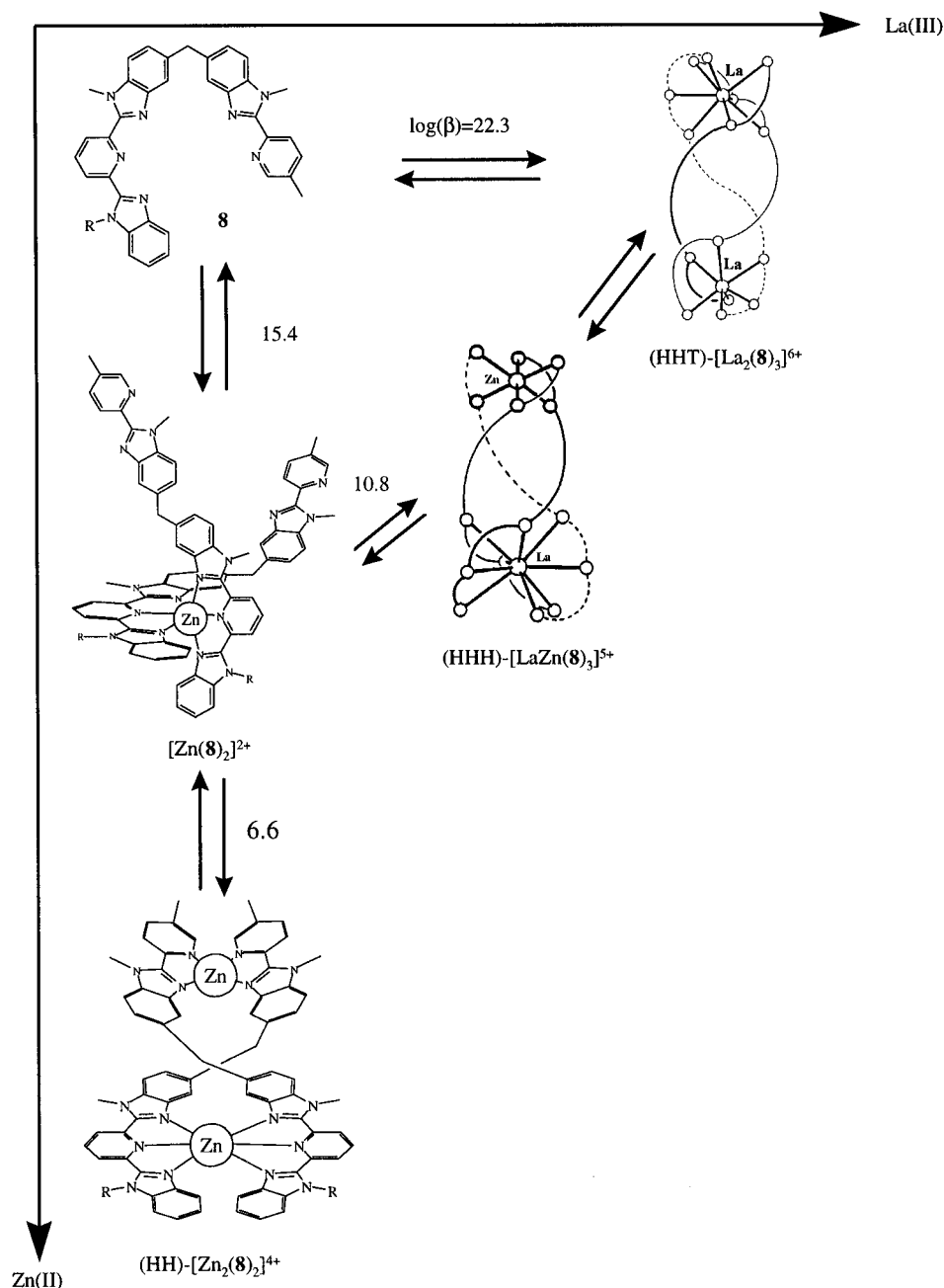


**Figure 46.** Self-assembly of **8** with La(III) and Zn(II). Stability constants are given as  $\log(\beta)$  and R is 3,5-dimethoxybenzyl.<sup>37</sup>

structural characterization of the triple-stranded helicates (HHH)-[LnZn(**8**)<sub>3</sub>]<sup>5+</sup> is based on <sup>1</sup>H NMR and high-resolution emission spectra using lanthanide metal ions as a structural paramagnetic and luminescent probe respectively.<sup>36,37</sup> Zn(II) lies in the facial pseudooctahedral site produced by the three bidentate binding units and acts as a noncovalent tripod which organizes the remaining tridentate binding units for their pseudotricapped trigonal prismatic coordination to Ln(III). Surprisingly, the reaction of **8** with Ln(III) (Ln = La–Eu) in the absence of d-block ions also produces selectively a heterotopic triple-stranded helicate (HHT)-[Ln<sub>2</sub>(**8**)<sub>3</sub>]<sup>6+</sup> despite the poor matching between the intrinsic informations of the ligands and those of the metal ions. The complicated <sup>1</sup>H-NMR spectra point to a C<sub>1</sub>-symmetrical head-to-tail arrangement of the strands which was confirmed by luminescence spectra compatible with the existence of a seven-coordinate and a eight-coordinate Ln(III) (Figure 6).<sup>36,37</sup> This su-

pramolecular complex (HHT)-[Ln<sub>2</sub>(**8**)<sub>3</sub>]<sup>6+</sup> is the only reported example of a saturated homonuclear heterotopic triple-stranded helicate

Zn(II) can be replaced by Fe(II), but the sterically more demanding d<sup>6</sup> Fe(II)<sup>188</sup> induces some distortion in the helical structure and prevents the structural contraction required for the complexation of heavy Ln(III) leading to the self-assembly of (HHH)-[LnFe(**8**)<sub>3</sub>]<sup>5+</sup> only for the larger Ln(III) (Ln = La–Eu).<sup>189</sup> New magnetic and thermochromic properties are associated with these self-assembled helicates since Fe(II) displays a spin-crossover equilibrium near room temperature.<sup>189</sup>

In order to increase the selectivity of the assembly process and the quantum yield of the emitting lanthanide complex, the terminal benzimidazole group of **8** has been replaced by a *N,N*-diethylcarbamoyl group in **109**. The quantitative formation of the heterotopic head-to-head triple-stranded helicate (HHH)-[LnZn(**109**)<sub>3</sub>]<sup>5+</sup> is observed even at very low

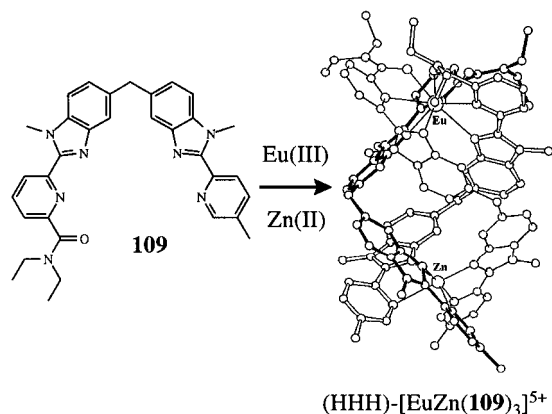


**Figure 47.** Self-assembly of the saturated heterotopic triple-stranded helicate (HHH)-[EuZn(**109**)<sub>3</sub>]<sup>5+</sup>. The representation of the complex on the right corresponds to the crystal structure found in the solid state.<sup>190</sup> (Reproduced with permission from ref 186. Copyright 1996 *Chimia*.)

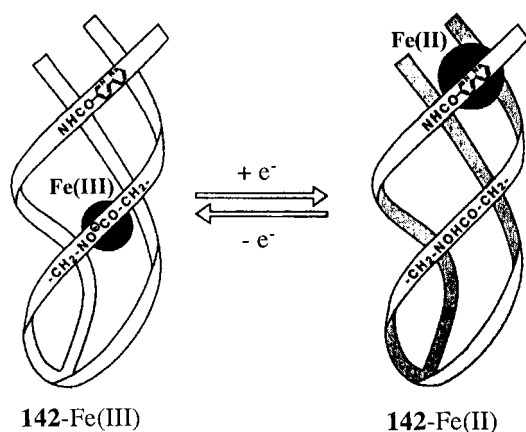


**Figure 48.** Schematic representation of triple-stranded helical complexes [Fe(**142**)]<sup>2+</sup> working as molecular switches based on redox properties of Fe<sup>III</sup>/Fe<sup>II</sup>.<sup>191</sup> (Reproduced with permission from ref 191. Copyright 1995 Macmillan Magazines Limited.)

concentration ( $10^{-4}$  M), and the X-ray crystal structure of (HHH)-[EuZn(**109**)<sub>3</sub>]<sup>5+</sup> confirms the triple-helical structure previously established in solution (Figure 47).<sup>150,190</sup> The luminescence intensity is increased by a factor  $10^3$ – $10^4$  when going from (HHH)-[EuZn(**8**)<sub>3</sub>]<sup>5+</sup> to (HHH)-[EuZn(**109**)<sub>3</sub>]<sup>5+</sup> which exemplifies the crucial influence of the binding units on the physicochemical properties of the lanthanide helicates.

Shanzer and co-workers recently synthesized heterotopic achiral **142** and chiral **143** podands possessing one "hard" hydroxamate and one "soft" bipyridine binding unit along the strand.<sup>191</sup> These new podands exhibit potential interest for the self-assembly of d–d heteronuclear head-to-head triple-stranded helicates (Figure 48).<sup>191</sup>

### 3. Unsaturated Triple-Stranded Helicates

The bis-monodentate pyridonate **9** is clearly not suitable for the self-assembly of saturated helicates with metal ions displaying large coordination numbers, but the bidentate nitrate anion may efficiently complete the vacant positions around Ln(III)<sup>183,192</sup> and Goodgame and co-workers have isolated and characterized the unsaturated homotopic triple-stranded helicate [Nd<sub>2</sub>(**9**)<sub>3</sub>(NO<sub>3</sub>)<sub>6</sub>] in the solid state (Figure 7).<sup>38</sup> The partial removing of the capping

NO<sub>3</sub><sup>-</sup> might lead to infinite linear polymeric triple-stranded helicates, but other geometries cannot be excluded.<sup>38</sup> A very simple tridentate ligand **144** has been shown to react with LnCl<sub>3</sub> (Ln = Y, Lu) in basic medium containing Na<sup>+</sup> to give the heterodinuclear complex [ClLu(**144**)<sub>3</sub>Na].<sup>193</sup> The <sup>1</sup>H NMR data imply dynamic processes in solution, but the lack of a C<sub>2</sub> axis passing through the ligand and the equivalence of the three strands strongly suggest the formation of the heterotopic C<sub>3</sub>-triple-stranded helicate which is confirmed by the X-ray crystal structure.<sup>193</sup> Lu(III) is seven-coordinated by three dimethylamino side arms, three bridging phenolate groups, and one terminal chloride anion while Na(I) is six-coordinated by the bridging phenolates and the three remaining dimethylamino side arms. A remarkable crystal packing is observed where the Lu–Cl vector of one residue points toward the Na(I) of the next helicate, thus forming a continuous string of helically wrapped complexes in the crystal.<sup>193</sup>

## V. Applications of Helicates

A considerable part of the research devoted to the helicates is academic and results from the design of aesthetically appealing helical and entwined supramolecular structures. Beyond this enjoyable aspect, the systematic investigation of the intrinsic informations encoded in the components yields an inroad into new technologies and new synthetic processes based on the detailed understanding of self-assembly and self-organization. This field has reached a point where it is now possible to consider some specific applications associated with these fascinating helical structures. A first attractive project is the introduction of self-assembled helicates as building blocks in helical macromolecular structures leading to new chiral and nonlinear properties.<sup>194</sup> Columnar right-handed helical superstructures based on complementary self-assembled hydrogen-bonded supramolecular complexes have been reported by Lehn and co-workers,<sup>195</sup> and a related transfer of molecular helical chirality to a larger supramolecular edifice using a double-stranded helicate has been proposed by Eisenbach, Newkome, and co-workers.<sup>114</sup> Their synthetic strategy aims to develop the 6,6'-bis-functionalized oligobipyridine unit **67** possessing long lipophilic organic chains which can generate double-stranded helical cores [Cu<sub>2</sub>(**67**)<sub>2</sub>]<sup>2+</sup> within the polymeric backbone.<sup>114</sup> An alternative approach uses the packing of helicates along their helical axis to produce helical columns of stacked complexes. This has been fortuitously observed in the crystal structures of the double-stranded helicate [Cu<sub>2</sub>(**48**)<sub>2</sub>]<sup>2+</sup> which forms adjacent infinite helical columns of opposite helicity (Figure 49)<sup>95</sup> and in packed dimers for (i) the double-stranded helicate (HH)-[CoAg(**7**)<sub>2</sub>]<sup>3+</sup> (the two units display identical helicity)<sup>34</sup> and (ii) the triple-stranded helicate (HHH)-[EuZn(**109**)<sub>3</sub>]<sup>5+</sup> (the two packed cations are related by a center of inversion).<sup>150,190</sup> Planned syntheses of infinite single-stranded [Cu<sub>n</sub>(**40**)<sub>n</sub>]<sup>n+</sup><sup>90</sup> and triple-stranded helicates derived from the building block {[Nd(**9**)<sub>3</sub>]<sub>n</sub>}<sup>(3n)+</sup> have been proposed,<sup>38</sup> but no detailed studies of the properties of these new materials have been reported.

The generation of dinuclear helicates produces metal-containing macrocyclic (for double-stranded

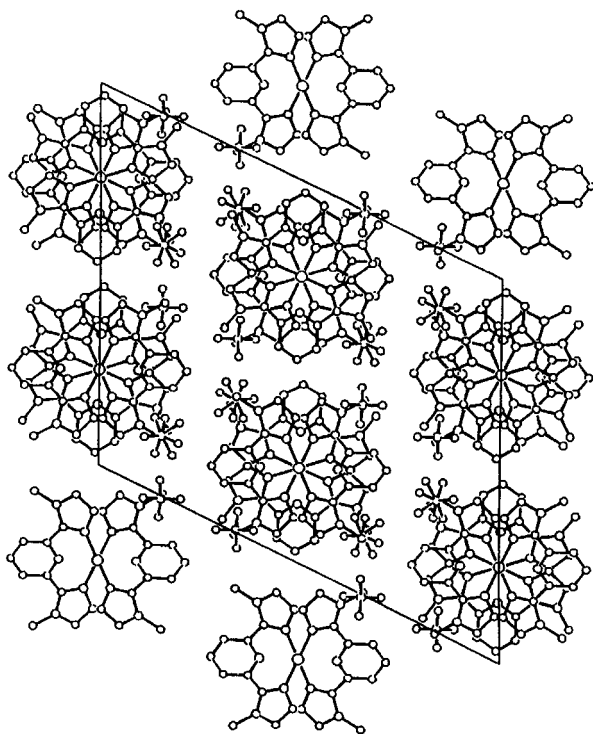


**Figure 49.** ORTEP view of the packing along the *b* axis of the unit cell showing the columns of packed double-stranded helicates  $[\text{Cu}_2(\mathbf{48})_2](\text{ClO}_4)_2$ .<sup>95</sup> Adjacent columns are of opposite helicity. (Reproduced with permission from ref 95. Copyright 1993 VCH Publishers.)

helicates), or macrobicyclic (for triple-stranded helicates) cavities constituted by the wrapped strands and the coordinated metal ions. Except for side-by-side helicates, this cavity is chiral and may lead to selective host-guest recognition processes. Systematic investigations of potential host cavities based on self-assembled double-stranded helicates have been reported by Beer and co-workers (ligands **76–80**)<sup>122</sup> and by Harding and co-workers (ligands **81–83** and **95–97**).<sup>123,124,139</sup> Until now, only few host-guest interactions have been clearly established, but (i) *o*- and *m*-dimethoxybenzene have been found to act as templating agents for the formation of the  $D_2$ -helical double-stranded helicate  $[\text{Zn}_2(\mathbf{83})_2]^{4+}$  where they probably occupy the intermetallic cavity<sup>124</sup> and (ii) alkali metal cations ( $\text{Li}^+$ ,  $\text{Na}^+$ ,  $\text{K}^+$ ) has been found

#### Chart 18

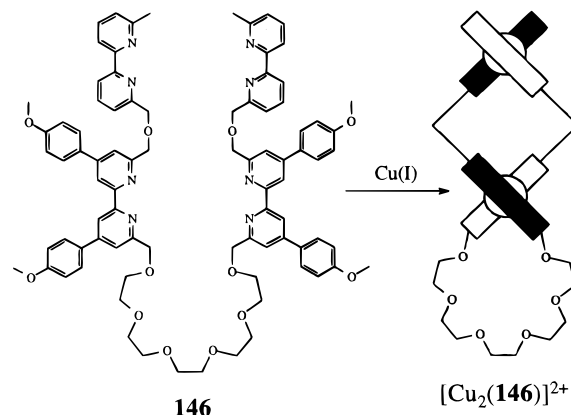
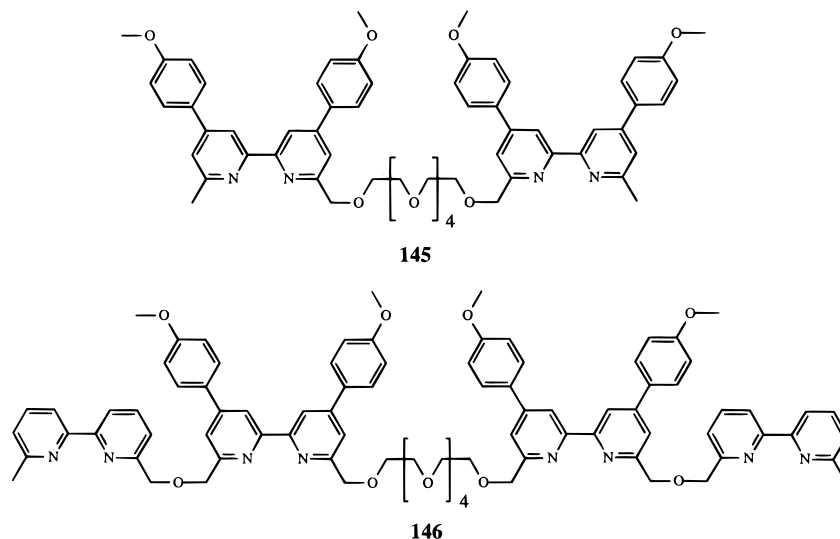


**Figure 50.** Formation of a pseudocrown ether cavity by self-assembly of the double-stranded helicate  $[\text{Cu}_2(\mathbf{146})]^{2+}$ .<sup>13</sup>

in the macrobicyclic cavity of the triple-stranded helicate  $[\text{Li}\text{Ti}_2(\mathbf{136})_3]^{3-}$ ,  $[\text{Na}\text{Ti}_2(\mathbf{137})_3]^{3-}$ , and  $[\text{K}_2\text{Ti}_2(\mathbf{138})_3]^{2-}$  in the solid state<sup>167,178,179</sup> and in solution for  $[\text{Na}\text{Ti}_2(\mathbf{137})_3]^{3-}$ .<sup>179</sup> A chloride anion has been observed to be strongly bound in the internal cavity of the circular double-stranded helicate  $[\text{Fe}_5(\mathbf{124})_5(\text{Cl})]^{9+}$  (Figure 44).<sup>182</sup> It has been suggested that the chloride anion may act as a template for the formation of this particular helicate. Nabeshima and co-workers have developed an alternative approach using acyclic polyether ligands connected to terminal bipyridine **145** or oligobipyridine units **146**<sup>13</sup> (Chart 18). Upon complexation to  $\text{Cu}(\text{I})$ , the self-assembly leading to the double-stranded helicate  $[\text{Cu}_2(\mathbf{146})]^{2+}$  simultaneously produces a chiral metal-containing pseudocrown ether suitable for complexation and recognition of alkali (Figure 50).<sup>13</sup> The mononuclear precursor  $[\text{Cu}(\mathbf{145})]^+$  indeed efficiently transports alkali metals in the metal-containing macrocyclic cavity with a high selectivity for  $\text{K}^+$  resulting from a balance between the cavity size and the electrostatic repulsion between the alkali ion and the copper metal ion coordinated to the bipyridine units of the artificial allosteric ionophore. In the dinuclear helicate  $[\text{Cu}_2(\mathbf{146})]^{2+}$ , the cooperative binding of  $\text{Cu}(\text{I})$  significantly increases the kinetic inertness which blocks the fast racemization observed for  $[\text{Cu}(\mathbf{145})]^+$  and provides a chiral pseudocrown ether cavity. Preliminary studies

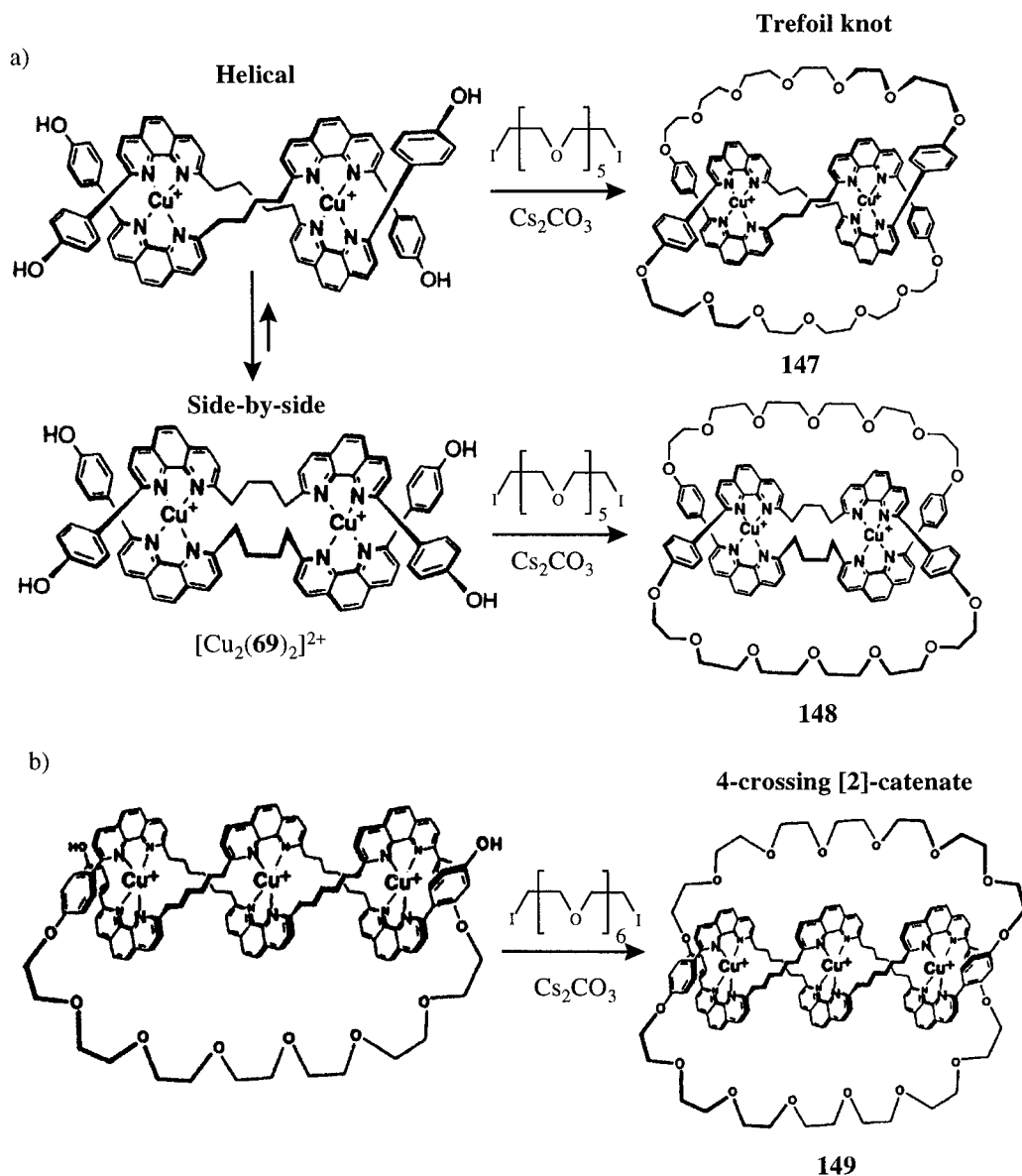


**Figure 51.** Metal-templated synthesis of (a) a molecular trefoil knot<sup>12,116</sup> and (b) a doubly interlocked [2]-catenane.<sup>199</sup> (Reproduced with permission from refs 116 and 199. Copyright 1992 and 1996 Gauthier-Villars Publishers.)

with potassium *L*-mandelate strongly suggest chiral host–guest interactions.<sup>13</sup>

The use of helicates in host–guest recognition processes is not limited to endoreceptors and Lehn and co-workers have taken advantage of the specific orientation of the bipyridine binding units in their double-stranded helicates to design exoreceptors.<sup>110,113</sup> The di- to pentanuclear double-stranded helicates  $[\text{Cu}_2(\mathbf{55})_2]^{2+}$ ,  $[\text{Cu}_3(\mathbf{4})_2]^{3+}$ ,  $[\text{Cu}_4(\mathbf{61})_2]^{4+}$ , and  $[\text{Cu}_5(\mathbf{63})_2]^{5+}$  strongly bind double-helical DNA and the binding affinity depends on the size of the helicate.<sup>113</sup> Although the helicates have probably multiple interacting sites, several elements point to major-groove binding. Single-strand cleavage of DNA is observed upon visible-light irradiation making these helicates promising candidates for the selective recognition, binding, and cleavage of oligonucleotides.<sup>113</sup> The attachment of thymidine groups on the periphery of the double-stranded helicate  $[\text{Cu}_3(\mathbf{60})_2]^{3+}$  might provide exoreceptors for thymidine–adenine–thymine interactions of the triple-helix type<sup>196</sup> with adenine–thymine pairs in the DNA.<sup>110</sup>

Dinuclear double-stranded helicates have been used by Dietrich-Buchecker, Sauvage, and co-workers

as precursors for the synthesis of topologically non-trivial trefoil knots and interlocked catenanes.<sup>12,116,117</sup> Their strategy requires the formation of stable polynuclear double-stranded helicates which then undergo a four-center cyclization of the appropriate termini (Figure 51).<sup>12</sup> Initial attempts used the demethylated dinuclear double-stranded helicate derived from  $[\text{Cu}_2(\mathbf{69})_2]^{2+}$  and led to the first knotted system **147** in only 3% yield.<sup>197</sup> The main limitation of this strategy is associated with an unfavorable thermodynamic equilibrium between the  $D_2$ -helical and the  $C_{2h}$ -side-by-side helicates (ratio 1:8); the latter conformer producing the unknotted bis-macrocyclic structure **148** (Figure 51a). Further investigations led to quantitative formation of the  $D_2$ -helical double-stranded helicate  $[\text{Cu}_2(\mathbf{71})_2]^{2+}$  with the benzene-1,3-diyl spacer, eventually leading to the final trefoil knot in 30% yield.<sup>117</sup> The formation of the knot induces a significant kinetic stabilization of the coordinated metal ions and controlled demetalation of only one metal ion produces a vacant tetrahedral coordination site which can be easily occupied by an entering metal ion leading to heterodinuclear CuAg and CuZn knotted complexes reminiscent of

heterodinuclear helicates.<sup>198</sup> Trinuclear double-stranded helicates are precursors of more complicated topologically nontrivial structures and the doubly interlocked [2]-catenate **149** has been detected in an intricate mixture of products (Figure 51b).<sup>199</sup> Several promising developments of topologically complex structures based on helicates have been proposed<sup>12</sup> and recently reviewed.<sup>15</sup> For double-stranded helicates, an odd number of metal ions provides a route to  $(n+1)$ -crossing-[2] catenanes while an even number of metals gives knotted single curves.<sup>12</sup> Extension of this strategy to a multicenter cyclization (six or more) has not yet been attempted, but the circular helicates  $[\text{Fe}_3(\mathbf{98})_3]^{6+}$ <sup>140</sup> and  $[\text{Fe}_5(\mathbf{124})_5(\text{Cl})]^{9+}$ <sup>182</sup> might be good candidates for the preparation of respectively trefoil and fivefoil knots while more complicated entwined or knotted structures might result from (i) triple-stranded helicate as precursors and (ii) the dimerization of semiknotted helical threads leading to the formation of molecular composite knots. Sauvage and co-workers have recently reported the first preparation of a composite trefoil knot obtained by the Glaser coupling of two semiknotted dinuclear double-stranded helicates.<sup>200</sup>

Careful consideration of space-filling models of double- and triple-stranded helicates shows that the wrapping of the strands produces compact structures where the metal ions are not easily accessible. Photophysical studies of the double-stranded helicates  $[\text{Cu}_2(\mathbf{34})_2]^{2+}$  and  $[\text{Cu}_2(\mathbf{68})_2]^{2+}$  have established that the metals are sufficiently protected from external interactions (i.e., solvent or anion quenching processes) to give significant luminescence of the MLCT level.<sup>126</sup> However, minor distortions of the coordination sites in the analogous double-stranded helicates  $[\text{Cu}_2(\mathbf{52})_2]^{2+}$  and  $[\text{Cu}_2(\mathbf{84})_2]^{2+}$  allow some interactions with the surrounding medium which completely quench the luminescence.<sup>126</sup> For triple-stranded helicates, the three closely packed strands are expected to protect more efficiently the metal ions as demonstrated by the long lifetime emission ( $\sim 2$  ms) of the  $^5\text{D}_0$  level of the mononuclear lanthanide precursor  $[\text{Eu}(\mathbf{44})_3]^{3+}$ .<sup>201</sup> However, the quantum yield in solution is low as a result of intramolecular quenching processes associated with the helically packed 2,6-bis-benzimidazole-pyridine ligands<sup>201</sup> and Piguet, Bünzli, and co-workers have suggested that the development of supramolecular UV  $\rightarrow$  visible light-converting devices based on triple-stranded helical lanthanide building blocks requires their introduction into heterotopic helicates where a thermodynamically stable and structurally rigid pseudooctahedral d-block metal ion occupies one coordination site.<sup>186,187</sup> According to this strategy, the first heterotopic triple-stranded helicates (HHH)- $[\text{LnZn}(\mathbf{8})_3]^{5+}$  (Ln = La–Lu) have been isolated recently and display the expected threaded structure with the d-block metal ions occupying the pseudooctahedral site defined by the three bidentate binding units of the strands (Figure 6). Despite protection of the lanthanide by the three strands, intramolecular quenching processes lead to only faint luminescence in (HHH)- $[\text{LnZn}(\mathbf{8})_3]^{5+}$  (Ln = Eu, Tb).<sup>36,37</sup> This drawback is avoided in the analogous, but strongly luminescent triple-stranded helicate (HHH)- $[\text{EuZn}(\mathbf{109})_3]^{5+}$  where carboxamide groups favor intra-

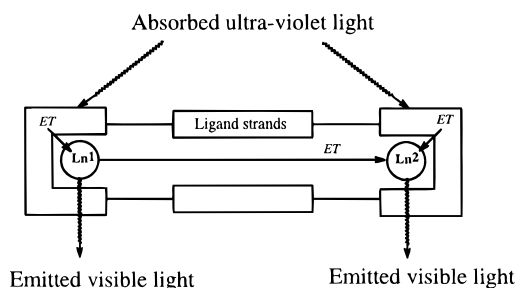


**Figure 52.** Schematic representation of an organized directional light-converting device based on a homotopic triple-stranded helicate with lanthanide metal ions  $\text{Ln}^1$  and  $\text{Ln}^2$ .<sup>186</sup> (ET: energy transfer). (Reproduced with permission from ref 186. Copyright 1996 Chimia.)

molecular ligand  $\rightarrow \text{Eu}^{\text{III}}$  energy transfer.<sup>150,190</sup> The introduction of two different  $\text{Ln}^{\text{III}}$  into the homotopic triple-stranded helicate  $[\text{EuTb}(\mathbf{98})_3]^{6+}$  has initiated the investigation of promising directional visible  $\rightarrow$  visible supramolecular light-converting devices (Figure 52).<sup>184</sup>

The recent preparation of the unsaturated heterotopic double-stranded helicate (HH)- $[\text{Ru}_2(\mathbf{7})_2(\text{C}_2\text{O}_4)]^{2+}$  offers promising possibilities for the development of photophysical and electrochemical devices.<sup>155</sup> Preliminary studies show that  $[\text{Ru}_2(\mathbf{7})_2(\text{H}_2\text{O})_2]^{4+}$  may be oxidized to Ru(IV) and Ru(VI) oxo species which are active catalysts for the oxidation of various organic substrates.<sup>155</sup> However, no reliable structure for the oxidized form of these catalysts has been established and it is not clear if the double-stranded helical structure is retained.

## VI. Characterization of Self-Assembled Helicates

The reversible labile noncovalent interactions involved in the assembly of supramolecular complexes provide molecular edifices in equilibrium with their components.<sup>1,25</sup> The characterization of the final complexes in solution is thus a challenge, but the detailed knowledge of the thermodynamic recognition processes occurring in solution is crucial for the design of stable helicates with predetermined structural and electronic properties.<sup>186</sup> Complete and detailed structural information may be readily obtained from X-ray crystal structures provided not only that the desired helicate is isolable in the solid state, but that it yields crystals suitable for X-ray diffraction studies. Most of the structural descriptions of helicates reported in the literature result from X-ray diffraction studies, but a total reliance on crystal structure determination poses several problems: (i) it is quite often impossible to grow suitable crystals for large supramolecular helicates and, when it is possible, disordered solvent molecules and counterions can give considerable problems for the resolution and refinement of the structure (see section VI.B) and (ii) the crystallization process may affect significantly the external conditions controlling the assembly process leading to structures in the solid state different from the species observed in solution. Therefore, the complete characterization of the species formed in solution is necessary, but it is particularly difficult for helicates because (i) these supramolecular complexes are labile, (ii) they often display complicated dynamic behavior in solution, and (iii) they bear positive or negative charges (only

few helicates are neutral)<sup>174</sup> and they are nonvolatile which severely limits the use of classical MS techniques and low-resolution solution-phase methods based on colligative properties for the determination of molecular weights.<sup>14,40</sup>

## A. Thermodynamic Self-Assembly and Solution Structures

NMR spectroscopy is often considered as the method of choice for characterizing helicates in solution and this is probably justified for the structural investigations of the final helicate (*vide infra*). However, NMR techniques suffer from two major drawbacks for the complete characterization of the thermodynamic processes: (i) large concentrations of helicates are required for recording NMR spectra which prevent the observation of poorly stable intermediates and (ii) dynamic equilibria on the NMR time scale between conformers or diastereomers may hinder the detailed characterization of multicomponent self-assemblies. Consequently, only a few complete solution studies of helicate self-assembly have been reported. However, the pioneer work of Lehn and co-workers dedicated to cooperativity<sup>43,46,47</sup> and self-recognition<sup>115</sup> in solution, and the application of the new soft electrospray-MS (ES-MS) technique<sup>202</sup> to the characterization of helicates by Hopfgartner, Piguet, and co-workers<sup>98,140</sup> and by Lehn and co-workers<sup>115</sup> have led to an efficient three-step procedure for characterizing helicate self-assemblies: (1) a reliable qualitative speciation of the intermediates and products involved in the assembly process is obtained by ES-MS titrations of the ligand strands with the metal ions, (2) the quantitative analysis is then obtained by mathematical fitting of spectrophotometric or potentiometric titrations obtained in the same conditions as those used for ES-MS, and (3) NMR spectroscopy associated with other techniques (electrochemistry, emission spectroscopy, etc.) is used for the structural investigation of the various complexes in solution.

### 1. Qualitative Speciation

First, the exact number of intermediates and helicates formed by the self-assembly must be estimated together with their relative and absolute stoichiometries. Before the development of ES-MS, no universal and reliable methods were available. Attempts using factor analysis<sup>203</sup> or single value decomposition<sup>204</sup> applied to spectrophotometric data<sup>29</sup> have led to satisfying speciations for homotopic double- and triple-stranded helicates with d-block metal ions,<sup>29,169</sup> but to oversimplifications in the assembly of triple-stranded helicates with 4f-block metal ions as a result of the correlation between the absorption spectra of the various intermediates.<sup>37,150,184</sup> The relative stoichiometry of the various components within supramolecular helicates has been tentatively addressed by using evolving factor analysis<sup>205</sup> or Job's plots<sup>206</sup> which are satisfying for simple assembly processes,<sup>174</sup> but inaccurate for complicated processes as exemplified by the dinuclear double-stranded helicate  $[\text{Cu}_2(\mathbf{44})_2]^{2+}$  which was first thought to spontaneously dissociate in solution to give the T-shaped mononuclear complex  $[\text{Cu}(\mathbf{44})]^+$ .<sup>94</sup> Subsequent conductivity and NMR measurements eventu-

ally established that the dinuclear helical structure was maintained in aprotic solvents.<sup>91</sup> The use of mass spectrometry as a chemical balance for molecular weights was considered as a promising technique quite early in the development of supramolecular chemistry, but the transfer of nonvolatile charged and weakly stable species into the gas phase was difficult. Fast atom bombardment MS (FAB-MS)<sup>207</sup> was first applied to the characterization of helicates after their isolation in the solid state<sup>62,64,82,130</sup> and it is still used in some isolated cases.<sup>30</sup>

FAB-MS requires solubilization or suspension of the complex in a liquid matrix (e.g., nitrobenzyl alcohol) deposited on a target which is then bombarded with neutral atoms (argon or xenon) to generate gas phase ions via a complex mechanism. Typical FAB-MS spectra of double-stranded helicates  $[\text{M}_2\text{L}_2]^{4+}$  show series of singly charged peaks corresponding to  $[\text{M}_2\text{L}_2(\text{X})_3]^+$ , where, for instance  $\text{M}(\text{II}) = \text{Mn}, \text{Fe}, \text{Cu}, \text{Cd}$ , and  $\text{X} = \text{PF}_6^-$ . Unfortunately, the monomer  $[\text{ML}]^{2+}$  is often observed as the base peak of the FAB-MS spectra, and it is difficult to establish clearly if it results from fragmentation occurring during the ionization process or from its existence as a chemical entity in the sample. Moreover, FAB-MS ionization can often lead to (i) matrix interferences especially in the low mass to charge range, (ii) fragmentation (often intense and preventing the detection of the molecular ion), (iii) reduction, or (iv) demetalation of the complexes. The application of UV-matrix-assisted laser desorption ionization (MALDI)<sup>208</sup> for the characterization of supramolecular complexes has not yet been demonstrated although this technique also requires dissolution of the complex in a matrix.<sup>209</sup> However, as a result of the relatively strong conditions of volatilization used in MALDI, extensive fragmentation of the complexes is expected. In general, the use of a matrix chemically different from the solvents in which the NMR and spectrophotometric studies are performed in solution can be a severe handicap for the correlation of the MS results with those obtained with other techniques.

Recently, considerable interest has been focused on electrospray ionization as a means of handling intractable, high-molecular weight compounds such as biopolymers.<sup>202</sup> Electrospray (ES) is a very soft atmospheric pressure ionization (API) technique where the sample solution is infused at flow rates typically in the range of 1–10  $\mu\text{L}/\text{min}$  through a stainless steel or a fused silica capillary sprayer. A charged aerosol of very fine droplets is generated by applying a high electric potential (4–6 kV) to the tip of the sprayer. Preformed ions in solution are then transformed into gas-phase ions by the rapid decrease of droplet size according to a mechanism which is not fully understood.<sup>210,211</sup> Gas-phase ions are then sampled from the atmospheric pressure into the high vacuum through an interface while neutral solvent molecules remain outside. Various mass analyzers (quadrupole, ion traps, time-of-flight, magnetic sectors, and ion cyclotron resonance mass spectrometers) have been used to separate these ions according to their  $m/z$  ratios.<sup>212</sup>

Desolvation and/or declustering of the analyte ions without causing fragmentation (up-front collision-induced dissociation)<sup>213</sup> can be performed in the

interface with the help of (i) heat, (ii) an inert curtain gas, or (iii) electric forces depending on the interface design. Pure electrospray was originally limited to very low flow rates (1–10  $\mu\text{L}/\text{min}$ ) and essentially organic solvent mixtures (methanol or acetonitrile). The spray process has been further optimized and different modifications of electrospray were developed including nanospray<sup>214</sup> and ion spray (IS-MS)<sup>215</sup> (pneumatically assisted electrospray).

Coordination and supramolecular complexes are typical examples of preformed ions in solution which are difficult to analyze by using classical mass spectrometry techniques. Chait and co-workers<sup>216</sup> first demonstrated the applicability of ES-MS for the analysis of  $[\text{Ru}(\text{bipy})_3]^{2+}$  in acetonitrile, methanol, or acetone. Applications to supramolecular self-assembly processes rapidly followed. Hopfgartner and co-workers<sup>98,140</sup> applied this technique to helicates and van Dorsselaer and co-workers to cylindrical metal-containing assemblies,<sup>43</sup> interlocked catenanes and knots,<sup>217</sup> and metal-containing macrocycles.<sup>218</sup>

One of the key features of ES-MS for the analysis of supramolecular complexes is the conservation of the charge state from the condensed phase into the gas phase leading to the reliable determination of the molecular weight of the supramolecular cationic complexes from signals at rather low to mass-to-charge value ( $m/z$ ) resulting from the multiply charged nature of the cations. The systematic application of this technique shows that ES-MS spectra qualitatively reflect the nature and the distribution of the different species present in solution. A large selection of solvents can be used for ES-MS analysis including water, methanol, acetonitrile, acetone, and chloroform. In order to limit decomplexation, ES-MS spectra of supramolecular complexes are recorded from relatively concentrated solutions for mass spectrometry (about  $10^{-4}$  M), and it appears essential to operate the instrument under rather unusual conditions (reduced multiplier gain, sprayer position, sprayer voltage)<sup>140,216</sup> which prevent saturation of the signal. Since electrospray ionization may be considered as an electrophoresis cell of a special type,<sup>219</sup> oxidation of stainless steel sprayers during the ionization process can severely affect the mass spectra, a fused silica sprayer should therefore be preferred.

One of the early ES-MS analyses of a supramolecular complex concerned the triple-stranded helicate  $[\text{Co}_2(\mathbf{5})_3](\text{ClO}_4)$  (1891.37  $\text{g mol}^{-1}$ ).<sup>98,140</sup> The ES-MS spectrum for a concentration of  $10^{-4}$  M in acetonitrile led to the almost exclusive observation of the cation  $[\text{Co}_2(\mathbf{5})_3]^{4+}$  at  $m/z$  373 with isotopic peaks separated by 0.25 Da which confirmed the charge 4+ borne by the cation (Figure 53). Further peaks that result from the association with perchlorate anions were observed at  $m/z$  530 and 846 and correspond to  $[\text{Co}_2(\mathbf{5})_3(\text{ClO}_4)]^{3+}$  and  $[\text{Co}_2(\mathbf{5})_3(\text{ClO}_4)_2]^{2+}$ , respectively. These associations between the cationic helicates and various counteranions ( $\text{CF}_3\text{SO}_3^-$ ,  $\text{PF}_6^-$ ,  $\text{ClO}_4^-$ ) are very common in ES-MS and have been tentatively attributed to electrostatic interactions.<sup>140</sup> It is worth noting that the relative intensities of these ions in the spectra strongly depend on the sprayer position. Under soft declustering conditions no significant fragmentation is observed which allows the

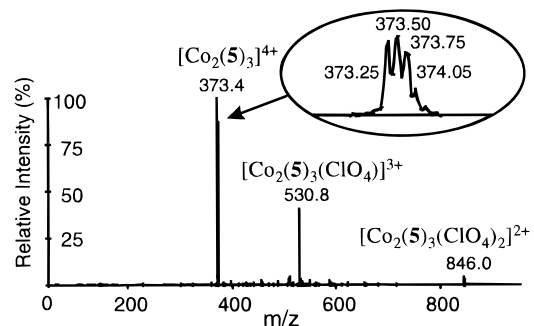


**Figure 53.** IS-MS spectrum of the dinuclear triple-helical complex  $[\text{Co}_2(\mathbf{5})_3](\text{ClO}_4)_4$  in acetonitrile.

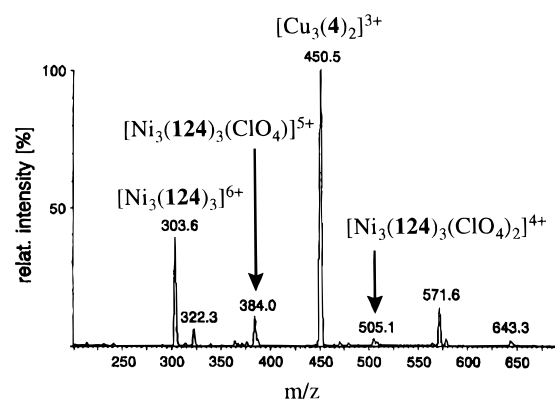


**Figure 54.** ES-MS spectrum of the mixture of the double-stranded helicate  $[\text{Cu}_3(\mathbf{4})_2]^{3+}$  and the triple-stranded helicate  $[\text{Ni}_3(\mathbf{124})_3]^{6+}$  in acetonitrile. (Reproduced with permission from ref 115. Copyright 1993 National Academy of Sciences USA.).

easy characterization of mixtures as demonstrated by Lehn and co-workers<sup>115</sup> during the self-recognition of the oligobipyridine strands **4** and **124** with the metal ions Cu(I) and Ni(II) in acetonitrile. In the ES-MS spectra, they only found peaks corresponding to the double-stranded helicate  $[\text{Cu}_3(\mathbf{4})_2]^{3+}$  ( $m/z$  450.3) and the triple-stranded helicate  $[\text{Ni}_3(\mathbf{124})_3]^{6+}$  ( $m/z$  303.6) complexes (Figure 54). No interference originating from the infusing solvent is observed.

The ES-MS characterization of a supramolecular complex requires a reliable assignment of its total charge. This is particularly critical for self-assembled dinuclear double-stranded helicates because the singly-charged monomer (for instance  $[\text{Cu}(\mathbf{45})]^+$ ) and the doubly-charged helicate ( $[\text{Cu}_2(\mathbf{45})_2]^{2+}$ ) display the same mass to charge ratio ( $m/z$  675.4) (Figure 55). The isotopic mass distribution shows peaks separated by 0.5 Da which is only compatible with the doubly charged species and the formation of the double-stranded helicate.<sup>98</sup> However, tandem MS-MS experiments have demonstrated that the dimer  $[\text{Cu}_2(\mathbf{45})_2]^{2+}$  fragments in the gas phase to give the monomer  $[\text{Cu}(\mathbf{45})]^+$ .<sup>140</sup> Thus the declustering energy for the analysis of such complexes should be kept as low as possible.

Unfortunately, the resolution of quadrupole instruments is limited to doubly or triply charged ions. For higher charge states magnetic sector or ion trap mass spectrometer are more adequate as exemplified by Ho and co-workers<sup>135</sup> who have used the isotopic mass distribution for the ES-MS characterization of the double-stranded helicate  $[\text{Cu}_2(\mathbf{93})_2]^{4+}$  with a magnetic sector instrument. An alternative approach for the determination of the charge state (and

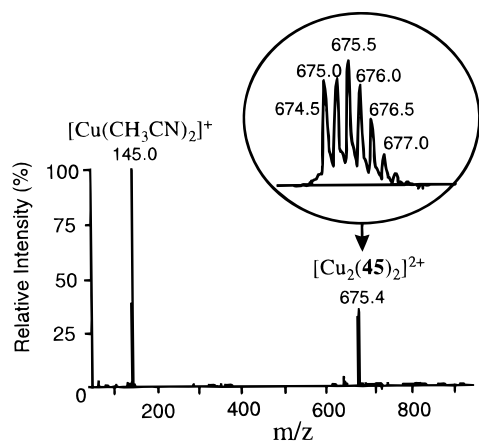


**Figure 55.** IS-MS spectrum of the dinuclear complex  $[\text{Cu}_2(\mathbf{45})_2](\text{ClO}_4)_2$  in acetonitrile.

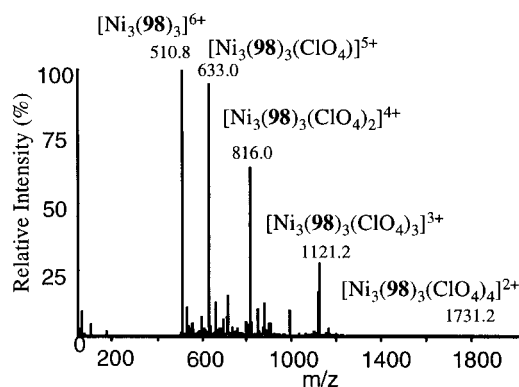


**Figure 56.** IS-MS spectrum of the circular helicate  $[\text{Ni}_3(\mathbf{98})_3](\text{ClO}_4)_6$  in acetonitrile.

the molecular weight of the helicate) is the use of peaks resulting from the association with counterions. For cationic supramolecular helicates, the association with counteranions ( $\text{ClO}_4^-$ ,  $\text{PF}_6^-$ ) produces an increase of the mass and a decrease of the total charge of the complex by one unit. The molecular weight of the complex can be thus determined as described for proteins.<sup>140</sup> Using this approach, the circular single-stranded helicates  $[\text{M}_3(\mathbf{98})_3]^{6+}$  ( $\text{M} = \text{Fe}, \text{Ni}$ ) have been first recognized by ES-MS while a double-stranded helical structure  $[\text{M}_2(\mathbf{98})_2]^{4+}$  was suggested from spectrophotometric results. The resolution of the mass spectrometer did not allow the direct determination of the charge state of the peak at  $m/z$  511 ( $[\text{Ni}_2(\mathbf{98})_2]^{4+}$  or  $[\text{Ni}_3(\mathbf{98})_3]^{6+}$ ), but the lack of the peak at  $m/z$  714 corresponding to the expected perchlorate adduct  $[\text{Ni}_2(\mathbf{98})_2\text{ClO}_4]^{3+}$  ruled out the double-helical structure. On the basis of the ions at  $m/z$  633, 816, 1121, and 1731, corresponding to perchlorate adducts of a 6+ charged species, it was possible to establish the existence of the circular helicate  $[\text{Ni}_3(\mathbf{98})_3]^{6+}$  in solution which has been confirmed later by NMR studies with various metal ions (Figure 56).<sup>140</sup> Recently, Lehn and co-workers<sup>182</sup> have reported a related ES-MS characterization of the circular double-stranded helicate complex  $[\text{Fe}_5(\mathbf{124})_5\text{Cl}]^{9+}$  where associations with  $\text{PF}_6^-$  has been observed in  $[\text{Fe}_5(\mathbf{124})_5\text{Cl}(\text{PF}_6)_{(2+n)}]^{(7-n)+}$  ( $n = 0-5$ ). The structure of this complex was confirmed by X-ray analysis.<sup>182</sup>

If the ES-MS analysis of supramolecular complexes with d-block metal ions is now relatively straightforward, some limitations have been found with

triple-stranded helicates containing lanthanide metal ions,  $\text{Ln}(\text{III})$ , which give only faint ES-MS response.<sup>150</sup> Only saturated lanthanide helicates may be easily observed with ES-MS while unsaturated helicates are very difficult to detect.<sup>37</sup> A recent study of macrocyclic complexes with alkali metal ions has suggested that the response factor in the ES-MS spectra mainly depends on the solvation energy.<sup>220</sup> This may explain why 4f-block helicates are more difficult to observe by ES-MS since  $\text{Ln}(\text{III})$  are known to display large solvation energies. Nevertheless, saturated homo- and heteropolynuclear triple-stranded helicates with 4f-block metal ions have been characterized successfully with ES-MS.<sup>140,150</sup>

In two cases, Van Dorsselaer and co-workers have found that the intensities of the supramolecular complexes observed in the ES-MS spectra are in good agreement with their relative amounts calculated from spectrophotometric titrations, suggesting that a quantitative ES-MS analysis is possible.<sup>43,221</sup> However, the response factors in ES-MS for the different species can be affected by numerous parameters which have not yet been fully investigated such as (i) total charge of the complex, (ii) the nature of the complex, (iii) the total concentration of ligands and metal ions in solution, (iv) the solvent and solvation processes, and (v) the declustering energy. Quantitative speciation by ES-MS should be considered with caution and may apply only in very specific cases.<sup>43,140,221</sup>

In conclusion, ES-MS is generally used for the qualitative speciation of the complex present in solution at different ligand to metal ratios. This information, combined with the quantitative spectrophotometric or potentiometric titrations obtained under similar conditions allows the elaboration of a chemical model for the assembly process. A first test is then readily made by dilution at a fixed ligand to metal ratio as illustrated in Figure 57 for the heterodinuclear triple-stranded helicate (HHH)- $[\text{EuZn}(\mathbf{109})_3]^{5+}$ .<sup>150</sup> For a total ligand concentration of  $10^{-4}$  M, only the heterodinuclear helicate  $[\text{EuZn}(\mathbf{109})_3]^{5+}$  and its adducts ions are observed in acetonitrile (Figure 57a). At  $10^{-5}$  M, the ES-MS spectrum reveals the formation of significant amounts of  $[\text{Zn}(\mathbf{109})_3]^{2+}$  and  $[\text{Zn}(\mathbf{109})_2]^{2+}$  in agreement with the stability constants proposed for the assembly process (Figure 57b).<sup>150</sup>

Finally, one of the very attractive features of API interface is the ability to perform up-front collision-induced dissociation (up-front CID) by varying an electric potential in the interface. Under low declustering or up-front CID conditions, solvent molecules or traces of free ligand can form clusters with the complex of interest which may confuse the interpretation of the ES-MS spectra.<sup>216</sup> A careful tuning of the declustering energy leads to a controlled desolvation and the observation of the bare complex. Further structural informations on composite mixtures or single species can be gained by collision-induced dissociation (CID) in the collision cell of a triple stage mass spectrometer<sup>140,222</sup> while the analyte of interest is isolated in the first mass analyzing quadrupole and the fragments recorded in the second mass analyzing quadrupole. Preliminary tandem mass spectrometric data suggest that interlocked

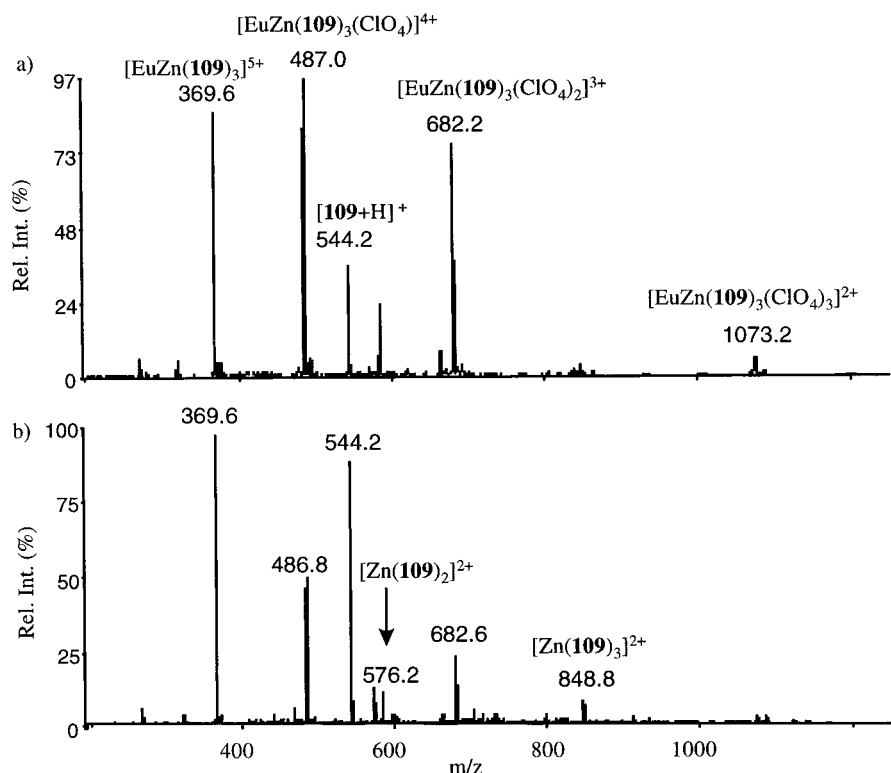


**Figure 57.** ES-MS spectra of the triple-stranded helicate (HHH)-[EuZn(**109**)<sub>3</sub>](ClO<sub>4</sub>)<sub>6</sub> in acetonitrile for a total ligand concentration of (a) 10<sup>-4</sup> M and (b) 10<sup>-5</sup> M.<sup>150</sup> (Reproduced from ref 150. Copyright 1996 American Chemical Society.)

complexes follow different fragmentation pathways compared with helicates.<sup>44,222</sup> Tandem ES-MS might apply not only to the determination of molecular weights of the complexes, but also to the partial elucidation of tertiary structures in polynuclear supramolecular complexes.

## 2. Quantitative Speciation

In contrast to supramolecular assemblies based on weak hydrogen bonding networks which are in rapid equilibrium with their components on the NMR time scale,<sup>40</sup> the coordination bonds involved in helicates are strong enough to prevent fast ligand exchange on the NMR time scale leading to separated and well-resolved NMR signals for the helicate and for its components. However, the stability constants are too large to allow the detection of significant quantities of intermediates in the concentrations used for NMR investigations, and NMR spectroscopy is thus inadequate to quantify the thermodynamic equilibria leading to the final helicates,<sup>223</sup> but it has been often used to determine the ratio between the various diastereomers or conformers formed in solution at the equilibrium if they do not interconvert rapidly on the NMR time scale. For instance, Sauvage, Dietrich-Buchecker, and co-workers have demonstrated that the side-by-side helicate [Cu<sub>2</sub>(**69**)<sub>2</sub>]<sup>2+</sup> is the major conformer in solution producing only low yields of trefoil knot **147** (Figure 51).<sup>12,116</sup> Harding and co-workers have similarly quantified the ratio of *D*<sub>2</sub>-helical vs *C*<sub>2h</sub>-side-by-side conformers formed during the self-assembly of the double-stranded helicates [M<sub>2</sub>(**L**)<sub>2</sub>]<sup>4+</sup> (L = **81**, **82**, **95**; M = Zn, Cd; Table 7).<sup>123,124,139</sup> In a detailed NMR investigation of the triple-stranded helicate [Ga<sub>2</sub>((*R,R*)-**12**)<sub>3</sub>]<sup>6-</sup> resulting from the diastereoselective self-assembly of (*R,R*)-**12** with Ga(III), Stack and Enemark were able to

estimate the differences in free energies between left-handed and right-handed diastereomers, while further studies with the enantiomeric strand (*S,S*)-**12** allowed the estimation of the energy differences between homo- and heterochiral helicates.<sup>53</sup> However, the quantitative characterization of the thermodynamic assembly process leading to the final helicate requires lower concentrations and/or less stable supramolecular complexes. Spectrophotometric titrations appear to be suitable even though the method of continuous variation<sup>206</sup> has been proved to be too restrictive to study the majority of self-assembly processes<sup>14</sup> (Job's plots have been used for the confirmation of the stoichiometry of a triple-stranded helicate [Fe<sub>2</sub>(**127**)<sub>3</sub>]).<sup>174</sup> Nonlinear least-squares fitting of multiple-wavelengths spectrophotometric data has been used by Williams, Piguet, and co-workers to extract global stability constants for the formation of double- and triple-stranded helicates<sup>25,29,36,37,44,98,150,184,189</sup> and by Lehn and co-workers for estimation of cooperativity in self-assemblies.<sup>43,47</sup> Figure 58a shows the variation of the absorption spectra upon titration of the ligand strand **58** with Cu(I) in solution. Lehn and Pfeil satisfactorily fit their data to the equilibria 1–4 in which three intermediates [Cu(**58**)]<sup>+</sup>, [Cu(**58**)<sub>2</sub>]<sup>+</sup>, and [Cu<sub>2</sub>(**58**)<sub>2</sub>]<sup>2+</sup> are involved (see section IV.B). The stability constants associated with these equilibria allow the calculation of criteria and tests for cooperativity<sup>45</sup> and the usual Scatchard plot:<sup>224</sup>  $r/[\text{Cu(I)}] = f(r)$  presents a concave downward curve typical of positive cooperativity ( $r$  is the average number of occupied sites; Figure 58b).<sup>47</sup> The direct potentiometric determination of the free concentration of Ag(I) during the self-assembly of the analogous helicate [Ag<sub>3</sub>(**59**)<sub>2</sub>]<sup>3+</sup> confirms this statement and leads to a similar concave Scatchard plot.<sup>46</sup>

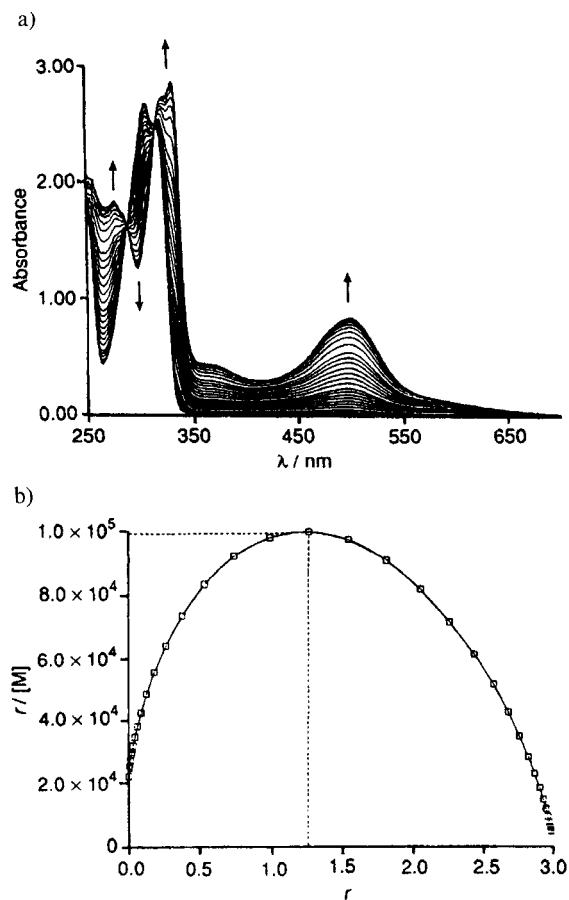


**Figure 58.** (a) Spectrophotometric titration of ligand **58** with Cu(I) in  $\text{CH}_2\text{Cl}_2/\text{CH}_3\text{CN}$  (1:1) and (b) Scatchard plot for the formation of the double-stranded helicate  $[\text{Cu}_3(\mathbf{58})_2]^{3+}$ .<sup>47</sup> (Reproduced with permission from ref 47. Copyright 1992 Royal Society of Chemistry.)

A simplified, but analogous analysis of spectrophotometric data developed by Williams and co-workers have led to the estimation of stability constants for homotopic triple-stranded helicates  $[\text{Co}_2(\mathbf{L})_3]^{4+}$  ( $\mathbf{L} = \mathbf{5}, \mathbf{126}$ ).<sup>29,169</sup> Application of this mathematical treatment to extended multicomponent self-assembly by Piguet, Bünzli, and co-workers provides stability constants for homo- and heterotopic double-<sup>44</sup> and triple-stranded helicates with 3d- and 4f-block metal ions (Figure 46).<sup>37,150,184,186,189</sup> This approach is limited to rather simple thermodynamic processes (maximum of 3–5 simultaneous equilibria) because of the significant correlation found between the UV absorption spectra of the various complexes which prevents reliable calculations for more than four absorbing species. For the self-assembly of the heterotopic triple-stranded helicate (HHH)- $[\text{LaZn}(\mathbf{109})_3]^{5+}$ , the complete characterization of the thermodynamic process should take into account the simultaneous treatment of nine equilibria involving four homonuclear complexes with La(III) ( $[\text{La}(\mathbf{109})_3]^{3+}$ ,  $[\text{La}_2(\mathbf{109})_3]^{6+}$ ,  $[\text{La}_2(\mathbf{109})_2]^{6+}$ ,  $[\text{La}_3(\mathbf{109})_2]^{9+}$ ), four homonuclear complexes with Zn(II) ( $[\text{Zn}(\mathbf{109})_3]^{2+}$ ,  $[\text{Zn}(\mathbf{109})_2]^{2+}$ ,  $[\text{Zn}_2(\mathbf{109})_3]^{4+}$ ,  $[\text{Zn}_2(\mathbf{109})_2]^{4+}$ ), and the heterodinuclear complex (HHH)- $[\text{LaZn}(\mathbf{109})_3]^{5+}$ .<sup>150</sup> Recently, the reliable qualitative speciation obtained by ES-MS under a set of specific conditions has been used to simplify the models for spectrophotometric titrations leading to satisfying quantitative speciations in complicated self-assembled supramolecular complexes if similar conditions are used for ES-MS and spectrophotomet-

ric investigations.<sup>43,150</sup> To the best of our knowledge, polarographic and voltammetric methods have not been applied to the quantitative speciation of helicates in solution except for the estimation of the stability constants of the heterodinuclear helicate (HHH)- $[\text{EuFe}(\mathbf{109})_3]^{4+}$  with the air-sensitive Eu(II) metal ion.<sup>225</sup>

### 3. Structural Characterization

The detailed qualitative and quantitative speciations in solution are neglected in the majority of publications dedicated to helicates and the structure of the final helicates in solution is investigated by NMR after isolation of the complexes in the solid state. This approach may be justified when one or more components or intermediates are poorly soluble as reported by Constable and co-workers for helicates derived from unsubstituted oligopyridine ligands.<sup>32</sup> The attention of the authors is generally focused on the aesthetically appealing helical structures which may be readily addressed by NMR techniques and compared with that found in the solid state. One magic aspect of helicates in solution is their rather high symmetry on the NMR time scale producing simple and clear NMR spectra. A preliminary counting of the observed signals is often sufficient to determine the principal symmetry elements, leading to a restricted choice of symmetry point groups provided that the structure of the helicate is retained in solution (this is seldom checked in the literature, but may be addressed by ES-MS at high concentrations). Van Koten and co-workers used this approach to assign the  $C_2$  point group to the head-to-tail double-stranded helicate (HT)- $[\text{Ag}_2((R,S)\mathbf{10})_2]^{2+}$ , and they demonstrated by multinuclear NMR that this complex is formed selectively among four possible diastereomers:<sup>142–144</sup> (i) steric constraints in the cyclohexyl bridge prevent the formation of side-by-side conformers, (ii) the observation of only two sets of  $^1\text{H}$  NMR signals for the protons of the pyridine rings implies a  $C_2$  axis, and (iii) a single signal in the  $^{109}\text{Ag}$ -NMR spectrum is only compatible with a  $C_2$ -axis perpendicular to the helical axis leading to a head-to-tail arrangement of the strands. Numerous helicates have been characterized similarly and this approach is particularly useful for the assignment of head-to-head vs head-to-tail conformers.<sup>146</sup> However, consideration only of the total number of signals in the NMR spectrum may correspond to a number of different possible point groups. Lehn and co-workers first recognized the usefulness of methylene protons in the  $^1\text{H}$  NMR spectrum for the determination of the structure adopted in the final helicate.<sup>50,51</sup> For the free ligand **4**, the protons of the methylene groups of the oxopropylene bridges are enantiotopic leading to singlets ( $A_2$  spin systems) in the  $^1\text{H}$ -NMR spectrum. Upon coordination to Cu(I) in the double-stranded helicate  $[\text{Cu}_3(\mathbf{4})_2]^{3+}$  (Figure 3), no symmetry element interconverts the hydrogen atoms connected to the same carbon atom leading to diastereotopic protons and doublets ( $AB$  spin systems) in the  $^1\text{H}$ -NMR spectra. The appearance of the  $AB$  spin system is considered as a test for the formation of the final helicate.<sup>50,51</sup> More precise structural information may be gained when the methylene groups are judiciously introduced into the ligand strands to test the presence of  $C_2$  or  $\sigma$  symmetry elements (Figure

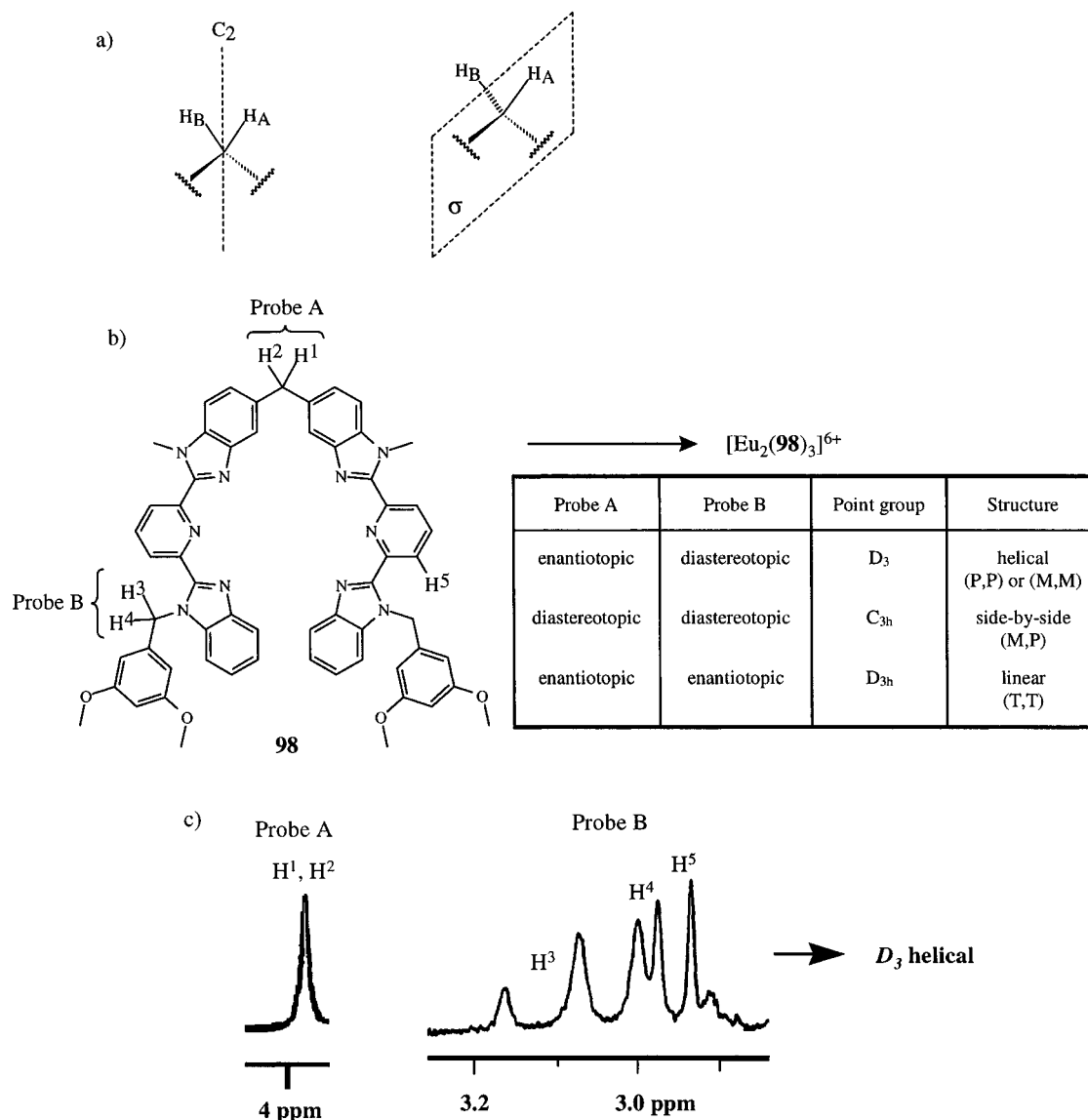


**Figure 59.** (a) Possible symmetry elements tested by a methylene probe, (b) principles of the determination of the point group for  $[\text{Eu}_2(\mathbf{98})_3]^{6+}$  using methylene probes, and (c)  $^1\text{H}$ -NMR spectra of probes A and B in the  $D_3$ -helical triple-stranded helicate  $[\text{Eu}_2(\mathbf{98})_3]^{6+}$ .<sup>184</sup>

59a). The systematic use of methylene probes was first developed by Piguet, Williams, and co-workers for the characterization of the double-stranded helicates  $[\text{Cu}_2(\mathbf{L})_2]^{2+}$  ( $\mathbf{L} = \mathbf{42}, \mathbf{45}, \mathbf{49}$ )<sup>91,95</sup> and then applied to the elucidation of the  $D_3$ -helical structures of  $[\text{Co}_2(\mathbf{L})_3]^{4+}$  ( $\mathbf{L} = \mathbf{5}, \mathbf{126}$ )<sup>29,169</sup> and  $[\text{Eu}_2(\mathbf{98})_3]^{6+}$ .<sup>184</sup> For the latter complex, the  $^1\text{H}$  NMR spectra display a  $A_2$  spin system for the central methylene unit of the bridge (probe A) and a  $AB$  spin system for the methylene probe B which is only compatible with a  $D_3$  point group (Figure 59b).<sup>184</sup> A similar approach has been later followed (i) by Albrecht and co-workers to assign a  $C_{3h}$ -side-by-side structure to the helicate  $[\text{Ti}_2(\mathbf{137})_3]^{4-}$  and a  $D_3$ -helical structure to  $[\text{Ti}_2(\mathbf{136})_3]^{4-}$ <sup>167,178</sup> and (ii) by Potts and co-workers to characterize double-stranded helicates derived from oligopyridine strands substituted with *S*-propyl groups.<sup>107,108,152</sup> The introduction of methylene probes is also useful for the investigation of dynamic interconversion between dinuclear right-handed (*P,P*) and left-handed (*M,M*) enantiomeric helicates because average symmetry elements result from fast exchange processes on the NMR time scale leading to the coalescence of diastereotopic signals.<sup>91,92</sup> Free energies for helical in-

terconversion in solution have been estimated for double-<sup>92</sup> and triple-stranded helicates from the investigation of the coalescence of  $AB$  spin system into  $A_2$  spin systems for lateral methylene or isopropyl probes using variable-temperature NMR experiments.<sup>176,178</sup>

Once the point group has been unambiguously assigned, further fine structural informations may be gained by the systematic use of aromatic ring current effects and nuclear Overhauser effects (NOEs). For self-assembled helicates of low symmetry derived from unsymmetrical ligands, NOEs are crucial for the elucidation of the structure and they have been successfully used for the structural characterization of heterodinuclear triple-stranded helicates<sup>34,150</sup> and for the first helicates containing sulfate anions.<sup>26</sup> Recently, the planned introduction of paramagnetic lanthanide metal ions possessing fast electronic relaxation rates into triple-stranded helicates has allowed reliable structural and electronic characterization in solution resulting from the separation of contact and pseudocontact contributions to the proton chemical shifts.<sup>150</sup>

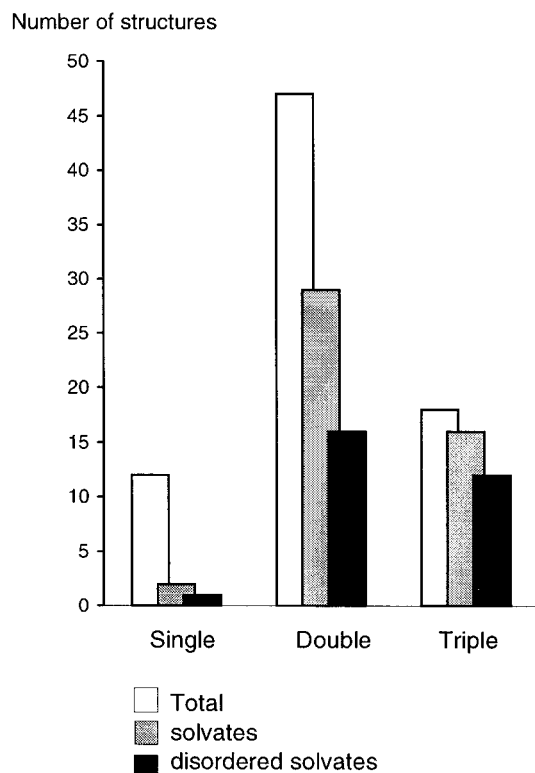


**Figure 60.** Distribution of single-, double-, and triple-stranded helicates (including the mononuclear complexes of section IV.A.1), showing the proportion of solvates and disordered solvates in the crystal structures.

## B. Crystal Structures of Helicates

Recently Atwood<sup>226</sup> in a short review devoted to diffraction studies of supramolecular compounds, showed clearly the major difficulties in the study of this class of compound as a crossing point between small and large molecule crystallography. All his remarks are also relevant to the X-ray diffraction analysis of helicates.

### 1. Crystal Growth and Handling

By way of preamble we can state that it is difficult to persuade such molecules to crystallize. The crystal growth of helicates, just like supramolecular compounds, is hard to handle and, depending on the solvents or counterions used, the resulting complex does not always correspond to the one expected. Their crystallization requires, in most cases, multi-solvent techniques such as layering or vapor diffusion.<sup>227</sup> These methods are based on the difference of solubility of the complex in the various solvents. On the other hand helicates are large-size entities and show a marked trend to form solvates (Figure 60). A judicious choice of the solvents of crystallization can avoid the formation of solvates which are frequently disordered in the crystals. In most cases, helicates are charged and lipophilic complexes, and this significantly limits their solubility in both polar and nonpolar solvents. Acetonitrile is often used as a good solvent together with diethyl ether, methanol, or ethanol as precipitating agents which are all excellent partners for the formation of inclusion compounds or solvates. It should be mentioned that the addition of an excess of counterion is also used with success in the crystallization of helicates.

In layering or vapor diffusion techniques the crystals grow in a closed system and the formation of good quality crystals does not imply that it will be easy to mount a crystal and use it for X-ray diffraction measurements. Depending on the volatility of the mixture of solvents used in the growth process it may well happen that when on picking up the crystal (or on opening the crystallization vessel) the crystals may dissolve rapidly or cover themselves with a precipitate. Moreover if the crystals are solvated (which is the case for more than 88% of the triple-stranded helicates, Figure 60), the solvent may rapidly diffuse out of the crystal once it is isolated from solution leading to a lack of crystallinity. It should be noted that the use of water as solvent could reduce these problems on account of its low volatility. Furthermore, when it is incorporated into the crystal, it is easier to model a monoatomic molecule (without hydrogen atoms) if the solvent molecules are indeed disordered.

Finally the molecular packing of such species is essentially guided by weak interactions and the crystals are particularly fragile when they form solvates. All crystal handling must thus be carried out quickly and gently without removing the crystals from the mother liquor. The use of polyfluorinated polyether (liquid Teflon)<sup>228</sup> or greases to prevent crystal degradation and low-temperature handling<sup>229</sup> and measurement are thus essential in the crystallographic study of this type of compound.

### 2. Choice of the Counterion

Helicates are generally cationic species and the choice of adequate counterions can be critical to the multicomponent self-assembly process. The aptitude of a given counterion to coordinate the metal in place of the organic ligand must be considered with attention ( $\text{NO}_3^- > \text{Cl}^- > \text{Br}^- > \text{CF}_3\text{SO}_3^- > \text{ClO}_4^- \cong \text{PF}_6^- \cong \text{BF}_4^-$ )<sup>230</sup> and  $\text{CF}_3\text{SO}_3^-$  or  $\text{NO}_3^-$  anions are sometimes bound to the metals. Highly symmetric anions such as  $\text{PF}_6^-$ ,  $\text{ClO}_4^-$ , although frequently used as noncoordinating counterions in helicates, generate considerable disorder (Figure 61). Overlarge or conformationally flexible counterions should be avoided as a potential source of problems. In some cases the presence of more than one counterion is a necessary condition to the formation of crystalline material.<sup>150, 225</sup> There are no general rules to choose an adequate counterion but  $\text{ClO}_4^-$  should be avoided in view of Figure 61.

### 3. Data Collection and Refinement

To minimize thermal motion and to prevent the degradation of the crystals by loss of the solvent of crystallization, low-temperature measurements are preferable. Nevertheless for a very few helicates phase transitions have been observed which lead to the destruction of the crystalline structure. The use of greases or polyfluorinated ethers to protect the crystal often hinders the accurate indexing of the faces and the dimensions of the crystal necessary to apply an absorption correction. Helicate crystals often diffract poorly and we can rarely hope for a resolution better than 1.1 Å. The number of unique reflections to be measured for such a resolution is often in the range of 10 000–20 000 and the use of

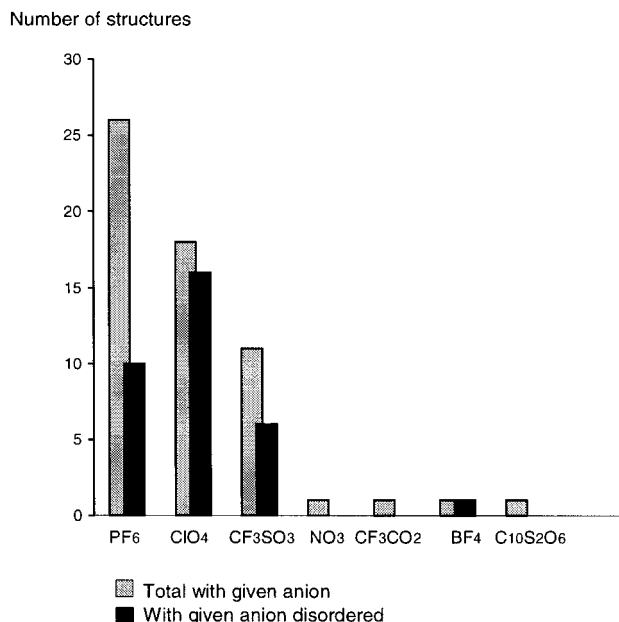


**Figure 61.** Distribution of counterions occurring in helicates with their proportion of disorder in the crystal structures.

an area detector (image plate or CCD) greatly improves the quality of the data and significantly reduces the measurement time. In most cases for a resolution range between 1.0 and 1.2 Å, only one-half (two-thirds in the best cases) of the reflections are observable ( $|F_o| > 4\sigma(|F_o|)$ ). This lack of diffraction data not only means that direct methods can fail, but leads also to poor data-to-parameter ratios preventing accurate treatment of the fine structure such as disorder or anisotropic atomic displacement parameters in the refinement. The choice of an adequate weighting scheme in the refinement is not trivial. The use of a normal statistical weight of  $1/\sigma^2(|F|)$  for the reflections tends to increase the effect of the highest intensities at low angle, detrimental to the weak, higher-angle reflections in which more information on the fine details of the structure is to be found. To balance this overestimation of the large low-angle amplitudes, some authors adopt unit weights or a weighting scheme taking into account the high-angle reflections of the form (for a refinement on  $|F|$ )  $\omega^{-1} = \sigma^2(|F|) + p|F|^2$  where  $p$  is obtained from the analysis of the variance. A survey of the recent literature concerning this type of compound shows that the conventional  $R$  values are high (often greater than 0.10), even for some unsolvated helicates.<sup>164</sup>

These structures are dominated by the packing of large cations with small anions and solvent molecules occupying the interstices. The helicates themselves are rarely subject to serious disorder (unless side chains are present) and often interstrand stacking interactions<sup>1,94,106,107,168</sup> stabilize the cation, whereas the anions or solvent molecules are partially or fully disordered. The usual procedure consists of including in the least-squares refinement the contribution of discrete atoms involved in the dynamic or static disorder in order to model the observed electron density in the disordered region. The discrete atomic sites involved in the disorder may or may not overlap and are generally represented with population parameters less than unity. From our own experience,

it is not unusual, mainly in highly charged helicates (+4 or +5) to have to search for a perchlorate or a trifluoromethanesulfonate anion in the residual electron density of about  $2 \text{ e}\text{\AA}^{-3}$ , clearly indicating that the anion is distributed over a large number of sites and orientations in the interstitial spaces of the crystal. In such conditions it is easy to understand that it is either difficult or impossible to distinguish a disordered acetonitrile from a disordered methanol or ethanol molecule.

In fact the interpretation and representation of the disorder require a great deal of work for the crystallographer to produce a chemically acceptable model which often requires constraints and/or restraints to obtain stable refinements. In some programs (SHELXL, PROLSQ, etc.) there is an automatic generation of constraints and restraints based on a connectivity interpretation of the chemical structure. In other programs (for example XTAL, SIR) these constraints or restraints must be specified individually, a time-consuming and tedious task (see for instance the structure of the circular double-stranded  $[\text{Fe}_5(\mathbf{124})_5\text{Cl}]^{9+}$  helicate where 126 032 restraints were applied in the refinement).<sup>182</sup>

In the case of highly disordered regions, the difference electron density cannot be interpreted in terms of a chemical model and the discrete-atom approach becomes difficult to apply in practice. It is surprising that the interesting alternative BYPASS of van der Sluis and Spek<sup>231</sup> has not achieved wider use, possibly due to its nonimplementation in commonly used X-ray program packages. This method uses the Fourier transform of the observed electron density in the disordered region (automatically identified by difference from the ordered part of the structure) as a contribution to the model structure factors in the refinement calculations. At the final stage of the refinement, an electron count of the disordered regions allows one to estimate the nature of the solvent molecules (or counterions) present in the structure. To our knowledge such a treatment has never been applied in the diffraction studies of helicates.

The above discussion clearly shows that the crystallographic problems arising during the crystal growing, structure solution, and refinement of helicates are greater than those arising in the field of small molecules. The major problems are those associated with the modeling of the disordered regions and in most cases this leads to a relatively low resolution and higher  $R$  values. A considerable amount of time is necessary to model the disordered counterions and solvent molecules in order to achieve sufficiently low conventional  $R$  values. Since the representation of the disordered or solvent part of the structure is of little interest to the chemist, it would seem that this is only a cosmetic but costly task dictated by the current standards required for publication of crystal structures. Indeed diffraction studies of such supramolecular compounds are a major source of frustration for the structural chemist as exemplified by the comments of Atwood:<sup>226</sup> "High  $R$  values may lead to difficulties in publication: many referees, editors, and journals now hold crystallographic structure determinations to the same standards, regardless of the compound, supramolecular

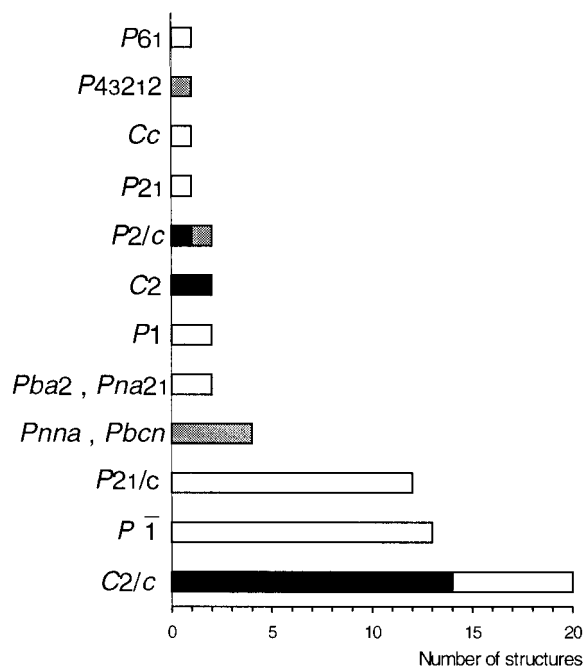


**Figure 62.** Distribution of helicites in space groups showing the presence of a crystallographic intramolecular symmetry:  $C_{2\perp}$  axis (black),  $C_{2\parallel}$  axis (gray) and no symmetry (white). ( $C_{2\perp}$ , 2-fold axis perpendicular to the helical axis;  $C_{2\parallel}$ : 2-fold axis parallel to the helical axis).

or small-molecule.” Some typical remarks from referees show their lack of experience of this class of compounds: “There is no excuse for publication of structures with diffractometer data refined to  $R$ -factors of 0.11, even with the disorder encountered”; “It is a low accuracy analysis”; “Data were collected only to a  $\theta$  value of  $21^\circ$  (MoKa), this is only a partial data set”; and “The data to parameter ratio is very poor”. These remarks are pertinent and exactly describe the intrinsic characteristics of this class of compound, which must be considered as different from that of small molecules.

#### 4. Molecular Symmetry and Crystal Packing

As described in section II the nature of the ligands in helicites is closely linked to their possible intramolecular symmetry. If we define the mean-square line passing through the metal ions as the helical axis ( $H_a$ ), the potential symmetry elements of the helical complex are as follows: one  $C_n$  axis parallel to  $H_a$  and  $n$   $C_2$  axes perpendicular to it, called  $C_{n\parallel}$  and  $C_{2\perp}$  respectively (with  $n = 2$  or  $3$ , Figures 10–12). Thus a homotopic double-stranded helicate (ligands of same denticity, same connectivity, same donor atoms) can ideally lead to  $D_2$  symmetry of the complex with a  $C_{2\parallel}$  and  $2$   $C_{2\perp}$ . For heterotopic helicites the number of possible intramolecular symmetries decreases according to the position of the binding sites along the ligand strand and to the nature of the central ions in polynuclear complexes. Chemically, these molecular symmetries are observed in solution by spectroscopic measurements, but from a crystallographic point of view these symmetries have never been fully observed. To the best of our knowledge the existence in the same helicate of two or more crystallographic symmetry elements has not yet been reported in the literature. The frequency distribution of helicites in different space groups and

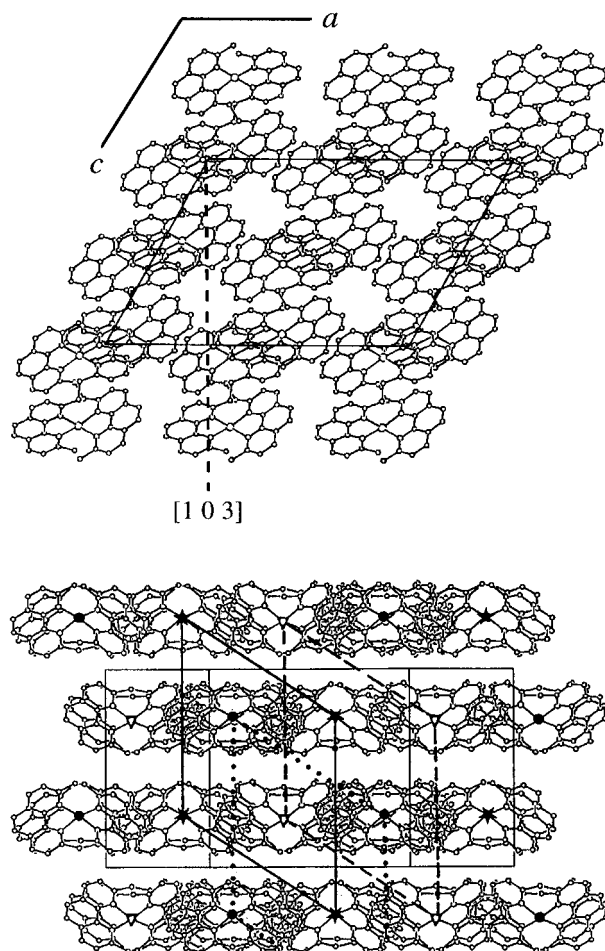


**Figure 63.** Projection on the monoclinic  $ac$  plane (top) and along the  $[1\ 0\ 3]$  direction (bottom) of the saturated homotopic helicate  $[\text{Cu}_2(\mathbf{34})_2]^{2+}$  showing a pseudo-hexagonal ABC close-packed arrangement in the space group  $C2/c$ . The helicate shows a crystallographic  $C_{2\perp}$  axis perpendicular to the pseudo-hexagonal  $[0\ 0\ 1]$  direction. Hydrogen atoms, counterions, and solvent molecules have been omitted for clarity.

their internal symmetry are reported in Figure 62. About one-third of helicites show the presence of an intramolecular symmetry (2-fold) axis of which one-half is perpendicular and one-half is parallel to the helical axis. In the most frequently occurring space group ( $C2/c$ ), 70% of the compounds show an internal symmetry which is exclusively a  $C_{2\perp}$  axis. Two-fold symmetries parallel to the helical axis are found for the most part in the crystal class  $mmm$ . It should be noted that no triple-stranded helicate shows a crystallographic 3-fold symmetry axis. The only related structure displaying such a symmetry is a mononuclear triple-stranded helical europium complex (i.e., it is not a helicate in the sense defined in section I).<sup>201</sup> This absence of ideal symmetry in the solid state originates mainly from intermolecular interactions in the crystal packing or from the presence of side chains with a high degree of freedom precluding a rigorous application of the symmetry.

Although helicites are ionic species, their molecular packing is essentially directed by weak interactions. Their general shape being almost cylindrical, their packing shows, in most cases, a definite directionality which is not observed in other supramolecular compounds such as fullerenes or calixarenes.<sup>226</sup> Parallel to their principal axis ( $H_a$ ) the

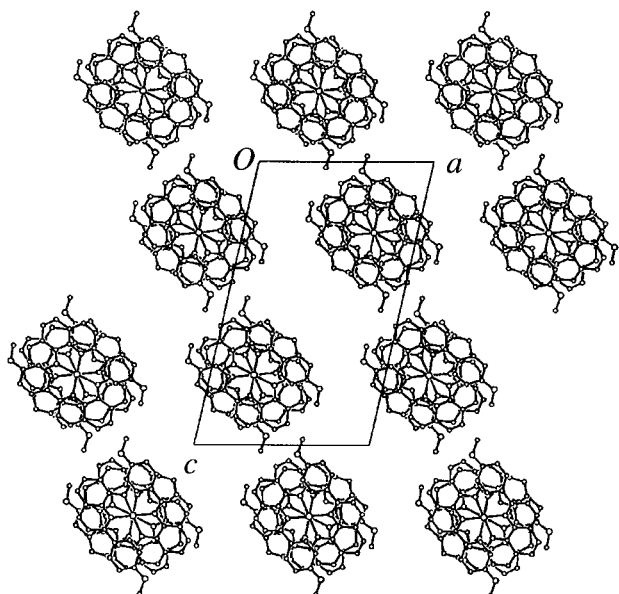


**Figure 64.** Projection on the  $ac$  plane of the crystal structure of the saturated homotopic helicate  $[\text{Cu}_2(\mathbf{71})_2]^{2+}$ <sup>117</sup> showing a pseudo-hexagonal AA close-packed arrangement in the space group  $P2/n$ . The complex shows a crystallographic  $C_{211}$  axis parallel to the pseudo-hexagonal  $[001]$  direction. Hydrogen atoms, counterions, and solvent molecules have been omitted for clarity.

molecules tend to align themselves to give the densest packing and leaving sufficient space in cavities or channels for the counterions. Since helicates are molecules possessing true or pseudo 2-fold symmetry,

it is not surprising that the most-frequently occurring space group is  $C2/c$ , a group of maximum density for packing such molecules.<sup>232</sup> In fact, we can demonstrate that the crystal structures of helicates, regardless of the crystal system in which they crystallize, can nearly always be described using deformed hexagonal unit cells (in a few cases a deformed tetragonal cell). As in the crystal packing of chain molecules,<sup>232</sup> the helicates form layers of hexagonal close packed cylindrical molecules and, depending on the packing of the layers, this leads to pseudo-hexagonal AA, AB or ABC close-packed arrangements.

All the reported helicate structures maintaining their  $C_{2\perp}$  in the crystal are found in the monoclinic system. Such a situation is observed in space groups containing some nontranslational 2-fold symmetry:  $C2/c$ ,  $C2$ , and  $P2/c$ . In most cases, the pseudo-hexagonal direction is to be found in the  $ac$  plane (i.e. perpendicular to the unique axis of the monoclinic system) and parallel to  $H_a$ . Depending on the transformation of the monoclinic unit cell to the pseudo-hexagonal cell, the molecular packing is formed of AA, AB or ABC close-packed arrangements (Figure 63). Two exceptions to this generalization are observed in space groups  $P2/n$  and  $I2/a$  where the helicates  $[\text{Cu}_2(\mathbf{71})_2]^{2+}$  and  $[\text{Cu}_2(\mathbf{48})_2]^{2+}$  maintain their  $C_{211}$  in the crystal.<sup>117</sup> Thus the structures show AA close-packed arrangements (columns of molecules) where the  $H_a$ , the pseudo-hexagonal direction and the unique axis of the monoclinic unit cell are parallel (Figures 49 and 64). The above-mentioned situation is also

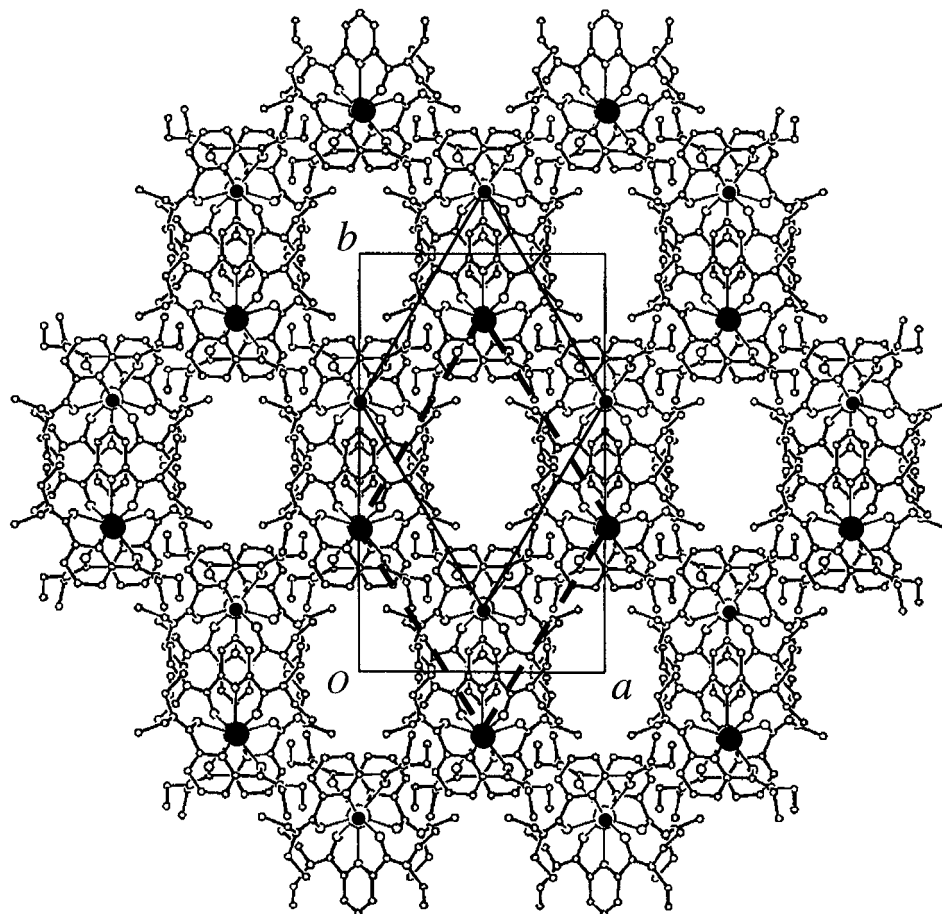


**Figure 65.** Projection along the monoclinic  $c$  axis of the mononuclear triple-stranded helical complex  $[\text{Eu}(\text{2,6-pyridinedicarboxylic acid-bisdiethylamide})_3]^{3+}$ <sup>233</sup> showing a pseudo-hexagonal AB close-packed arrangement in the space group  $C2/c$ . Hydrogen atoms, counterions, and solvent molecules have been omitted for clarity.

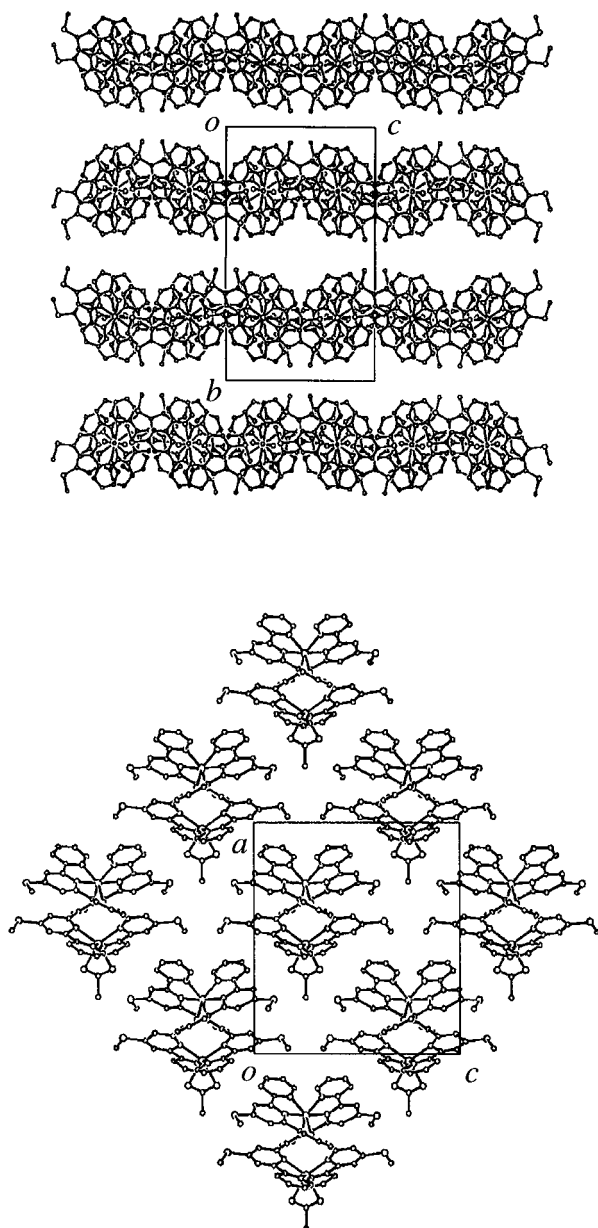


**Figure 66.** Projection, on the  $bc$  plane (top), of the crystal structure of the unsaturated helicate  $(\text{HH})\text{-}[\text{Ni}_2(\mathbf{20})_2(\text{OAc})]^{3+}$  in the space group  $Pnna$ . Each layer (bottom) shows a pseudotetragonal arrangement of the cations. The crystallographic  $C_{211}$  axis of the complex is perpendicular the pseudotetragonal  $[0\ 0\ 1]$  direction. Hydrogen atoms, counterions, and solvent molecules have been omitted for clarity.

frequently observed in many double- or triple-stranded mononuclear complexes (Figure 65) where the molecular shape is closely related to a sphere which contrasts with the elongated cylinders observed for helicates.<sup>233</sup>

For helicates possessing a crystallographic  $C_{211}$  axis, except for the above-mentioned case, the crystal packing is less compact since all observed structures adopt a true<sup>128</sup> or pseudotetragonal arrangement (Figure 66). In all cases,  $H_a$  is perpendicular to the pseudotetragonal direction. It should be noted that the four compounds involved in orthorhombic space groups  $Pnna$ <sup>62,107,108</sup> and  $Pbcn$ <sup>97</sup> do not possess a  $C_{2\perp}$  axis and their unit cell parameters are close to tetragonal.

In conclusion, we can say that the mere knowledge of the unit cell parameters and space group as well

as the number of molecules per asymmetric unit allows (if  $Z$  is less than the number of Wyckoff sites) the estimation with a high probability of the nature and the location of the molecular symmetry. Moreover, following the form of the matrix to transform the true unit cell to the pseudohexagonal (or pseudotetragonal) system, an evaluation of the direction of the principal axis of the helix in the unit cell can be obtained together with the type of close-packed arrangement before solving the crystal structure. It should be noted that such information can play an important role in the success of direct methods or Patterson interpretation at the stage of structure solution.

## VII. Summary and Outlook

During the last decade, intense activity has been focused on the preparation of aesthetically appealing helicates and the various combinations of intrinsic informations leading to homotopic homostranded helicates have been explored for oligo-mono-, oligo-bi- and oligo-tridentate ligand strands (Table 1). The control of the encoded structural and electronic informations leading to the selective production of the final symmetrical homotopic helicate is now well-established and extension of this approach inspired by the induced fit concept<sup>234</sup> has led to new active fields of research in chemical topology,<sup>15</sup> inorganic materials,<sup>6</sup> and clusters.<sup>27</sup> If we consider the chemical challenge of preparing a quadruple-stranded helicate, we can reasonably imagine that the first member of this new series will be synthesized according to one of the following possibilities: (i) oligo-monodentate strands with square-planar four-coordinate metal ions or (ii) oligo-bidentate strands with square antiprismatic eight-coordinate metal ions. The preparation of homostranded heterotopic helicates has been much less studied as suggested by the missing entries of Table 2. This probably arises from the increased difficulty in encoding sufficient intrinsic informations in unsymmetrical ligands for the selective recognition of different metal ions under thermodynamic control. However, heteronuclear and heterotopic helicates possess an intrinsic directionality and offer fascinating possibilities for the development of molecular devices having predetermined properties and functions (light-conversion, nonlinear optic, etc.). The high degree of structural programming and control in these supramolecular architectures: (i) distance between the metal ions, (ii) protection of the metal ions, (iii) electronic and structural properties of the coordination sites, and (iv) selective attachment of structurally organized peripheric groups for exogenous recognition have been hardly explored and only few pioneer works are concerned with the planned development of helicates for specific applications. In this context, the development of heterostranded helicates will be also interesting for the possible combination of the different electronic properties of the ligands with those of the metal ions (charge separating devices, selective RNA sequencing agents, etc.). We have no doubts that academic and aesthetic interests will lead to further developments in helicates, but we do think that the enormous potential applications of helicates, and particularly of heteronuclear and heterotopic heli-

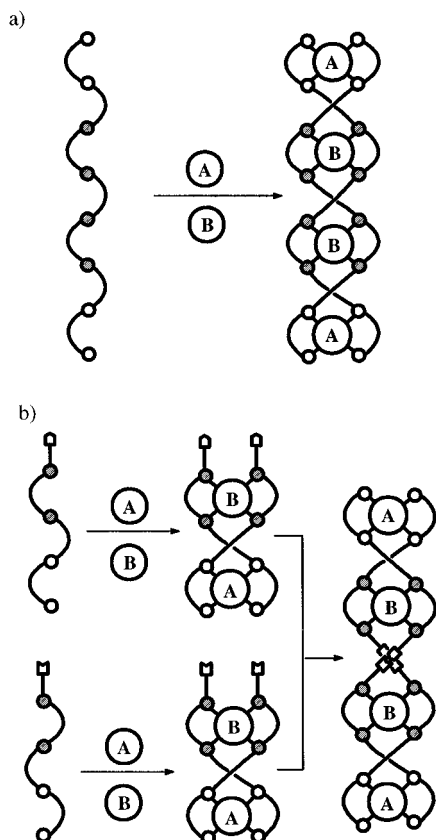
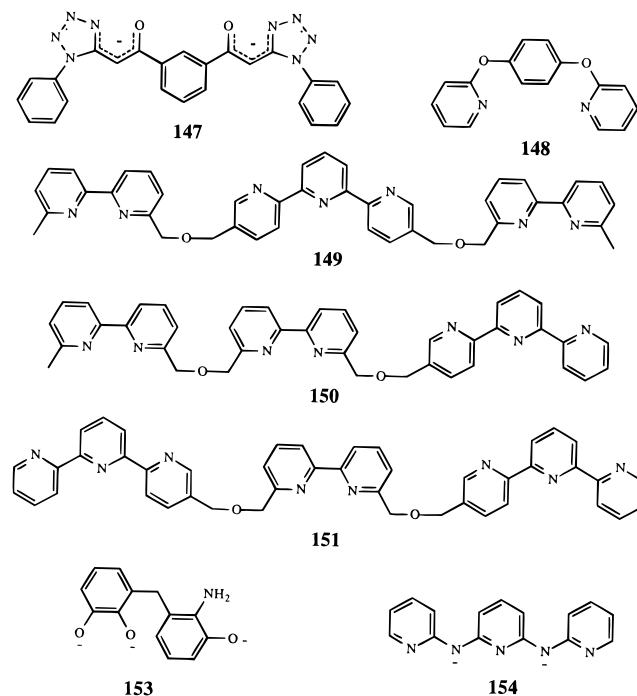


**Figure 67.** (a) Classical and (b) step-by-step self-assembly of a heterotetranuclear double-stranded helicate.

icates will become a considerable driving force in that field in the next future.

Helicates obtained by self-processes have clearly initiated a revolution from classical coordination concepts toward extended supramolecular concepts in which the coordination bond has become a tool for the construction of larger organized architectures capable of further recognition processes based on various noncovalent interactions such as stacking interactions, hydrogen bonding, or van der Waals interactions. The main limitation of this approach results from the tedious and often complicated preparation of instructed ligand strands suitable for helicate self-assembly. This is particularly sensitive for polynuclear complexes and a large part of the publications in that field concerns dinuclear helicates. However, the global consideration of noncovalent interactions to build organized architectures provides an attractive solution to this problem with the design of inert helical building blocks which may assemble to give the final planned helicates (Figure 67). Much work has been devoted to helicates since 1987 when this term was first introduced by Lehn and co-workers.<sup>1</sup> Structural control and molecular programming have been significantly explored and improved, but the use of self-assembly to provide self-organized functional supramolecular helicates is still in its infancy. Helicates will probably suffer from the competitions of other fascinating inorganic and metal-containing assemblies such as grids, racks, ladders, cylinders, and symmetry-driven clusters but they will keep a predominant place if their promising potential applications as molecular and supramolecular functional devices are confirmed and developed.

**Chart 19**



### VIII. Addendum

Between the submission and the acceptance of this review, some significant publications devoted to helicates have appeared in the literature.<sup>235–241</sup> Three of them report the detailed characterization of homotopic double-stranded helicates  $[\text{Cu}_5(\mathbf{L})_2]^{5+}$  ( $\mathbf{L} = \mathbf{63}, \mathbf{64}$ ),<sup>235</sup>  $[\text{Zn}_2(\mathbf{147})_2]$  which exists as a dimeric cluster  $[\text{Zn}_4(\mathbf{148})_4]$ <sup>236</sup> and  $[\text{Ag}_4(\mathbf{148})_2(\text{OH}_2)_2]^{2+}$ .<sup>237</sup> Recent significant advances in the field of heteronuclear heterotopic double-stranded<sup>238,239</sup> and triple-stranded<sup>240</sup> helicates merit further comments.

Lehn and Smith<sup>238</sup> have synthesized the segmental ligands **149–151** (Chart 19) which possess various sequences of bidentate and tridentate binding units separated by oxypropylene spacers. According to ES-MS and <sup>1</sup>H-NMR data, **149** self-assembles with suitable a 2:1 mixture of Cu(I) and Fe(II) to give the programmed double-homostranded heterotopic helicate  $[\text{CuFeCu}(\mathbf{149})_2]^{4+}$  where two Cu(I) occupy the terminal *pseudotetrahedral* binding site produced by the bipyridine units of each strand while Fe(II) lies in the central *pseudo-octahedral* site defined by the two terpyridine subunits.<sup>238</sup> This heterotrimeric helicate is closely related to the dinuclear double-stranded helicates (HH)- $[\text{CoAg}(\mathbf{7})_2]^{3+}$ <sup>34</sup> and (HH)- $[\text{FeAg}(\mathbf{107})_2]^{3+}$ <sup>148</sup> where selective self-assembly has been shown to result from correct matching between the bidentate and tridentate binding units with tetrahedral (Ag(I)) and octahedral (Co(II), Fe(II)) metal ions. According to this approach, **150** produces the double-homostranded heterotopic helicate (HH)- $[\text{Cu}_2\text{Fe}(\mathbf{150})_2]^{4+}$  where the sequence of the metal ions is changed. The use of Cu(II), which displays a preference for pentacoordination, leads to the formation of the double-heterostranded homotopic helicate  $[\text{Cu}_3(\mathbf{149})(\mathbf{151})]^{6+}$  in which each Cu(II) is coordinated by a bipyridine and a terpyridine unit of each strand as previously described for  $[\text{Cu}_3(\mathbf{4})(\mathbf{6})]^{6+}$ .<sup>30</sup> This new series of heterotopic helicates suggests that the previously identified metal ion-directed strand com-

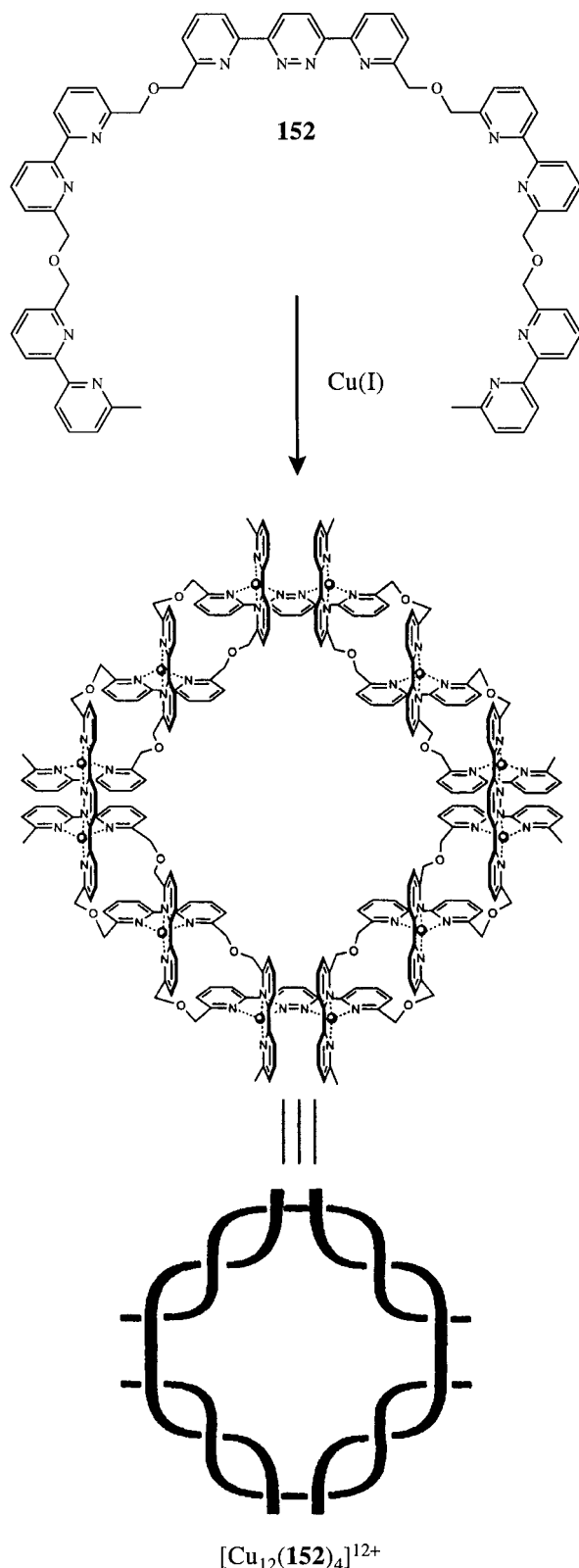


**Figure 68.** Self-assembly of a nanocyclic supramolecular architecture based on four linked double-stranded helical sections.

combination of dinuclear helicate self-assembly<sup>29,34,44</sup> may be extended to trinuclear helicates leading to broader perspectives for molecular programming.<sup>238</sup> A fascinating new advance in this field concerns the combination of different structural motifs in the segmental ligand **152**. Oligobipyridine units coded for helicate self-assembly with Cu(I) are connected to a central bispyridyl-pyridazine unit coded for the

preparation of square shaped species.<sup>239</sup> Reaction with Cu(I) produces selectively the nanocyclic dodecanuclear complex  $[\text{Cu}_{12}(\mathbf{152})_4]^{12+}$  which is composed of four intertwined strands displaying four linked dinuclear double-helical sections of alternating chiralities (Figure 68).<sup>239</sup> In the crystal structure, four  $\text{PF}_6^-$  anions and solvent molecules occupy the central hollow cavity.

The segmental ligand **153** synthesized by Albrecht and Fröhlich<sup>240</sup> allows the self-assembly of the homodinuclear heterotopic head-to-tail triple-stranded side-by-side helicates (HHT)- $[\text{Ti}_2(\mathbf{153})_3]^-$  and (HHT)- $[\text{Ga}_2(\mathbf{153})_3]^{3-}$  according to NMR data. Upon reaction with a mixture of Ti(IV) and Ga(III), the  $C_3$ -symmetrical heterodinuclear side-by-side helicate  $[\text{GaTi}(\mathbf{153})_3]^{2-}$  is obtained selectively as demonstrated by its crystal structure.<sup>240</sup> These observations are closely related to the self-assembly of (HHT)- $[\text{La}_2(\mathbf{8})_3]^{6+}$  and (HHH)- $[\text{LaZn}(\mathbf{8})_3]^{5+}$  discussed in section IV.C.2).<sup>36,37</sup>

Finally, Peng and co-workers<sup>241</sup> have recently reported the first quadruple-stranded helicate. As predicted in the conclusion of this review, the first quadruple-stranded helicate results from the assembly of an oligo-monodentate ligand **154** with metal ions compatible with square planar geometries. The resulting pentanuclear unsaturated helicates  $[\text{M}_5(\mathbf{152})_4\text{X}_2]$  ( $\text{M} = \text{Co(II)}$ ,  $\text{X} = \text{NCS}^-$ ;  $\text{M} = \text{Ni(II)}$ ,  $\text{X} = \text{Cl}^-$ ) possess pseudo- $D_4$  symmetries associated with four *syn-syn-syn-syn* wrapped deprotonated strands about the metal ions. The distances between the metal ions are short (2.229–2.277 Å for  $\text{M} = \text{Co}$ ; 2.346–2.385 Å for  $\text{Ni(II)}$ ) and imply metal–metal bonding. The three central metal ions are thus pseudooctahedrally coordinated by four N-donor atoms of the ligand strands forming an equatorial plane and two metal ions in the apical positions. The two terminal metal ions are in very similar environment except for a complementary anion occupying one apical position ( $\text{NCS}^-$  for  $\text{Co(II)}$  and  $\text{Cl}^-$  for  $\text{Ni(II)}$ ).<sup>241</sup>

## IX. Acknowledgments

C.P. thanks the Werner Foundation for a fellowship. This work is supported through grants from the Swiss National Foundation for Scientific Research.

## X. References

- (1) Lehn, J.-M.; Rigault, A.; Siegel, J.; Harrowfield, J.; Chevrier, B.; Moras, D. *Proc. Natl. Acad. Sci. U.S.A.* **1987**, *84*, 2565.
- (2) Vögtle, F. *Supramolecular Chemistry*; John Wiley & Sons: Chichester 1991; Chapter 2.
- (3) Dietrich, B.; Viout, P.; Lehn, J.-M. *Macrocyclic Chemistry*; VCH: Weinheim, 1993.
- (4) Watson, J. D.; Crick, F. H. C. *Nature* **1953**, *171*, 737. Saenger, W. *Principles of Nucleic Acid Structure*; Springer: New York, 1984.
- (5) Constable, E. C. *Nature* **1990**, *346*, 314.
- (6) Lehn, J.-M. *Supramolecular Chemistry*; VCH: Weinheim, 1995.
- (7) Lindsey, J. S. *New J. Chem.* **1991**, *15*, 153.
- (8) Cramer, F. *Chaos and Order, The Complex Structure of Living Systems*; VCH: Weinheim, 1993.
- (9) Piguët, C.; Bünzli, J.-C. G. *Eur. J. Solid State Inorg. Chem.* **1996**, *33*, 165. Bünzli, J.-C. G.; Froidevaux, P.; Piguët, C. *New J. Chem.* **1995**, *19*, 661.
- (10) Sleiman, H.; Baxter, P.; Lehn, J.-M.; Rissanen, K. *J. Chem. Soc., Chem. Commun.* **1995**, 715. Chambron, J.-C.; Dietrich-Buchecker, C. O.; Nierengarten, J.-F.; Sauvage, J.-P.; Solladié, N.; Albrecht-Gary, A.-M.; Meyer, M. *New J. Chem.* **1995**, *19*, 409. Hanan, G. S.; Arana, C. R.; Lehn, J.-M.; Fenske, D. *Angew. Chem., Int. Ed. Engl.* **1995**, *34*, 1122. Baxter, P.; Hanan, G. S.; Lehn, J.-M. *Chem. Commun.* **1996**, 2019.

- (11) Baxter, P.; Lehn, J.-M.; Fischer, J.; Youinou, M. T. *Angew. Chem., Int. Ed. Engl.* **1994**, *33*, 2284.
- (12) Sauvage, J.-P. *Acc. Chem. Res.* **1990**, *23*, 319. Dietrich-Buchecker, C. O.; Sauvage, J.-P. *Chem. Rev.* **1987**, *87*, 795.
- (13) Nabeshima, T.; Inada, T.; Furukawa, N.; Hosoya, T.; Yano, Y. *Inorg. Chem.* **1993**, *32*, 1407. Nabeshima, T. *Coord. Chem. Rev.* **1996**, *148*, 151.
- (14) Lawrence, D. S.; Jiang, T.; Levett, M. *Chem. Rev.* **1995**, *95*, 2229.
- (15) Amabilino, D. B.; Stoddart, J. F. *Chem. Rev.* **1995**, *95*, 2725. Philp, D.; Stoddart, J. F. *Angew. Chem. Int. Ed. Engl.* **1996**, *35*, 1154.
- (16) Constable, E. C. *Chem. Ind.* **1994**, 56.
- (17) Ernst, R. E.; O'Connor, M. J.; Holm, R. H. *J. Am. Chem. Soc.* **1967**, *89*, 6104.
- (18) Muetterties, E. L. *J. Am. Chem. Soc.* **1968**, *90*, 5097; **1969**, *91*, 1636.
- (19) Bisson, A. P.; Carrer, F. J.; Hunter, C. A.; Waltho, J. P. *J. Am. Chem. Soc.* **1994**, *116*, 10292.
- (20) Mislow, K.; Gust, D.; Finocchiaro, P.; Boettcher, R. J. *Top. Curr. Chem.* **1974**, *47*, 1.
- (21) Durham, D. A.; Frost, G. H.; Hart, F. A. *J. Inorg. Nucl. Chem.* **1969**, *31*, 833. Skelton, B. W.; Waters, A. F.; White, A. H. *Aust. J. Chem.* **1996**, *49*, 137.
- (22) Hulliger, J. *Angew. Chem., Int. Ed. Engl.* **1994**, *33*, 143.
- (23) Harris, C. M.; Mc Kenzie, E. D. *J. Chem. Soc. (A)* **1969**, 746.
- (24) Cahn, R. S.; Ingold, C.; Prelog, V. *Angew. Chem., Int. Ed. Engl.* **1966**, *5*, 385.
- (25) Williams, A. F.; Piguet, C.; Carina, R. in *Transition Metal in Supramolecular Chemistry*, Fabbri, L., Poggi, A., Eds.; Kluwer Academic Publishers: 1994; p 404.
- (26) Sanchez-Quesada, J.; Seel, C.; Prados, P.; de Mendoza, J. *J. Am. Chem. Soc.* **1996**, *118*, 277.
- (27) Beissel, T.; Powers, R. E.; Raymond, K. N. *Angew. Chem., Int. Ed. Engl.* **1996**, *35*, 1084. Raymond, K. N.; Caulder, D. L.; Powers, R. E.; Beissel, T.; Meyer, M.; Kersting, B. *Proceedings of the Robert A. Welch Foundation 40<sup>th</sup> Conference on Chemical Research: Chemistry On The Nanometer Scale*, Texas, 1996. Saalfrank, R. W.; Burak, R.; Reihers, S.; Löw, N.; Hampel, F.; Stachel, H.-D.; Lentmaier, L.; Peters, K.; Peters, E.-M.; von Schnering, H. G. *Angew. Chem., Int. Ed. Engl.* **1995**, *35*, 993.
- (28) Healy, P. C.; Engelhardt, L. M.; Patrick, V. A.; White, A. H. *J. Chem. Soc., Dalton Trans.* **1985**, 2541. Dobson, J. F.; Green, B. E.; Healy, P. C.; Kennard, C. H. L.; Pakawatchai, C.; White, A. H. *Aust. J. Chem.* **1984**, *37*, 649.
- (29) Piguet, C.; Bernardinelli, G.; Bocquet, B.; Quattropiani, A.; Williams, A. F. *J. Am. Chem. Soc.* **1992**, *114*, 7440.
- (30) Hasenknopf, B.; Lehn, J.-M.; Baum, G.; Fenske, D. *Proc. Natl. Acad. Sci. U.S.A.* **1996**, *93*, 1397.
- (31) Mislow, K. *Chimia* **1986**, *40*, 395.
- (32) Constable, E. C. *Tetrahedron* **1992**, *48*, 10013. Constable, E. C. *Prog. Inorg. Chem.* **1994**, *42*, 67. Constable, E. C. In *Comprehensive Supramolecular Chemistry*; Atwood, J. L.; Davies, J. E. D., MacNicol, D. D., Vögtle, F., Eds. Pergamon: Oxford, 1996; Chapter 6.
- (33) Constable, E. C.; Elder, S. M.; Healy, J.; Ward, M. D. *J. Am. Chem. Soc.* **1990**, *112*, 4590.
- (34) Constable, E. C.; Walker, J. V. *J. Chem. Soc., Chem. Commun.* **1992**, 884. Constable, E. C.; Edwards, A. J.; Raithby, R.; Walker, J. V. *Angew. Chem., Int. Ed. Engl.* **1993**, *32*, 1465.
- (35) Shriver, D. F.; Atkins, P. W.; Langford, C. H. *Inorganic Chemistry*; Oxford University Press: Oxford, 1990; pp 152, 197.
- (36) Piguet, C.; Hopfgartner, G.; Williams, A. F.; Bünzli, J.-C. G. *J. Chem. Soc., Chem. Commun.* **1995**, 491.
- (37) Piguet, C.; Rivara-Minten, E.; Hopfgartner, G.; Bünzli, J.-C. G. *Helv. Chim. Acta* **1995**, *78*, 1541.
- (38) Goodgame, D. M. L.; Hill, S. P. W.; Williams, D. J. *J. Chem. Soc., Chem. Commun.* **1993**, 1019.
- (39) Barley, M.; Constable, E. C.; Corr, S.; McQueen, R. C. S.; Nutkins, J. C.; Ward, M. D.; Drew, M. G. B. *J. Chem. Soc., Dalton Trans.* **1988**, 2655.
- (40) Whitesides, G. M.; Simanek, E. E.; Mathias, J. P.; Seto, C. T.; Chin, D. N.; Mammen, M.; Gordon, D. M. *Acc. Chem. Res.* **1995**, *28*, 37. Aakeröy, C. B.; Seddon, K. R. *Chem. Soc. Rev.* **1993**, 397.
- (41) Shetty, A. S.; Zhang, J.; Moore, J. S. *J. Am. Chem. Soc.* **1996**, *118*, 1019 and references therein.
- (42) Purcell, K. F.; Kotz, J. C. *Inorganic Chemistry*; W. B. Saunders Company: Philadelphia, 1977; pp 636, 717.
- (43) Marquis-Rigault, A.; Dupont-Gervais, A.; Baxter, P. N. W.; Van Dorsselaer, A.; Lehn, J.-M. *Inorg. Chem.* **1996**, *35*, 2307.
- (44) Piguet, C.; Hopfgartner, G.; Bocquet, B.; Schaad, O.; Williams, A. F. *J. Am. Chem. Soc.* **1994**, *116*, 9092.
- (45) Perlmutter-Hayman, B. *Acc. Chem. Res.* **1986**, *19*, 90.
- (46) Garrett, T. M.; Koert, U.; Lehn, J.-M. *J. Phys. Org. Chem.* **1992**, *5*, 529.
- (47) Pfeil, A.; Lehn, J.-M. *J. Chem. Soc., Chem. Commun.* **1992**, 838.
- (48) Brewster, J. H. *Top. Curr. Chem.* **1974**, *47*, 29.
- (49) Meurer, K. P.; Vögtle, F. *Top. Curr. Chem.* **1985**, *127*, 1.
- (50) Zarges, W.; Hall, J.; Lehn, J.-M.; Bolm, C. *Helv. Chim. Acta* **1991**, *74*, 1843.
- (51) Lehn, J.-M.; Rigault, A. *Angew. Chem., Int. Ed. Engl.* **1988**, *27*, 1095.
- (52) Van Stein, G. C.; Van Koten, G.; Vieze, K.; Brevard, C.; Speck, A. L. *J. Am. Chem. Soc.* **1984**, *106*, 4486.
- (53) Enemark, E. J.; Stack, T. D. P. *Angew. Chem., Int. Ed. Engl.* **1995**, *35*, 996.
- (54) Corey, E. J.; Cywin, C. L.; Noe, M. C. *Tetrahedron Lett.* **1994**, *35*, 69.
- (55) For a review, see: Vögtle, F.; Weber, E. *Angew. Chem., Int. Ed. Engl.* **1979**, *18*, 753.
- (56) Goedken, V. L.; Christoph, G. G. *Inorg. Chem.* **1973**, *12*, 2316.
- (57) Wester, D.; Palenik, G. J. *J. Chem. Soc., Chem. Commun.* **1975**, 74. Wester, D.; Palenik, G. J. *Inorg. Chem.* **1976**, *15*, 755.
- (58) Struckmeier, G.; Therwall, U.; Fuhrhop, J.-H. *J. Am. Chem. Soc.* **1976**, *98*, 278.
- (59) Constable, E. C.; Drew, M. G. B.; Forsyth, G.; Ward, M. D. *J. Chem. Soc., Chem. Commun.* **1988**, 1450.
- (60) Gheysen, K. A.; Potts, K. T.; Hurrell, H. C.; Abruna, H. D. *Inorg. Chem.* **1990**, *29*, 1589.
- (61) Constable, E. C.; Walker, J. V.; Tocher, D. A.; Daniels, M. A. M. *J. Chem. Soc., Chem. Commun.* **1992**, 768.
- (62) Constable, E. C.; Daniels, M. A. M.; Drew, M. G. B.; Tocher, D. A.; Walker, J. V.; Wood, P. D. *J. Chem. Soc., Dalton Trans.* **1993**, 1947.
- (63) Constable, E. C.; Martinez-Manez, R.; Cargill Thompson A. M. W.; Walker, J. V. *J. Chem. Soc., Dalton Trans.* **1994**, 1585.
- (64) Constable, E. C.; Elder, S. M.; Raithby, P. R.; Ward, M. D. *Polyhedron* **1991**, *10*, 1395.
- (65) Constable, E. C.; Chotalia, R.; Tocher, D. A. *J. Chem. Soc., Chem. Commun.* **1992**, 771.
- (66) Youinou, M.-T.; Ziessel, R.; Lehn, J.-M. *Inorg. Chem.* **1991**, *30*, 2144.
- (67) Yao, Y.; Perkovic, M. W.; Rillema, D. P.; Woods, C. *Inorg. Chem.* **1992**, *31*, 3956.
- (68) Pinkerton, M.; Steinrauf, L. K. *J. Mol. Biol.* **1970**, *49*, 533.
- (69) Vögtle, F.; Sieger, H. *Angew. Chem., Int. Ed. Engl.* **1977**, *16*, 396.
- (70) Saenger, W.; Brand, H. *Acta Crystallogr.* **1979**, *B35*, 838.
- (71) Weber, E.; Saenger, W.; Vögtle, F.; Sieger, H. *Angew. Chem., Int. Ed. Engl.* **1979**, *18*, 226.
- (72) Raschhofer, W.; Open, G.; Müller, W. M.; Vögtle, F. *Chem. Ber.* **1978**, *111*, 1108.
- (73) Bell, T. W.; Jouselin, H. *J. Am. Chem. Soc.* **1991**, *113*, 6283.
- (74) Deuschel-Cornioley, C.; Stoeckli-Evans, H.; von Zelewsky, A. *J. Chem. Soc., Chem. Commun.* **1990**, 121.
- (75) Shannon, R. D. *Acta Crystallogr.* **1976**, *A32*, 751.
- (76) Ho, P. K. K.; Cheung, K. K.; Peng, S. M.; Che, C. M. *J. Chem. Soc., Dalton Trans.* **1996**, 1411.
- (77) Fu, Y.; Sun, J.; Li, Q.; Zhou, Z.; Dai, W.; Wang, D.; Mak, T. C. W.; Hu, H.; Tang, W. *Chem. Commun.* **1996**, 1549.
- (78) Fu, Y.; Sun, J.; Li, Q.; Chen, Y.; Dai, W.; Wang, D.; Mak, T. C. W.; Tang, W.; Hu, H. *J. Chem. Soc., Dalton Trans.* **1996**, 2309.
- (79) Mizutani, T.; Yagi, S.; Honmaru, A.; Ogoshi, H. *J. Am. Chem. Soc.* **1996**, *118*, 5318.
- (80) Constable, E. C.; Ward, M. D.; Tocher, D. A. *J. Am. Chem. Soc.* **1990**, *112*, 1256.
- (81) Constable, E. C.; Chotalia, R. *J. Chem. Soc., Chem. Commun.* **1992**, 64. Chotalia, R.; Constable, E. C.; Neuburger, M.; Smith, D. R.; Zehnder, M. *J. Chem. Soc., Dalton Trans.* **1996**, 4207.
- (82) Constable, E. C.; Ward, M. D.; Tocher, D. A. *J. Chem. Soc., Dalton Trans.* **1991**, 1675.
- (83) Burke, P. J.; McMillin, D. R.; Robinson, W. R. *Inorg. Chem.* **1980**, *19*, 1211. Federlin, P.; Kern, J.-M.; Rastegar, A.; Dietrich-Buchecker, C.; Marnot, P. A.; Sauvage, J.-P. *New J. Chem.* **1990**, *4*, 9.
- (84) Iwamoto, R. *Bull. Chem. Soc. Jpn.* **1973**, *46*, 1114.
- (85) Iwamoto, R. *Bull. Chem. Soc. Jpn.* **1973**, *46*, 1123.
- (86) Cathey, C. J.; Constable, E. C.; Hannon, M. J.; Tocher, D. A.; Ward, M. D. *J. Chem. Soc., Chem. Commun.* **1990**, 621.
- (87) Thummel, R. P.; Hery, C.; Williamson, D.; Lefoulon, F. *J. Am. Chem. Soc.* **1988**, *110*, 7894.
- (88) Bardwell, D. A.; Barigelletti, F.; Cleary, R. L.; Flamigni, L.; Guardigli, M.; Jeffery, J. C.; Ward, M. D. *Inorg. Chem.* **1995**, *34*, 2438.
- (89) Balzani, V.; Juris, A.; Venturi, M.; Campagna, S.; Serroni, S. *Chem. Rev.* **1996**, *96*, 759.
- (90) Gelling, O. J.; Feringa, B. L. *J. Am. Chem. Soc.* **1990**, *112*, 7599.
- (91) Gelling, O. J.; Van Bolhuis, F.; Feringa, B. L. *J. Chem. Soc., Chem. Commun.* **1991**, 917.
- (92) Rüttimann, S.; Piguet, C.; Bernardinelli, G.; Bocquet, B.; Williams, A. F. *J. Am. Chem. Soc.* **1992**, *114*, 4230.
- (93) Williams, A. F.; Carina, C.; Charbonnière, L.; Desmartin, P.; Piguet, C. *Thermodynamic and Kinetic Stability of Polynuclear Complexes in Physical Supramolecular Chemistry*; Echegoyen, L., Kaifer, A. E., Eds.; Nato AST Series, 1996, p. 379.
- (94) Bernardinelli, G.; Kübel-Pollak, A.; Williams, A. F. *Chimia* **1992**, *46*, 155.
- (95) Piguet, C.; Bernardinelli, G.; Williams, A. F. *Inorg. Chem.* **1989**, *28*, 2920.
- (96) Carina, R. F.; Bernardinelli, G.; Williams, A. F. *Angew. Chem., Int. Ed. Engl.* **1993**, *32*, 1463.
- (97) Constable, E. C.; Edwards, A. J.; Hannon, M. J.; Raithby, P. R. *J. Chem. Soc., Chem. Commun.* **1994**, 1991.

- (97) Potts, K. T.; Keshavarz-K., M.; Tham, F. S.; Abruna, H. D.; Arana, C. *Inorg. Chem.* **1993**, *32*, 4450.
- (98) Hopfgartner, G.; Piguet, C.; Henion, J. D.; Williams, A. F. *Helv. Chim. Acta* **1993**, *76*, 1759.
- (99) Phifer, C. C.; McMillin, D. R. *Inorg. Chem.* **1986**, *25*, 1329.
- (100) Drew, M. G. B.; Lavery, A.; McKee, V.; Nelson, S. M. *J. Chem. Soc., Dalton Trans.* **1985**, 1771.
- (101) Petoud, S.; Bünzli, J.-C. G.; Schenk, K.; Piguet, C. *Inorg. Chem.*, in press.
- (102) Bin Silong, S.; Kildea, J. D.; Patalinghug, C.; Skelton, B. W.; White, A. H. *Aust. J. Chem.* **1994**, *47*, 1545.
- (103) Paolucci, G.; Stelluto, S.; Sitran, S.; Ajo, D.; Benetollo, F.; Polo, A.; Bombieri, G. *Inorg. Chim. Acta* **1992**, *193*, 57.
- (104) Lehn, J.-M.; Sauvage, J.-P.; Simon, J.; Ziessel, R.; Piccinni-Leopardi, C.; Germain, G.; Declercq, J.-P.; Van Meerssche, M. *Nouv. J. Chim.* **1983**, *7*, 413.
- (105) Gisselbrecht, J.-P.; Gross, M.; Lehn, J.-M.; Sauvage, J.-P.; Ziessel, R.; Piccinni-Leopardi, C.; Arrieta, J. M.; Germain, G.; Van Meerssche, M. *Nouv. J. Chim.* **1984**, *8*, 661.
- (106) Constable, E. C.; Hannon, M. J.; Martin, A.; Raithby, P. R.; Tocher, D. A. *Polyhedron* **1992**, *11*, 2967. Constable, E. C.; Elser, S. M.; Hannon, M. J.; Martin, A.; Raithby, P. R.; Tocher, D. A. *J. Chem. Soc., Dalton Trans.* **1996**, 2423.
- (107) Potts, K. T.; Keshavarz-K., M.; Tham, F. S.; Abruna, H. D.; Arana, C. *Inorg. Chem.* **1993**, *32*, 4422.
- (108) Potts, K. T.; Keshavarz-K., M.; Tham, F. S.; Abruna, H. D.; Arana, C. *Inorg. Chem.* **1993**, *32*, 4436.
- (109) Harding, M.; Koert, U.; Lehn, J.-M.; Marquis-Rigault, A.; Piguet, C.; Siegel, J. *Helv. Chim. Acta* **1991**, *74*, 594.
- (110) Koert, U.; Harding, M. M.; Lehn, J.-M. *Nature* **1990**, *346*, 339. Harding, M. M.; Lehn, J.-M. *Aust. J. Chem.* **1996**, *49*, 1023.
- (111) Garrett, T. M.; Koert, U.; Lehn, J.-M.; Rigault, A.; Meyer, D.; Fischer, J. *J. Chem. Soc., Chem. Commun.* **1990**, 557.
- (112) Woods, C. R.; Benaglia, M.; Cozzi, F.; Siegel, J. S. *Angew. Chem., Int. Ed. Engl.* **1996**, *35*, 1830.
- (113) Schoentjes, B.; Lehn, J.-M. *Helv. Chim. Acta* **1995**, *78*, 1.
- (114) Eisenbach, C. D.; Schubert, U. S.; Baker, G. R.; Newkome, G. R. *J. Chem. Soc., Chem. Commun.* **1995**, 69.
- (115) Krämer, R.; Lehn, J.-M.; Marquis-Rigault, A. *Proc. Natl. Acad. Sci. U.S.A.* **1993**, *90*, 5394.
- (116) Dietrich-Buchecker, C. O.; Sauvage, J.-P.; Kintzinger, J.-P.; Maltèse, P.; Pascard, C.; Guilhem, J. *New J. Chem.* **1992**, *16*, 931. Dietrich-Buchecker, C. O.; Nierengarten, J.-F.; Sauvage, J.-P.; Armaroli, N.; Balzani, V.; De Cola, L. *J. Am. Chem. Soc.* **1993**, *115*, 11237.
- (117) Dietrich-Buchecker, C. O.; Sauvage, J.-P.; DeCian, A.; Fischer, J. *J. Chem. Soc., Chem. Commun.* **1994**, 2231.
- (118) Dietrich-Buchecker, C. O.; Sauvage, J.-P.; Armaroli, N.; Ceroni, P.; Balzani, V. *New J. Chem.* **1996**, *20*, 801.
- (119) Constable, E. C.; Hannon, M. J.; Tocher, D. A. *Angew. Chem., Int. Ed. Engl.* **1992**, *31*, 230. Constable, E. C.; Hannon, M. J.; Tocher, D. A. *J. Chem. Soc., Dalton Trans.* **1993**, 1883.
- (120) Constable, E. C.; Hannon, M. J.; Edwards, A. J.; Raithby, P. R. *J. Chem. Soc., Dalton Trans.* **1994**, 2669.
- (121) Müller, E.; Piguet, C.; Bernardinelli, G.; Williams, A. F. *Inorg. Chem.* **1988**, *27*, 849.
- (122) Beer, P. D.; Wheeler, J. W.; Moore, C. P. *J. Chem. Soc., Dalton Trans.* **1992**, 2667.
- (123) Bilyk, A.; Harding, M. *J. Chem. Soc., Dalton Trans.* **1994**, 77.
- (124) Bilyk, A.; Harding, M. *J. Chem. Soc., Chem. Commun.* **1995**, 1697.
- (125) Ziessel, R.; Youinou, M.-T. *Angew. Chem., Int. Ed. Engl.* **1993**, *32*, 877.
- (126) Juris, A.; Ziessel, R. *Inorg. Chim. Acta* **1994**, *225*, 251.
- (127) Bonnet, R.; Davies, J. E.; Hursthouse, M. B. *Nature* **1976**, *262*, 326.
- (128) Sheldrick, W. S.; Engel, J. *J. Chem. Soc., Chem. Commun.* **1980**, 5. Sheldrick, W. S.; Engel, J. *Acta Crystallogr.* **1981**, *B37*, 250.
- (129) Bell, T. W.; Cragg, P. J.; Drew, M. G. B.; Firestone, A.; Kwok, D.-I. *Angew. Chem., Int. Ed. Engl.* **1992**, *31*, 348.
- (130) Bell, T. W.; Jousselein, H. *Nature* **1994**, *367*, 441.
- (131) Airey, A. L.; Swiegers, G.; Willis, A. C.; Wild, B. S. *J. Chem. Soc., Chem. Commun.* **1995**, 695.
- (132) Comba, P.; Fath, A.; Hambley, T. W.; Richens, D. T. *Angew. Chem., Int. Ed. Engl.* **1995**, *34*, 1883. Comba, P.; Fath, A.; Huttner, G.; Zsolnai, L. *Chem. Commun.* **1996**, 1885.
- (133) Tiecco, M.; Testaferri, L.; Tingoli, M.; Chianelli, D.; Montanucci, M. *Synthesis* **1984**, 736.
- (134) Constable, E. C.; Edwards, A. J.; Martinez-Manez, R.; Raithby, P. R. *J. Chem. Soc., Dalton Trans.* **1995**, 3253.
- (135) Ho, P. K. K.; Peng, S. M.; Wong, K. Y.; Che, C. M. *J. Chem. Soc., Dalton Trans.* **1996**, 1829.
- (136) Sauvage, J.-P.; Ward, M. D. *Inorg. Chem.* **1991**, *30*, 3869.
- (137) Crane, J. D.; Sauvage, J.-P. *New J. Chem.* **1992**, *16*, 649.
- (138) Hasenkopf, B.; Lehn, J.-M. *Helv. Chim. Acta* **1996**, *79*, 1643.
- (139) Bilyk, A.; Harding, M. M.; Turner, P.; Hambley, T. W. *J. Chem. Soc., Dalton Trans.* **1994**, 2783. Bilyk, A.; Harding, M. M.; Turner, P.; Hambley, T. W. *J. Chem. Soc., Dalton Trans.* **1995**, 2549.
- (140) Hopfgartner, G.; Piguet, C.; Henion, J. D. *J. Am. Soc. Mass Spectrom.* **1994**, *5*, 748.
- (141) Piguet, C.; Bocquet, B.; Müller, E.; Williams, A. F. *Helv. Chim. Acta* **1989**, *72*, 323. Bochet, C. G.; Piguet, C.; Williams, A. F. *Helv. Chim. Acta* **1993**, *76*, 372.
- (142) Van Stein, G. C.; Van der Poel, H.; Van Koten, G.; Spek, A. L.; Duisenberg, A. J. M.; Pregosin, P. S. *J. Chem. Soc., Chem. Commun.* **1980**, 1016.
- (143) Van Stein, G. C.; Van Koten, G.; Passenier, H.; Steinebach, O.; Vrieze, K. *Inorg. Chim. Acta* **1984**, *89*, 79.
- (144) Van Stein, G. C.; Van Koten, G.; Vrieze, K.; Spek, A. L.; Klop, E. A.; Brevard, C. *Inorg. Chem.* **1985**, *24*, 1367.
- (145) Constable, E. C.; Heirtzler, F. R.; Neuburger, M.; Zehnder, M. *Supramol. Chem.* **1995**, *5*, 197.
- (146) Constable, E. C.; Heirtzler, F. R.; Neuburger, M.; Zehnder, M. *Chem. Commun.* **1996**, 933.
- (147) Constable, E. C.; Edwards, A. J.; Raithby, P. R.; Smith, D. R.; Walker, J. V.; Whall, L. *Chem. Commun.* **1996**, 2551.
- (148) Piguet, C.; Bocquet, B.; Hopfgartner, G. *Helv. Chim. Acta* **1994**, *77*, 931.
- (149) Piguet, C.; Bernardinelli, G.; Williams, A. F.; Bocquet, B. *Angew. Chem., Int. Ed. Engl.* **1995**, *34*, 582.
- (150) Piguet, C.; Bünzli, J.-C. G.; Bernardinelli, G.; Hopfgartner, G.; Petoud, S.; Schaad, O. *J. Am. Chem. Soc.* **1996**, *118*, 6681.
- (151) Constable, E. C.; Holmes, J. M.; Raithby, P. R. *Polyhedron* **1991**, *10*, 127.
- (152) Potts, K. T.; Keshavarz-K., M.; Tham, F. S.; Gheysen Raiford, K. A.; Arana, C.; Abruna, H. D. *Inorg. Chem.* **1993**, *32*, 5477.
- (153) Constable, E. C.; Neuburger, M.; Smith, D. R.; Zehnder, M. *Chem. Commun.* **1996**, 1917.
- (154) Constable, E. C.; Ward, M. D.; Drew, M. G. B.; Forsyth, G. A. *Polyhedron* **1989**, *8*, 2551.
- (155) Ho, P. K. K.; Cheung, K. K.; Che, C. M. *Chem. Commun.* **1996**, 1197.
- (156) Baker, A. T.; Craig, D. C.; Dong, G. *Inorg. Chem.* **1996**, *35*, 1091.
- (157) Jonassen, H. B.; Douglas, B. E. *J. Am. Chem. Soc.* **1949**, *71*, 4094. Stratton, W. J.; Busch, D. H. *J. Am. Chem. Soc.* **1960**, *82*, 4834.
- (158) Potts, K. T.; Horwitz, C. P.; Fessak, A.; Keshavarz-K., M.; Nash, K. E.; Toscano, P. J. *J. Am. Chem. Soc.* **1993**, *115*, 10444.
- (159) Onggo, D.; Goodwin, H. A. *Aust. J. Chem.* **1991**, *44*, 1539.
- (160) Serr, B. R.; Andersen, K. A.; Elliott, C. M.; Anderson, O. P. *Inorg. Chem.* **1988**, *27*, 4499.
- (161) Ferrere, S.; Elliott, C. M. *Inorg. Chem.* **1995**, *34*, 5818.
- (162) Elliott, C. M.; Derr, D. L.; Ferrere, S.; Newton, M. D.; Liu, Y.-P. *J. Am. Chem. Soc.* **1996**, *118*, 5221.
- (163) Larson, S. L.; Hendrikson, S. M.; Ferrere, S.; Derr, D. L.; Elliott, C. M. *J. Am. Chem. Soc.* **1995**, *117*, 5881.
- (164) Krämer, R.; Lehn, J.-M.; DeCian, A.; Fischer, J. *Angew. Chem., Int. Ed. Engl.* **1993**, *32*, 704.
- (165) Zurita, D.; Baret, P.; Pierre, J.-L. *New J. Chem.* **1994**, *18*, 1143.
- (166) Albrecht, M. A.; Riether, C. *Chem. Ber.* **1996**, *129*, 829. Albrecht, M. A.; Riether, C. *Synlett.* **1995**, 309.
- (167) Albrecht, M. A.; Kotila, S. *Angew. Chem., Int. Ed. Engl.* **1995**, *34*, 2134.
- (168) Williams, A. F.; Piguet, C.; Bernardinelli, G. *Angew. Chem., Int. Ed. Engl.* **1991**, *30*, 1490.
- (169) Piguet, C.; Bernardinelli, G.; Bocquet, B.; Schaad, O.; Williams, A. F. *Inorg. Chem.* **1994**, *33*, 4112.
- (170) Charbonnière, L. J.; Bernardinelli, G.; Piguet, C.; Sargeson, A. M.; Williams, A. F. *J. Chem. Soc., Chem. Commun.* **1994**, 1419.
- (171) Wilkins, R. G. *Kinetics and Mechanisms of Reaction of Transition Metal Complexes*, 2nd ed.; VCH: Weinheim, 1991; p 265.
- (172) Charbonnière, L. J.; Gilet, M.-F.; Bernauer, K.; Williams, A. F. *Chem. Commun.* **1996**, 39. Charbonnière, L. J.; Williams, A. F.; Frey, U.; Merbach, A. E.; Kamalaprjya, P.; Schaad, O. *J. Am. Chem. Soc.* **1997**, *119*, 2488.
- (173) Carrano, C. J.; Raymond, K. N. *J. Am. Chem. Soc.* **1978**, *100*, 5371. Carrano, C. J.; Cooper, S. J.; Raymond, K. N. *J. Am. Chem. Soc.* **1979**, *101*, 599.
- (174) Sarrow, R. C.; White, D. L.; Raymond, K. N. *J. Am. Chem. Soc.* **1985**, *107*, 6540.
- (175) Enemark, E. J.; Stack, T. D. P. *Inorg. Chem.* **1996**, *35*, 2719.
- (176) Kersting, B.; Meyer, M.; Powers, R. E.; Raymond, K. N. *J. Am. Chem. Soc.* **1996**, *118*, 7221.
- (177) Kersting, B.; Telford, J. R.; Meyer, M.; Raymond, K. N. *J. Am. Chem. Soc.* **1996**, *118*, 5712.
- (178) Albrecht, M. A.; Kotila, S. *Angew. Chem., Int. Ed. Engl.* **1996**, *35*, 1208.
- (179) Albrecht, M. A.; Röttle, H.; Burger, P. *Chem. Eur. J.* **1996**, *2*, 1264.
- (180) Albrecht, M. A.; Kotila, S. *Chem. Commun.* **1996**, 2309.
- (181) Libman, J.; Tor, Y.; Shanzer, A. *J. Am. Chem. Soc.* **1987**, *109*, 5880.
- (182) Hasenkopf, B.; Lehn, J.-M.; Kneisel, B. O.; Baum, G.; Fenske, D. *Angew. Chem., Int. Ed. Engl.* **1996**, *35*, 1838.
- (183) Bünzli, J.-C. G.; Milicic-Tang, A. in *Handbook on the Physics and Chemistry of Rare Earths*, Gschneider, K. A. J., Eyring, L. Eds.; Elsevier Science Publishers: Amsterdam, 1995; Vol. 21, Chapter 145.
- (184) Piguet, C.; Bünzli, J.-C. G.; Bernardinelli, G.; Hopfgartner, G.; Williams, A. F. *J. Am. Chem. Soc.* **1993**, *115*, 8197.
- (185) Bernardinelli, G.; Piguet, C.; Williams, A. F. *Angew. Chem., Int. Ed. Engl.* **1992**, *31*, 1621.

- (186) Piguet, C. *Chimia* **1996**, *50*, 144.
- (187) Piguet, C.; Bünzli, J.-C. G.; Bernardinelli, G.; Williams, A. F. *J. Alloys Compd.* **1995**, *225*, 324.
- (188) Vanquickenborne, L. G.; Pierloot, K. *Inorg. Chem.* **1981**, *20*, 3673.
- (189) Piguet, C.; Rivara-Minten, E.; Hopfgartner, G.; Bünzli, J.-C. G. *Helv. Chim. Acta* **1995**, *78*, 1651.
- (190) Piguet, C.; Bernardinelli, G.; Bünzli, J.-C. G.; Petoud, S.; Hopfgartner, G. *J. Chem. Soc., Chem. Commun.* **1995**, 2575.
- (191) Zelikovich, L.; Libman, J.; Shanzler, A. *Nature* **1995**, *374*, 790.
- (192) Piguet, C.; Williams, A. F.; Bernardinelli, G.; Moret, E.; Bünzli, J.-C. G. *Helv. Chim. Acta* **1992**, *75*, 1697.
- (193) Hogerheide, M. P.; Jastrzebski, J. T. B.; Boersma, J.; Smeets, W. J. J.; Spek, A. L.; Van Koten, G. *Inorg. Chem.* **1994**, *33*, 4431.
- (194) Prasad, P. N.; Williams, D. J. *Introduction to Non Linear Optical Effects in Molecules and Polymers*, John Wiley & Sons: Chichester, 1991.
- (195) Gulik-Krzywicki, T.; Fouquey, C.; Lehn, J.-M. *Proc. Natl. Acad. Sci. U.S.A.* **1993**, *90*, 163.
- (196) Griffin, L. C.; Kiessling, L. L.; Beal, P. A.; Gillespie, P.; Dervan, P. B. *J. Am. Chem. Soc.* **1992**, *114*, 7976. Giovannangeli, C.; Montenay-Garestier, T.; Rougée, M.; Chassignol, M.; Thuang, N. T.; Hélène, C. *J. Am. Chem. Soc.* **1991**, *113*, 7775.
- (197) Dietrich-Buchecker, C. O.; Sauvage, J.-P. *Angew. Chem., Int. Ed. Engl.* **1989**, *28*, 189.
- (198) Dietrich-Buchecker, C. O.; Sauvage, J.-P.; Armaroli, N.; Ceroni, P.; Balzani, V. *Angew. Chem., Int. Ed. Engl.* **1996**, *35*, 1119.
- (199) Nierengarten, J.-P.; Dietrich-Buchecker, C. O.; Sauvage, J.-P. *J. Am. Chem. Soc.* **1994**, *116*, 375. Nierengarten, J.-P.; Dietrich-Buchecker, C. O.; Sauvage, J.-P. *New J. Chem.* **1996**, *20*, 685.
- (200) Carina, R. F.; Dietrich-Buchecker, C. O.; Sauvage, J.-P. *J. Am. Chem. Soc.* **1996**, *118*, 9110.
- (201) Piguet, C.; Bünzli, J.-C. G.; Bernardinelli, G.; Williams, A. F. *Inorg. Chem.* **1993**, *32*, 4139. Piguet, C.; Bünzli, J.-C. G.; Bernardinelli, G.; Bochet, C. G.; Froidevaux, P. *J. Chem. Soc., Dalton Trans.* **1995**, 83.
- (202) Fenn, J. B.; Mann, M.; Meng, C. K.; Wong, S. F.; Whitehouse, C. M. *Science* **1989**, *246*, 64.
- (203) Malinowski, E. R.; Howerly, D. G. *Factor Analysis in Chemistry*, J. Wiley: New York, 1991.
- (204) Henry, H.; Hofrichter, J. *Methods in Enzymology*; Brand, L., Johnson, M. L., Eds.; Academic Press: 1992; Vol. 210, p 129.
- (205) Gampp, H.; Maeder, M.; Meyer, M.; Zuberbühler, A. D. *Talanta* **1985**, *32*, 95.
- (206) Hill, Z. D.; MacCarthy, P. *J. Chem. Educ.* **1986**, *63*, 162.
- (207) Pachuta, S. J.; Cooks, R. G. *Chem. Rev.* **1987**, *87*, 647.
- (208) Karas, M.; Hillenkampf, F. *Anal. Chem.* **1988**, *60*, 2299.
- (209) Przybylski, M.; Glocker, M. O. *Angew. Chem., Int. Ed. Engl.* **1996**, *35*, 806.
- (210) Fenn, J. B.; Mann, M.; Meng, C. K.; Wong, S. F.; Whitehouse, G. M. *Mass Spectrom. Rev.* **1990**, *9*, 37.
- (211) Hager, D. B.; Dovichi, N. J.; Klassen, J.; Kebarle, P. *Anal. Chem.* **1994**, *66*, 3944.
- (212) Burlingame, A. L.; Boyd, R. K.; Gaskell, S. J. *Anal. Chem.* **1996**, *68*, 599R.
- (213) Caldecourt, V. J.; Zakett, D.; Chou, J. C. *Int. J. Mass Spectrom. Ion Phys.* **1983**, *49*, 233.
- (214) Wilm, M. S.; Mann, M. *Int. J. Mass Spectrom. Ion Proc.* **1994**, *136*, 167.
- (215) Bruins, A.; Covey, T. R.; Henion, J. D. *Anal. Chem.* **1987**, *59*, 2642.
- (216) Katta, V.; Chowdhury, S. K.; Chait, B. T. *J. Am. Chem. Soc.* **1990**, *112*, 5348. For a review see Colton, R.; D'Agostino, A.; Traeger, J. C. *Mass Spectrom. Rev.* **1995**, *14*, 79.
- (217) Bitsch, F.; Dietrich-Buchecker, C. O.; Khémis, A.-K.; Sauvage, J.-P.; Dorsselaer, A. V. *J. Am. Chem. Soc.* **1991**, *113*, 4023.
- (218) Romero, F. M.; Ziessel, R.; Dupont-Gervais, A.; Dorsselaer, A. V. *Chem. Commun.* **1996**, 551.
- (219) Blades, A. T.; Ikonomou, M. G.; Kebarle, P. *Anal. Chem.* **1991**, *63*, 2109.
- (220) Leize, E.; Jaffrezic, A.; Dorsselaer, A. V. *J. Mass Spectrom.* **1996**, *31*, 537.
- (221) Leize, E.; Dorsselaer, A. V.; Krämer, R.; Lehn, J.-M. *J. Chem. Soc., Chem. Commun.* **1993**, 990.
- (222) Hopfgartner, G.; Piguet, C. *42<sup>nd</sup> ASMS Conference on Mass Spectrometry* **1994**.
- (223) Bryant, R. G. *J. Chem. Educ.* **1983**, *60*, 933. Hynes, M. J. *J. Chem. Soc., Dalton Trans.* **1993**, 311.
- (224) Scatchard, G. *Ann. N. Y. Acad. Sci.* **1949**, *51*, 660.
- (225) Piguet, C.; Bünzli, J.-C. G.; Bernardinelli, G.; Hopfgartner, G.; Rivara-Minten, E. *J. Chem. Soc., Dalton Trans.* **1997**, 421.
- (226) Atwood, J. L. In *Proceedings of the NATO Advanced Research Workshop on Physical Supramolecular Chemistry*; Echegoyen, L., Kaifer, A. E., Eds.; Kluwer Academic Publisher: Dordrecht, The Netherlands, 1996; p 261.
- (227) Van der Sluis, P.; Hezemans, A. M. F.; Kroon, J. *J. Appl. Crystallogr.* **1989**, *22*, 340. Jones, P. G. *Chem. Br.* **1981**, *17*, 222.
- (228) RS 3000 and Hostinert 216 by Riedel-deHaën, D-30926 Selze, Germany.
- (229) Kottke, T.; Stalke, D. *J. Appl. Crystallogr.* **1993**, *26*, 615.
- (230) Bünzli, J.-C. G.; Merbach, A. E.; Nielson, R. M. *Inorg. Chim. Acta* **1987**, *139*, 151.
- (231) Van der Sluis, P.; Spek, A. L. *Acta Crystallogr.* **1990**, *A46*, 194.
- (232) Kitaigorodsky, A. I. *Molecular Crystals and Molecules*, Academic Press Inc.: London, 1973.
- (233) Renaud, F.; Piguet, C.; Bernardinelli, G.; Bünzli, J.-C. G.; Hopfgartner, G. *Eur. J. Chem.*, in press.
- (234) Voyer, N.; Lamothe, J. *Tetrahedron* **1995**, *51*, 9241. Koshland, D. A. *Angew. Chem., Int. Ed. Engl.* **1994**, *33*, 2375.
- (235) Marquis-Rigault, A.; Dupont-Gervais, A.; Van Dorsselaer, A.; Lehn, J.-M. *Chem. Eur. J.* **1996**, *3*, 1395.
- (236) Saalfrank, R. W.; Harbig, R.; Nachtrab, J.; Bauer, W.; Zeller, K.-P.; Stalke, D.; Teichert, M. *Eur. J. Chem.* **1996**, *2*, 1363.
- (237) Hartshorn, C. M.; Steel, P. J. *Inorg. Chem.* **1996**, *35*, 6902.
- (238) Smith, V. C.; Lehn, J.-M. *Chem. Commun.* **1996**, 2733.
- (239) Funeriu, D. P.; Lehn, J.-M.; Baum, G.; Denske, D. *Chem. Eur. J.* **1997**, *3*, 99.
- (240) Albrecht, M.; Fröhlich, R. *J. Am. Chem. Soc.* **1997**, *119*, 1656–1661.
- (241) Shieh, S. J.; Chou, C. C.; Lee, G. H.; Wang, C. C.; Peng, S. M. *Angew. Chem., Int. Ed. Engl.* **1997**, *36*, 56.

CR960053S